Living biointerfaces to direct stem cell fate

Michaela Petaroudi

(BSc Hons)

Submitted in fulfilment of the requirements for the Degree of

Doctor of Philosophy (PhD)

Centre for the Cellular Microenvironment

College of Science and Engineering

University of Glasgow

G12 8LT

Abstract

Cellular therapeutics is a constantly evolving field within tissue engineering and regenerative medicine, that aims to provide clinically relevant solutions for tissue repair applications. Currently, the most commonly used methods of tissue regeneration revolve around the use of stem cells, due to their inherent potential to self-renew and differentiate, driving damaged tissue repair. However, the scarcity of suitable donors, the variety of challenges associated with primary stem cell isolation, the lack of controllable ways to direct differentiation into specific lineages, and insufficient numbers of engraftable cells, have hindered the extensive and efficient use of stem cells in clinical settings. These issues, that stem from the lack of understanding of the underlying mechanisms driving stem cell differentiation, have created the need for the study of stem cell behaviour and the chemical and mechanical stimuli that influence their fate decisions.

In an attempt to understand the specific mechanisms that drive stem cell survival, proliferation and differentiation, research efforts have been focused on the engineering of physiologically relevant cell microenvironments, that could mimic the natural stem cell niche. The endeavour to provide close niche analogues has driven the evolution of such efforts from initially simple cell culture methods, based on the use of stem cell expansion media containing soluble growth factors, to the development of dynamic surfaces, bioactive 3D substrates and bioprinted scaffolds with the aim to provide close representations of the target cell niche. Given their enormous clinical potential to treat a variety of hematological disorders and heal major tissue injuries respectively, Hematopoietic (HSCs) and Mesenchymal stem cells (MSCs) have been the two most widely used cell types in cellular therapeutics. Currently, most common scientific efforts for the expansion of HSCs have been focused on cell cultures with the external addition of niche growth factors including stem cell factor, thrombopoietin and FMS-like tyrosine kinase 3 ligand (FLT3L). In contrast, research on clinical applications of MSCs has focused on identifying the soluble cues that drive cell differentiation into specific lineages, such as bone repair. However, despite the variety of scientific studies aiming to increase the therapeutic uses of both stem cell types, progress is still slow in the development of efficient ways to produce clinically relevant cell numbers to address the increasing need for cellular grafts.

Active biomaterials have recently received increased scientific attention due to their intrinsic ability to exert instructive or stimulating effects on cells and tissues by engineering the material's responsiveness to internal or external stimuli that can promote tissue repair and regeneration. In particular, living interfaces have the potential to actively produce and deliver growth factors of interest to the cultured cells and guide their behaviour to improve tissue regeneration, providing a promising opportunity to substantially enhance the efficacy of tissue engineering and regenerative medicine.

In this work, we have genetically engineered the non-pathogenic bacterial species *Lactococcus lactis* (*L. lactis*) to produce recombinant human CXCL12, thrombopoietin, and VCAM1 and have combined these populations with the previously developed FN-expressing *L. lactis* to create bone marrow niches *ex vivo*. The purpose of this work is to engineer a platform that could directly influence stem cell fate by actively stimulating the cultured cells by the recombinant proteins and by added 3D elements, such as poly(ethylene) glycol hydrogels. The successful development of such a system could have significant potential in cellular therapeutics, as it could provide a variety of physiologically relevant, niche mimicking stimuli to encourage stem cell survival and proliferation. In particular, our platform could be used to maintain HSCs and MSCs in a naïve state, while also encouraging their self-renewal and proliferation. In alignment with the increasing demand for HSC and MSC transplants for clinical applications, our work could provide insights into the most optimal culture methods that would encourage the proliferation of the cultured stem cells, in order to produce clinically relevant cell numbers for the cellular therapeutics. In parallel, our system could be used as a platform to study a variety of aspects of the bone marrow, such as the effects of specific soluble and mechanical stimuli on stem cell fate in healthy and deregulated conditions. The results of this thesis suggest that *L. lactis* can be used as a versatile tool to produce a variety of recombinant proteins. Its ability to form stable biofilms enables the bacteria to act as a living interface between the substrate below and the stem cells seeded above. We report that HSCs cultured on top of *L. lactis* biofilms show notable expansion, and decreased tendency to differentiate, both in 2D where the HSCs are seeded directly above the biofilms, and in 3D where the stem cells are maintained in a hydrogel, on top of the biofilms. In parallel, we report that MSCs cultured on our living interfaces display

maintenance of their naïve, stem-like phenotype, without showing commitment to differentiated cell lineages.

In the future, this tuneable, biocompatible system can be engineered to produce any recombinant protein or small molecule and deliver it to any cultured cell type. These expressed factors can be either secreted or presented as a membrane protein on the bacteria, providing opportunities for both soluble and mechanical stimulation of the cultured cells. The variety of combinations of recombinantly expressed factors and cultured cell types provide the opportunity for the development of different niche-mimicking microenvironments that can be tailored to address different clinical needs. In total, our active biointerface provides a proof of concept that living materials can be successfully engineered and used in biomedical applications.

Table of contents

List of abbreviations

2D	2 Dimensional
3D	3 Dimensional
3PGA	3-Phosphoglyceric Acid
ABC	ATP-Binding Cassette
ALCAM	Activated Leukocyte Cell Adhesion Molecule
Ang	Angiopoietin
APTES	(3-aminopropyl)triethoxysilane
ATP	Adenosine Triphosphate
BIT	Bovine Insulin and Transferrin
BM	Bone Marrow
BMP2	Bone Morphogenetic Protein 2
BSA	Bovine Serum Albumin
CAMs	Cell Adhesion Molecules
Cm	Chloramphenicol
CXCL12	C-X-C motif chemokine 12
CXCR4	C-X-C motif chemokine receptor 4
DNA	Deoxyribonucleic Acid
DNTPs	Deoxynucleotide Triphosphates
E. coli	*Escherichia coli*
ECM	Extracellular Matrix
EFSA	European Food Safety Authority
ELISA	Enzyme Linked Immunosorbent Assay
EMP pathway	Embden-Meyerhof-Parnas pathway
Ery	Erythromycin
ETC	Electron Transport Chain
FA	Focal Adhesion
FBP	Fructose-1,6-Biphosphate
FBS	Foetal Bovine Serum
FDA	Food and Drug Administration
FLT3L	FMS-like Tyrosine Kinase 3 Ligand
FN	Fibronectin
FOXO3	Forkhead Box O-3
G6P	Glucose-6-Phosphate
GAPDH	Glyceraldehyde 3-Phosphate Dehydrogenase
GelMA	Gelatin Methacryoyl
GFP	Green Fluorescent Protein
GRAS	Generally Recognized As Safe
GTP	Guanosine Triphosphate
HSC	Hematopoietic Stem Cell
ICAM1	Intercellular Adhesion Molecule 1
ICW	In-Cell Western
IgSF	Immunoglobulin Superfamily
IL	Interleukin
JAK	Janus kinase
L. lactis	*Lactococcus lactis*

LAB	Lactic Acid Bacteria
LAMP	Loop Mediated Isothermal Amplification
LDH	Lactate Dehydrogenase
LPS	Lipopolysaccharide
MMP	Matrix Metalloproteinases
MSC	Mesenchymal Stem Cell
NAD	Nicotinamide Adenine Dinucleotide
NICE	Nisin-Controlled Inducible Expression
OPN	Osteopontin
OSX	Osterix
P/S	Penicillin/Streptomycin
PAA	Polyacrylamide
PBS	Phosphate-buffered Saline
PCR	Polymerase Chain Reaction
PDMS	Polydimethylsiloxane
PEG	Poly(ethylene glycol)
PEGMAL	PEG-Maleimide
PEGSH	PEG-Dithiol
PEP	Phosphoenolpyruvate
PI3K	Phosphoinositide-3 Kinase
PTS	Phosphotransferase System
QPS	Qualified Presumption of Safety
RCA	Rolling-Circle Amplification
RGD	The arginine-glycine-aspartic acid tri-peptide sequence
RNA	Ribonucleic Acid
RT	Room Temperature
S/Ie	Sulfamethoxazole
SCF	Stem Cell Factor
SpA	*Staphylococcus aureus* protein A
TALENs	Transcription Activator-Like Effector Nucleases
Tet	Tetracycline
TGF-β	Transforming Growth Factor β
TMB	3,3’,5,5’-tetramethylbenzidine
TPO	Thrombopoietin
UC	Umbilical Cord
UCB	Umbilical Cord Blood
UPT	Uridine-5’-Triphosphate
Usp45	Unknown Secreted Protein 45
UV	Ultraviolet
VCAM1	Vascular Cell Adhesion Protein 1
VLA	Very Late Antigen
VPM	The crosslinking peptide GCRDVPMSMRGGDRCG
ZFNs	Zinc Finger Nucleases

List of tables

List of equations

List of figures

Acknowledgements

This thesis is the result of 4 years of work, inside and out of the lab. It has survived long evenings spent on the lab bench or in front of a computer screen, countless of paper reading and a pandemic. In the aftermath, this work reflects not only the raw data and results presented in the pages that follow, but a collective effort displayed by both individual work, and the endless support and encouragement provided by a few very special people, who I will always be grateful to.

First, I would like to express my immense gratitude to my supervisors, Professors Manuel Salmeron-Sanchez and Matt Dalby for always providing me with valuable guidance and advice. Thank you for your patience and support, I will always be thankful and feel incredibly lucky to have had you as my mentors throughout this journey.

Next, I would like to convey my deepest appreciation and thankfulness to my supervisor, colleague and now dear friend Aleixandre Rodrigo-Navarro. From the very beginning you so openly shared your expertise with me, guiding me through each step of the way, but have also always been there to support me with the frustrations, setbacks and challenges I found along the way. I am truly grateful your patience, help and support and I hope I have never let you down. Thank you for always been there, in good and bad times, and I will truly miss working with you.

I would also like to thank my supportive family, and especially my wonderful aunt, Evi. You know how much of a special place you hold in my heart; I would not have been the person I am today without your endless support before and during my PhD.

Finally, I would like to thank all of my colleagues in CeMi. You are a wonderful bunch, and I will always cherish the fun times we had together, in and out of the lab. Thank you Oana and Cris, for your great support and advice. And thank you Marianela, Ola and Lydia, for listening to my rants and being the most wonderful friends, anyone could wish for. It has been such a great experience, minus some small lab failures. I even enjoyed the writing!

Chapter 1. Introduction

1.1. Summary of the thesis

The objective of this work is to engineer active microenvironments for the expansion of stem cells for cellular therapeutics. Inspired by the bone marrow (BM) niche, we have genetically modified the non-pathogenic bacterial species *L. lactis* to produce the key BM cytokines CXCL12, thrombopoietin and VCAM1, that have been associated with the maintenance and self-renewal of the two clinically significant BM-residing stem cell types; Hematopoietic and Mesenchymal Stem Cells (HSCs and MSCs). Our proposed system is based on the living interface between *L. lactis* biofilms that produce the above recombinant proteins and HSCs or MSCs in order to reproduce a BM mimicking niche *ex vivo*. Co-cultures between the engineered biofilms and HSCs have displayed that the recombinant proteins produced by the bacteria encourage the maintenance of the HSCs in an undifferentiated state, while also inducing their expansion in a similar way as traditional methods featuring the use of cytokine cocktails. The same trend has been observed in 3D, where the HSCs are encapsulated in PEG hydrogels in the co-cultures with the bacteria. Similarly, we report that our culture system has the potential to maintain MSCs in a naïve, undifferentiated state for up to 2 weeks in culture. In total, we provide proof-of-concept data that *L. lactis* can be used as an active biomaterial to direct stem cell fate. We envision that our system can be used in the future to produce clinically significant stem cell numbers for cellular therapeutics.

1.2. Tissue engineering and regenerative medicine / smart biomaterials

Tissue engineering is widely described as an interdisciplinary subfield of regenerative medicine, that combines the basic principles of biology and engineering in order to provide a functional substitute for organs with impaired function in a variety of clinical settings[1]. Its potential to heal or replace tissues and organs damaged by age, disease, or trauma, as well as to restore congenital defects has placed tissue engineering in the spotlight of current research on regenerative medicine[2]. Commonly used approaches are based on the engineering of microenvironments that provide the biochemical and mechanical stimuli to direct cultured stem cells into pre-designed applications of interest, such as specific cell differentiation to mature tissue or stem cell maintenance and expansion for transplant

development[3]. Such strategies involve the isolation of the cells of interest from a donor, the engineering of the appropriate *ex-vivo* culture microenvironment, the engineering of the new tissue and its transplantation into the recipient (Figure 1.1). Of key importance in the successful development of the transplants are the culture conditions and the materials used to direct the development of the target tissue. The development of such optimal conditions has given rise to the manufacturing of novel biomaterials, that directly impact cell proliferation and tissue development. Key characteristics of most biomaterials are their biocompatibility and cell toxicity profile, their mechanical and physical properties, that can be tailored to mimic the tissue of interest, their size, shape, surface texture and porosity, as well as their bioactivity[4].

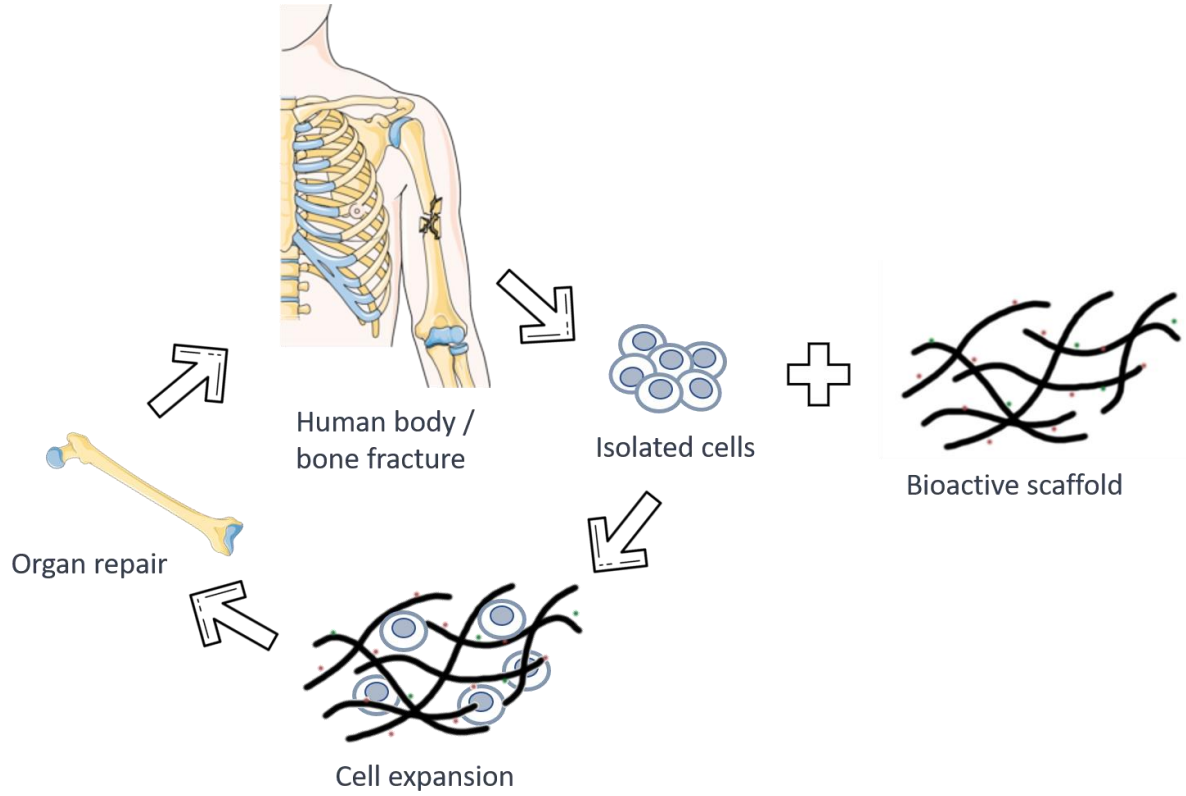

Figure 1.1 Tissue engineering. Cells are isolated from a donor in order to repair a damaged tissue. A bioactive scaffold is engineered to resemble the properties of the target tissue. The cells are incubated, expanded, or differentiated in the scaffold before their final transplantation to the recipient.

Despite the endless clinical possibilities of novel biomaterials, their biocompatibility, safety and efficacy still remains a challenge[5]. However, rigorous scientific research is making huge progress in developing biocompatible polymers with optimal chemical and physical

properties that provide close analogues of the human organs or tissues of interest. 3D bioprinting and the development of decellularized scaffolds are aiming to address the challenges associated with the complex organization of different cell types within each organ[6], while a variety of different natural and synthetic polymers are being explored to ensure biocompatibility and reduced immunogenic reactions[7].

1.3. Stem cells in Tissue Engineering

After the selection and optimisation of an appropriate material scaffold with the desired mechanical and chemical properties, every tissue engineering approach requires a source of cells. Stem cells have been widely used in regenerative medicine due to their high self-renewal and differentiation capacity, that makes them excellent candidates as therapeutic methods for a variety of clinical conditions. Some of the most popular tissue sources in regenerative medicine include induced pluripotent stem cells (iPSCs), MSCs and HSCs. iPSCs are artificial stem cells produced from somatic cells through co-expression of defined pluripotency-associated factors, that can typically proliferate and self-renew indefinitely *in vitro* and further differentiate into derivatives of all three primary germ layers. Because of their unique features, iPSCs have been associated with numerous biomedical applications in basic research, drug screening, toxicological studies, disease modelling, and cellular therapeutics. In regenerative medicine, iPSCs have been reported to successfully differentiate into different kinds of tissue, including cardiovascular and hematopoietic lineages, sperm, and retinal cells[9]. Nevertheless, despite of their promising regenerative potential, iPSCs have been associated with a variety of clinical challenges, including tumorigenicity due to incorrect patterning, genomic instability or genetic abnormalities, as well as the observed immunogenicity they have often exhibited in clinical settings. Therefore, we have decided to exclude iPSCs from the studies conducted as part of this work[10].

MSCs have also been used in tissue engineering research due to their wide availability and well-established culture, expansion and differentiation methods as well as their immunomodulatory properties[9]. MSCs can be isolated from a variety of tissues (figure 1.2), with bone marrow-derived MSCs (BM-MSCs) being the most widely used in cell therapies[10]. Currently, MSCs are mainly used as a tool to treat joints degeneration, bone and cartilage

reconstruction, and are widely used in plastic surgeries, aesthetic medicine, cardiovascular diseases, endocrine and nervous system conditions, and in the repair of damaged musculoskeletal tissues[11]. However, despite their numerous advantages, the high numbers of MSCs needed for cell therapeutics often pose a significant limitation in clinical settings. Most studies aiming to develop clinical grafts have focused on the differentiation of MSCs towards the target tissue, in order to provide end-stage lineage cells to reduce healing times and increase clinical efficiency[12]. Nevertheless, this differentiation process has been directly linked with proteome modifications resulting in the loss of expression of genes involved in the maintenance of stemness and the subsequent decrease in the expansion potential of the cells, resulting in overall low cell numbers[13]. In particular, the cell numbers reported to have been achieved in previous studies range in the millions and are much lower compared to the gold standard required for applications in cellular therapeutics (eg. 10^8 nucleated cells is needed per bone marrow transplant).

This can be a significant drawback considering the high MSC numbers needed for clinical trials, posing an urgent need for the creation of novel MSC expansion methods that result in clinically relevant cell numbers, that maintain their stem-like phenotype and characteristics. Such platforms could also provide a solution to the often observed heterogeneity of MSCs used in grafts that could reduce the efficiency of their therapeutic applications[14].

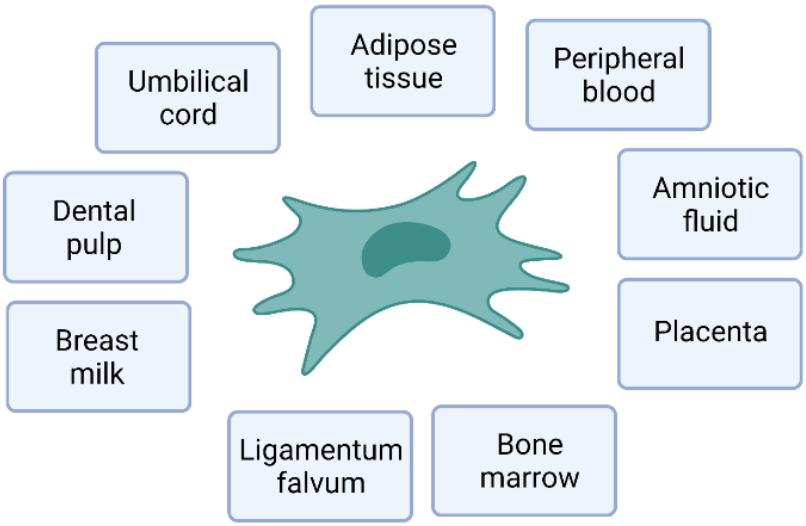

Figure 1.2. Common mesenchymal stem cell (MSC) sources. Primary MSCs reside and can be isolated from a variety of sources. For clinical applications, MSCs are most commonly isolated from the bone marrow or the umbilical cord.

One of the most common applications of MSCs in regenerative medicine has been its use as a therapeutic tool to repair bone and cartilage defects. The limited supply of autologous bone and cartilage, increased operation time and blood loss and increased donor site morbidity associated with autologous bone grafts[15], combined with the high risk of rejection or infection caused by allografts[16] have increased the popularity of MSCs as a therapeutic approach. A variety of stem cell-based approaches have been employed to encourage bone and chondral defect repair. Intravascular injections, including intravenous and intra-arterial injections have been used to administer doses of MSCs that circulate around the body and migrate to the damaged site, enhancing tissue repair[17]. Nonetheless, the initial large numbers of MSCs required for successful healing, combined with increased risk of "first pass effect," where MSCs could be trapped in small vessels drastically reducing the effectiveness of the method[18]. As an alternative, recent tissue engineering strategies have aimed to combine biomaterials, MSCs and growth factors in order to improve bone repair. Electrospun[19,20], 3D printed[21,22], polymeric[23] or decellularized matrix scaffolds[24] have been explored as potential mechanisms to encourage MSC differentiation into bone or cartilage tissue with the aim to provide successful therapies. Despite the promising potential of a variety of approaches, the issue of the production of the large quantities of MSCs required for cell therapeutics remains an obstacle to optimal bone and cartilage defect treatment.

Hematopoietic stem cells (HSCs) have also gained scientific interest due to their significant clinical potential in tissue regeneration and, in particular, in restoring hematopoietic disorders. This significant advantage has placed HSCs in the spotlight of experimental and clinical haematology, making them the most commonly used stem cell type in cellular therapeutics. However, the lack of donors, combined with the increasing need for HSC transplants has created an urgent need for the identification of alternative sources of HSCs or the development of novel ways for their expansion. Furthermore, in contrast with MSCs, HSCs cannot be as easily isolated in the required high numbers, have a high mortality rate *ex-vivo*, and there is a lack of standardised methods for their efficient and reliable expansion in *in vitro* culture[25]. Despite the growing understanding of the mechanisms of stem cell expansion and manipulation by the scientific community, crucial questions regarding the specific mechanisms of stem cell survival, expansion and fate manipulation *in vitro* remain unanswered. This problem constitutes the current limitations associated with stem cell

therapies, that can give rise to medical complications such as implant failure, undesired immune responses, lack of efficacy or even neoplasm formations[26].

To address this issue, efforts to expand HSCs *ex-vivo* have been focused on the development of dynamic biomaterials inspired by the specific natural microenvironments of the stem cells. In studies in 2D, a variety of substrates of varying topography[27], elasticity[28], and ligand presentation[29,30] were explored for their potential to maintain and expand HSCs. Apart from mimicking the mechanical characteristics of the target tissue, other novel approaches are designed to also provide soluble chemical stimuli to the cultured cells[31,32]. Further efforts have been focused on co-cultures between HSCs and other BM niche cells, including stromal cells[33,34], osteoblasts[35], vascular and endothelial cells[36,37] and MSCs[38,39]. More recently, efforts have focused on the dimensionality of engineered microenvironments, incorporating 3D scaffolds or hydrogels of controlled geometry and physical as well as biochemical properties[40,41]. To provide a more accurate representation of the BM microenvironment, a variety of the above-mentioned culture models have been combined, with the resulting cultures featuring cells residing in the niche acting as a feeder layer, and 3D hydrogels providing both biochemical and mechanical support to the HSCs[42,43]. Finally, bioreactors[44,45] and organ-on-a-chip approaches[46] have also been explored for their potential to stimulate HSC expansion and proliferation for clinical applications. The end goal of all such studies has been to create a culture method or bioreactor with precisely controlled characteristics that can be tailored to mimic the natural niches of stem cells, providing users with the opportunity to study and understand the spatiotemporal effects of the microenvironment to the cultured cells and ultimately create the optimal conditions for transplant development in clinical settings[47,48].

1.4. The bone marrow microenvironment

HSCs have been the first stem cell type to be successfully used in clinical applications, and the only stem cell type routinely used to cure a variety of haematological disorders[49]. Their regenerative potential lies on their ability to differentiate and give rise to mature effector blood cell types[50]. Due to their regulation of hematopoiesis, outlined in figure 1.3, HSCs have the potential reconstitute the whole hematopoietic system in the case of haematological disorders[51]. Their central role and huge potential in regenerative medicine has created the need for a robust understanding of HSC biology, with a view to discovering ways for their expansion and regeneration *ex-vivo*. Therefore, major scientific focus has been placed in studying their natural niche, the BM. Despite vigorous research in understanding the variety of signals that support HSC stemness and self-renewal in the BM, our understanding still remains insufficient and our task to successfully expand HSCs in order to create life-saving transplants is still incomplete[52]. This is largely due to the complexity of the BM microenvironment, that displays various oxygen and pH gradients as well as stiffness and porosity and consists of a large number of different cell types, all producing a wide array of cytokines at different levels[53]. Efforts to understand the niche and the most important factors that affect HSC survival and regeneration have broken down the niche into discrete components, including the cellular, chemical and mechanical parts of the microenvironment.

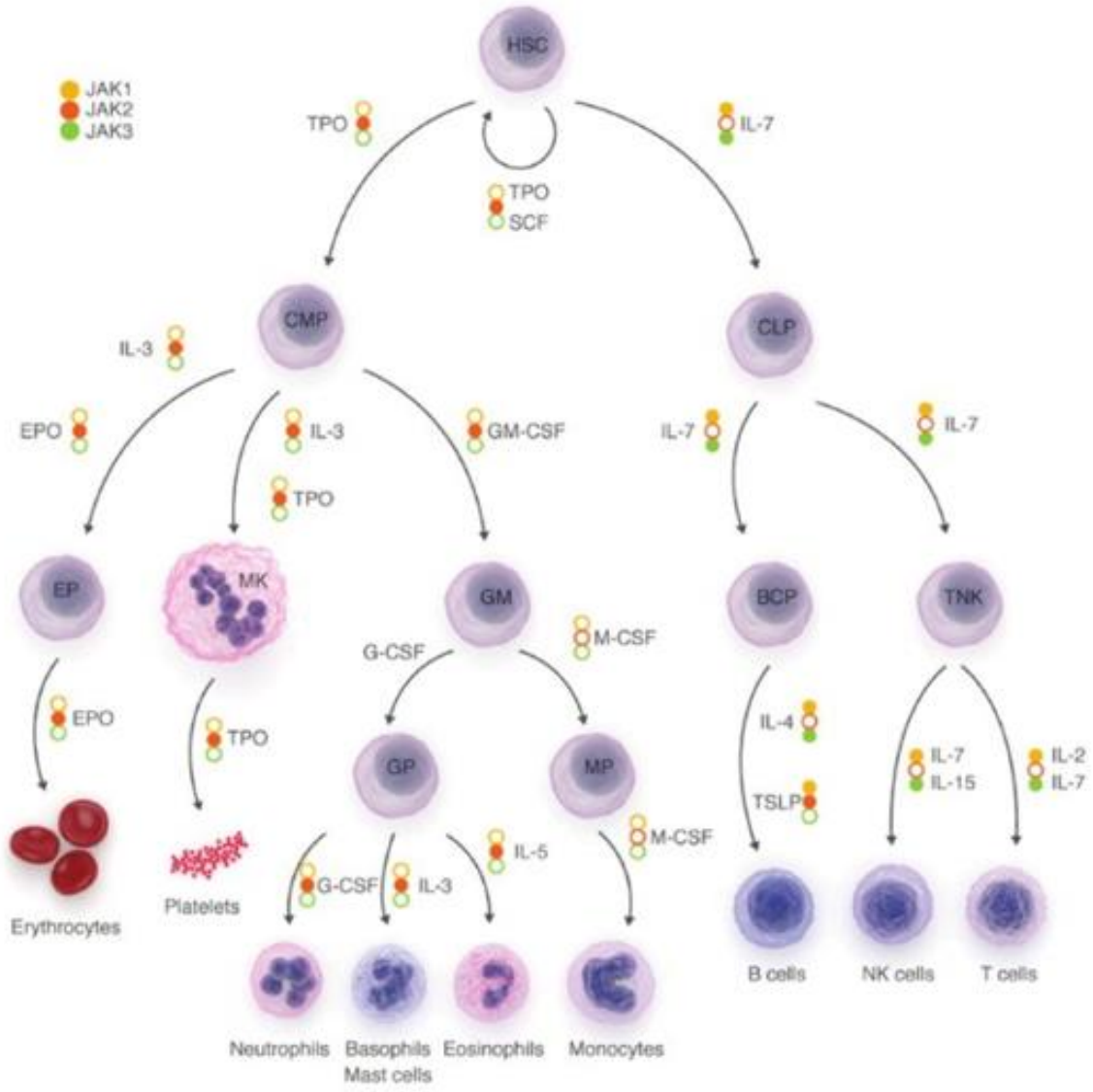

Figure 1.3. The process of hematopoiesis. Multipotent HSCs can differentiate into common lymphoid (CLP) or myeloid (CLM) progenitors that in turn can differentiate and give rise to mature blood cells. A variety of soluble signals and their receptor-associated Janus kinase (JAK) have been identified as the driving forces of these differentiation events, with the most important ones being shown next to the respective arrows. HSC: hematopoietic stem cell; CMP: common myeloid progenitor; CLP: common lymphoid progenitor; GM: granulocyte macrophage progenitor; BCP: B cell progenitor; TNK: T and natural killer cell progenitor; EP: erythroid progenitor; Mk: megakaryocyte; GP: granulocyte progenitor; MP: macrophage progenitor; TPO: thrombopoietin; SCF: stem cell factor; IL: interleukin; GM-CSF: granulocyte/monocyte colony-stimulating factor; G-CSF: granulocyte colony-stimulating factor; M-CSF: monocyte colony-stimulating factor; TSLP: thymic stromal-derived lymphopoietin. Adapted from L. Springuel et al. (2015).[54].

The HSC niche consists of a variety of cells, such as osteoblasts, mesenchymal stem cells (MSCs), adipocytes and stromal cells, that secrete a variety of chemical signals that influence HSC fate[55]. Furthermore, HSCs are regulated through hormonal and sympathetic nervous system signals as well as chemokines and adhesion proteins secreted by the other cells present in the BM. The physical characteristics of the BM play a critical role in HSC regulation. The stiffness of the niche, combined with the ligands present, have been shown as important determinants of the lineage specification of HSCs[56].

1.4.1. Cellular components

The bone marrow microenvironment features a variety of different cell types, each of which contributes to the overall homeostasis of the niche. Furthermore, the signals produced by these cell populations are critical for HSC maintenance and expansion depending on the needs of the organism. A schematic representation of the bone marrow niche and its most important cellular and chemical components for HSC homeostasis is depicted in figure 1.4.

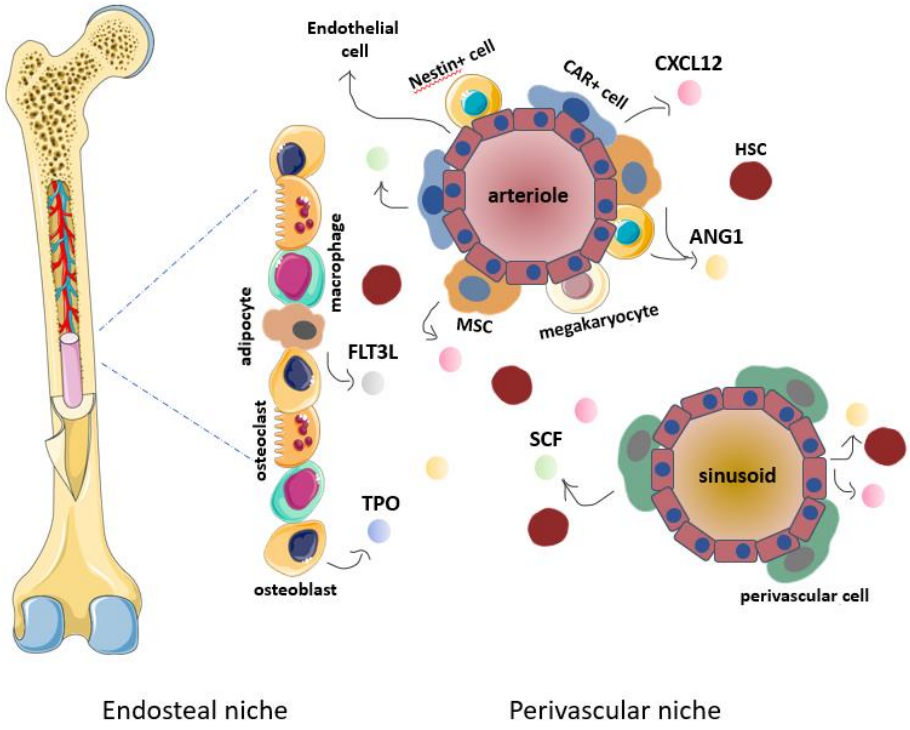

Figure 1.4. The bone marrow microenvironment. Within the BM, HSCs reside in two distinct niches, the endosteal (left) and the perivascular niche (right). In both microenvironments they communicate with different cell populations that contribute to their maintenance and proliferation by the secretion of different signals.

Studies of the localisation of HSCs in the bone marrow have placed the cells in two distinct niches, the endosteal and the perivascular. In both cases, the cells appear to be in close proximity to osteogenic lineage cells, while HSCs with the highest hematopoietic potential appear to adhere to the endosteal matrix[57]. Apart from providing attachment and homing for HSCs through annexin-2 expression[58], osteoblastic cells tightly regulate haematopoiesis through Notch signalling[59]. Thrombopoietin (TPO) secretion by osteoblasts, also regulates homing and HSC quiescence[60].

MSCs that can differentiate into both osteogenic lineage cells, as well as adipocytes and chondrocytes, are another major component of the BM niche. Perivascular CXCL12-expressing mesenchymal progenitors are especially important in HSC maintenance as they induce cell maintenance and are associated with increased repopulation activity[61]. Additionally, MSCs have been reported to produce angiopoietin-1 (ANG1) and stem cell factor (SCF), key cytokines for HSC expansion and self-renewal.

Endothelial cells present in the BM, also serve as a source of secreted ANG1, CXCL12 and SCF[62]. Furthermore, through deletion of E-selectin, endothelial cells can induce HSC quiescence and therefore regulate HSC proliferation[63]. Stromal cells are another component present in the perivascular HSC niche that also secrete maintenance factors and contribute in HSC expansion and proliferation[64]. Furthermore, stromal N-cadherin and SCF expression has been shown as a key regulator of HSC fate[65]. Stromal cell lines have also been used in *ex-vivo* cultures to support HSC maintenance and self-renewal[66]. Neuronal and glial cells have also been implicated in HSC fate decisions, inducing their mobilisation through CXCL12 production and quiescence through transforming growth factor β (TGF-β) signaling[67].

Except for the direct impact of some BM cell types on HSC regulation through the secretion of soluble and adhesion proteins, research has also identified indirect signals that have an impact on HSCs[68]. Osteoblasts are one of the key regulators of the endosteal BM niche and a great example of an indirect regulator of HSC fate. Attachment of HSCs to nestin+ osteoblasts has been suggested to contribute to their maintenance, in a way that has not been directly linked to otherwise influencing HSC function[69]. Osteoclasts have also been linked to HSC maintenance through the regulation of calcium levels in the BM. The release of hydroxyapatite-bound calcium from osteoclasts has been reported to retain HSCs in the endosteal niche, promoting homing and quiescence[70]. Furthermore, the degradation of the

bone matrix by osteoclasts causes a release of soluble factors such as bone morphogenetic proteins and transforming growth factor-β that have been linked to different HSC fate decisions[71,72].

1.4.2. Chemical stimuli

The effect of the cellular components of the BM on HSCs is mediated through chemical signals in the forms of adhesion molecules or soluble cytokines. The CXCL12/CXCR4-mediated signalling pathway has been reported to regulate HSC homing, engraftment and survival in the BM. By binding to its receptor CXCR4, CXCL12 activates the very late antigen 4 and 5 (VLA-4, VLA-5), and $\alpha_L\beta_2$integrins in CD34+ cells and directs their interaction with their receptors vascular cell adhesion protein 1 (VCAM-1) and Intercellular Adhesion Molecule 1 (ICAM-1), contributing in the maintenance of the stem cells in their niche[73]. Furthermore, the interplay between CXCL12 and transforming growth factor-b (TGF-β) has been suggested to regulate the balance between HSC quiescence and cell cycle progression. Activation of the phosphoinositide-3 kinase (PI3K)/Akt/mTOR signalling cascade and Forkhead box O-3 (FOXO3) activated phosphorylation by CXCL12 appears to promote cell cycle entry in HSCs, promoting their proliferation. In contrast, activation of TGF-β has shown an inhibitory effect on CXCL12 promoting HSC quiescence[74]. SCF expression by stroma cells, endothelial cells, and adipocytes plays an essential role in the survival, migration, and differentiation of hematopoietic stem progenitor cells (HSPCs) and directly regulate haematopoiesis[75,76]. BM adipocyte secreted SCF in particular, promotes the regeneration of hematopoietic stem cells in studies after irradiation[77], while SCF-producing arteriolar endothelial cells has been found to promote HSC recovery after myeloablation[78].

A number of different BM cells have been associated with TPO production, a primary cytokine-regulator of HSC fate. MSCs, osteoblasts and BM stromal cells have been reported to produce TPO[79]. However, deletion of TPO from hematopoietic cells, osteoblasts, or bone marrow mesenchymal stromal cells has been suggested to not directly affect HSC number or function. A recent study has suggested that hepatocytes are a major source of TPO and even though they are not physically present in the BM, they have a direct effect on HSC maintenance[80].

Apart from secreted signalling factors, oxygen has been suggested to play an important role on the regulation of HSCs. The BM microenvironment has been described as a hypoxic niche[81], with oxygen availability directing HSC localisation and metabolic activity[82,83]. HSCs have been reported to prefer low to rich oxygen conditions[84]. A mathematical model describing the oxygen pressure distribution within the BM microenvironment has suggested that HSCs should reside in a hypoxic niche while a recent study has reported that the HSC niche with the highest regenerative and self-renewal capacity is located in the trabecular bone area[85]. Hypoxic culture conditions have been reported to induce a 27-fold expansion of CD34+/CD38- HSCs compared to normoxic conditions. Umbilical cord blood (UCB)-derived HSCs seemed to raise their numbers resulting in a four-fold increased expansion in 5% compared to 21% O_2[86]. This low oxygen environment has been shown to induce HIF-1a and vascular endothelial growth factor (VEGF) as well as CXCR4 expression, factors that are important in HSC maintenance and regeneration[87]. The enhanced expansion of HSC in hypoxic conditions has also been supported by studies on the metabolic profile of HSCs. Long-term hematopoietic stem cells (LT-HSC) have been shown to produce low levels of ATP and to use cytoplasmic glycolysis instead of mitochondrial oxidative phosphorylation for their metabolic requirements, which implies their residence in a hypoxic environment[88].

1.4.3. Mechanical stimuli

The BM is a biophysically diverse microenvironment with a stiffness ranging from soft marrow and adipose tissue (<1 kPa), to surrounding cell membranes (1–3 kPa), to developing osteoid (>30 kPa)[89]. The mechanical properties of the matrix significantly impact stem cell behaviour[90], and in the BM niche have a regulatory effect on haematopoiesis[91]. Inspired by the BM, a variety of studies have examined the impact of biomechanical forces and substrate stiffness on HSC fate. The 3D architecture of engineered matrices for HSC maintenance (hydrogels/scaffolds) have demonstrated a relationship between dimensionality and cell viability as well as cytoskeletal organization. HSC viability seems to be reduced in stiffer environments, and they acquire a more spread phenotype. High ligand density also seems to have an impact on HSCs, resulting in more rounded cells with decreased collagen ligand density in hydrogels[92]. Cell adhesion has also been linked to matrix stiffness, with stiffer matrices enabling better HSPC attachment[93]. The physical and

mechanical properties of extracellular matrix (ECM) proteins have also been shown to impact HSC fate. The physical properties of the protein tropoelastin were required to increase the percentage of HSCs in culture, an effect that is thought to take place because of elastin binding protein/elastin-laminin receptor-mediated mechanotransduction[94].

1.5. Cell adhesion and mobility

Like every living system, stem cells continuously interact with their microenvironment and the (bio)chemical and mechanical stimuli it provides. Cells sense and respond to these forces, through the processes of mechanosensing and mechanoresponding. These processes, defined as the ability of cells to perceive the mechanical properties of the ECM and responding to it, result in changes in cellular behaviour, including motility, morphological changes, proliferation, differentiation and polarity formation, as well as tissue remodelling[95,96]. The main way of interaction between the cells and their surroundings, including the ECM and other cell types residing in it, is mediated through cell adhesion molecules (CAMs). There are a variety of different CAMs include integrins[97], cadherins[98], selectins[99], members of the immunoglobulin superfamily (IgSF) including nectins[100], and others such as mucins[101], all playing different roles in cell-ECM or cell-cell adhesion interactions.

Integrins are large heterodimers consisting of transmembrane α- and β-units that cluster to form the complete receptor in the plasma membrane. In humans there are 18 integrin α subunits and 8 β subunits that can combine to form 24 αβ combinations, each having distinct functions in regulating cell-ECM interactions[102]. Integrins bind to a wide variety of ligands in the ECM via specific motifs located on niche molecules (e.g. the arginine-glycine-aspartic acid tri-peptide (RGD) sequence found in fibronectin, vitronectin, and laminin[103]) and, together with other proteins such as talins, vinculins and paxillins are the key regulators of focal adhesion (FA) formation, mediating cell adhesion and migration[104] (figure 1.5).

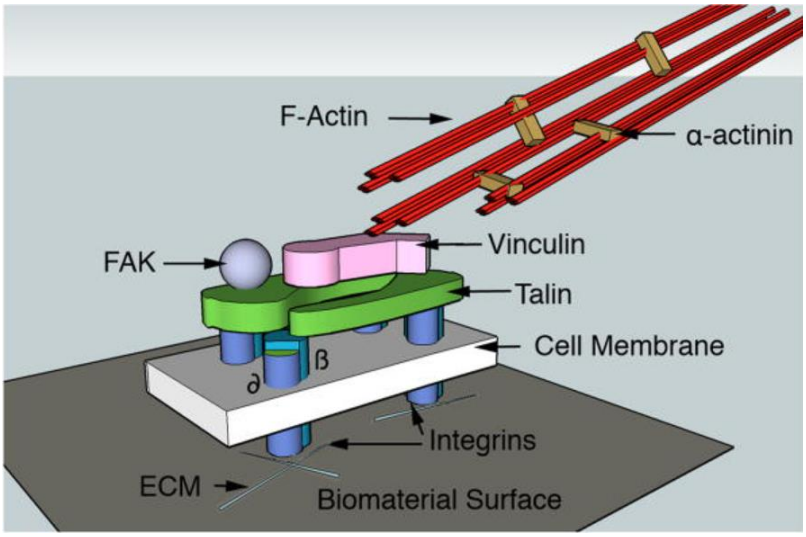

Figure 1.5. Schematic representation of some of the most important molecular interactions occurring at the focal adhesion development stage. Focal adhesions are macromolecular structures provide points of adhesion between the cell cytoskeleton, via F-actin, and the extracellular matrix (ECM). Furthermore, they provide biochemical signalling, through the regulated interactions of focal adhesion associated signalling molecules, regulating mechanotransduction-dependent changes in cellular function and behaviour[105].

The initial stages of FA development involve the formation of focal attachments; cellular protrusions, such as filopodia and lamellipodia. These are relatively weak, transient clusters, with length less than 1 μm, serve as the initial attachment point of the cell to the substrate and as a start for cell migration[106]. As the leading edge of the cell advances, the weak focal attachments are replaced by focal complexes (1-5 μm in length) that can further mature to form FAs (>5 μm in length)[107], after the recruitment of additional proteins such as a-actin and the Rho and focal adhesion kinases[108]. Further maturation of the FAs can result in the formation of fibrillary adhesions, which are larger macromolecular structures consisting of integrin-rich focal complexes[109].

The importance of the formation of FAs and the central role of cell attachment and interaction with the ECM has been highlighted in a variety of studies. Their tight involvement in normal physiological events such as cellular adhesion, movement, cytoskeletal structure and intracellular signaling pathway regulation imply increased adverse effects in the event of FA deregulation. More precisely, it has been established that failure to establish normal FAs can be directly linked to cellular apoptosis[110], while disruptions in FA turnover are also associated with tumor development and cancer metastasis[111,112].

Cell migration is a highly organized and regulated process orchestrated by a variety of intra- and extracellular factors, that demonstrates cellular responses to the rapidly changing ECM. Integrins play a key role in the transmission of forces between the cytoskeleton and the ECM directly regulates the tension redistribution inside the cell, resulting in conformational changes and subsequent cytoskeletal reorganization. This results in complex cell movements driven by actin movement, in a process known as retrograde flow[113]. The increase in traction stress around the FA sites and its implications in cell movement and migration has been described as the molecular clutch[114]. The molecular clutch is driven by FAs and is initially activated by the interaction between the ECM-bound integrins and the cytoskeleton of the immobilized cell. As forces from the cytoskeleton are propagated towards the substrate, actin polymerization at the FA site drives the formation of forward membrane protrusions, that in turn form FAs and pull the cell forwards. In the absence of migration signals, the clutch would disengage, resulting in faster retrograde flow and the cessation of the development of membrane protrusions[115].

Since mechanosensing has been identified as one of the key innate cellular behaviour, the study and the establishment of FA dynamics has been widely studied for its involvement in directing cell fate. ECM stiffness[116], elasticity and viscosity[117], as well as substrate architecture and topography have been identified as crucial regulators of cellular mechanosensitivity, with direct implications in the regulation of cell functions. A variety of different platforms have been developed to better understand the influence of ECM elasticity on cell function. Synthetic polymers such as polydimethylsiloxane (PDMS)[118], hydrogels made from polyacrylamide (PAA)[119] or poly (ethylene glycol) (PEG)[120] and even natural substrates, such as decellularized ECM[121] have been manufactured with varying mechanical properties with the aim of mimicking the natural cell niche and subsequently manipulating cell activities.

Cell adhesion and spreading was among the first aspects of cell behaviour linked to substrate mechanical properties. Cell spreading has been reported to increase as a function of stiffness and stress relaxation properties of the matrix[122]. In contrast, soft substrates have been linked to smaller, more round cell morphologies. Furthermore, FA disassembly rate has been reported to be higher on soft ECMs with stiffness ranging from 1 to 5 kPa, and lower on stiffer substrates (5-50 kPa), suggesting that cells form more stable attachments to

stiffer ECMs[123]. This observation has been supported by the increased activation and clustering of integrins observed in cells cultured on stiffer matrices, where higher expression of mechanosensory and mechanotransductor proteins, including integrins and the downstream FA complex proteins has been recorded[124]. At a molecular level, the reduction in FA turnover on soft matrices has been linked to decreased levels of integrin β_1[125], while integrin α2 upregulation has been observed on stiffer matrices[126]. Furthermore, the expression of integrin subunits α_1, α_2, α_5, α_v, β_1, and β_3 have been reported to change in a stiffness- and cell type-dependent manner[127]. Other integrins, such as integrin $\alpha_5\beta_1$, have been specifically linked to precisely controlling cell migration on substrates of varying stiffness[128]. During migration, the FAs are recycled intracellularly and transported to the leading end of the cell, allowing for the creation of new attachments that push the cell forward. This FA turnover is highly regulated by integrin clustering at the initial steps of adhesion, resulting in stable FA formation that are then disassembled due to microtubule extension and subsequent integrin internalization from the cell surface[129].

In addition to their roles in cell adhesion and migration, integrins play an important role in transducing biochemical signals into the cell, inducing a variety of cell responses that include cell quiescence, proliferation or differentiation[130]. The changes in surface receptor composition, integrin subunit expression, and nuclear shape of MSCs mediated by integrins in response to matrix stiffness has been associated with specific responses, such as immuno-modulatory and angiogenic properties, as well as TGF-β1-induced differentiation[131]. Higher substrate stiffness has also been linked to MSC commitment towards the osteogenic lineage[132], while medium and lower stiffness ECMs have been suggested to induce MSC differentiation towards myoblasts[133] and neurons respectively[134]. The variety of cell responses to different properties of their ECM has therefore opened new avenues for biomaterials design, the properties of which could be tailored specifically to direct cell behaviour for targeted biomedical applications.

1.6. Dynamic surfaces and living interfaces

As indicated by the complex, dynamic nature of living organisms and the various cellular microenvironments within them, cells are responsive to a variety of physical and chemical stimuli, necessary for their survival and proliferation. The study of the different cell niches and their characteristics suggest that cell fate and behaviour is not only affected by signalling molecules but also by oxygen gradients[135], pH[136,137], as well as the physical characteristics of the environment they reside in, such as its architecture[138], topography[139], stiffness[140,141] and porosity[142]. Inspired by the high complexity of these interactions, novel biomaterials have increasingly shifted towards complex, dynamic culture methods that have the potential to more closely mimic cellular natural niches[143]. Traditional static culture methods that require external stimulation or addition of growth factor cocktails has been replaced with dynamic surfaces, 3D culture microenvironments or bioreactors that have the ability to provide cultured cells with a variety of stimuli provided by the systems or the materials themselves, without the need for external manipulation[144,145,146]. The high association between cellular biological responses and cues derived by the extracellular matrix (ECM) has been widely studied. Cell migration[147], attachment[148,149] and differentiation[150] are some of the major processes affected by the composition and mechanical properties of the ECM. Although the basic components of the ECM (including water, proteins, growth factors and polysaccharides) are well understood[151], the differences in topography and composition between the different tissues and the complexity of the biochemical interactions between the cell types it encloses has challenged efforts to recreate its dynamic nature in culture. Furthermore, the constant enzymatic[152,153] and non-enzymatic[154,155] remodelling that characterises the ECM, combined with the post-translational modifications of its components[156] has increased the need for the development of dynamic culture systems in order to mimic biological processes and achieve the cellular responses of interest.

To mimic the dynamic nature of the ECM, different bioactive 2D and 3D cell culture platforms have been developed. Photodegradable hydrogels with controlled chemical properties[157], bio-responsive polymers designed to release proteins of interest in response to changes in enzymatic levels[158] as well as mechanoresponsive[159] and electroactive substrates[160] have attempted to mimic natural characteristics of the ECM to achieve the

target cellular responses. Light-responsive materials have also been an increasingly used approach in efforts to mimic ECM-cell interactions[161]. The most common mechanism of light-induced signalling in these cases involves the removal of a caging group that reveals an RGD (arginine-glycine-aspartic acid) domain, which mediates integrin-regulated cell adhesion and downstream signalling[162,163]. Dynamic materials have also been developed based on chemical click reactions that can provide additional functionalities as well as the desired mechanical properties that mimic the ECM for biomedical applications[164,165]. Finally, temperature[166] and pH[167]-regulated materials have been reported in the literature as potential cell culture substrates that could dynamically regulate cell responses. Combined, these smart biomaterials have been reported to actively control cultured cell fate and achieve a variety of programmed responses such as expansion and self-renewal[168] or differentiation towards a lineage or cell type of interest[169,170] .

Living interfaces is an emerging field of living materials, characterised by the effort of more closely mimicking dynamic cellular niches by incorporating the extra complexity of a living component as part of the engineered ECM. Most current approaches are focused on engineered living materials, that are mostly based on *Escherichia coli* (*E. coli*) biofilms[171]. While *E. coli* is not ideal for co-cultures with human cells for biomedical applications due to its high production of lipopolysaccharides and endotoxins[172] that are associated with the initiation of immune responses[173], different groups have attempted the engineering of biomaterials based on amyloids[174], curli fibres[175] or bacterial cellulose[176] secreted by biofilms of the bacteria. The amyloid-based materials have been inspired both by the wide availability of the fibres to both bacteria and humans[177] and by their structural and biological properties. More precisely, their ability to provide a substrate for cell adhesion[178], their capacity for surface modification and functionalisation[179], combined with their high tensile strength and resistance proteolysis[180] have made amyloid-based living materials popular for biomedical applications. The possibilities offered by *E. coli* curli fibres on biosensor development, nanoparticle biotemplating, substrate adhesion and covalent immobilization of proteins to create functional biomaterials, have also been explored in a variety of studies[181,182]. Finally, cellulose has been used as a basis for living materials because of its natural abundance, ability to form 3D networks with high porosity, increased mechanical strength and stability, high water-holding capability as well as good

biocompatibility[183]. These desirable material properties have resulted in the development of cellulose-based biomaterials for a variety of different applications ranging from scaffold development for cell cultures[184], to bone repair[185] and neural interface applications[186].

A class of living biointerfaces have recently been developed by our team[187,188] and others[189], as an effective tool to manipulate cell behaviour. While studies featuring bacteria and human cell co-cultures have been reported in the literature, they are largely uncommon, and they are focused on investigating host-pathogen interaction dynamics[190]. In the past few years, a small number of studies have investigated the possibility of using genetically engineered bacteria as a biomaterial that could direct the fate of different cell types. In this system, the bacteria were cultured as a biofilm that was then used as a substrate for C2C12 and MSC cultures. More precisely, the non-pathogenic gram positive bacterial species *Lactococcus lactis (L. lactis)* has been genetically engineered to present the FN III_{7-10} fragment on its cell wall and has been shown to drive the differentiation of cultured C2C12 myoblasts to myotubes[191]. A schematic representation of the bacterial expression of FN III_{7-10}, and the culture system is depicted in figure 1.6. The same bacteria have been further engineered to produce bone morphogenetic protein 2 (BMP-2) and have shown to support MSC attachment and trigger osteogenic differentiation[187,192]. The ability of bacteria to be used as a living biointerface to provide signals to cultured cells has been further explored by teams using genetically engineered endotoxin-free strains of *E. coli* to mediate light-regulated bacteria-cell interactions[193].

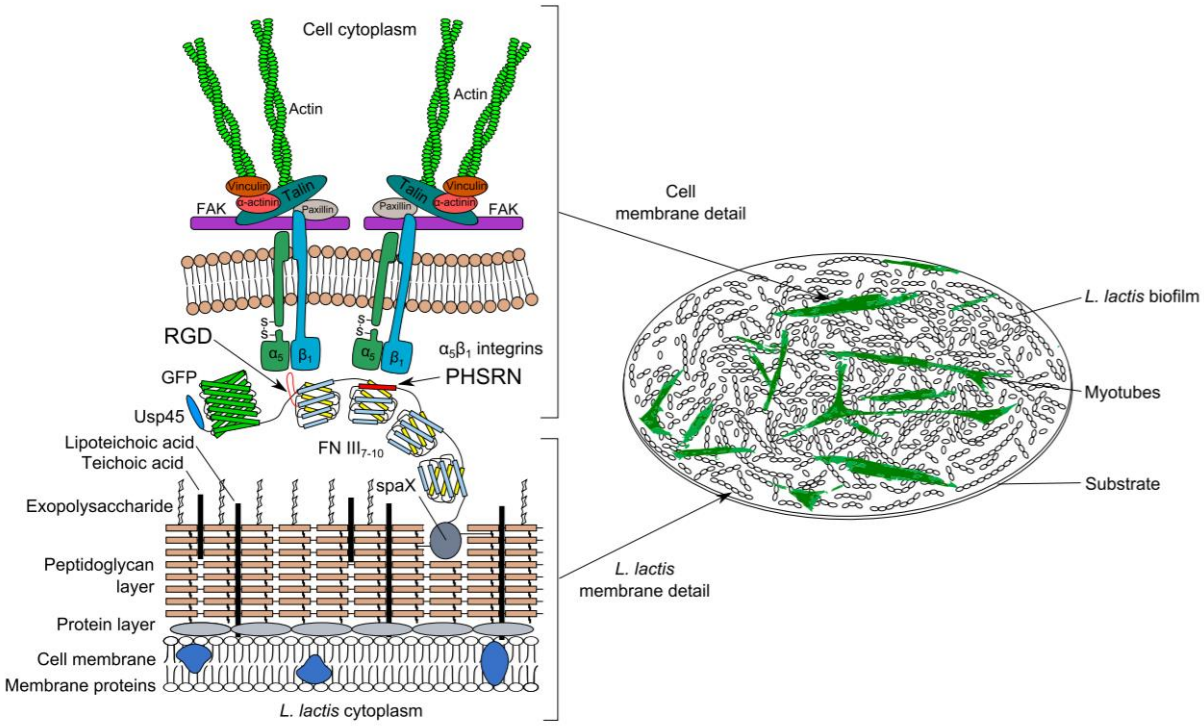

Figure 1.6. Conceptual sketch of the expressed III_{7-10} fragment in *L. lactis* (left) and the co-culture system (right). The membrane localisation of the FN fragment and its expecting interaction with the the $\alpha_5\beta_1$ integrin on the MSC outer membrane allows for MSC adhesion on the biofilm and interaction with the recombinant protein[194].

We are aiming to build on previous proof of concept research to develop a more ambitious system where *L. lactis*-based living biointerfaces can be used as a substrate for the development of *ex-vivo* bone-marrow mimicking microenvironments. We envision a system where different populations of genetically engineered *L. lactis* would produce different cytokines and adhesion peptides in order to manipulate HSC and MSC behaviour. The development of such a platform would provide us with the opportunity to study bacteria-stem cell interactions and possibly provide a microenvironment where stem cell fate can be externally mediated in an efficient, dynamic way.

1.7. Genetic engineering

Genetic manipulation has been a method used throughout history, from positive crop selection starting thousands of years ago, to modern gene editing for clinical applications. While little was known about the precise genetic effects plant selection and selective animal breeding, it has taken humans thousands of years to understand the mechanism behind the

advantageous traits they had been selecting for. In more recent years, genetic engineering started as a scientific method in the 1930s, when chemical methods or ionising radiation were used to induce genetic alterations in the form of mutations in the target organism. Despite the random nature of this process, these methods have established the foundations on which modern targeted gene manipulation is based on. From the discovery that a specific gene controls a biochemical reaction in 1941[195], to the first gene editing in human embryos in 2015[196], genetic engineering has developed advanced tools and precise methods of targeted gene alterations and holds promising potential as a cure or even prevention method for a variety of clinical applications. There are many examples of genetic manipulation, including the insertion of foreign genes into an organism, the alteration of a specific gene or part of it (mutagenesis), or the activation, silencing or altering of the expression level of a gene. They can be accomplished by a variety of different techniques, including gene editing by sequence specific nucleases, such as meganucleases[197], zinc finger nucleases (ZFNs)[198], transcription activator-like effector nucleases (TALENs)[199], and the clustered regularly interspaced palindromic repeats (CRISPR)/Cas9 nuclease system[200]. Other possible methods include RNA interference[201], antisense oligonucleotides[202] and ribozymes[203]. In this work, we have used the method known as Gibson assembly, a robust exonuclease-based method to assemble DNA seamlessly and in the correct order, that will be covered in more detail later.

Bacterial engineering and recombinant DNA technology has been established as an important tool in all areas of life. From medical applications in the development of vaccines and pharmaceuticals to biofuel production[204], natural product biosynthesis[205] and carbon fixation[206], bacterial engineering has gained popularity among both researchers, the industry and the clinic. *E. coli* in particular, has been used for years as a microbial factory for the recombinant protein production in clinical settings[207]. More precisely, the synthesis of human serum albumin[208] and insulin[209] by *E. coli* has been established as a safe and efficient source of recombinant proteins to treat clinical conditions such as advanced liver cirrhosis[210] and diabetes[211]. In recent years, the bacterial species *L. lactis* has also gained traction in research and the clinic due to its promising uses in biomedicine. Despite its common association with dairy product production, genetic engineered *L. lactis* has recently been used as a delivery vehicle expressing and delivering human recombinant interleukin 10 (IL-

10) in inflammatory bowel disease patients[212] and has also been explored as a vaccine delivery agent providing protection against other bacteria, such as *Helicobacter pylori*[213] and *Listeria monocytogenes*[214]. Furthermore, gram-positive species has been engineered to produce B vitamins, primarily folate (B11) and riboflavin (B2)[215], the anti-thrombotic agent subtilisin QK-2[216], as well as anti-cancer peptides[217]. The wide variety of applications of genetically engineered *L. lactis* has boosted the development of gene manipulation tools and techniques and has established the species as an economically and clinically valuable asset. In this work, we have chosen to work with genetically engineered *L. lactis*, for reasons that will be discussed later.

An overview of genetic engineering is schematically represented in figure 1.7. The process starts with the selection of an appropriate host. As discussed above, these can be bacteria or even plant[218] and mammalian cells[219]. Once a suitable host has been selected, an appropriate genetic vector must be chosen. A wide variety of vectors are available, ranging from plasmids[220] to artificial chromosomes[221]. All vectors have a set of characteristics that make them suitable for carrying and expressing genetic material in a host cell. The first component is the origin of replication, a sequence that will be recognized by the host cell and note the start of replication of the vector and genetic material of interest and will specify the number of copies of the vector in a cell. Another important component of a successful vector is the selection marker, that will confer a selective advantage to positive transformants[222]. Moreover, to ensure the expression of the gene of interest in the vector, an appropriate promoter must be selected. The choice of promoter is based on the desired expression mode of the gene of interest. Based on the outcome of the application, the two major categories of promoters are constitutive and inducible promoters[223]. While constitutive promoters are always “on”, inducible promoters require activation by an external signal, most commonly being temperature[224], pH[225], light[224] or chemicals[226].

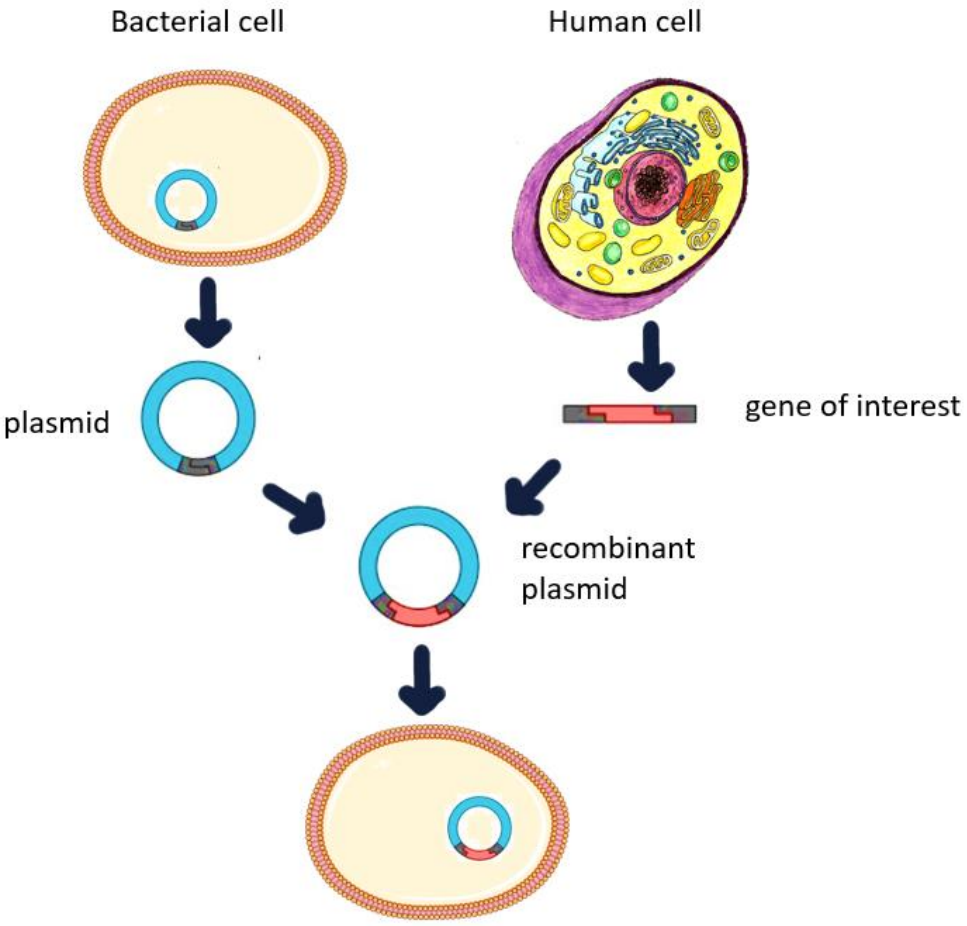

Figure 1.7. Schematic overview of genetic engineering. An appropriate vector (plasmid) is isolated and amplified along with the gene of interest. The selected gene is then inserted into the vector and the construct is then inserted into an appropriate host.

After deciding on the correct vector and the desirable components for the expression of our gene of interest, the target DNA sequence needs to be obtained, amplified and inserted into the chosen vector. The amplification step is performed using a polymerase chain reaction assay (PCR), that creates a large number of exact copies of our DNA sequence of interest to maximise the chances of its successful incorporation into the selected vector. Developed in the late 1980s, the PCR has proven a highly specific and efficient technique for DNA amplification[227], that is schematically represented in figure 1.8. This versatile assay includes a step-by-step process starting with the denaturation of double-stranded DNA to separate the complementary strands, followed by the annealing of pre-designed primers to the dissociated DNA strands. The primers are then involved in an extension reaction catalyzed by a thermostable DNA polymerase, that when repeated creates a huge number of the DNA

sequences of interest[228]. At the end of the PCR cycle, the end mixture contains a variety of proteins, including the polymerase, the sequence and primers, free nucleic acids and deoxynucleotide triphosphates (dNTPs). To isolate the amplified sequence of interest, the PCR product needs to be purified using a method that will be discussed in section 3.2.3. The next step involves the ligation of the amplified DNA fragment and the chosen vector. This is usually achieved using restriction enzymes, that cut and linearise the destination vector generating blunt or sticky ends where the foreign DNA fragment can be annealed and a DNA ligase that will ligate the linearized vector with the amplified sequence. The ligation step is mediated by the creation of a phosphodiester bond in the sugar backbone between the two DNA sequences resulting in the insertion of the chosen DNA sequence at the exact desired point[229].

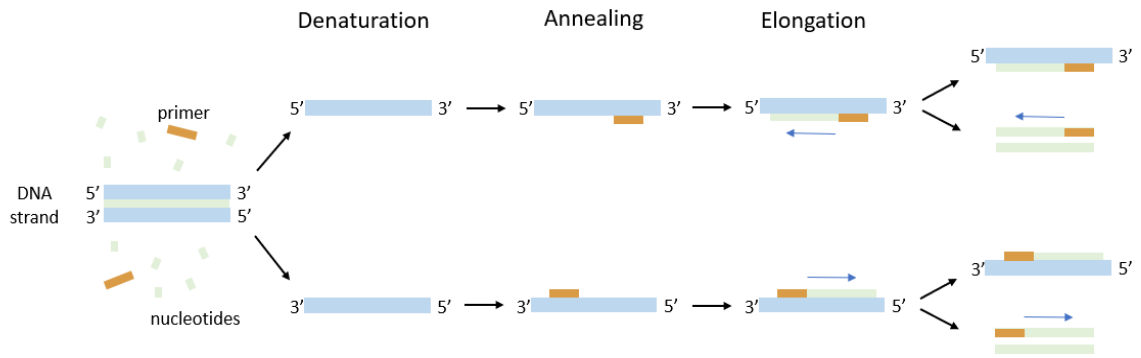

Figure 1.8. Overview of the polymerase chain reaction technique (PCR). During the denaturation the reaction is heated at 98 °C for 30 seconds to break the hydrogen bonds between the strands and separate them. The reaction temperature is then lowered to 50-65 °C according to the characteristics of the primers for 30 seconds to allow the primers to anneal to the template strands. Strand elongation takes place at 72 °C, the optimal temperature for the Taq DNA polymerase to add deoxyribonucleotide triphosphate (dNTPs) to the strands. The amount of the sequence of interest doubles with each thermal cycle, leading to an exponential amplification represented by $2^{(\#\ of\ cycles)}$.

Over the years and across different disciplines, the PCR has been used for a variety of applications, ranging from genotyping, cloning and mutagenesis to forensics and paternity testing. While PCR was the first nucleic acid amplification method developed and remains the most widely used and preferred technique since its invention by Mullis[230], a number of alternative amplification methods have also been developed. These include the loop

mediated isothermal amplification (LAMP)[231], rolling-circle amplification (RCA)[232] and ligase chain reaction (LCR)[233].

Once the desired DNA fragment is incorporated into a vector, the complete assembly can be inserted into the host cell. In the case of bacteria, this can be mainly achieved either by electroporation or by heat shock transformation in certain species. Heat shock transformation is used optimally for gram negative bacteria. The process is based on the creation of small pores on the bacterial membrane caused by an increase in temperature. Initially, the cells are incubated at 0°C in a calcium-rich medium and then are transferred in a water bath at 42°C, where they are incubated for a few seconds. The electrostatic repulsion between the DNA and bacterial membrane is counteracted by the calcium chloride present in the medium in which the bacteria and DNA of interest are incubated[234]. This environment allows the foreign DNA to attach on the bacterial membrane of gram-negative cells and quickly be taken up during the pore formation. In contrast, gram-positive bacteria, such as *L. lactis*, have a thicker peptidoglycan layer that is not easily disrupted by a heat shock. Therefore, transformation of gram-positive cells requires a high voltage electric shock to allow the foreign DNA to enter the bacterial cell. To increase the efficiency of electrotransformation, the bacterial cells need to be made electrocompetent. This process involves the overnight growth of the desired bacterial cells in glycine-rich medium that acts as a cell wall weakening agent[235]. Upon the introduction of the millisecond-long high voltage electric pulse, tiny pores will open up on the bacterial cell wall and close within nanoseconds. If any DNA is present in the medium surrounding the bacterial cells, some may be taken up into the cell before the cell wall pores close.

Following the transformation, a selective marker is used to separate the bacteria that have successfully taken up the DNA to the wild type cells. This can be achieved by the incorporation of one or more antibiotic resistance genes in the plasmid that carries the DNA strand of interest, followed by incubation of the cells in a medium containing the same antibiotic. Only the cells that have successfully taken up and can express the plasmid will survive and grow in the media. Other screening methods include the incorporation of fluorescent proteins in the plasmid, such as green fluorescent protein (GFP). Bacteria that have taken up the plasmid will express GFP under normal growth conditions and can be selected for upon illumination using a fluorescence microscope or flow cytometry.

Over the past few years, gene editing tools and methods have revolutionized our understanding of complex diseases and conditions and provided novel avenues to explore and cure clinical conditions. The endless possibilities offered by genetic engineering can be tailored to address environmental issues, from biofuel development to carbon fixation in engineered microorganisms to preventing and curing genetic and acquired conditions in humans. In the context of this thesis, genetic engineering has been used as a tool to develop a platform that will both contribute to our understanding of the complex dynamic interplay between different components of the bone marrow microenvironment to attempt the expansion of HSCs for clinical applications.

1.8. *L. lactis*, origins and uses

1.8.1. *Lactococcus lactis*

Lactococcus lactis (*L. lactis*) is a Gram-positive, non-motile, non-sporulating spherical or ovoid-shaped bacterium, with a size about 1.2 by 1.5 µm[236]. Originating from the family of *Streptococci*, *Lactococcus lactis* has three subspecies, *lactis*, *cremoris*, and *hordinae*[237] and is classified in the category of lactic acid bacteria (LAB) because of its metabolic ability to ferment sugars into lactic acid[238]. This particular property has been exploited for centuries in milk fermentation and therefore dairy product production, making the species economically valuable and rendering its generally recognized as safe (GRAS) status by the Food and Drug Administration (FDA)[239]. Furthermore, its small-sized fully sequenced genome (2.3 Mbp), and the wide availability of compatible genetic engineering tools have made *L. lactis* a desirable model organism for genetic engineering[240].

1.8.2. Origin and uses

Despite commonly being associated with dairy products, LAB were initially isolated from plants. They naturally reside in the phyllosphere (the aboveground surfaces of a plant), where they can be found in relatively low cell numbers (10^2 to 10^4 CFU/g), but rapidly increase in cell densities following the harvest of plant leaves and fruits and exposure to humid, low oxygen environments[241].

Apart from its common use for centuries in the fermentation of cheese and yoghurt, *L. lactis* has gained popularity as a microbial cell factory that has been used in a variety of applications, gaining a qualified presumption of safety (QPS) status by the European Food Safety Authority's (EFSA) scientific panels[242]. Its current uses range from vitamin[243], multivitamin and health supplement production[244,245] to vaccine delivery[246,247]. The species has also been used as a probiotic[248], as well as a vector for the delivery of functional proteins to mucosal tissues of patients[249]. In medicine, *L. lactis* has been used as a tool with therapeutic potential for a variety of diseases such as colitis[250] and necrotizing enterocolitis[251]. Finally, specific strains of *L. lactis* have been shown to have antioxidant and anticancer effects[252] while others have been used for cosmetic purposes as they display evidence of skin health and status improvement[253] or even as sweetener producers[254,255]. Additionally, recombinant protein producing strains of *L. lactis* have been successfully used in clinical attempts for the management and treatment of inflammatory bowel disease[256,257]. Table 1.1 provides a further summary of recombinant proteins produced in *L. lactis* for biomedical applications.

Aside of biomedicine and the food industry, LAB are also used for biomass feedstock production[258] as well as for the conversion of plant tissues such as alfalfa into silage for animal feed while ensuring its preserved and enhanced nutritional value and sanitary qualities[259]. Other efforts have focused on the use of *L. lactis* for ethanol production as an energy source[260] and for the fermentation of plant-based substrates into industrial-grade lactic acid for the manufacture of polylactide bioplastics[261].

Recombinant protein	**Application**	**Expression vector**	**Promoter**	**Protein display**	**Ref**
Trefoil Factor (TFF)	Inflammatory Bowel Disease	pTREX-derived	P1 (pH dependent)	Secreted	[262]
Low calcium response V (LcrV)	Inflammatory Bowel Disease	pTREX-derived	PUsp45 (constitutive)	Secreted	[262]
IL-10	Inflammatory Bowel Disease	Chromosome integrated	PthyA (constitutive)	Secreted	[262]

IL-10	Crohn's Disease	pOR19	P1 (constitutive)	Secreted	[263]
IL-27	Inflammatory Bowel Disease	pT1NX-derived	P1 (pH dependent)	Secreted	[262]
Catalase	Inflammatory Bowel Disease	pSEC:KatE	PnisA (inducible)	Cytoplasmic	[262]
Murine IL-10	Inflammatory Bowel Disease	pLB263	PgroESL (Inducible)	Secreted	[262]
Pro-insulin/IL-10	Type 1 diabetes	pT1NX-derived	P1 (pH dependent)	Secreted	[262]
HSP65-6P277	Type 1 diabetes	pCYT:HSP65-6P277/pHJ: HSP65-6P277	PnisA (inducible/ constitutive)	Cytoplasmic/Secreted	[262]
GAD65 and IA-2	Type 1 diabetes	-	-	Secreted	[262]
Single-chain insulin analog, SCI-57	Diabetes	pNZPnisA:uspSCI-57	PnisA (inducible)	Secreted	[262]
Glucagon like peptide-1 (GLP-1)	Type 2 Diabetes	pUBGLP-1	PgroESL (inducible)	Secreted	[262]
HPV-16 E7 antigen	Cancer	pLB263	-	-	[262]
HPV-16 E7	Cervical cancer	pMG36e	P32 (constitutive)	Cytoplasmic	[262]
Staphylococcal nuclease	Staphylococcal infection	pLB263	PgroESL (inducible)	Secreted	[262]
VP8	Rotavirus infection	pNZ8048	PnisA (inducible)	Secreted/cell anchored/ cytoplasmic	[262]
Ara h 2	Peanut allergy	pNZ8148	PnisA (inducible)	Secreted/cell anchored/ cytoplasmic	[262]
Der p2	Dust mite allergy	pNZ8148	PnisA (inducible)	Secreted/cell anchored/	[262]

				cytoplasmic	
Pneumococcal surface protein A	Streptococcus pneumoniae infection	pTREX1	P1 (pH dependent)	Cytoplasmic	[262]
hemagglutinin 1 (HA1)	Avian influenza virus	pMG36e	-	Cytoplasmic	[262]
Leptin	Body weight control	pSEC:lep	PnisA (Inducible)	-	[262]
Murine IL-18	Immune response enhancement on mucosal surfaces	pNZ8149	PnisA (Inducible)	Secreted	[264]
KiSS-1	Colon carcinoma	pNZ401	PnisA (Inducible)	Secreted	[265]
TNF-related apoptosis-inducing ligand (TRAIL)	Cancer	pNZ8124	PnisA (Inducible)	Secreted	[266]
IL-17A	Cancer	pLB333	groESL	Secreted	[267]
Hepatitis E virus antigen	Hepatitis E virus infection	pNZ8149-inaQN-ORF2	PnisA (Inducible)	Surface-displayed	[268]

Table 1.1 Recombinant proteins produced in *L. lactis* for biomedical applications.

1.9. Phylogenetic characteristics of *L. lactis*

The earliest taxonomic classification of the LAB has been considered the contribution of Orla-Jensen (1919, 1942), who characterised the members of the group depending on their cellular morphology, mode of glucose fermentation, range of growth temperature, and sugar utilization patterns. LAB have been collectively described as Gram-positive, non-motile, non-spore-forming, rod- or coccus-shaped organisms that ferment carbohydrates, primarily glucose, and higher alcohols to mainly lactic acid, often also producing CO_2 and ethanol metabolites[269]. Further to these parameters, growth rate, pH, salt and alkaline tolerance as well as type of metabolic end product produced have also been used to classify LAB. In more recent years, gene sequencing has replaced the traditional morphological classification of species. More precisely, the sequence of the small subunit ribosomal RNA (16S/18S rRNA) and other genes such as cytochrome oxygenase subunit 1 (CO1)[270] have

been the target sequences for organism classification, with the former being the most commonly used[271].

By 16S/18S rRNA sequencing and their G-C content, LAB can be placed in the low G-C branch of Eubacteria. As shown in figure 1.9, Gram positive bacteria form two main lines of descent, one with a high G-C content (*Actinomyces*) and one with a low G-C content (*Clostridium*) that contains the LAB supercluster. LAB are generally classified into four families and seven genera, as follows: family *Lactobacillaceae* including the genera *Lactobacillus* and *Pediococcus*, family *Leuconostocaceae* made up of genera *Oenococcus* and *Leuconostoc*, family *Enterococcaceae* with the genus *Enterococcus* and family *Streptococcaceae* containing the genera *Lactococcus* and *Streptococcus*. Based on 16S rRNA as a variety of selected genes, a strong phylogenetic relationship exists among the genera *Lactococcus*, *Streptococcus* and *Enterococcus* (figure 1.10).

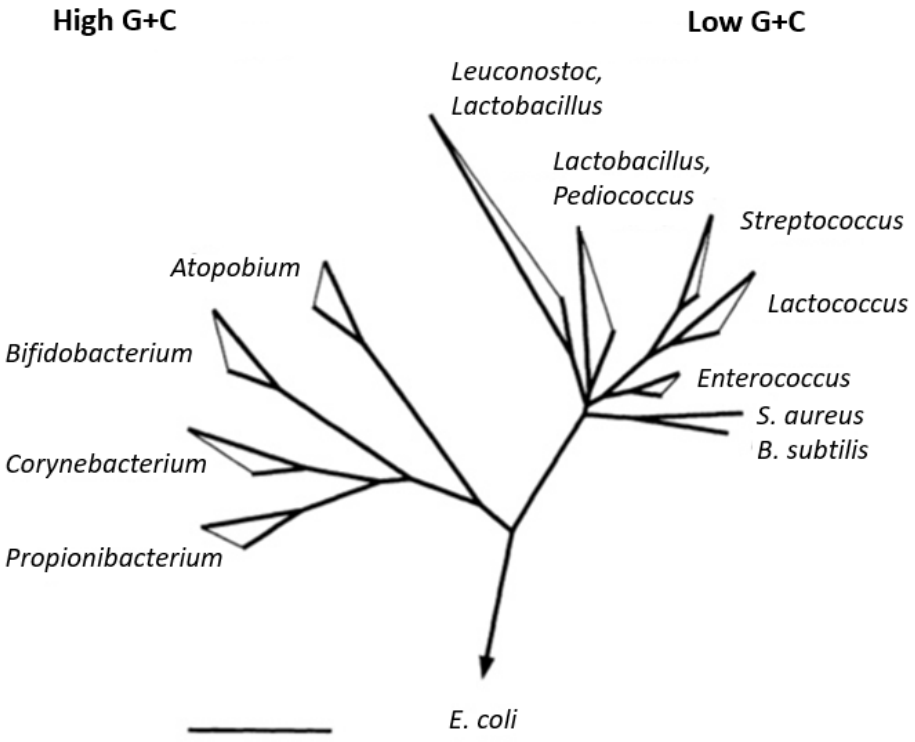

Figure 1.9. Phylogenetic tree of Gram-positive bacteria. The bar indicates 10% expected sequence divergence. Adapted from Schleifer and Ludwig (1995)[272].

Despite their classification in the same cluster of microorganisms, the term 'lactic acid bacteria' does not reflect a phyletic class, but rather the common metabolic similarities of this heterogeneous bacterial group, the most important of which is the capacity to ferment

sugars primarily into lactic acid. Other differences observed between the different species of LAB are on their oxygen tolerance as well as fermentation characteristics. More precisely, even though LAB are generally characterised as facultative anaerobes, many species can tolerate oxygen. Furthermore, LAB can be divided into three groups based on fermentation characteristics: obligately homofermentative, producing mainly lactic acid, as well as facultatively heterofermentative and obligately heterofermentative, that produce a variety of fermentation end-products, including lactic, acetic, and formic acids, ethanol and carbon dioxide, as mentioned above.

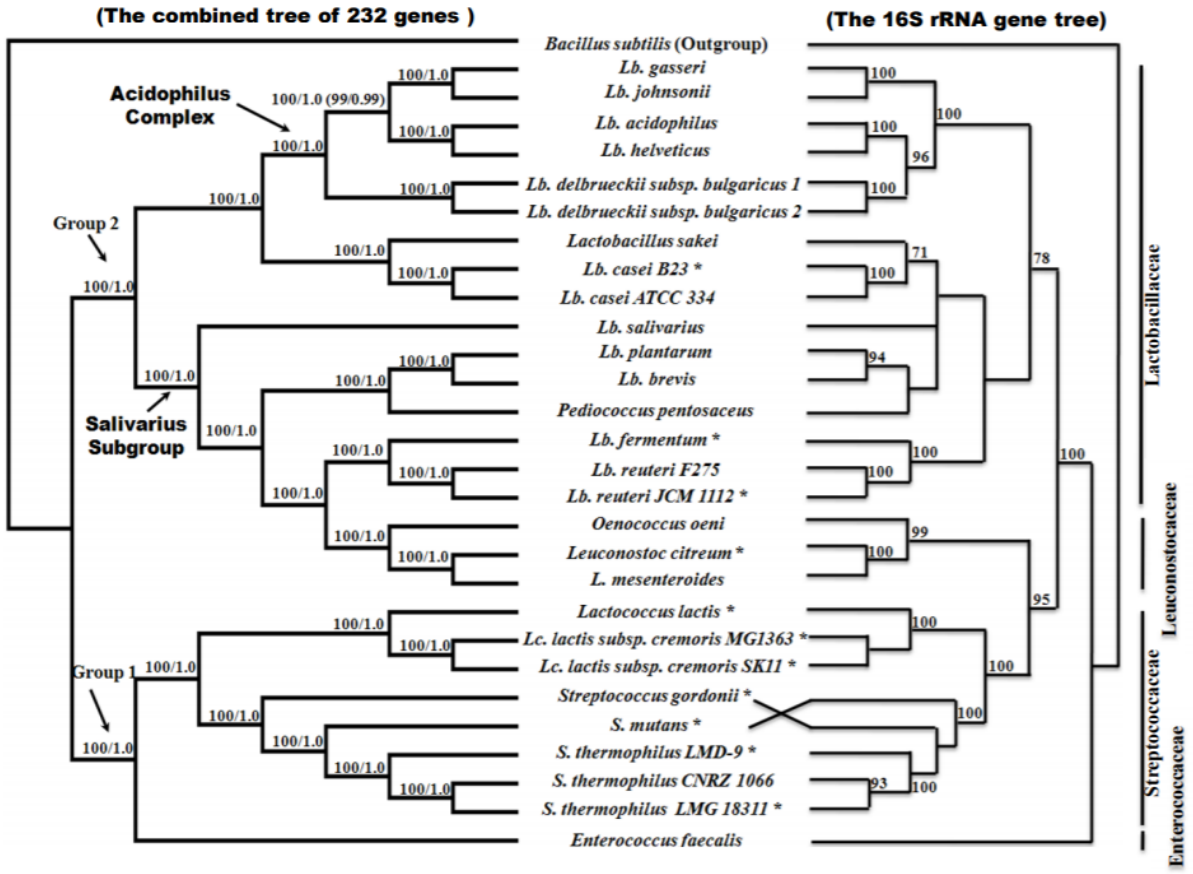

Figure 1.10. Partitioned Bayesian/ML tree topology inferred from selected 232 genes and the 16 S rRNA gene tree of 29 species of LAB. ML bootstrap supports and Bayesian posterior probabilities are shown above the branches. Figure adapted from Zhang et al (2011)[273].

1.10. Why *L. lactis*

LAB have a long history of use in many aspects of human life. From their industrial applications and importance in dairy product production[274,239] to more recent uses in medicine as drug delivery systems and role in vaccine production[247], the species has proven

of high economic and clinical importance. It has been associated with a GRAS status by the FDA and a QPS status by the European Food Safety Authority's (EFSA) scientific panels[242].

Compared to the traditionally used for protein production gram-negative bacteria, *L. lactis* provides an attractive alternative for biomedical applications due to its physical characteristics[275]. One of the major concerns of using bacteria in tissue cultures is lipopolysaccharide (LPS) production, that has been associated with inflammatory responses and anaphylactic shock in animals and humans[276,277]. Being gram positive, *L. lactis* does not produce LPS, which makes it a suitable substrate for human tissue culture. Furthermore, *L. lactis* features low exopolysaccharide (EPS) production that allows the interaction of human cells with membrane proteins expressed on the bacterial membrane. Low EPS are also important for optimal secretion of soluble recombinant proteins. This property is particularly important for this work as it facilitates the interaction between the mammalian cells, the soluble recombinant CXCL12 and TPO, as well as the membrane bound fragment of FN $III_{7\text{-}10}$ and VCAM1 produced by the genetically engineered strain NZ9020.

Another important characteristic of *L. lactis*, particularly for our system, is its ability to spontaneously form biofilms[278] on a variety of substrates. This feature has been exploited by previous studies in order to use *L. lactis* as a biomaterial to direct stem cell fate[279,280]. In these studies, *L. lactis* biofilms have been shown to be stable and viable for up to 4 weeks in culture and has been classified as a living biointerface that can support stem cell adhesion and differentiation.

Moreover, *L. lactis* is a well characterised species and the first LAB to have its full genome sequenced[281]. There are currently more than 80 individual, fully sequenced lactococcal plasmids[280] as well as a variety of recombinant protein expression systems[282,283]. The core proteome of the species has also been recently characterised and quantified and has provided an insight into cellular processes, signalling and cell cycle control[284,285].

Except for its desirable natural properties, a variety of gene editing tools have been developed for genetic engineering applications in *L. lactis*. Targeted Group II Introns[286], the P170[287] and CRISPR-Cas9[288] systems, the nisin-controlled inducible expression (NICE) system[289] as well as other single and dual plasmid systems[290] have been developed for precise and efficient gene manipulation in the species. The most commonly used method of gene transfer in *L. lactis*, and the technique used in this work, is through bacterial plasmids.

In this method, the plasmid is cut open at a specific site using a restriction enzyme, following the mixing of open plasmid and gene of interest and the incorporation of the gene into the plasmid, using a DNA ligase.

L. lactis has also been successfully used to direct stem cell fate of mouse and human stem cells. Our work has been inspired by the proof of concept provided by previous research, that suggested the suitability of *L. lactis* for co-cultures with mouse and human cells in order to induce specific cellular responses[291,292].

In this work, we are using the pT2NX plasmid, which has been designed and developed by Dr A. Rodrigo-Navarro and Dr J. Hay[293] in the Centre for the Cellular Microenvironment, at the University of Glasgow, and is derived from the PT1NX plasmid by the substitution of the erythromycin with the chloramphenicol resistance gene. The plasmids are depicted in figure 1.11 and details of the pT2NX plasmid design are shown in table 4. pT1NX has been developed by Dr L. Steidler[294] and has been extensively used as a vector for recombinant protein production in LAB[295,296].

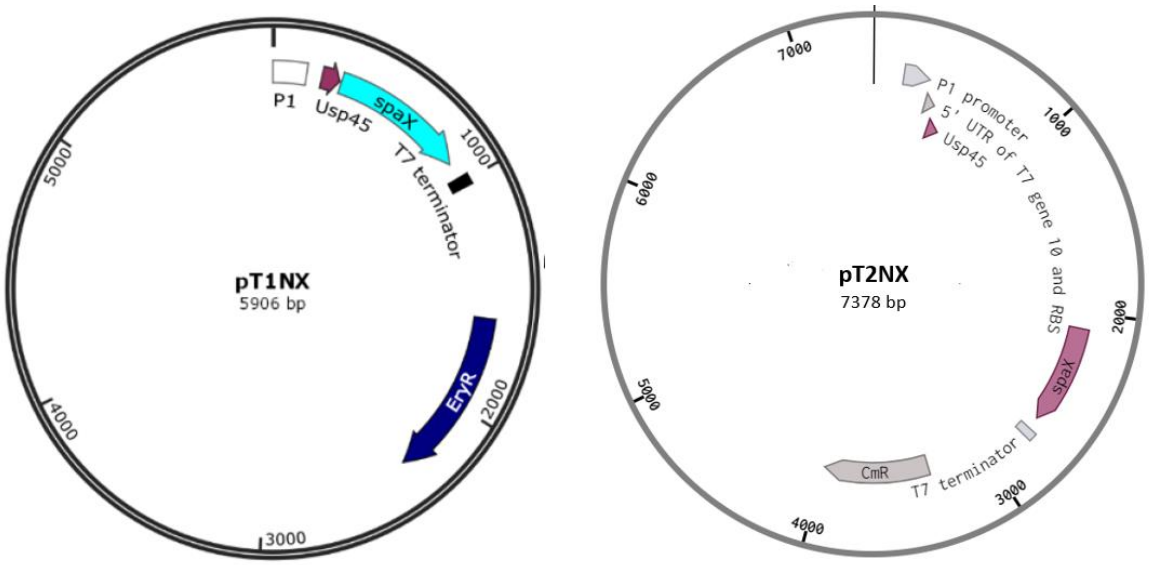

Figure 1.11. Graphical illustration of the *L. lactis* plasmids pT1NX and pT2NX. The plasmid maps feature the constitutive P1 promoter, Usp45 secretion peptide, *S. aureus* protein A anchor and T7 terminator that are shared between the two plasmids. pT1NX bears erythromycin resistance, while pT2NX contains the chloramphenicol resistance gene.

pT2NX, like pT1NX, bears the P1 lactococcal promoter, that is constitutively expressed and the phage T7 gene 10 (T7g10) 5'-UTR and RBS and the T7 terminator for the control of mRNA synthesis. The terminator is derived by the T7 *E. coli* originating phage[297]. The

plasmid also features the *usp45* gene, encoding for the Usp45 (unknown secreted protein 45) secretion peptide found in a number of LAB[298]. This secretion peptide comprises the first 27 residues of the native N-terminal region of Usp45, has no known biological activity and has been previously used to optimise the expression and secretion of the desired recombinant proteins by the bacteria[299]. More precisely, in our plasmid designs, the gene encoding the protein of interest is inserted downstream the *usp45* gene, ensuring that upon expression the recombinant proteins will be tagged with Usp45 and secreted from the cell. Additionally, pT2NX features the *Staphylococcus aureus* protein A (SpA) C-terminal fragment. This 42 kDa protein found in the cell wall of the bacterial species (gene name *spax*) functions as an anchorage protein and allows for the production and presentation of membrane-bound recombinant proteins[300]. The SpA has been previously characterised and shown to comprise of an LPXTG motif on its carboxy-terminus, a hydrophobic core of approximately 30 amino acid residues, and a positively charged (Arg- or Lys-rich) tail[301]. Of particular interest for recombinant protein presentation is the LPXTG motif, that mediates chemical coupling of the desired protein to the bacterial cell wall. A proteolytic cleavage of the peptide between the threonine (T) and glycine (G) of its LPXTG motif, followed the formation of a covalent bond between the C-terminus of SpA to the pentaglycine peptide in the peptidoglycan layer of the cell wall of *L. lactis*[302]. The amide bond formed between the C-terminal threonine and the free amino groups of the peptidoglycan cross bridge, ensures the extracellular presentation of the engineered proteins by the bacteria.

Primer	Sequence 5'-3'	3' Annealing Temperature
Forward chloramphenicol	'TTCTATGAGTCGCTTTTG'	56.9 °C
Reverse chloramphenicol	'GTAATCACTCCTTCTTAATTACAAATTTTTAG'	56.9 °C
pT1NX Forward	'AATTAAGAAGGAGTGATTACATGAACTTTAATAAAATTGATTTAGACAATTG'	57.3 °C
pT1NX Reverse	'TACAAAAGCGACTCATAGAATTATAAAAGCCAGTCATTAGG'	57.3 °C

Table 1.2. Primers and annealing temperatures for the incorporation of a chloramphenicol resistance gene in pT1NX, for the creation of pT2NX. Table adapted from Hay, J. (2018)[292].

Together, the SpA and Usp45 proteins create possibilities for the design of both secreted and membrane bound recombinant proteins in *L. lactis*. This is particularly important for the purpose of this work, as the bone marrow microenvironment is a highly complex niche, characterised by the presence of both biochemical and mechanical signalling. These can take the form of either secreted molecules and cytokines or adhesion proteins presented by its cellular components. Therefore, any effort to create a representative *ex-vivo* BM analogue would have to incorporate both chemical and mechanical signalling in the engineered platform. For the purpose of this work, we have selected four key proteins present in the BM that have been highly associated with HSC survival and self-renewal[303,304] and have expressed them in the pT2NX plasmid. We have engineered *L. lactis* to secrete soluble recombinant human CXCL12 and TPO as well as the membrane bound extracellular signalling fragment of VCAM1 and the FN_{7-10} fragment. A schematic representation of the recombinant protein expression system used in this work is depicted in figure 1.12.

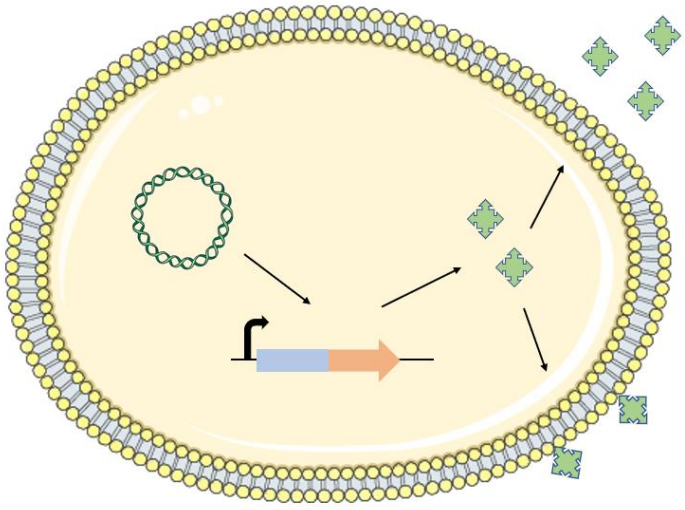

Figure 1.12. Schematic overview of the engineered protein production in *L. lactis*. The constitutively expressed pT2NX plasmid activates transcription of the protein of interest under the P1 Lactococcal promoter. The presence of the SpA anchor will determine whether the protein will be secreted, or cell wall-bound.

1.11. Bacterial metabolism

1.11.1. LAB metabolism

Because of their central role in both industrial, research and medical applications, a variety of studies have focused their interest in understanding the major metabolic processes of LAB. This group of bacteria employ three major pathways for hexose fermentation; the glycolytic (Embden-Meyerhof-Parnas) pathway, the "bifid shunt" (Bifidus) pathway and the 6P-Gluconate pathway[305]. As shown in figure 1.13, all three fermentation processes have glucose as the starting substrate. Their difference is based on alternative strategies for breaking down the substrate and the carbon skeleton of the downstream metabolites which results to the production of different end products.

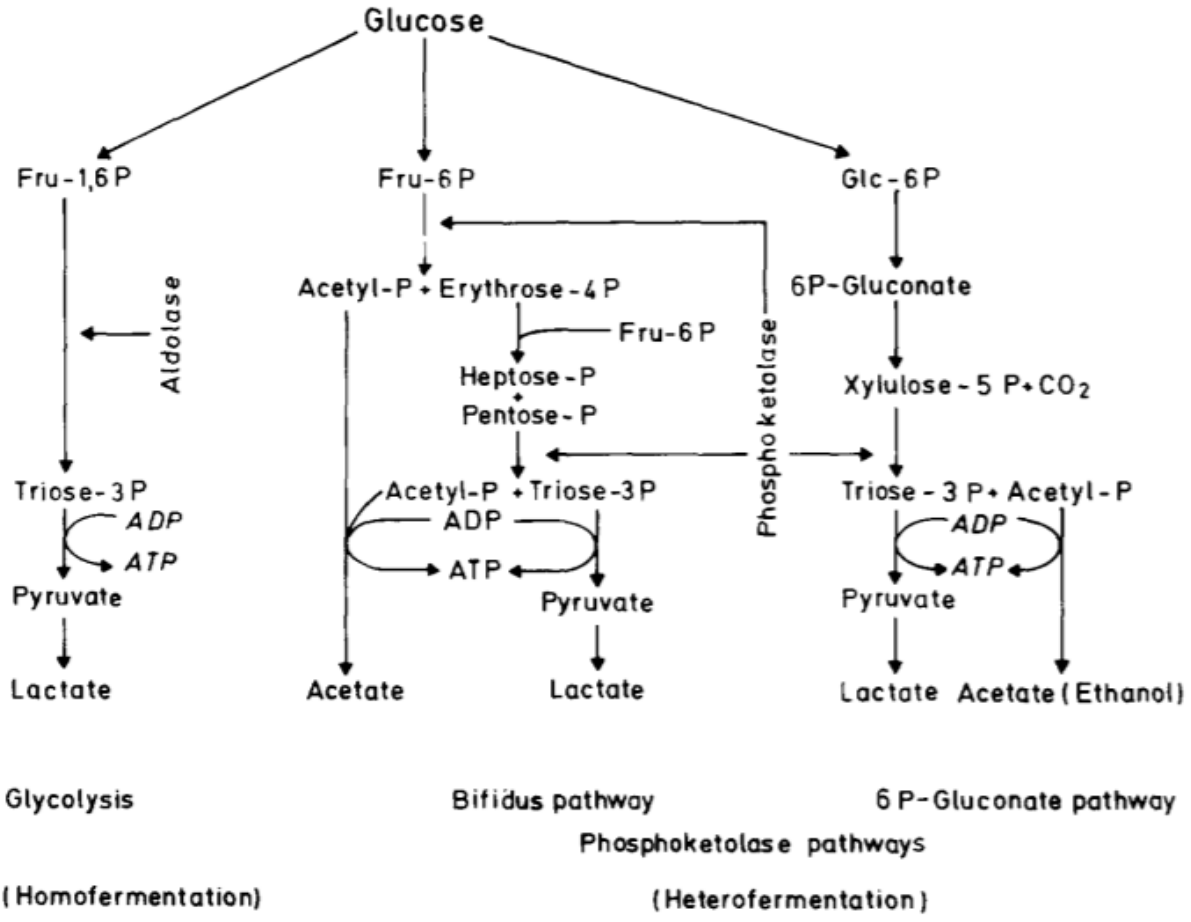

Figure 1.13. The main pathways of glucose fermentation in LAB. Adapted from Kandler, O (1983)[305].

The first step of bacterial metabolic processes is the transport of carbohydrates across the cytoplasmic membrane. There are three major uptake systems for sugars in bacteria: the phosphoenolpyruvate (PEP) phosphotransferase system (PTS)[306], ion-linked sugar transport and adenosine triphosphate (ATP)-dependent sugar transporter systems[307]. The most commonly used and best characterised system of sugar uptake in LAB, PTS-mediated sugar uptake, is initiated by the binding of the transported sugar to the membrane component of the PEP. The sugar then gets phosphorylated by an ATP-dependent phosphocarrier protein (HPr)[308,] and enters the cytoplasm. Once internalised, the substrate is converted to downstream metabolites producing energy in the form of ATP. Ion-dependent sugar translocation is mediated through the uptake of sugars via secondary transport systems (permeases)[309]. Once in the cytoplasm, the free sugar is phosphorylated by a kinase and enters a downstream metabolic pathway. An example of ion-linked sugar transport system and the first to be discovered and characterised in *L. lactis* has been the secondary transport system for lactose. Canonical bacterial ABC importers are dependent predominantly on high-affinity substrate-binding proteins domains (BPDs) that capture the substrate and deliver it to the transporter. In ATP-dependent sugar transport, the nutrient is taken up by ATP-dependent ATP-binding cassette (ABC) permeases. Energy harnessed by ATP induces a conformational change of the transporter that allows for the passing of the target molecule into the bacterial cell[310]. Furthermore, ATP-dependent sugar transport has been shown to be important in cases where the PTS system is inhibited. Upon PEP inhibition, it has been reported that an ATP-dependent metabolite-activated HPr kinase and a sugar-phosphate phosphatase are activated in an ATP-dependent way[311] . After their activation, they reversibly phosphorylate serine 46 in the phosphocarrier protein HPr, allowing for the transport of sugars in the cell and activating the respective downstream metabolic pathways[312]. A schematic description of the HPr phosphorylation and activation by PEP and ATP respectively is presented in figure 1.14.

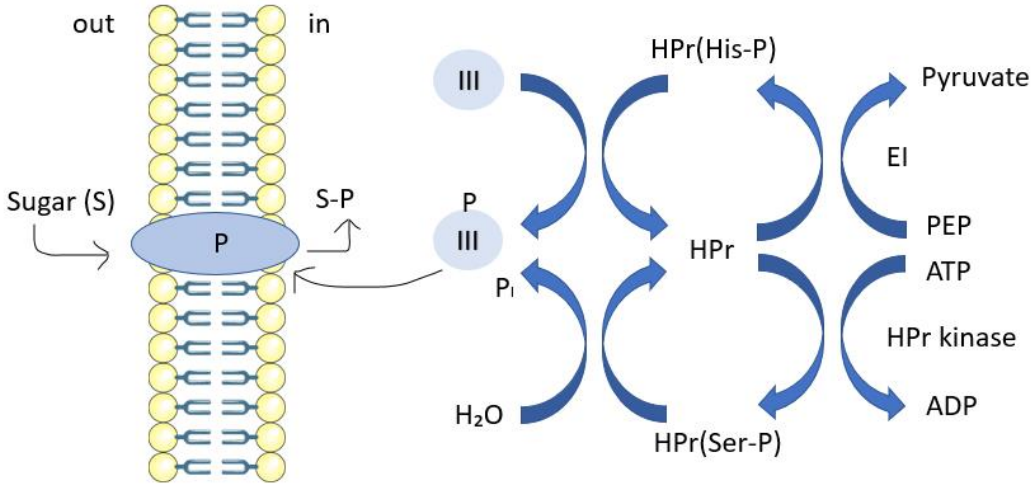

Figure 1.14. Mechanisms of HPr phosphorylation during sugar uptake in LAB. HPr is activated by PEP (top) or ATP (bottom) in an EI or HPr kinase-mediated way respectively.

Glycolysis is the main carbon metabolic pathway occurring in *Streptococci*, *Pediococci*, homofermentative *Lactobacilli*, as well as the species featured in this work, *L. lactis*. During this process, glucose is phosphorylated by hexokinase[313] and converted to glucose-6-phosphate, and further downstream to fructose-6-phosphate and fructose 1,6-bisphosphate, that is then metabolised into glyceraldehyde-3-phosphate, through an aldolase-mediated process and then converted to pyruvate and finally lactate[314]. *Leuconostoc* and heterofermentative *Lactobacilli* generate metabolic energy through the Embden-Meyerhof-Parnas (EMP) pathway or the 6-P-Gluconate pathway[315], while *Bifidobacteria* ferment glucose through the "bifid shunt" central fermentative pathway[316]. In both cases, glucose gets metabolised to end products including CO_2, lactate and acetate or ethanol. This procedure is powered by the initial oxidation of glucose or fructose 6-phosphate to resulting trioses and acetyl-phosphate, followed by conversion to pyruvate and lactate. Acetate can also result as an end product of the metabolism of fructose 6-phosphate to acetyl-phosphate, erythrose-4-phosphate and H_2O with the release of a molecule of ATP[317]. Additionally, ethanol can also be produced from the conversion of xylose-5-phosphate to equimolar amounts of glyceraldehyde 3-phosphate and acetylphosphate, through an ATP-yielding reaction[318].

Other than the main metabolic products of hexose fermentation described above and depicted in figure 1.14, different ratios of lactate, acetate and CO_2, as well as keto and hydroxy acids[319], primary alcohols, aldehydes, ketones, and organic acids may be produced as a result of homolactic and mixed acid fermentation of different substrates[320]. Moreover, pyruvate may not only be converted to lactate and acetate[321] but also to several other products by alternative mechanisms depending on the growth conditions and properties of the particular species. More precisely, metabolic engineering has provided new opportunities for the conversion of pyruvate into a variety of industrially important compounds, such as aromatic compounds (eg. acetaldehyde), sweeteners (eg. L-alanine) and other sugar alcohols with applications in the food and pharmaceutical industries[322].

1.11.2. *L. lactis* metabolism

Depending on their glycose metabolic pathways, LAB are divided in two categories, homolactic and heterolactic, using the glycolytic EMP pathway and the phosphoketolase (6-phosphogluconate) pathway, respectively. The main outcome of the EMP pathway is the generation of two molecules of ATP from one molecule of glucose, through subsequent phosphorylation of downstream regulators. On the contrary, the phosphoketolase pathway yields one molecule of ATP per molecule of glucose utilised, along with one molecule of lactic acid, ethanol and CO_2[323].

Lactococcus lactis is a homofermentative lactic acid bacterium. It primarily metabolises glucose to lactic acid for the production of adenosine triphosphate (ATP) for biosynthesis and more than 95% of the metabolised sugar is converted to fermentation products(Figure 1.15)[324]. The metabolism of the species has been studied in different media and has been reported as characterized by a lactate yield of about 1.7 mol/mol of glucose[325]. For sugar uptake, the bacterium use transport ATPase membrane channels that utilises a H^+ gradient to create a proton-motive force that drives the transport of ions and metabolites into the cell. This transport method is both utilised by permeases and the PTS system, that constitute the two main metabolic systems of *L. lactis*. *L. lactis* uses the glycolytic EMP pathway, through which almost all glucose is metabolised into L-(+)-lactic acid, following the steps described in the section above. Glucose metabolism is achieved through the catalysis of consecutive redox reactions, with nicotinamide adenine dinucleotide (NAD+) and its

reduced form NADH playing a pivotal role. More precisely, during energy metabolism, NAD+ is oxidised, forming NADH, which actively drives the mitochondrial electron transport chain (ETC) to fuel oxidative phosphorylation[326]. Under anaerobic conditions, glucose is metabolised to either lactate, via lactate dehydrogenase (LDH), or to formate, ethanol and acetate at a carbon ratio of 1:1:1 via pyruvate formate lyase [327]. In contrast, in the presence of oxygen, a metabolic shift in by product formation is observed, and the main metabolites secreted become acetate, acetoin, pyruvate and CO_2[328].

Except for glucose, *L. lactis* can metabolise other sugars such as mannose, fructose and galactose. Uptake of mannose and fructose is either permease or PTS-dependent[329], while transport of galactose is mediated by the PTS. Galactose then enters the glycolytic pathway at the glyceraldehyde-3-phospate level, while mannose and fructose are metabolised via the EMP pathway. Finally, the species can metabolise disaccharides, such as lactose. Upon entry in the cytoplasm via a lactose-specific PTS (*lac*-PTS), the phosphorylated disaccharide is split into glucose and galactose-6-phosphate in a phospho-β-galactosidase-mediated reaction, that enter the EMP pathway[330].

The strain used in this work, *L. lactis* NZ9020, is a lactate dehydrogenase (*ldh*)-deficient strain, in which two out of the three *ldh* genes have been knocked out[331]. In anaerobic conditions, the metabolic activity and levels of sugar fermentation of the strain drop significantly and the main metabolic end products include small amounts formate, ethanol and butanediol[332]. NADH has been reported to play an important role in the reducing steps of the pathway that mediates the conversion of pyruvate to the aforementioned end products[333]. The combination of reduced metabolic activity and the lack of lactic acid as a metabolic end product are of major importance for the applications of this specific bacterial strain in this work. These desirable properties have provided us with the opportunity to culture the bacteria in a monolayer biofilm and achieve long, stable co-cultures of biofilms and human stem cells, as will be described later.

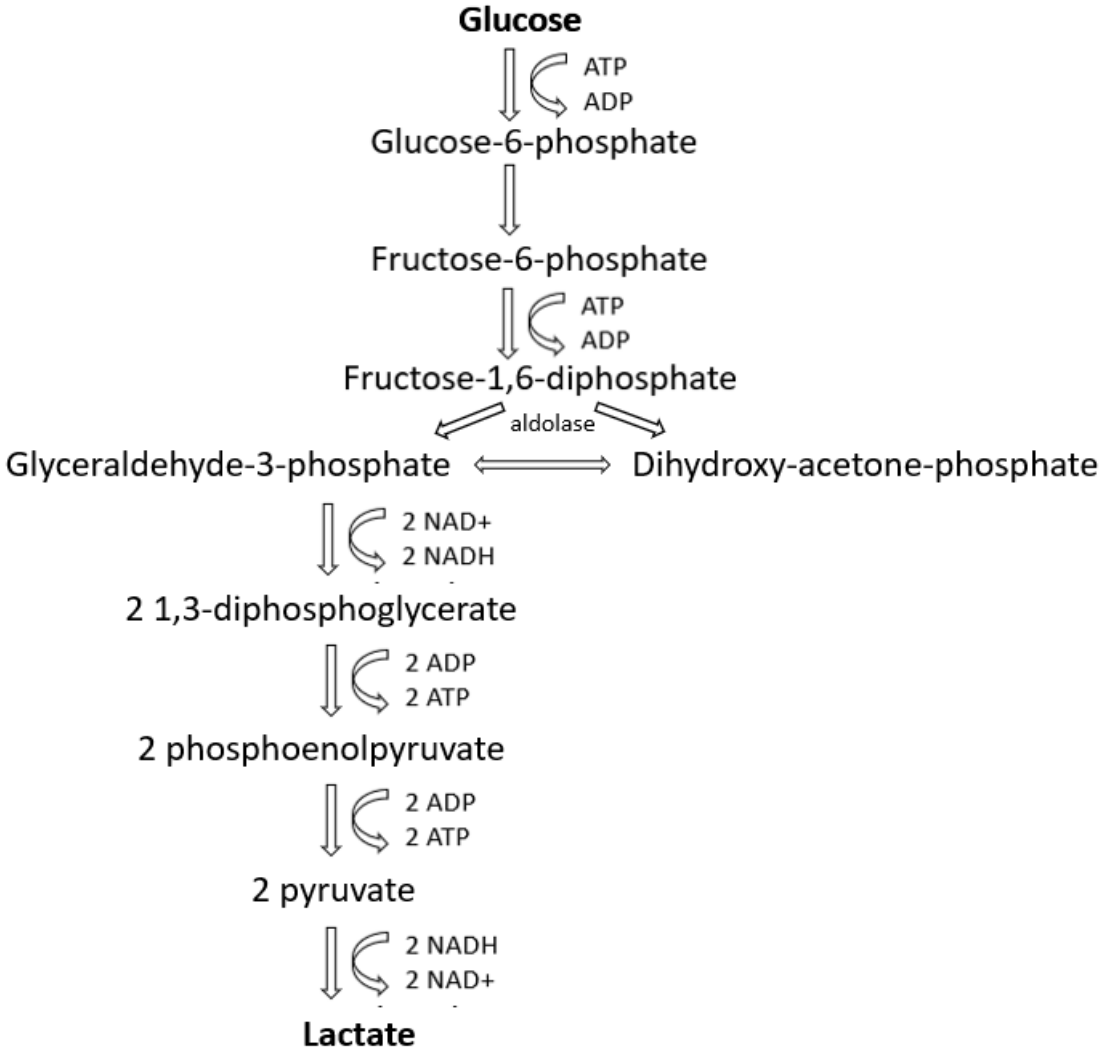

Figure 1.15. Homolactic fermentation pathway in *L. lactis*. Glycolysis yields lactate as the end product.

Studies on the metabolism of *L. lactis*, have revealed that different culture conditions result in the production of different levels of metabolites. When cultured aerobically, *L. lactis* mainly produces lactate (final concentration, 31.4 ± 1.1 mM), followed by acetate (6.7 ± 0.7 mM). Furthermore, acetoin and 2,3-butanediol can also be detected in *L. lactis* cultures in the presence of oxygen. In anaerobic conditions, glucose is almost completely metabolised to lactate, with acetate only being produced in trace amounts (37.4 ± 0.3 mM vs 0.5 ± 0.1 mM respectively)[334]. When switched from anaerobic to aerobic conditions, an increase in α-acetolactate synthase flux is observed in the metabolism of *L. lactis*, resulting in acetoin-diacetyl production that has been used as a flavour enhancer in the dairy industry[335]. While this is the case for most *L. lactis* strains, lactate dehydrogenase (*ldh*)-deficient mutants (such

as the NZ9020 strain used in this work) produce different end products as a result of the different culture conditions. *Ldh*-deficient strains display a shift from homolactic fermentation to a mixed acid fermentation characterised by an almost complete loss of lactate production with acetoin as their main metabolic end product[336].

1.11.3. Metabolism during glucose depletion in LAB

A schematic overview of the metabolic activities during glucose depletion in LAB is shown in figure 1.16. Shortly before glucose is depleted in limited resource media, ATP and Uridine-5'-triphosphate (UTP) production starts to decrease, but without significantly affecting the bacterial growth rate. Following glucose depletion ATP and guanosine triphosphate (GTP) concentrations drop to extremely low levels, resulting in a near protein synthesis shutdown. In contrast to the general decrease of protein production, the downshift in carbon and energy source associated with glucose starvation is also marked by an up regulation of the FruR, CcpA, ArgR and AhrC regulons[337,338,339]. Furthermore, the ribosomal dimerization factor YfiA has been reported to be highly expressed during glucose starvation in *L. lactis*, playing a role in keeping the cells at a growth competent state[340]. In glucose starved LAB, the depletion of glucose-6-phosphate (G6P) results in the inactivation of pyruvate kinase. Consequently, phosphoenolpyruvate (PEP) accumulates in a high concentration, which leads to an inhibition of LD production. In anaerobic conditions, the lack of LD combined with the gradual decrease in the levels of pyruvate results in the depletion of NAD+ and subsequent inactivation of glyceraldehyde 3-phosphate dehydrogenase (GAPDH). This gives rise to a residual amount of fructose-1,6-biphosphate (FBP) that provides the cells with a small amount of ATP through the phosphoglycerate kinase reaction, which could be used as a secondary mechanism to restart glycolysis. On the contrary, in aerobic conditions the reduction in pyruvate due to the lack of glucose results in an increase in intracellular NAD+, that is produced by NADH oxidase. FBP gets metabolised in a reaction downstream mediated by GAPDH, that results in subsequent accumulation of 3-Phosphoglyceric acid (3PGA) and PEP, and finally pyruvate and ATP production.

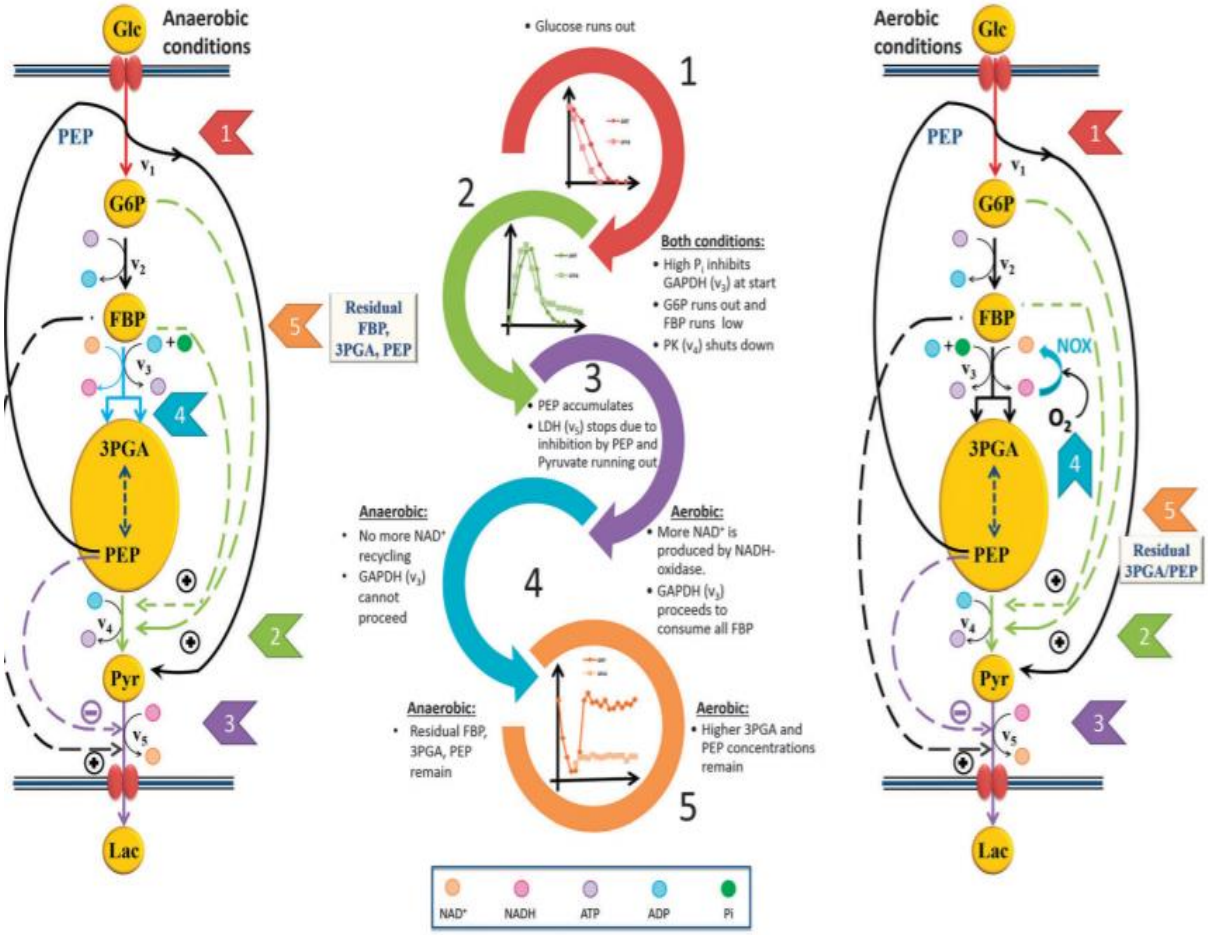

Figure 1.16. Cascade of events resulting from glucose depletion in aerobic and anaerobic conditions. Despite the different response mechanisms during the metabolic "shut down", the cells retain some 3PGA and PEP when glucose runs out both in the presence and absence of oxygen[341].

1.12. Aims of the project

Stem cells have attracted major clinical interest because of their significant therapeutic potential for a variety of otherwise untreatable medical conditions. However, the large cell numbers required for cellular therapies have created an urgent need for novel platforms that would encourage increased cell proliferation and expansion, in order to meet the increasing clinical demands for stem cell grafts. Therefore, major scientific interest has been focused on creating *ex-vivo* stem cell niches that closely resemble the natural stem cell microenvironment. Such platforms would both widen the understanding of all aspects of cellular and niche biology by the scientific community and provide a better alternative to

traditional culture methods that have so far failed to meet the growing demand for large cell numbers for stem cell transplantation.

Two of the most clinically significant stem cell types are mesenchymal and hematopoietic stem cells, both achieving recognition for their potential to repair major bone, muscular, and chondral defects and reconstitute the haematopoietic system in the event of haematological disorders, respectively. Since both stem cell types majorly reside in the BM, scientific attention has been focused on the study and engineering of BM-resembling niches in the lab. The complexity of the BM niche has urged researchers to create culture systems that provide both physical and chemical stimuli in a dynamic manner, in order to regulate stem cell fate, resulting in a variety of studies reporting the engineering of microenvironments and culture methods that bear different characteristics of the BM[342,343].

The dynamic nature of stem cell niches involves a high level of interaction between the cells and their surroundings, where one can change and remodel the other, resulting in conformational changes of the material and changes in cell behaviour. However, most current approaches are based on external chemical signal stimulation and 2D or 3D materials that despite their sophistication often lack active components. A novel approach that promises to reduce the need for external stimulation by providing stem cells with the necessary chemical signals in a controlled, dynamic way is the incorporation of living biointerfaces in the culture system. The bacteria can be engineered to produce a variety of both soluble and adhesion signalling molecules, creating a living, dynamic, self-regulated environment to control stem cell behaviour. Such a system can be tailored to different applications, including the maintenance of naïve stem cells and their proliferation for increased stem cell number manufacturing for cellular therapeutics.

In this work we aim to create cell culture platforms, inspired by the BM microenvironment in order to achieve MSC maintenance and proliferation, as well as HSC expansion for therapeutic applications.

Our primary goal is to genetically engineer *L. lactis* to produce a variety of recombinant soluble and adhesion molecules that are important in mediating stem cell fate decisions in the BM. These include CXCL12, TPO, VCAM1 and FN.

- CXCL12 has been found to be highly expressed throughout the BM and is particularly important in the musculoskeletal system by mediating cell localization. It plays important roles in the regulation of both hematopoietic and mesenchymal progenitor cells, that require CXCL12 stimulation for their localization, homing, survival, and proliferation[348].
- TPO has been associated with normal BM function: its loss is connected to bone marrow failure and thrombocytopenia, whilst higher expression levels drive HSC and MSC maintenance[349].
- VCAM1 has also been found to be highly expressed in the BM, enhancing cell adhesion and homing. Its expression has been linked with the regulation of hematopoiesis and the retention of HSCs in their niche[350].
- Fibronectin has also been associated with the maintenance of BM homeostasis, including the retention, homing, and maintenance of MSCs and HSCs[351]. In addition to the adhesive effects of FN to the cellular components of the BM, this interaction has been described as essential for the maintenance of the naïve phenotype and differentiation potential of BM-residing stem cells[352].

This work aims to then explore the co-culture dynamics between *L. lactis* biofilms and MSCs, with a view to providing a close representation of the BM. We plan to explore whether our platform would allow MSCs to adhere and migrate on the biofilms and remodel their microenvironment in 3D experiments, in a way similar to their behaviour in the BM. We also aim to explore the potential of the biointerface to mediate MSC phenotype maintenance in long term cultures, and the way such cultures would impact the differentiation potential of MSCs. The final purpose of this work is to investigate the capacity of our living interface to instigate HSC maintenance and expansion in both 2D and 3D cultures.

Specifically, this work has been conducted according to the following objectives:

1. The identification of the most relevant cytokines for the engineering of a BM-mimicking HSC niche, according to literature. The aim of the work is to engineer a BM analogue, for MSC and HSC expansion. Hence, it is important to identify the appropriate niche signalling factors that have been associated with the maintenance

of both stem cell types in a naïve, undifferentiated state, while at the same time promote their self-renewal and expansion.

2. The genetic engineering of *L. lactis* NZ9020 to produce the above selected cytokines of interest.
3. The expression and characterisation of the recombinant cytokines.
4. The effect of the biointerface on MSC and HSC viability in co-culture experiments.
5. The assessment of the effect of the expressed cytokines on MSCs.
6. The effect of the recombinant cytokines on HSCs.
7. The study of the potential of 3D HSC cultures to induce stem cell maintenance and expansion.
8. Establishment of a 3D, bioactive culture system, where the HSCs are encapsulated in a hydrogel and supported by the recombinant proteins produced by the biofilms.

Chapter 2. Materials and Methods

The following chapter describes some general methods used throughout this work. More specific details are outlined in the specific chapters that follow.

2.1. Bacterial Culture

L. lactis was cultured in anaerobic conditions, in M17 medium (Formedium). The medium recipe, as provided by the manufacturer, includes:

- Pancreatic digest of casein: 5 g/l
- Soy peptone: 5 g/l
- Beef extract: 5 g/l
- Yeast extract: 2.5 g/l
- Ascorbic acid: 0.5 g/l
- Magnesium sulphate: 0.25 g/l
- Disodium glycerophosphate: 19 g/l

For media preparation, 36.24 grams of powdered M17 is resuspended in 1 litre distilled water. When dissolved, the media has a pH of 6.9 ± 0.2 at 25 °C. The liquid medium is then sterilised in an autoclave at 126 °C for 30 minutes. Upon cooling, and when the medium reaches room temperature, 0.5 % w/v sterile glucose and 10 µg/ml of antibiotic of choice are added. In our work, the *L. lactis* strain incorporates a plasmid carrying the chloramphenicol acetyltransferase gene to provide chloramphenicol (Cm) resistance. Therefore, this has been the antibiotic used in all culture conditions unless otherwise specified. The addition of sterile glucose and antibiotic after the autoclave sterilisation of the M17 liquid medium is important to prevent the antibiotic from degrading in this high temperature and to prevent the Maillard reaction between glucose (a reducing sugar) and the aminoacids present in the medium. In this thesis, the complete medium made up of M17 + 0.5 % w/v glucose + 10 µg/ml Cm will be referred to as GM17. *L. lactis* is grown in a standing culture at 30 °C in anaerobic conditions. The stationary phase of growth is usually met within 8 hours and the bacteria slowly begin to sediment and form a pellet at the bottom of the culture tube.

2.2. Surface preparation

In this work we have used hydrophilic D263M borosilicate glass coverslips (Avantor, VWR UK) as the substrate on which biofilms were formed. Given the increased and more stable, long-term interaction and attachment to bacteria on hydrophobic surfaces, we tested a variety of silanes for their potential to maintain a viable biofilm with high surface coverage in a process that will be described in more detail in a later section.

To achieve a homogeneous, hydrophobic surface, clean and dry glass coverslips were submerged in Sigmacote® siliconizing reagent (Sigma-Aldrich, ref: SL2-100ML). Sigmacote® is a solution of a chlorinated organopolysiloxane in heptane that readily forms a covalent, microscopically thin film on glass. It reacts with surface silanol (Si–OH) groups on glass, almost instantaneously, to produce a neutral, hydrophobic film that can be used for stronger and more stable attachment of the bacteria on the glass coverslip. The coverslips were then washed in distilled water to remove any excess solution as well as any HCl residues. In order to produce a more durable coating, after the heptane had evaporated, the siliconized coverslips were oven-dried at 100 °C for 30 minutes.

2.3. *L. lactis* Biofilm production and viability

The method used in this work to develop a *L. lactis* biofilm was adapted from Burmolle, Webb et al. (2006)[344]. A frozen glycerinate stock of *L. lactis* was kept at -80 °C and used to streak a fresh GM17, 1 % agar plate that was incubated at 30 °C overnight. During this incubation period, several 1-2 mm colonies had grown. A single colony was selected and inoculated in 10 ml fresh GM17 medium until the culture reached an optical density of 0.3-0.5 at 600 nm. A part of the bacterial culture, depending on the application, was then poured over an appropriate surface in a multiwall plate, the plate was grown then overnight in anaerobic conditions at 30 °C.

After the biofilm was formed, the media was removed, and the surface was washed with sterile PBS three times. The purpose of the washes is to remove the planktonic phase bacteria that have not adhered to the surface in order to avoid the complete colonisation of the well due to excessive proliferation of the bacteria. In this way, we can ensure that the *L.*

lactis that remains in the well is in the form of a monolayer biofilm, adherent to our surface of interest.

For biofilm viability, we used the FilmTracer™ LIVE/DEAD® Biofilm Viability Kit (ThermoFisher). The assay provides a two-colour fluorescence assay of bacterial viability, based on membrane integrity that stains live cells green and dead cells red. Biofilms were produced as described above, were cultured in either GM17 or IMDM, and were maintained for a variety of timepoints depending on the needs of each experiment. The assay involves washing the biofilms with a 0.9% NaCl solution and then incubating the biofilms in a 1:1 solution of SYTO 9 and propidium iodide. After 15 minutes of incubation in the dark, the assay is stopped, and the samples are visualised using a Zeiss AxioObserver epifluorescence microscope. The results are processed by image analysis, through measuring the number of green-stained (viable) and red-stained (non-viable) cells in each field of view.

2.4. Human stem cell cultures

2.4.1. Human mesenchymal stem cell (MSC) culture

The mesenchymal stem cells (MSC) used in this work were purchased from PromoCell. They were self-renewing multipotent cells that have the ability to differentiate into a wide variety of cell types, such as adipocytes, chondrocytes, osteoblasts, myocytes, and ß-pancreatic islets cells. The cells were isolated from the bone marrow of human donors and cryopreserved in PromoCell's freezing medium Cryo-SFM. Each batch of MSCs was quality control-tested for cell morphology, proliferation potential, adherence rate, viability and diverse viral diseases (HIV, hepatitis). After their isolation, they were characterized by flow cytometric analysis of a panel of markers, including CD73/CD90/CD105 and CD14/ CD19/CD34/CD45/HLA-DR as proposed by the International Society for Cellular Therapy (ISCT)[345]. After purchase of a cryopreserved vial of MSCs, the cells were cultured and expanded to create a stock. The cell growth medium was made up of DMEM supplemented with 100 µM sodium pyruvate (Sigma), 1% MEM Non-essential amino acid solution (100×) (Sigma), 1.1 mM L-glutamine (Sigma), 10 % FBS and 1 % Cm. For standard cell culture, the MSCs were cultured in plastic flat bottom flasks in a humidified incubator at 37 °C, 5% CO_2.

2.4.2. Human hematopoietic stem cell culture

CD34 is a glycosylated transmembrane protein that has been widely used as a marker for primitive blood- and bone marrow-derived progenitor cells, especially for hematopoietic and endothelial stem cells[346]. These cells first originate as embryonic stem cells in the inner cell mass of blastocysts and give rise to all hematopoietic cells, including all terminally differentiated blood cells. In our work, we are interested in the maintenance and expansion of naïve HSCs. Because of the extremely small number of these cells in the body and the difficulty of isolating and preserving a large number of the true HSC population, we have selected to use the bone marrow derived CD34+ cell mix for our experiments. The CD34 marker indicates two main cellular subpopulations, hematopoietic and endothelial progenitor cells, that can be used for expansion and differentiation studies and can be further narrowed down into specified sub populations using a panel of different markers.

The CD34+ cells used in this work have been purchased from AllCells. The cells are collected by clinicians from the posterior iliac crest of a healthy donor. A 50 ml aspirate is drawn from each hip from a maximum of 2 sites using multiple syringes. The aspirate is filtered to remove clots and bone chips, and then pooled to normalize cell concentration between draws. CD34+ cells are then isolated from the sample and are cryopreserved. Once defrosted, the cells are cultured overnight in IMDM medium (Sigma) supplemented with 20% of a supplement containing bovine serum albumin (BSA), bovine insulin and transferrin (BIT), 10% L-glutamine and 10 μg/ml chloramphenicol. In order to preserve the naïve phenotype, the culture medium is supplemented with 100 ng/ml thrombopoietin (TPO) and stem cell factor (SCF) and 50 ng/ml FMS-like tyrosine kinase 3 ligand (FLT3L). The following day, the cells are ready to be seeded in the culture microenvironments of interest. In the co-culture experiments, where we are investigating the potential of the recombinant cytokines expressed by the bacteria in regulating HSC fate, these maintenance cytokines are not added to the medium. The cells are then cultured in plastic well plates in a humidified incubator at 37 °C, 5% CO_2. All experiments performed in this work last 5 days, without media changes, unless stated otherwise. For the 2D experiments, the CD34+ cells were seeded at a density of $2.5 \cdot 10^5$ cells/ml, while in 3D the cell concentration in the cultures was 10^6 cells/ml, according to current standards.

2.4.3. Mammalian cell and biofilm co-cultures

All MSC-bacteria experiments were performed in clear, sterile 24-well polystyrene plates (ThermoFisher). A standing culture of *L. lactis* was prepared the day before the experiment. Dry, sterile, hydrophobic coverslips were transferred to the bottom of each well of the plate and a biofilm was formed as described previously. The following day, the biofilms were washed three times and 10,000 human bone marrow MSCs per cm^2 were seeded on top of each biofilm. For viability experiments, we used MSCs of passage 3 or 4, while for spreading, adhesion and differentiation experiments we used stem cells of passage 2 or 3. The cells were maintained in DMEM medium (Dulbecco's modified eagle medium, ThermoFisher) supplemented with 4.5 g/L glucose and 10 % foetal bovine serum (FBS). In order to maintain the bacterial monolayer and avoid excessive *L. lactis* proliferation, we used an antibiotic cocktail that we developed and optimised as part of this work, containing 10 μg/ml of chloramphenicol, 5 μg/ml sulfamethoxazole, 5 μg/ml tetracycline and 2.5 μg/ml erythromycin, supplemented with 5 μg/ml hemin. Hemin allows *L. lactis* to switch to an aerobic metabolism when cultured in aerobic conditions, diminishing the production of lactic acid to allow for long term co-cultures with human stem cells, without the risk of lowering the pH of the culture medium enough to endanger the viability of the human cells.

For the CD34+ cell and bacteria co-cultures we used clear, sterile, non-tissue culture 24- well plates. As described above, for each condition, a biofilm was created on a Sigmacote-coated coverslip and was placed at the bottom of each well. CD34+ cells were seeded at a density of $25 \cdot 10^4$ cells/ml on top of each biofilm, as well as in empty control wells, depending on the conditions of each experiment. The cells were cultured in each condition for 5 days without media changes at 37 °C, 5% CO_2 and the populations were analysed using flow cytometry.

2.5. Hydrogel formation

2.5.1. Fibronectin PEGylation

Fibronectin (FN, YoProteins, 3 mg/mL) was initially denatured in a buffer containing 5 mM Tris(2-carboxyethyl)phosphine hydrochloride (TCEP, pH 7, Sigma) and 8 M urea (Acros Organics, 99.5%) in phosphate buffer saline (PBS, Gibco, pH 7.4) for 15 min at room temperature (RT). Then, 4-arm-PEG-maleimide (PEGMAL, 20 kDa, LaysanBio) was added at a molar ratio FN:PEGMAL 1:4, and the reaction was incubated for 30 min at RT. After PEGylation, the remaining non-reacted cysteine residues were blocked by alkylation using 14 mM iodoacetamide (Sigma) in PBS at pH 8. After the 2 h incubation, the product of the reaction was dialysed using a Mini-A-Lyzer, MWCO 10 KDa, (ThermoFisher) against PBS for 1 hour at room temperature (RT). The protein solution was then precipitated using nine volumes of cold absolute ethanol and by mixing using a vortex mixer. The reaction was then incubated at −20 °C overnight. The following day, the mixture was centrifuged at 15,000 g and 4 °C for 15 min, the supernatant was discarded, and the protein pellet was washed with cold 90% ethanol. After another centrifugation step at 15,000 g and 4 °C for 5 min, the supernatant was removed, the pellets were dried and further solubilised using 8 M urea at a final protein concentration of 2.5 mg/mL. Finally, the solution was dialysed against PBS for 1 h at RT and stored in the freezer for further use.

2.5.2. Laminin PEGylation

Lyophilised laminin-521 (BioLamina) was resuspended at a concentration of 0.5 mg/ml in sterile PBS in a sterile laminar flow hood. The mixture was shaken for 5 minutes in a vortex mixer to ensure that the protein had properly dissolved. A sterile dialysis membrane was activated in the laminar flow hood, using sterile MiliQ water, and the laminin mixture was added to the membrane. The mixture was dialysed against sterile sodium bicarbonate ($NaHCO_3$) for 1 hour at 4°C. After the dialysis, the laminin mixture was transferred to a sterile low protein binding microcentrifuge tubes (Sigma) and an appropriate amount of AC-PEG-NHS diluted in sodium bicarbonate was added to the tube. This amount was calculated according to the amount of laminin being PEGylated (eg. 8.2 µl per 50 µg of laminin). The reaction was incubated on a shaking mixer at room temperature for 2 hours. After the

incubation period, the mixture was spun down in a microcentrifuge tube, the pellet was resuspended and was transferred to an activated, sterile dialysis membrane, where the mixture was dialysed against sterile PBS for 1 hour at 4°C. The dialysed solution was then stored in the freezer for further use.

2.5.3. Hydrogel preparation

The PEG and PEG-FN hydrogels used in this work were formed using a Michael-type addition reaction under physiological pH and temperature according to a previously published protocol by Phelps et al. (2010)[4]. For the FN-functionalised hydrogels, PEGylated FN was added to different amounts of PEGMAL (5% or 10%) at a concentration of 1 mg/mL. To crosslink the hydrogels, we used either PEG-dithiol (PEGSH, 2 kDa, Creative PEGWorks) or mixtures of PEGSH and the protease-degradable peptide VPM, flanked by two cysteine residues (VPM peptide, GCRDVPMSMRGGDRCG, purity 96.9%, Mw 1696.96 Da, GenScript). The thiolated crosslinker was added always at the end, at a molar ratio 1:1 maleimide:thiol to ensure full crosslinking. In experimental setups that required the encapsulation of cells in the hydrogels, the cells of interest were always mixed with the PBS, protein and PEGMAL before the addition of the crosslinker. Gelation occurred for 30 min at 37 °C, in a humidified incubator. The PEG only hydrogels were manufactured in the same way, without the addition of the PEGylated FN.

The laminin hydrogels were fabricated according to the procedure outlined by Dobre *et al.* (2021). PEGylated laminin was added to PEG-AC and PBS, at a concentration of 0.5 mg/ml. The hydrogels were crosslinked in a similar way as the fibronectin hydrogels described above, using either PEG-dithiol, or mixtures of PEGSH and the protease-degradable peptide VPM. Gelation occurred for 30 min at 37 °C, in a humidified incubator.

2.6. Image analysis

Images were acquired using a Zeiss AxioObserver Z1 fluorescence microscope (unless stated otherwise) fitted with a 12-bit monochrome Andor camera. Depending on the experiment, 10, 20 and 40× objectives were used, and images were saved in 16-bit per channel monochrome TIFF format. Image analysis was performed using Fiji-ImageJ[347]. Cell area was

determined by capturing images of the actin channel of the immunofluorescence. In this work, this corresponds with staining with Alexa Fluor 488 antibody (Thermo). After acquisition, the images were loaded on the ilastik software (version 1.0)[348], where pixel classification and background removal was performed. The use of ilastik was particularly advantageous as it enabled more accurate distinction between the object of interest and the background. By performing pixel classification, it estimated the probability that each pixel belongs to either foreground or background. The resulting probability maps could be used directly for quantitative analysis[349]. A mask of the original image was generated by performing simple segmentation, that was exported in PNG format for further analysis. The images were then fed into the Fiji-ImageJ software, where a binary format of the image was generated. The size of the cells was calculated using the Particle Analysis command.

Chapter 3. Bacterial Engineering

Summary

This chapter focuses on the genetic engineering and use of the bacterial species *L. lactis* as an active biomaterial. Initially, our work has focused on bacterial engineering, involving cloning and transformation of the bacteria with plasmids that carry the genetic sequence for the expression of recombinant human CXCL12, TPO and VCAM1. Following successful protein expression, we performed protein characterisation and confirmed that our proteins of interest are expressed at physiologically relevant levels. We then assessed the ability of *L. lactis* to form biofilms, as well as their viability and surface coverage in different culture media. We also studied the biofilm formation dynamics on substrates of different coatings to determine the optimal conditions for bacterial culture, that would in the future enable the most efficient biofilm and stem cell co-culture. Our results show the successful expression and production of CXCL12, TPO and VCAM1 in *L. lactis*, and suggest that the bacteria can be cultured in a biofilm that shows good surface coverage and high viability for up to 9 days in different media. Furthermore, our data supports that the different bacterial populations have similar growth kinetics and can therefore be used in combinations in the same biofilm. Finally, we have identified Sigmacote as the most suitable treatment for our substrates, as it encourages the strongest bacterial adhesion and highest surface coverage.

3.1. Introduction

Microorganisms have been around for millions of years, however, their first discovery has been accredited to Robert Hooke and Antoni van Leeuwenhoek during the period 1665-83[350]. Since their discovery and characterisation, the impact and implications of microorganisms in every aspect of our lives has been extensively studied. Pathogenic and non-pathogenic bacteria have been studied for their effects on human and animal health, as well as their impact on the environment, driving and evolving our medical research and general understanding of the world[351,352]. Furthermore, microorganisms have been associated with a variety of other activities, such as ecosystem maintenance through carbon and nitrogen fixation[353] and oxygen production[354]. Therefore, microbes have gained interest

as integral parts of human lives and ecosystems and have widened our understanding of ourselves and our surroundings.

Except for their natural abilities, the advent of biotechnology has created opportunities for engineering microorganisms to display desirable characteristics that can be used for a variety of applications. From food biotechnology and the onset of the dairy industry to biofuel production[355] and medicine or vaccine development[351,356], bacteria have been used in a variety of industrial and clinical settings. The first genetic engineering experiments in microorganisms date back to 1943, when DNA from the bacterium *Streptococcus pneumonia* was successfully transformed into a different bacterial species[357]. This research has marked the onset of a plethora of efforts to introduce foreign DNA in bacteria and has set the starting block for the development of new tools for efficient and precise genetic manipulation techniques.

The most common method of genetic engineering in bacteria is the use of plasmids. These extrachromosomal genetic elements capable of stable autonomous replication in a cell and was first introduced by Joshua Lederberg in 1952[358]. Despite their early discovery, plasmids only gained prominence among scientists in the 1970s, replacing in part the use of the bacteriophage λ that was up to that point the tool of choice for the study of bacterial genetics and genome engineering[359]. Plasmids are small circular pieces of DNA, common to many bacteria[360] as well as archaea[361], yeast[362] and plants[363]. They can replicate autonomously, and their main function is to provide functional advantages to the hosts, such as antibiotic resistance, degradative functions and in some cases virulence and toxins. All natural occurring plasmids contain an origin of replication that controls the number of plasmids present in each host cell, and a number of genes that provides a desirable trait to the host[364]. Except for the basic characteristics necessary for recombinant protein production (promoter, 5'-UTR and ribosome binding sites, polylinker for restriction sites or any other appropriate sequence for gene insertion, and terminator), plasmids designed for genetic engineering applications typically feature a selection marker that will facilitate the screening of the transformants carrying the marker. A schematic representation of a typical plasmid is shown in figure 3.1. Plasmids are normally smaller in size compared to the genome of the host organism; however, each cell of the host may contain a copy number, ranging from one to sometimes hundreds[365].

Genetic engineering has provided a variety of tools and endless possibilities for science, industry and medicine. Using plasmids as vectors, scientists can incorporate any DNA fragment or gene of interest and precisely control its expression levels, while ensuring that the foreign DNA inserted will be replicated and maintained by the host. *L. lactis* in particular, has had a long history of beneficial use in human culture. From its key role in the dairy industry[366], to the development of probiotics[367] and vaccines[368], *L. lactis* has been largely associated with a central role in industrial and clinical applications. Furthermore, the increasing number of effective molecular tools developed for LAB have created the opportunity for many members of the family to be used as cell factories for the production of recombinant proteins of interest. The non-pathogenic nature of these bacteria combined with their capacity for recombinant protein production has also enabled scientists to use them as gene delivery systems. To this day, *L. lactis* has been used as a DNA delivery system[369], as a vaccine carrier against brucellosis[370], tuberculosis[371] and *Streptococcus pyogenes* infections[372], as well as a therapeutic protein delivery system for a variety of diseases including Crohn's disease[373] and ulcerative colitis[374]. The huge therapeutic potential of LAB and their ability to produce and deliver clinically significant molecules, holds promises for novel, more affordable future treatment solutions.

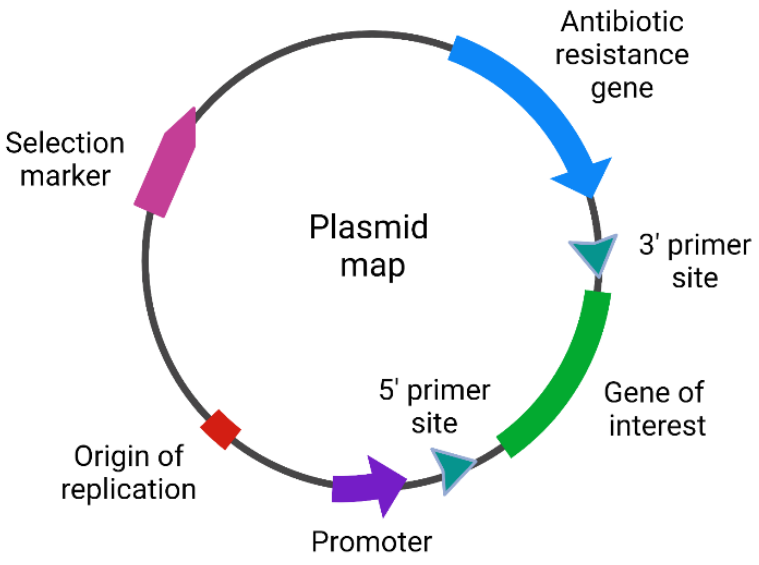

Figure 3.1. Typical plasmid map. All natural and synthetic plasmids contain an origin of replication and a gene of functional interest to the host (here: antibiotic resistance gene). Engineered plasmids also feature a heterologous DNA fragment (inserted gene) and a promoter that regulates its expression. Designed primers insert the gene at a specific position after the promoter. A selection marker is used to identify successfully transformed cells.

In this work, we are proposing a different use of genetically engineered *L. lactis*. Our aim is to develop a platform that controls and directs stem cell fate through the expression different recombinant proteins produced by *L. lactis* biofilms. We envision a tuneable platform that can be tailored to meet different clinical needs, including MSC and HSC cell and niche regulation for cell therapeutic applications. More precisely, our goal is to create a dynamic, biointerface-based culture system that maintains the stem-like phenotype of MSCs in long term cultures and stimulates stem cell proliferation. Such a system would bear high clinical significance, as it would produce increased cell numbers that maintain their desirable healing potential and stem-like properties, for cell therapeutics. In parallel, we aim to use a similar setting in order to mimic the bone marrow microenvironment, with a view to maintaining and expanding HSCs for biomedical applications.

In both cases, the engineered niche we envision, is based on *L. lactis* biofilms that have been engineered to produce recombinant human CXCL12 and TPO, as well as the extracellular, signalling part of VCAM1 and the $III_{7\text{-}10}$ part of FN. All four proteins are normally expressed in the BM, the natural niche of both MSCs and HSCs, and have been associated with HSC maintenance and proliferation. To our knowledge, there have been no studies directly examining the effects of these proteins on MSC behaviour. Therefore, our study aims to both provide insight into the effect of recombinant BM niche factors on MSC fate and study the way the expression of these factors affects cell behaviour. The flexibility of the suggested system will allow the user to select different combinations of recombinant proteins and create different platforms for the study of microenvironment conditions on different stem cell types and for the potential use of these novel culture methods for clinical or biomedical applications.

3.2. Materials and Methods

3.2.1. Cloning

All cloning reported in this work was performed using the pT2NX plasmid developed by Dr A. Rodrigo-Navarro and Dr J. Hay from the commercially available pT1NX[375]. pT1NX was originally a gift from Dr. Vicente Monedero (Institute for Agrochemistry and Food Technology, IATA, Spain) and its map is depicted in figure 3.2. pT2NX was created by

replacing the erythromycin resistance gene in pT1NX with a chloramphenicol acetyltransferase gene, to confer chloramphenicol resistance to the host, resulting in the plasmid shown in figure 3.3.

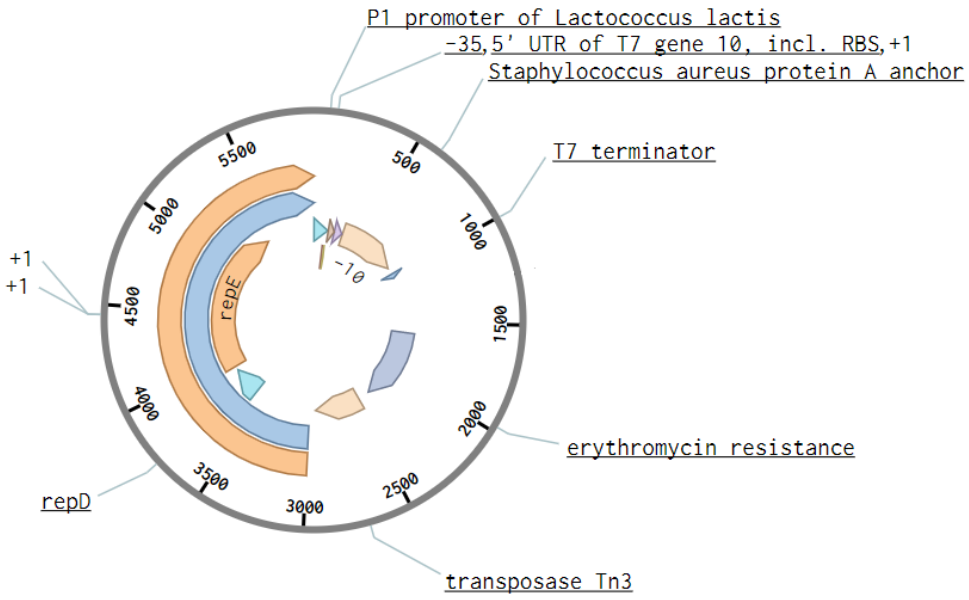

Figure 3.2. Annotated plasmid map of pT1NX. The plasmid features the P1 lactococcal promoter, the *S. aureus* protein A anchor (spaX), the T7 terminator, as well as an erythromycin resistance gene.

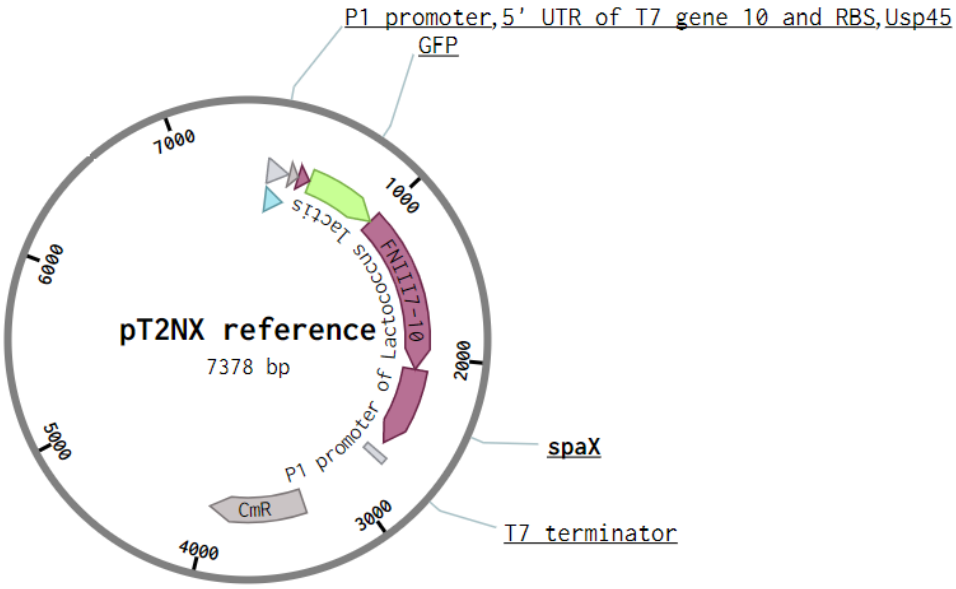

Figure 3.3. Plasmid map of pT2NX. The plasmid bears the P1 promoter of *Lactococcus lactis*, the T7 terminator and a chloramphenicol (Cm) resistance gene. The plasmid also features the FN $III_{7\text{-}10}$ gene that is fused to the *S. aureus* protein A and GFP.

This work was largely based on modifying the pT2NX plasmid to produce different recombinant proteins in *L. lactis*. Since CXCL12 and TPO are secreted cytokines, we removed the *S. aureus* protein A anchor from pT2NX and inserted the proteins in-frame after the Usp45 secretion peptide. This peptide was selected since the *usp45* gene of *L. lactis* encodes the major extracellular protein of lactococci, and hence Usp45 has been used in a variety of studies to produce secreted recombinant proteins in *L. lactis*[376]. In contrast, to achieve presentation of VCAM-1 and the FN fragment $III_{7\text{-}10}$ on the bacterial cell wall, we cloned the cell adhesion protein after the anchor. To achieve maximum efficiency of recombinant protein production in *L. lactis*, the proteins of interest were first optimised for expression in our vector system using an online codon optimisation tool, provided by Integrated DNA Technologies (IDT, Belgium)[377]. Furthermore, to allow easier protein quantification, a 6xHis tag was added to either the N or the C-terminus of the optimised sequences, depending on the positioning of the signalling part of each protein. A comprehensive list of the genetic elements used in this work is displayed in supplementary table 1. After codon optimisation for expression in *L. lactis*, the whole human CXCL12 and TPO genes as well as the extracellular, biologically active fragment of VCAM-1 (purchased from IDT as double-stranded, uncloned DNA gBlocks) were cloned in the pT2NX plasmid. The primers used for cloning are described in table 3.1. The plasmid and primer design was performed using Benchling, a commercial cloud-based bioinformatics platform[378] and the final constructs were created using Gibson assembly in a way that will be described in more detail in the relevant section. Finally, the plasmids containing the genes of interest were transformed into electrocompetent *L. lactis* NZ9020, according to the methods described below.

Primer	5'-3' sequence	3' annealing temperature
CXCL12 Forward	CCCATCACCACCATCATCACATGAATGCAAAAGTTGTTGT	54°C
CXCL12 Reverse	TTGTCTTCCTCTTTTGGATCTTATTTATTCAATGCTTTTTCA	54°C
pT2NX for CXCL12 Forward	AAAAAGCATTGAATAAATAAGATCCAAAAGAGGAAGACAACA	63°C

pT2NX for CXCL12 Reverse	ATGTGATGATGGTGGTGATGGGCGTAAACACCTGACAACG	63°C
TPO Forward	CGTTGTCAGGTGTTTACGCCATGGAGTTAACCGAACTTCT	61°C
TPO Reverse	TTAGTGATGATGGTGGTGATGTCCCTCCTGACTAAGGTTTTG	61°C
pT2NX for TPO Forward	CATCACCACCATCATCACTAACTAGTAGATCCGGCTGCTAAC	65°C
pT2NX for TPO Reverse	AGAAGTTCGGTTAACTCCATGGCGTAAACACCTGACAACG	65°C
VCAM-1 Forward	CGTTGTCAGGTGTTTACGCCTTCAAGATAGAGACTACGCC	61°C
VCAM-1 Reverse	GCCGTGATGATGGTGGTGATGCTCCGGTGAAAAGTAATCTTT	61°C
pT2NX for VCAM-1 Forward	CATCACCACCATCATCACGGCGATCCAAAAGAGGAAGACAACAAC	65°C
pT2NX for VCAM-1 Reverse	GGCGTAGTCTCTATCTTGAAGGCGTAAACACCTGACAACG	65°C

Table 3.1. Primers for the cloning of CXCL12, TPO and VCAM-1 in pT2NX.

3.2.2. Preparation of electrocompetent *L. lactis*

A 5 mL culture of plasmid-free *L. lactis* was grown overnight at 30°C in M17 medium (Formedium) supplemented with 1 % v/w glycine, 0.5 M sucrose and 0.5% w/v glucose. The following day, the whole culture was transferred into 200 mL of fresh M17 with 1 % v/w glycine, 0.5 M sucrose and 0.5% w/v glucose and was incubated at 30 °C until it reached an optical density (OD) of 0.2-0.3 at 660 nm. The cells were then harvested by centrifugation at 3,000 g for 10 minutes at 4 °C. This pellet was washed 3 times in a sterile ice-cold solution of 10 % v/v glycerol and 0.5 M sucrose in ultrapure water. Following the washes, the cells were resuspended in 1 % of the same wash solution and aliquoted at volumes of 50 µL, flash-frozen in liquid nitrogen and stored at -80°C. Freshly made electrocompetent cells are reported to keep their competency for at least 6 months[379].

3.2.3. Polymerase chain reaction (PCR)

Polymerase chain reaction (PCR) is a nucleic acid amplification technique that is based on the ability of a thermostable DNA polymerase to synthesize a new strand of DNA complementary to the provided template strand. This is an automated process based on the activity of the heat resistant DNA polymerase from the thermophilic bacterium, *Thermus aquaticus* (Taq) and is able to create thousands of identical copies using a simple set of reagents and a basic heating and cooling (denaturing and annealing) thermocycling machine. Because DNA polymerase can add a nucleotide only onto a pre-existing 3'-OH group, it requires the use of a set of primers that anneal at the upstream 5’ and downstream 3’ ends of the target DNA fragment to be amplified. Provided with a mix of free deoxynucleosides triphosphate containing adenine (dATP), cytosine (dCTP), guanine (dGTP), thymine (dTTP), the forward and reverse primers (3’ and 5’ annealing primers) and the appropriate buffer, Taq polymerase can amplify the DNA sequence between the two primers during a series of denaturing and annealing steps. In this work the commercially available Q5 high-fidelity polymerase (New England Biolabs) was used.

The general steps of the PCR involve an initial denaturation step for 30 seconds at 98 °C, a denaturation step for 30 seconds at 98 °C, an annealing step based on the primer sequence, a fragment extension step at 72 °C with time depending on the length of the amplified fragment and a final extension at 72 °C for 2 minutes. All PCRs were performed in a ProFlex PCR thermocycler (Applied Biosystems).

Specifically, the cycles and temperatures used for the amplification of the plasmids and CXCL12, TPO and VCAM1 used in this work are presented in table 3.2.

Step	CXCL12	pT2NX for CXCL12	TPO	pT2NX for TPO	VCAM1	pT2NX for VCAM1
Denaturation	1 x 98 °C, 30 sec	1 x 98 °C, 30 sec	1 x 98 °C, 30 sec	1 x 98 °C, 30 sec	1 x 98 °C, 30 sec	1 x 98 °C, 30 sec
Denaturation	35 x 98 °C, 10 sec	35 x 98 °C, 10 sec	35 x 98 °C, 10 sec	35 x 98 °C, 10 sec	35 x 98 °C, 10 sec	35 x 98 °C, 10 sec
Annealing	35 x 57 °C, 30 sec	35 x 65 °C, 30 sec	35 x 61 °C, 30 sec	35 x 65 °C, 30 sec	35 x 61 °C, 30 sec	35 x 65 °C, 30 sec
Extension	35 x 72 °C, 17 sec	35 x 72 °C, 2’ 40’’	35 x 72 °C, 35 sec	35 x 72 °C, 2’ 40’’	35 x 72 °C, 1’ 10’’	35 x 72 °C, 2’ 40’’
Final Extension	1 x 72 °C, 2 mins	1 x 72 °C, 2 mins	1 x 72 °C, 2 mins	1 x 72 °C, 2 mins	1 x 72 °C, 2 mins	1 x 72 °C, 2 mins

Table 3.2. PCR setups. Details of the PCR cycles performed to amplify the CXCL12, TPO and VCAM1 sequences, as well as their respective plasmids.

Following the PCR, the size of the DNA fragments amplified can be purified and evaluated by gel electrophoresis. For PCR purification, we used the QIaquick PCR Purification Kit (Qiagen, ref: 28104), according to the provider’s instructions. Briefly, 5 volumes of binding buffer PB were added to the PCR mix, which was then transferred to a QIaquick column. The column was centrifuged at >16,000 g for 60 seconds. 750 µL of washing buffer PE was then added to the sample, and the column was centrifuged again and dried. Finally, 50 µL of 10 mM tris-HCl buffer was added in order to elute the DNA, and the column was centrifuged again for 2 minutes. The purified PCR mix was then run in an agarose gel to determine the size and yield of the fragments of interest.

3.2.4. Gibson Assembly (GA)

Developed by Dr Daniel G. Gibson, this exonuclease-based method can be used to assemble DNA seamlessly and in the correct order and has been used in this work to incorporate the proteins of interest into a plasmid vector. This isothermal reaction features three enzymatic activities: a 5’ exonuclease that generates long overhangs, a polymerase that fills in the gaps of the annealed single strand regions, and a DNA ligase that seals the nicks of the annealed and filled-in gaps[380]. A schematic overview of the process is depicted in figure 3.4.

In this work, we used the Gibson Assembly Master Mix (New England Biolabs, ref: E2611L). Briefly, the PCR amplified fragments and vectors of interest were mixed at a ratio of 2:1 with an equal volume of Gibson Assembly Master Mix. The reaction was incubated for 20 minutes at 50 °C and the assembled construct was transformed into electrocompetent *L. lactis*.

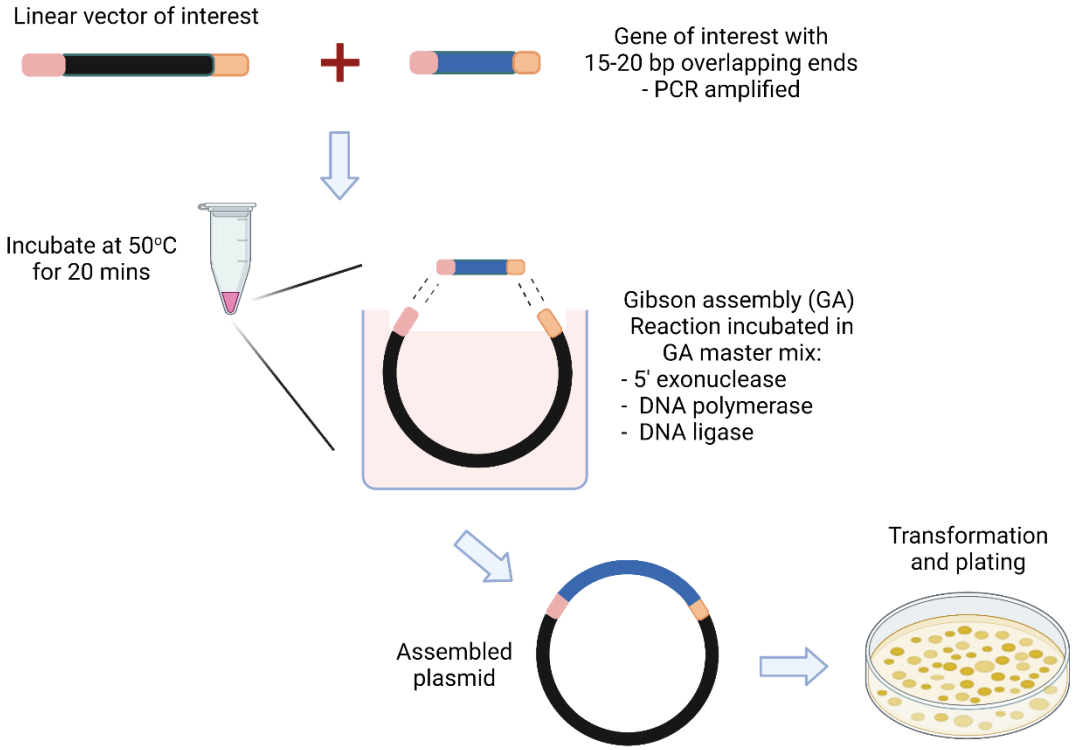

Figure 3.4. Gibson Assembly overview. The 5´ T5 exonuclease chews back the 5´ end sequences, exposing the complementary sequence for annealing. A Phusion DNA polymerase then fills in the gaps on the annealed regions and a Taq DNA ligase seals the nick and covalently links the DNA fragments together.

3.2.5. Transformation of electrocompetent *L. lactis*

Electrocompetent *L. lactis* NZ9020 were thawed on ice for 10 minutes prior to transformation. 100 ng of the plasmid of interest was added to the cells, that were then transferred to a chilled 1-mm gap electroporation cuvette (VWR). A 2000 V pulse was applied to the cell suspension with a time constant of around 5 msec, using an Eppendorf Eporator® (Eppendorf), to allow the insertion of the plasmid into the bacterial cell. The bacteria were then rapidly transferred into chilled recovery medium, made up of M17 containing 0.5% w/v glucose, 20 mM $MgCl_2$, and 2 mM $CaCl_2$. After 5 minutes of incubation

in the recovery medium on ice, the bacterial suspension was incubated at 30°C for two hours. The bacteria were harvested by centrifugation at 3,000 g for 3 minutes and plated on M17 agar selection plates containing 0.5% w/v glucose and 10 µg/mL chloramphenicol.

3.2.6. Plasmid isolation from *L. lactis*

After the protein of interest was inserted into the plasmid and the plasmid assembly was transformed in *L. lactis*, our next step was to isolate this plasmid to sequence it. This process is crucial in order to verify the insertion of the correct DNA sequence at the precise location in the plasmid. To do that, we used the QIAprep Miniprep system (Qiagen), that is based on DNA adsorption on a silica membrane in the presence of high salt and allows for efficient plasmid purification from a cell lysate. Initially, a 10 mL overnight culture of *L. lactis* expressing the plasmid of interest is centrifuged at 3000 g for 5 minutes. The pellet is washed once with PBS and transferred to a solution containing 30 mg/mL lysozyme that helps hydrolysing the polysaccharide cell wall. After a 30-minute incubation at 37 °C in a ThermoMixer C (Eppendorf) shaking incubator, the cells are pelleted at 7,000 g for 3 min and processed using the kit's instructions. The protocol is an adaptation of the usual alkaline-SDS lysis where 250 µL NaOH 0.2 M and 3% SDS is used to solubilize the membrane and denature the proteins and genomic DNA present in the sample. Then 350 µL sodium acetate 3M at pH 4.8 is added to precipitate the solubilized proteins, membrane and genomic DNA while the supercoiled plasmid DNA renatures and stays in solution. The mix is centrifuged at 12,000 g for 10 minutes to pellet the insoluble debris.

The supernatant, containing the plasmid, is then transferred to a QIAprep 2.0 silica spin column that retains the plasmid during two consecutive washing steps with buffer PE, until the plasmid is eluted using nuclease-free water or 50 mM Tris-HCl at pH 8.5. More precisely, the DNA binds to the silica membrane in the presence of high concentrations of chaotropic salts, in a process driven by dehydration and hydrogen bond formation, which competes against weak electrostatic repulsion. During the elution step, these salts are removed with an alcohol-based solution and the DNA is released from the membrane using a low-ionic-strength solution such as Tris buffer or water. The concentration of the plasmid is then measured using a nanodrop UV-visible spectrophotometer (ThermoFisher) and its size is assessed using agarose gel electrophoresis.

3.2.7. Agarose gel preparation

0.8 % agarose (Bio-Rad) gels were used to visualise the PCR fragments, as well as the linearised plasmids used in this work. Briefly, 1 µg of plasmid was mixed with gel loading dye (Qiagen) and was added to the agarose gel stained with SYBR safe (Invitrogen). 2-Log DNA Ladder (0.1-10 KB) (New England Biolabs) was added as a marker and gels were run at 120V until the bands of the ladder could be seen separately. The gel was visualised using a Bio-Rad GelDoc XR gel imager using a 365 nm UV light source.

3.2.8. Plasmid sequencing

Samples were sent to Source Bioscience using the Sanger SpeedREAD™ service. 100 ng/µL of plasmid DNA and 3.2 pmol/µL of the primer shown in table 3.3 was sent to the service and these were sequenced using standard Sanger sequencing. In brief, the process involves the generation of DNA fragments of different lengths and their separation by gel electrophoresis. The labelled nucleotides at the end of each fragment are then excited by a laser and the light emitted by each excited nucleotide can be tied to the correct base. The chromatograms generated by this sequencing method were aligned to the *in-silico* sequences using the Clustal Omega algorithm integrated on the Benchling online software platform.

Primer	**Sequence**
pT2NX	cgttgtcaggtgtttacgcc

Table 3.3. Primer for sequencing of the pT2NX plasmid.

3.2.9. Isolation of cell wall-associated proteins from *L. lactis*

The amount of VCAM1 produced by *L. lactis* was determined by according to the protocol *Isolation and solubilization of gram-positive bacterial cell wall-associated proteins*, described by Cole et al (2008)[381]. An overnight culture was transferred to a sterile centrifuge tube and the cells were harvested by centrifugation at 7560g for 20 mins at 4 °C. The supernatant was discarded and the pellet was placed on ice for 5 minutes. The bacteria were resuspended in 5 mL of cold TE buffer (50 mM Tris-HCl, 1 mM EDTA, pH 8.0) containing 1mM phenylmethylsulfonyl fluoride (PMSF, Sigma). The cells were centrifuged at 7,560 g for 20

mins at 4°C and the wash step was repeated twice. Next, the mutanolysin mix was prepared by dissolving 10,000 units of chromatographically purified mutanolysin from *Streptomyces globisporus* (Sigma) in 2 mL of chilled filter sterilised 0.1 M K_2HPO_4 (pH 6.2) to prepare a working solution of 5,000 units/mL. The bacterial pellet was resuspended in 1.15 mL of ice-cold mutanolysin mix, followed by incubation for 2h at 37°C with shaking (200 rpm). After the incubation step, the cells were spun at 14,000 g for 5 mins at room temperature, and the supernatant containing the previously membrane-associated proteins of interest was collected. Mutanolysin cell wall extracts can be stored for at least 2 years at –20 °C.

3.2.10. Enzyme Linked Immunosorbent Assay (ELISA)

To detect and characterise the levels of recombinant protein production by *L. lactis*, we used the His Tag ELISA Detection Kit from GenScript. In this assay, a His-tagged protein of known molecular weight (M.W. 12.7 kD) is pre-coated on the microwell plate provided. 50 µl of His Tag protein standard of varying concentrations provided in the kit or samples containing His-tagged proteins was added to each well, followed by an addition of 50 µL of Anti-His monoclonal antibody. In this work, the samples used were either the supernatant of *L. lactis* cultures expressing the soluble proteins CXCL12 and TPO, or the cell wall extracts from cultures, obtained after the mutanolysin-mediated extraction of cell wall associated proteins, in the case of VCAM1. The plate was sealed and incubated at room temperature for 30 minutes. Each well of the plate was then washed three times with 250 ul washing solution. After the final washing step, all residual liquid was removed from the wells by patting the plate on a dry paper towel. Next, 100 µL of antibody tracer was added to the wells and the plate was sealed again and incubated at room temperature for 30 minutes. After the incubation, the washing steps were repeated and again the plate was dried as described above. 100 µL of 3,3’,5,5’-tetramethylbenzidine (TMB) substrate was added to the wells and the plate was incubated at room temperature for 10-15 minutes. The rection was stopped by adding 50 µl of stop solution to each well and the absorbance of the plate was read on an Infinite 200 PRO NanoQuant Plate Reader (Tecan) at 450 nm. After the reaction, a standard curve was generated by plotting the absorbance on the vertical axis versus the His-tagged standard concentration on the horizontal axis. The amount of His-tagged protein

in the samples is then determined by extrapolating the absorbance value of each sample to the standard curve.

3.3. Results

In order to create a biointerface-based system for the study of stem cell behaviour, we selected to conduct our experiments using the NZ9020 strain of *L. lactis*. Compared to other *L. lactis* strains, NZ9020 is a more suitable candidate for bacterial and mammalian cell co-cultures as two out of its three lactate dehydrogenase (*ldh* and *ldhB*) genes have been knocked out[382]. This resulting *ldh*$^-$ mutant strain is associated with a significantly reduced lactate production as a fermentation end product. This is vital for our work, as a high production of lactic acid would drastically reduce the pH of the medium, rendering the conditions unsuitable for a bacterial and mammalian cell co-culture. Therefore, use of the NZ9020 strain contributes to the maintenance of a more stable, neutral pH in the culture system. The strain originates from the NZ9000 strain of *L. lactis*, where the two missing *ldh* genes have been knocked out and as a part of the gene editing process the strains shows erythromycin and tetracycline resistance.

3.3.1. Protein production and characterisation

We have selected four key proteins that are present in the BM and contribute to HSC maintenance and homeostasis and have produced them in *L. lactis* NZ9020. These signalling factors (CXCL12, TPO, VCAM1 and FN) have been constitutively produced by the bacteria, in the pT2NX plasmid and under the regulation of the P1 lactococcal promoter. Initially, we designed the sequences for human CXCL12 and TPO, as well as the extracellular segment of VCAM1, that contains the signalling part of the peptide, for production in our bacteria. All gene sequences were codon optimised for expression in *L. lactis*. The optimised sequences of CXCL12, TPO, VCAM1 and the FN $III_{7\text{-}10}$ fragment were obtained from Uniprot. For simplicity purposes, we refer to the bacteria populations by the protein they are expressing, (eg, the CXCL12-expressing *L. lactis* population is referred to as CXCL12, and *L. lactis* expressing the FN $III_{7\text{-}10}$ fragment is referred to as FN). A schematic representation of the recombinant proteins produced by *L. lactis* used in this work and the promoter-His-tag-protein assemblies is depicted in figure 3.5. To facilitate protein detection and

characterisation, our sequences were tagged with a His-tag in either the N- or C-terminal of each protein, depending on the positioning of the signalling part of each molecule. Furthermore, for efficient attachment of VCAM1 and FN to the extracellular membrane of *L. lactis*, we used the *S. aureus* protein A domain (SpA). This anchor peptide contains the LPXTG motif, that can be recognized and cleaved by the membrane-bound transpeptidase sortase A (SrtA), and subsequently covalently incorporated into the peptidoglycan layer of *L. lactis*, resulting in the presentation of the protein of interest on the extracellular membrane of the bacterial cell wall[300]. All engineered proteins have been fused to the Usp45sp signal peptide that allowed for their secretion by the bacteria[383].

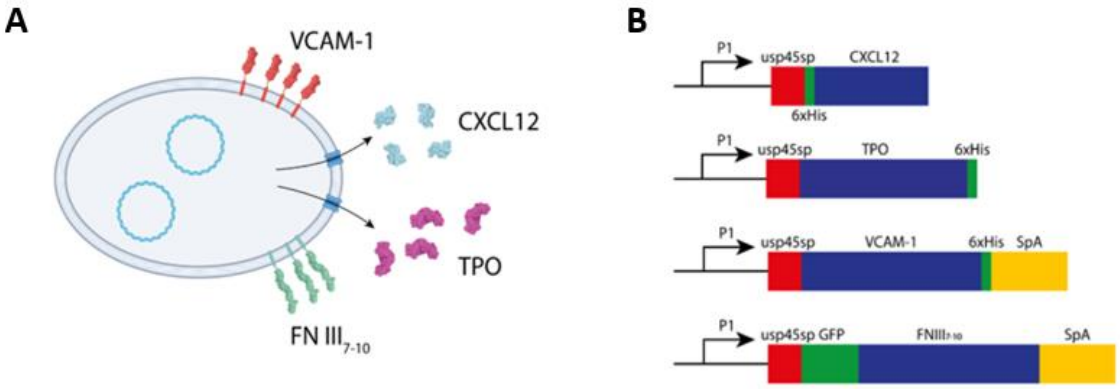

Figure 3.5. Recombinant protein production in *L. lactis*. (A) *L. lactis* NZ9020 was transformed with plasmids carrying ORFs for human CXCL12, TPO, VCAM-1 and FN III7-10. TPO and CXCL12 were secreted extracellularly using the lactococcal Usp45 secretion peptide. VCAM-1 and $FNIII_{7-10}$ were cloned upstream the *S. aureus* protein A domain (SpA). (B) Schematic of the plasmid constructs. All proteins were placed under the control of the constitutive lactococcal P1 promoter followed by the phage T7 gene 10 RBS. Usp45sp was used as a secretion signal, followed by the gene of interest and *S. aureus* protein A for cell wall binding.

After the genes encoding the proteins of interest and the plasmid were obtained and amplified, we assessed the success of the PCR by agarose gel electrophoresis. This technique separates fragments by size using an electric current that will pull the negatively charged DNA fragments towards the positive end of the gel. The gel is then visualised and the different DNA fragments can be seen as individual bands, the sizes of which are determined by comparing them to a standard of known molecular weight.

As shown in image 3.6, the pT2NX as well as the DNA sequences that encode for the selected proteins have been correctly amplified as they have the expected length when

compared to a pre-stained protein ladder containing known molecular weight proteins. As shown in the imaged gel, the plasmid and our proteins of interest have the correct length in base pairs that is displayed in table 3.4.

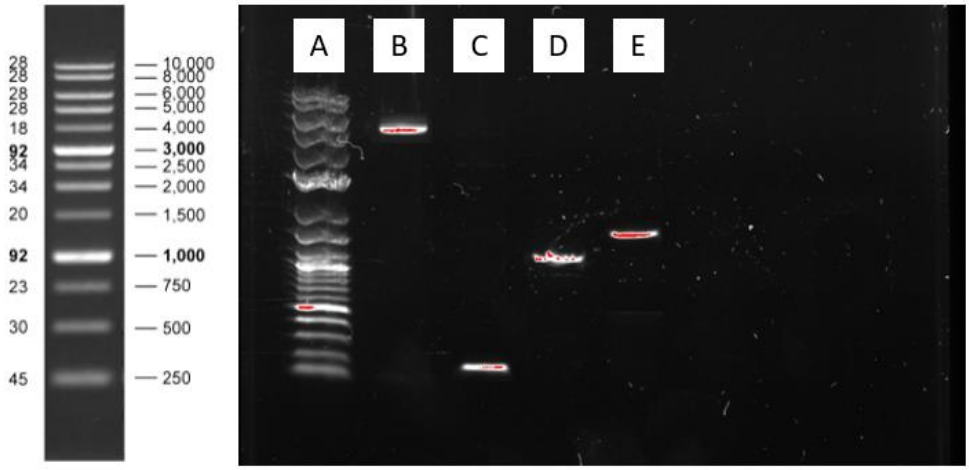

Figure 3.6. Gel electrophoresis image featuring the amplified nucleotide sequences of pT2NX, CXCL12, TPO and VCAM1. A) 2-log DNA ladder (NEB), B) pT2NX, C) CXCL12, D) TPO, E) VCAM1 amplicons. A descriptive depiction of the DNA ladder and the band sizes (left) and base pairs (right) are also shown on the left part of the image.

DNA Fragment	**length**
pT2NX	5764 bp
CXCL12	288 bp
TPO	1080 bp
VCAM1	2043 bp
FN	1107 bp

Table 3.4. The length in base pairs of the pT2NX plasmid and the DNA sequences encoding the four proteins used in this work.

After the verification of the correct plasmid and insert size, the two parts were ligated using Gibson assembly[384] and the end construct was transformed into *L. lactis* NZ9020. After the electroporation, transformants were seeded on selective plates, individual colonies were picked and cultured in GM17-C medium and plasmid was isolated and sequenced. The sequencing results were analysed on the Benchling online platform and were compared to the original sequences. A match between the compared sequence ensures that the original

DNA sequence has been incorporated in a correct manner in the specified region of the plasmid according to our original design. The proteins expressed in NZ9020 are fused with a 6xHis-tag to facilitate their detection and quantification. The levels of protein expressed by the bacteria were assessed using a His-tag ELISA assay. This was performed on the supernatant of standing bacteria cultures, obtained during the stationary phase in the case of CXCL12 and TPO, and at the lysate obtained from the isolation and solubilization of the bacterial cell wall-associated proteins in the case of VCAM1. CXCL12 was produced at 280.32 ng/mL, TPO at 175.4 ng/mL and VCAM1 at 99.18 ng/mL (figure 3.7 A). Furthermore, the recombinant protein concentration was measured in biofilms, where different populations of NZ9020 producing different proteins were co-cultured in the same biofilm. After 3 days of culture, the protein concentration was assessed using a His-tag ELISA assay, in the same way as the quantification of the individual expressed proteins. Different combinations of the populations produced different levels of 6xHis-tagged proteins when the bacteria were cultured in biofilms, as shown in figure 3.7 B. The difference between protein levels in graphs C and D is based on the directly proportional relationship between the number of bacteria and the amount of recombinant protein produced; standing cultures produce much higher protein quantities (A) than biofilms (B). Furthermore, some variation can be noted between the different combination of strains on each biofilm. This can be attributed to the difference on the absolute number of bacteria in each condition, as the procedure of biofilm formation is not a standard method and depends highly on uncontrollable variables that can affect the number of bacteria that attach to our substrate and form the biofilm, the strength of that attachment and any potential bacterial dissociation from the biofilm during the washing steps. In any case, the level of protein produced by the biofilms falls within the physiologically relevant range that has been observed in the bone marrow of mice[385]. More precisely, CXCL12 has been measured to be produced at around 220 ng/ml in the murine BM, while no absolute expression values have been determined for VCAM1, TPO or FN in the BM[386].

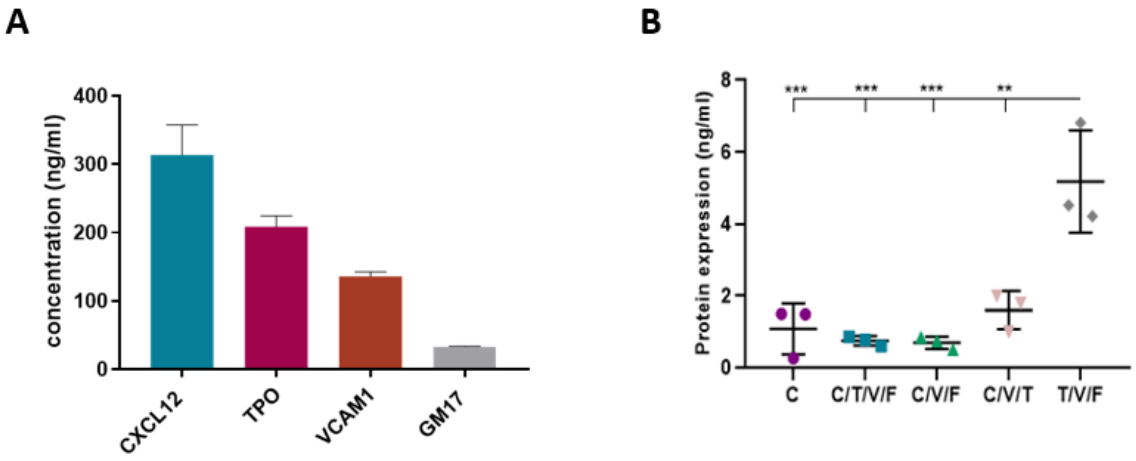

Figure 3.7. Recombinant protein production by *L. lactis* NZ9020. A) Protein was isolated from a standing culture of *L. lactis* NZ9020, during the stationary phase. Quantification was performed using a His-Tag ELISA. B) Protein production measured after 3 days of culture in NZ9020 biofilms. Statistical differences were determined using a one-way ANOVA with a Tukey post-hoc test and an alpha = 0.05 between the conditions are depicted using asterisks, where: *p < 0.05, **p < 0.01 and ***p < 0.001.

3.3.2. Growth monitoring of the different bacterial populations

In order to closely mimic the BM microenvironment, different combinations of the recombinant cytokines had to be provided to the system and the cultured HSC at the same time. Therefore, it was necessary to co-culture different bacterial populations that express different recombinant proteins at the same time, in the same biointerface. To make sure that this is possible and make sure that no one bacterial population would outcompete the others, we measured the growth kinetics of each population. Same amounts of overnight cultures of CXCL12, TPO, VCAM1 and FN $III_{7\text{-}10}$ expressing NZ9020 were cultured for 1000 minutes and the OD_{600} of each was measured every 10 minutes (figure 3.8).

As shown, all bacterial growth curves follow the same trend, however, there are apparent differences between the growth rates of different populations (figure 3.8 A). While the EMPTY, CXCL12 and TPO-producing bacteria grow at very similar speeds, the VCAM1 and FN-producing population seem to have an observably slower growth rate. This lower growth rate is supported by the lower growth constant values and higher doubling times (figure 3.8 B), suggesting that these two protein fragments pose a higher metabolic burden to *L. lactis*. This difference between the strains is expected and is directly proportional to the size and complexity of each molecule produced by the bacteria. In the case of CXCL12 and TPO, the

small size of the proteins does not significantly impact the growth kinetics or metabolism of *L. lactis* when compared to the EMPTY bacteria. In contrast, the larger, more complex VCAM1 and FN have a noticeable effect on the bacterial growth and doubling time. Nevertheless, this effect can be managed by the use of the antibiotic mix described in section 3.3.3, that was developed and used in this work. This works by slowing down the bacterial metabolism, maintaining *L. lactis* in a lower metabolic state that permits recombinant protein production but restricts cell doubling.

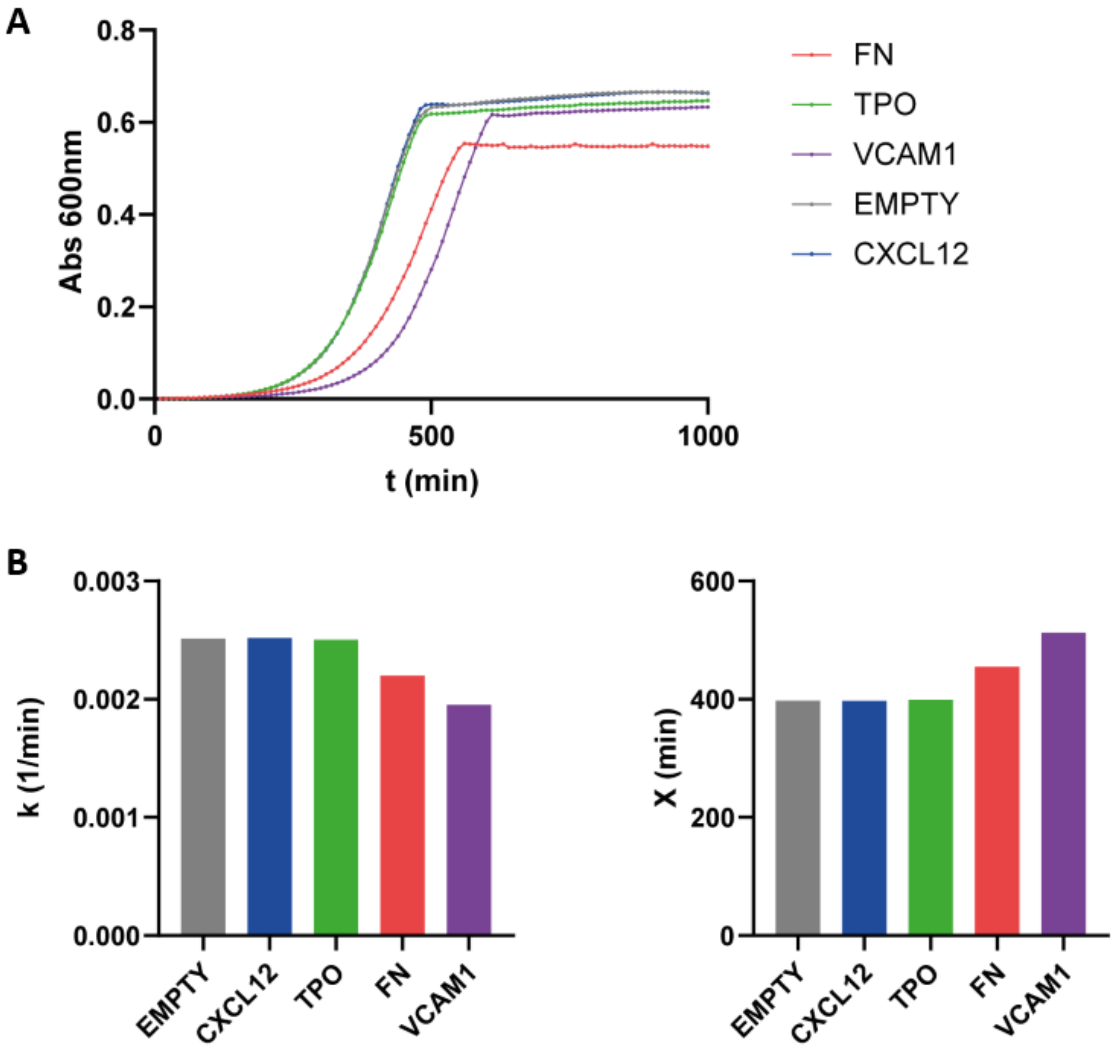

Figure 3.8. Growth kinetics of *L. lactis* populations. A) Growth kinetics, as absorbance measured at λ=600 nm over the course of 1000 minutes every 10 minutes. The strains expressing TPO, CXCL12 and the control strain present similar kinetics in terms of growth constant k and shorter doubling time. As expected per values shown in C), CXCL12 and TPO-producing strains show higher expression levels compared to VCAM-1, where lower growth constant values and higher doubling times suggest that the expression VCAM-1 and FN impose a higher metabolic burden on the cells, consequentially yielding lower protein expression.

3.3.3. Biofilm viability characterization

This work is largely based on the ability of *L. lactis* NZ9020 to form biofilms and produce the recombinant proteins of interest in order to induce specific stem cell behaviours. To achieve this, we first evaluated the ability of *L. lactis* to form biofilms that remain viable and produce detectable amounts of the engineered proteins.

Previous in-house studies have suggested that the longest HSC culture time that can be achieved without the need for a media change is 5 days, therefore, it was of paramount importance to ensure that the biofilms remain viable for this length of time. Previous work on biofilm formation on coverslips for co-culture experiments has suggested that *L. lactis* forms biofilms and remains viable on glass coverslips for up to 4 days[387]. Despite the hydrophilic nature of glass, it has become apparent that uncoated surfaces result in weak adhesion forces, that are insufficient for the retention of the bacteria in a monolayer for longer periods of time. To overcome this obstacle, previous work has supported that the use of the synthetic polymer poly (ethyl acrylate) (PEA) as a coating for glass coverslips results in increased biofilm stability that lasts over 4 weeks, with the viability remaining unaffected[187]. For the purpose of our study, we required a coating that enables a longer biofilm attachment than glass but without necessarily as high adhesion dynamics as PEA offers. Moreover, the hydrophobicity of the coating had to be considered, as it has been described as an important factor in mediating bacterial adhesion on substrates[388]. Given the naturally hydrophobic surface of the bacterial strain *L. lactis* NZ9020 used in this work[389] and the hydrogen-bonding forces that would surround the hydrophobic moieties, selecting a more hydrophobic substrate than glass could provide a stronger attachment for the bacteria[390].

The effect of hydrophobicity on surface interaction dynamics has been described in detail in the extended Derjaguin-Landau-Verwey-Overbeek model (XDLVO)[391]. In terms of the interactions between the bacterial cells and the substrate, the model describes a two-step adhesion process. Initially, the electrostatic repulsion between the negatively charged cell and surface create an energy barrier that allows the bacteria to approach but not directly interact with the substrate. Once the bacterial cell approaches the surface closer, it enters a lower repulsive energy barrier that allows for a first, reversible approach and interaction between the bacteria and the substrate. Once attached, the bacteria will start producing adhesion structures, such as pili, fimbriae and lipopolysaccharides, that will encourage the

adhesion of other bacteria and the ultimate formation of a biofilm[392,393]. Biofilms are be formed on most natural substrates[394] and their formation time and mechanics depend on a variety of factors, including nutrient availability, the ionic strength of the medium and properties of the substrate[395]. The stages of biofilm formation are described in figure 3.9.

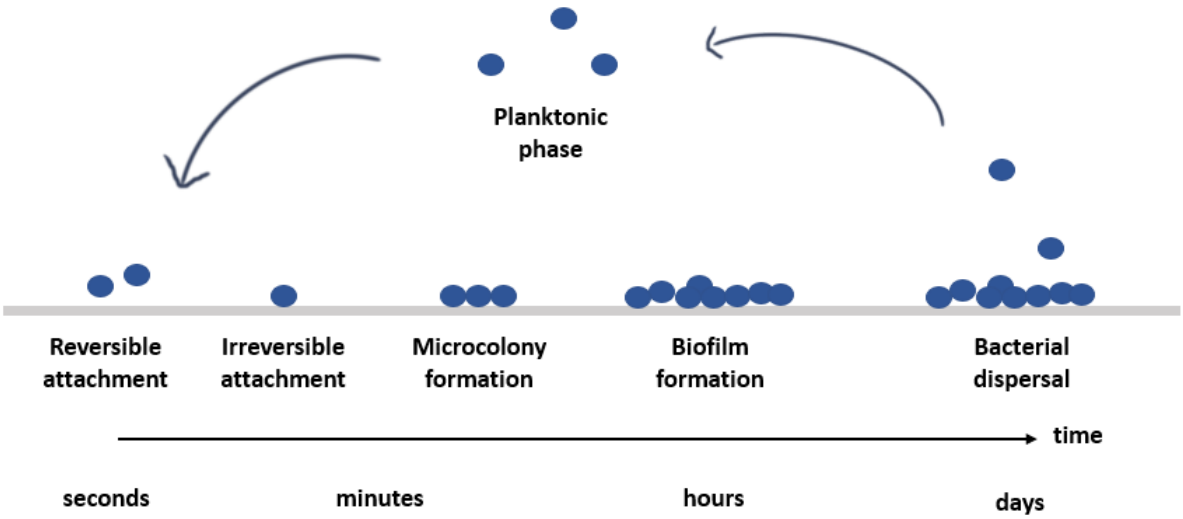

Figure 3.9. The stages of biofilm formation. At an early phase, a few bacterial cells approach and reversibly attach to a given surface. Within minutes, the adherent bacteria initiate the biogenesis of adherent structures that recruit more bacteria and solidify their attachment to the substrate. The formation of the biofilm continues through the stationary phase of the culture. Depending on the strength of the interaction between the biofilm and the substrate, bacterial cells start to detach after a period of time, as the adhesion dynamics between the bacteria and surface drop.

Once in an appropriate medium, *L. lactis* will form biofilms on any available substrate and proliferate continuously. For optimal conditions, the species require the availability of a carbon source, most commonly a sugar, that will be metabolised into lactic acid. This creates a challenge for any system based on a co-culture between *L. lactis* and mammalian cells as extensive bacterial proliferation will both deplete the medium of the starting nutrient and result in a build-up of lactic acid, reducing the pH of the media. To address this issue, previous research has suggested that the use of tetracycline (TC) at 10 µg/mL is sufficient to impede bacterial metabolism without negatively affecting mammalian cells for up to 4 days[387]. This effect is mediated by the binding of the antibiotic to the 30S subunit of bacterial ribosomes that impedes bacterial protein synthesis by restricting the binding of aminoacyl-tRNA (transfer Ribonucleic acid) to the ribosomal acceptor (A) site[396] as shown in figure 3.10.

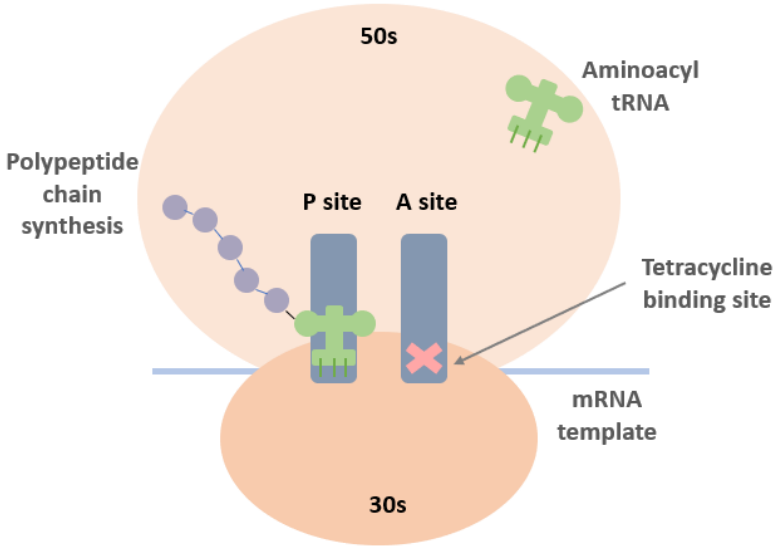

Figure 3.10. Tetracycline mechanism of action. The antibiotic binds to the A site of the 30s bacterial ribosomal subunit, preventing tRNA binding and inhibiting bacterial protein synthesis.

Since a typical HSC culture conducted in this work lasts 5 days and the shortest culture of MSCs that allow for the detection of a start of differentiation is 14 days, it was imperative to develop a method that will prevent bacterial overgrowth, while ensuring that the biofilm remains viable and the recombinant proteins are still secreted. To achieve this, we tested a variety of other antibiotics, for further inhibition of the metabolism of *L. lactis*.

The strain used in this work carries a chloramphenicol (Cm) resistance gene. Therefore, to prevent other bacteria from growing in the media, our culture conditions always include Cm added to the GM17 culture media or any other cell culture media used in each experiment. To test the effect of different antibiotics on *L. lactis* viability, we performed an overnight culture of a NZ9020 biofilm in a variety of different antibiotic conditions. On top of Chloramphenicol, we used sulfamethoxazole (S/le) at a concentration of 5 µg/mL and erythromycin (Ery) at 5 µg/mL, as well as a combination of Tet, S/le and Ery (at 10 µg/mL, 5 µg/mL and 5 µg/mL respectively), named Antibiotic mix. Sulfamethoxazole is a inhibits the synthesis of dihydrofolic acid due to its structural similarity to para-aminobenzoic acid (PABA), an endogenous substrate crucial in folic acid synthesis. The antibiotic competitively inhibits dihydropteroate synthase, the enzyme responsible for bacterial conversion of PABA to dihydrofolic acid, that downstream leads to the inhibition of tetrahydrofolate production and ultimately the synthesis of bacterial purines that lead to the inhibition of DNA

synthesis[397]. On the other hand, erythromycin exerts its bacteriostatic properties by inhibiting protein synthesis. Ery binds to the 23S ribosomal RNA molecule in the 50S subunit of the bacterial ribosome inducing a conformational change that prevents the exiting of the growing peptide chain[398]. This reversible interaction stops bacterial growth through the resulting halt in protein release from the ribosome. This particular property is especially advantageous for use in co-cultures of human and bacterial cells, as human cells have different ribosomes and therefore the antibiotic has no inhibitory effect on mammalian protein synthesis. Furthermore, we used hemin at a concentration of 5 ug/mL as an aerobic metabolism promoter. In *L. lactis* cultures, hemin has been found to suppress lactic acid production indirectly via switching to aerobic respiration and has been used to prevent undesirable shifts of the pH because of bacterial metabolism[399].

In the effort of suppressing or at least diminishing the production of lactic acid, we aimed to maintain a high biofilm viability and density, while also ensuring that the bacteria will not escape the biofilm and overpopulate our co-culture system. Figure 3.11 depicts biofilm behaviour in different *L. lactis* cultures in a variety of antibiotics. More precisely, a biofilm was developed on a sterile glass coverslip and was incubated for 24 hours in GM17 + Cm (base culture medium for *L. lactis*, control) plus another antibiotic of interest or a combination of the tested antibiotics. Our results suggest that NZ9020 viability remained high, above 99% in all conditions (figure 3.11 A, B). A small statistical difference was observed between the viability of the biofilm cultured in the antibiotic mix with the addition of hemin, compared to the culture containing just the antibiotic mix as well as compared to the control. However, this difference is small when the extremely high viability (99.9%) is taken into consideration, so the difference can be ignored for the purpose of our study. Similar differences were observed in the recorded biofilm density between the condition containing hemin and the antibiotic mix, control and media containing Tet. Our experiment recorded a higher number of bacteria per field of view in the media containing the antibiotic mix compared to the other conditions. Nevertheless, a clear biofilm was observed in all conditions. Notably, the viability of the biofilms where the antibiotics were used remained comparable to the control, which is expected, as the antibiotics used in this work only aim to slow down the metabolism of the bacteria and have no bactericidal effect at the concentrations used.

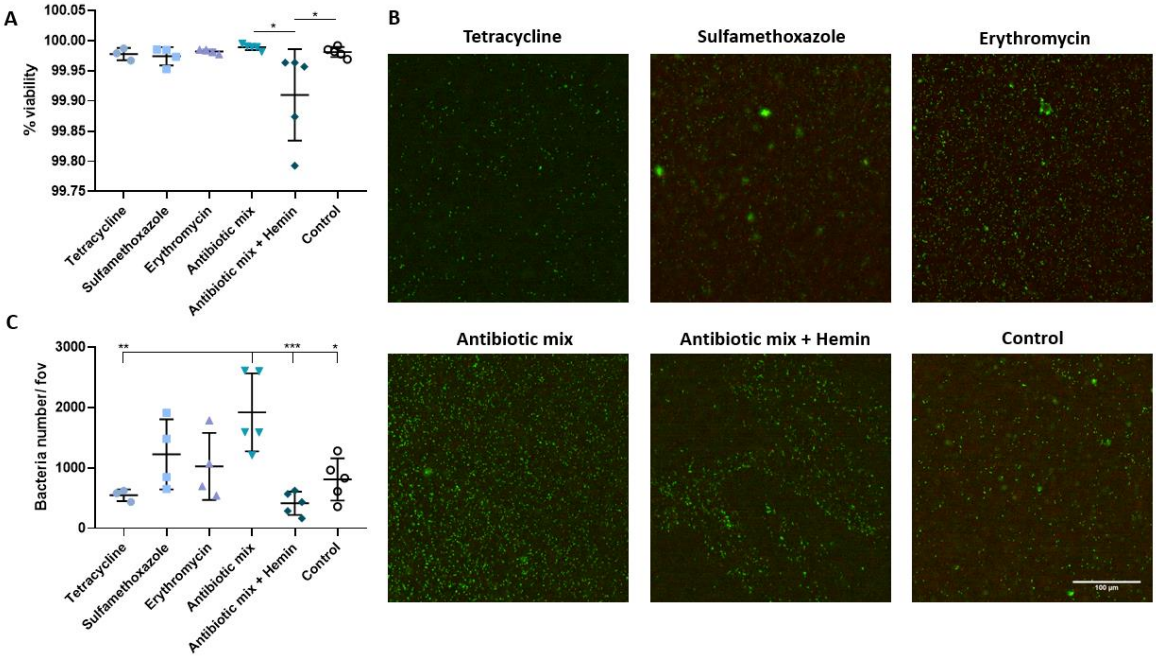

Figure 3.11. Biofilm viability and density in different antibiotics. A) NZ9020 biofilm viability after a 24h incubation in the different antibiotic conditions. Tetracycline, Sulfamethoxazole and erythromycin were used at a concentration of 5 µg/mL, and they were all combined at the same concentrations to make the Antibiotic mix. Hemin was also used at 5 µg/mL. B) Representative images of the bacterial cell viability assay for biofilms in each of the antibiotic conditions, showing live bacteria in green and dead bacteria in red. C) Biofilm density, described by the number of bacteria measured per field of view. All biofilms were cultured in GM17 + chloramphenicol, which is also the condition used as a control, plus the antibiotic of interest described in each condition. Antibiotic mix: GM17 + chloramphenicol + tetracycline + erythromycin. The statistical differences between the conditions, as measured by a one-way ANOVA test, are represented with asterisks, where * $p \leq 0.05$, ** $p \leq 0.01$ and *** $p \leq 0.001$. Scale bar: 100 µm.

Collectively, our results confirm the maintenance of a high biofilm viability in all antibiotics, while also showing that a biofilm can be formed and maintained in all conditions. Yet, when observed under the microscope, some of the conditions revealed a planktonic phase of NZ9020 above the biofilm, which is non-optimal for our system. More precisely, in all conditions except the biofilms cultured in the antibiotic mix with or without hemin bacteria that had escaped the biofilm have been observed. Some enlarged representative images of the bacteria viability assay discussed above clearly demonstrate this issue in figure 3.12. Here, bacteria can be viewed in different planes, a lower plane where the biofilm is attached on the glass coverslip and appear clear and focused and an upper, out of focus plain, where the planktonic bacteria can be seen. Examples of this planktonic phase are demonstrated with arrows in figure 3.12.

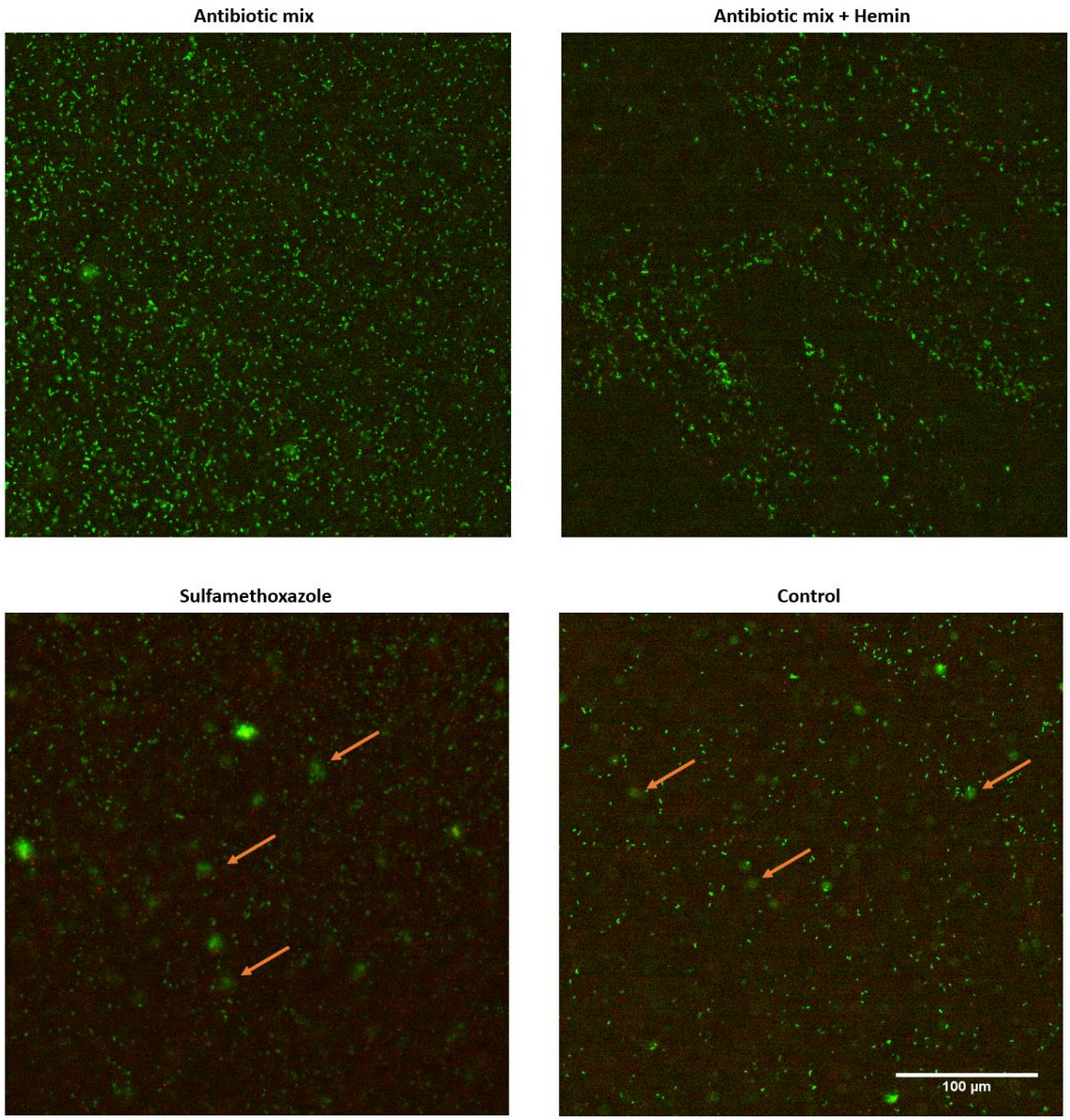

Figure 3.12. *L. lactis* biofilms. In the images in the top row the biofilm has been cultured in base medium plus the antibiotic mix, with or without hemin respectively, and is depicted as a green fluorescent monolayer. In cultures containing only base medium (control) or base medium + Sulfamethoxazole, bacteria appear to escape the biofilm, forming a planktonic phase inside the well (shown with arrows).

Consequently, we have chosen to add the antibiotic mix (Cm, Tet, S/Ie and Ery, at 10 µg/mL, 5 µg/mL, 5 µg/mL and 5 µg/mL, respectively) plus hemin to our co-culture experiments, as this condition has been found to both sustain high biofilm viability and maintain the bacteria in the biofilm and as a monolayer, preventing them from escaping. We chose to control the bacterial growth dynamics using an antibiotic cocktail rather than genetic manipulation

since our system was optimised and aimed at short term cultures, made out of a frozen stock. The timescales of bacteria and stem cell cultures were short enough (< ??) to prevent the development of antibiotic resistance by the bacteria, and since each biofilm was made from a frozen bacterial stock the possibility of the development of antibiotic resistance in our system was negligible. However, we acknowledge that if this system were to be used for longer timescales (e.g. in clinical applications), the possibility of alternative methods of regulating the bacterial growth such as genetic engineering should be considered.

Furthermore, since HSCs are cultured in IMDM media, we tested the viability of biofilms in GM17 and IMDM. In both cases, the biofilms were developed overnight in GM17 and were then either maintained in GM17 or IMDM with media changes every 4 days. The viability was measured after 10 days and the results are displayed in figure 3.13. The fluorescence images represent the visualized results of the Live/Dead assay, after which the live bacteria appear green, while the dead bacteria obtain a red colour upon illumination. The two-colour fluorescence assay used, features the SYTO® 9 green fluorescent nucleic acid stain and the red-fluorescent nucleic acid stain, propidium iodide. While SYTO® 9 penetrates and stains nucleic acids in all cells, propidium iodide penetrates only bacteria with damaged membranes, causing a reduction in the SYTO® 9 stain fluorescence. This results in the retention of the green fluorescent colour by the live bacteria and the red fluorescent colour by the damaged, dead bacteria.

The Live/Dead assay results suggest that the bacteria remain viable after 10 days, while a slight increase in viability is also observed with time. No statistical difference has been observed between the conditions, culture media or timepoints, suggesting that the biofilms can be cultured in either medium and they will retain high viability for the duration of our experiments.

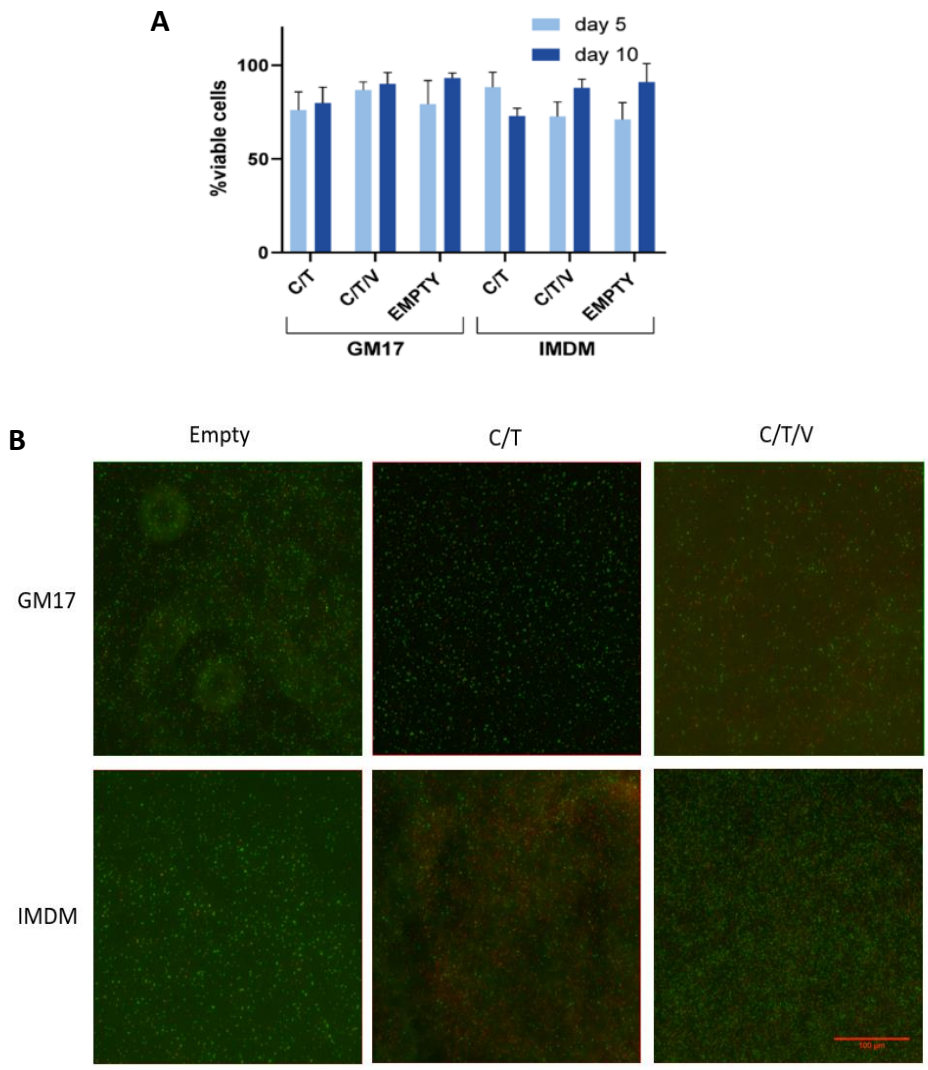

Figure 3.13. Biofilm viability in GM17 and IMDM. (A) viability of the biofilms used in the co-culture experiments, produced by combining CXCL12 (C), TPO (T) and VCAM-1 (V) at different ratios and the control strain, were determined after 5 or 10 days using the FilmTracer viability kit. Viability values do not show a statistically significant difference (p-value ≥ 0.05) between the different strains and time points. (B) Representative images of the Live/Dead assay for biofilm viability after 5 days of culture.

3.3.4. Surface treatment for efficient biofilm production

Despite the ability of *L. lactis* to form viable biofilms on a variety of substrates, these biofilms are often unstable and detach after a few days, depending on the shear forces acting on them[400]. As described above, surfaces with hydrophobic properties display an increased biofilm attachment. In our work, it is imperative that we maximise the strength and time of biofilm attachment to the substrate and avoid the escaping of bacteria from the biofilm, as this will increase the chances of uncontrolled proliferation of the bacteria. This in

turn would result in the complete acidification of the media and its complete depletion from nutrients, something that would negatively impact the survival of the co-cultured mammalian stem cells.

Since the biofilms used in this work have been developed on glass coverslips, we selected two different silanes as coatings and tested their properties in culture. A variety of different coatings have been used in the literature to improve the adhesion and immobilization of cells on different materials[401,402,403]. Two of the most commonly used silanes for such applications are (3-aminopropyl)triethoxysilane (APTES)[404] and Sigmacote[405]. To determine the optimal conditions for the development of stable *L. lactis* biofilms we developed and maintained the bacteria in monolayers on coverslips coated with both silanes for 5 and 10 days. The glass coverslips were initially sterilised by sonication in 70% ethanol and dried at 80 °C, followed by UV-irradiation for 30 minutes. Then the coverslips were coated with the silanes according to the manufacturer's protocols. Biofilms were developed overnight on the different surfaces and the viability as well as the surface covering of each biofilm was assessed as shown in figure 3.14.

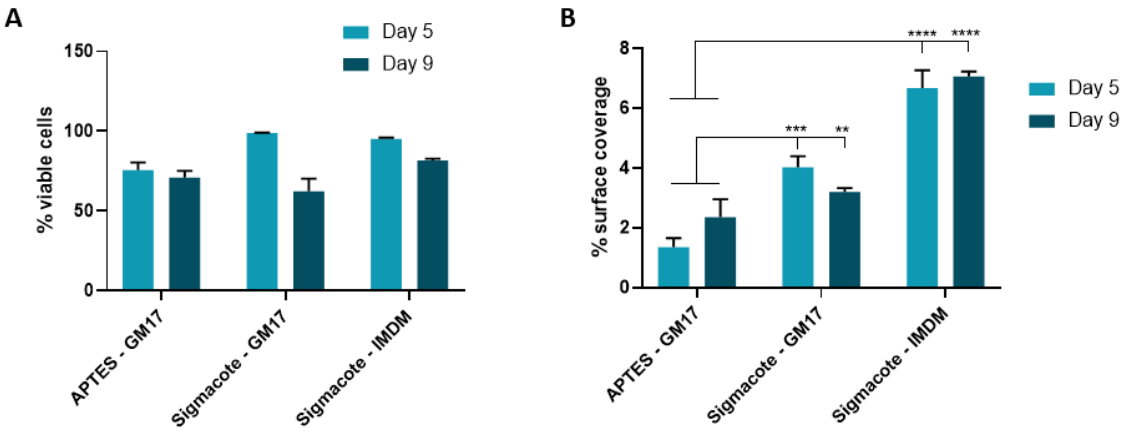

Figure 3.14. Biofilm characterization. (A) Biofilm viability on the different tested surfaces and culture media, in this case GM17 and IMDM were used to compare the different culture conditions and their effect on the bacterial biofilm. No statistically significant differences were found ($p \geq 0.05$) between the different time points or conditions. (B) Biofilm area density, as in percentage of area covered by the bacterial biofilm, was determined for the same conditions used in (A) at the same time points. The results were generated by subtracting the total area of the biofilm that appears as dark spots on the brighfield images, from the total area imaged. Surfaces treated with Sigmacote kept a higher biofilm density compared to APTES, and IMDM showed the higher values. The statistical differences between the conditions, as measured by a one-way ANOVA test, are represented with asterisks, where * $p \leq 0.05$, ** $p \leq 0.01$ and *** $p \leq 0.001$.

Our findings suggest that biofilm viability remained unaffected by either coating (p-value ≥ 0.05) at both time points and in both media (figure 3.14 A). The viability data is consistent with previous research that has indicated that both Sigmacote and APTES can be used in bacterial[406,407] and human cell[408] cultures without displaying any cytotoxic effects. Similarly, bacteria have been shown to be able to colonise a variety of surfaces and successfully form biofilms[409]. This property has proven especially problematic in medical areas, where biofilms of pathogenic bacteria in particular pose a threat to patients and their recovery[410]. In contrast, our work requires that the biofilm remains strongly attached to the substrate so that the bacteria remain in a state of low metabolic activity, ensuring that the media will not be depleted by nutrients and acidified due to excessive bacterial metabolism. Our effort to maintain a balance between a low bacterial metabolic activity and physiologically relevant production of recombinant proteins can be achieved by culturing the biofilm on Sigmacote-treated glass coverslips. According to our results depicted in figure 3.14 B, Sigmacote treatment of our substrate can both achieve a stable biofilm attachment and a higher surface coverage compared to APTES. Compared to the high bacterial viability on the silane coating, Sigmacote has been selected as the coating of preference for the rest of this work.

3.4. Discussion

L. lactis is a non-pathogenic, gram positive lactic acid bacterium that has been used for centuries in food fermentation and the production of dairy products. In recent years, its fully sequenced genome and GRAS characteristics have fuelled research on its potential applications in medicine and healthcare through genetic engineering for therapeutic protein delivery. The wide variety of gene manipulation tools that have been developed for *L. lactis* has enabled both constitutive and inducible production of small molecules and recombinant proteins of interest for specific clinical applications. In recent studies, *L. lactis* has been genetically engineered to produce cancer-fighting cytokines, such as IL-17A[411], anti-human cytotoxic T lymphocyte-associated antigen 4 [412] as well as the KiSS-1 peptide[413], in an effort to fight a variety of cancers including gastrointestinal tract and human papilloma virus (HPV)-induced cancer. Furthermore, *L. lactis* has been also suggested as an effective vaccine delivery vector as it grows very efficiently *in vitro*, it lacks lipopolysaccharide (LPS), its

metabolism and growth or death can directly be mediated with the use of antibiotics, and their genetic material does not integrate into the host genome. According to these attributes, a variety of vaccines have been produced, with the most successful and promising one being a human papillomavirus type 16 E7 oncogene oral vaccine that has passed the first stage clinical trials in 2020 and will be proceeding in stage II in the near future[414]. The aforementioned clinical advantages have solidified the position of *L. lactis* as a tool of great scientific potential and has encouraged further research on the endless possibilities it provides for medicine.

Despite its recently obtained recognition as a clinically significant tool, *L. lactis* has not gained the popularity of the gold standard for bacterial protein production, currently held by *E. coli*. Its unparalleled fast growth kinetics associated with easily achieved high-density cultures, the readily available, inexpensive culture media and the wide array of established transformation strategies have made *E. coli* the bacterium of choice for most mainstream recombinant protein production applications[415]. However, except for the difficulty of expressing certain heavily post-translationally modified human proteins and the accumulation of others in inclusion bodies[416], *E. coli*-based protein production can also be subject to LPS and endotoxin contamination[417], that requires labour intensive procedures to remove them before the expressed protein can be safely administered to humans. Furthermore, due to the high expression of ECM proteins by *E. coli*, some expressed recombinant proteins can get trapped in the matrix, making their isolation and purification especially demanding[418].

In contrast, the low LPS produced by *L. lactis* and the lack of considerable ECM production from its biofilms, makes the species an attractive alternative for medical applications. In our study in particular, the co-culture of bacteria and mammalian cells would not have been possible had we chosen a species that produces LPS and an extensive ECM, due to the induced inflammatory responses and the difficulty of the mammalian cells to access the recombinant proteins produced by the biofilm due to the secreted bacterial ECM. This work has been based on previous studies where FN and BMP2 were produced in *L. lactis* MG1363[191,187] and NZ9000/NZ9020[188] respectively, and have been shown to directly impact and influence stem cell behaviour.

For the purpose of our study, we have expressed CXCL12, TPO and VCAM1 in *L. lactis* NZ9020. The genetic engineering of the bacteria has been performed using Gibson assembly, a versatile technique that utilises primer overlaps to allow precise annealing of multiple fragments of interest. Given the plasmid backbone and the protein sequence of interest, we could perform PCR to elongate and produce multiple copies of both, that could then be ligated and produce a final assembly containing the complete plasmid and target protein gene, that could be inserted and expressed by *L. lactis*.

We have demonstrated that physiologically relevant expression levels of CXCL12, TPO and VCAM1 can be produced in *L. lactis* NZ920 and expressed constitutively in the pT2NX plasmid. In particular, we have designed and achieved the production of soluble CXCL12 and TPO, that are secreted by the bacteria after expression with the use of the Usp45 secretion peptide. In contrast, we have chosen to only express and produced the extracellular part of VCAM1, that also contains the signalling part of the protein and describe the production and display of the peptide on the extracellular membrane of *L. lactis*, using the *S. aureus* protein A anchoring protein. In all cases, the recombinant proteins were tagged with a 6-His tag, that facilitated their optimal characterisation after isolation[419]. The tag was added to either the N- or the C- terminal of each protein depending on the localisation of its signaling part, in order to ensure the tag did not interfere with protein functionality. For example, the signalling part of CXCL12 is located near its C-terminus, therefore the 6-His tag was placed on the N-terminus of the protein to prevent major structural changes that would interfere with its normal activity. The levels of the expressed proteins were assessed using a His-Tag protein detection kit. This kit is based on competitive ELISA, where a His-tagged protein of known molecular weight is pre-coated on the provided microwell plate and protein standards are used to generate a reference standard curve, from which the target protein concentration in our samples can be extrapolated.

We have achieved a physiologically relevant expression of all proteins of interest, at a similar level to previously reported recombinant BMP2 expression levels in NZ9020, as shown in table 3.5. Our results suggest that CXCL12 was expressed at a higher concentration compared to TPO, and that both soluble protein expression was higher than VCAM1. This observation can be explained by the size difference of the aforementioned proteins, where the smaller and less complex signalling molecules are expressed in higher amounts than the

larger, more complex ones. Accordingly, monitoring of the growth rate of the different engineered *L. lactis* populations displayed the same trend. The populations expressing smaller molecules (CXCL12 and TPO) had a similar growth rate to the EMPTY bacteria, while the bacteria producing VCAM1 and FN appeared to grow at a significantly slower rate compared to the rest of the populations. Therefore, we can conclude that the different recombinant proteins pose different levels of metabolic strain on *L. lactis*, depending on their size and tertiary structure complexity.

Recombinant protein	**Expression level (average ± SD, n=3)**
CXCL12	280.32 ± 43.84 ng/mL
TPO	175.4 ± 15.82 ng/mL
VCAM1	99.18 ±6.74 ng/mL
BMP2	299 ng/mL
FN III_{7-10}	5.84 ng/cm^2

Table 3.5. Quantification of *L. lactis* recombinant protein expression. Displayed are the values obtained by the His-Tag ELISA performed on samples obtained in this work (CXCL12, TPO, VCAM1) and the expression levels of proteins engineered previously (BMP2, FN III_{7-10}). It should be noted that values required for differentiation in the literature are not currently available or with wide ranges preventing meaningful comparison.

Our data also suggests that *L. lactis* can form biofilms that remain viable in a variety of media, suggesting the suitability of the bacteria for co-cultures with mammalian cells in their culture media. More precisely, since the aim of this work is to create an *ex-vivo* bone marrow analogue, we compared the biofilm viability in GM17 (*L. lactis* media) to IMDM (HSC media), demonstrating that there is no statistical difference between the two conditions.

Furthermore, for a successful bacterial-human stem cell co-culture, it has been important to establish the optimal conditions that would both provide a viable, actively protein-producing biofilm and ensure that the bacteria will not escape the biofilm, overgrow and overpopulate the co-culture. We therefore assessed biofilm viability in a variety of different antibiotics in order to determine the most effective antibiotic mix conditions that maintain the desired co-culture balance. Our results suggest that when cultured in a mix of

Chloramphenicol, Sulfamethoxazole, Erythromycin, Tetracycline and Hemin, *L. lactis* retains high viability, while also remaining in a stable biofilm, attached to the provided substrate.

While previous research has shown that *L. lactis* biofilms attach and remain stable on glass coverslips for 4-5 days, the need for longer cultures urged us to find a way to increase the adhesion dynamics between the bacteria and the substrate. Taking into account that a stronger attachment can be achieved by increasing the hydrophobicity of the substrate, we tested the bacterial viability and surface coverage on two different silanes. According to our data, both APTES and Sigmacote maintained a high biofilm viability after 9 days. Sigmacote also provided a higher surface coverage compared to APTES, so we chose this coating for all further experiments.

3.5. Conclusion

The work described in this chapter shows that *L. lactis* has been successfully engineered to produce recombinant CXCL12, TPO and VCAM1 in a constitutive manner with bacteria attached to a surface. All proteins are produced at different concentrations and the respective bacterial populations display different growth rates, according to the specific characteristics of each produced protein.

Furthermore, we provide evidence that biofilms producing different recombinant proteins remain viable for more than 9 days when cultured in both the *L. lactis* media, GM17, and in HSC maintenance media, IMDM. We have also assessed the impact of different antibiotics as a control mechanism of *L. lactis* growth, with an aim to achieving a low bacterial metabolism that would prevent bacterial overgrowth. Based on our data, we suggest that NZ9020 biofilms cultured in the antibiotic mix described above is sufficient to maintain the bacteria in a biofilm monolayer, in a high-viability, lower-metabolic state, that still produces the engineered proteins of interest.

Finally, we tested the efficiency of two different silanes, APTES and Sigmacote on biofilm viability and surface coverage. Our results suggest that while high viability is maintained in biofilms cultured on substrates treated with either silane, Sigmacote yields a better surface coverage by the biofilm and has been selected as the preferred coating for future work.

The results discussed in this chapter have laid the foundations for the development of a BM analogue based on genetically engineered bacteria. Our aim has been to utilise the biofilm as an active support mechanism for stem cell culture, that will provide the essential soluble and adhesion factors to direct stem cell behaviour. The successful genetic engineering, protein quantification and the achievement of the optimal conditions for a viable, stable and long-lasting biofilm have been of great importance for the co-culture experiments described in later chapters.

Chapter 4. Bacteria-MSC interactions

Summary

This chapter is focused on the interaction between *L. lactis* biofilms and human BM-derived human MSCs. These interactions were studied in co-culture experiments, where the MSCs were co-cultured with biofilms of genetically engineered *L. lactis*, producing CXCL12, TPO, VCAM1 and FN, alone or in different combinations. Initial studies involved the analysis of stem cell adhesion and spreading on the biofilms, as well as evaluation of cell viability in the co-culture experiments. Furthermore, the phenotype of MSCs cultured on different biofilms was evaluated in an effort to use the biofilms as a substrate to control stem cell behaviour. Finally, we tracked the movement and characterised the migration patterns of MSCs on different biofilms.

Our results suggest that the presence of *L. lactis* and its use as a substrate for human MSC cultures has no negative impact on cell's viability. Additionally, MSCs attached and spread on the different biofilms and showed different morphologies, depending on the recombinant protein produced in each condition. Finally, MSC phenotype analysis displayed evidence that the biofilms induced the maintenance of a BM-resembling, stem-like phenotype on the cells, while at the same time preventing their osteogenic and adipogenic differentiation. This observation was consistent with and without the presence of a hydrogel in the cultures, with a clear maintenance of stemness markers and downregulated expression of osteogenic markers compared to the control.

We also performed tracking experiments to determine the movement patterns of MSCs on the different *L. lactis* biofilms, with and without the presence of a hydrogel covering the cells. Our analysis suggests that the MSCs migrate following random paths when cultured on all biofilms and cover large distances in 2D. In the presence of a degradable hydrogel, MSCs displayed the ability to degrade and remodel their microenvironment, as they migrated at higher average speeds and followed larger movement trajectories compared to the non-degradable gel condition. Therefore, we suggest that our engineered biointerface-based microenvironment has the potential to mimic the native BM conditions, resulting in the maintenance of a naïve MSC phenotype that retains its differentiation potential, while at

the same time allowing for physiological cell movement and migration in both 2D and in the presence of degradable hydrogels.

4.1. Introduction

Since their discovery in 1676[420], bacteria and their interaction with humans and other species have been closely observed and studied by the scientific and medical communities. In the early years following the first discovery of microorganisms, bacteria have attracted increased interest in two main emergent areas, medicine and food production[421]. With science advances, and despite the bad reputation of many pathogenic species as infectious agents, several non-pathogenic species have been identified and studied due to their health and economically beneficial properties.

Outside the direct use of *L. lactis* for drug production and administration, the possibility of enabling their use as stem cell fate manipulation mechanism have not yet been explored in detail. Stem cells have been identified as a very promising solution to a variety of clinical conditions because of their unique capacity to differentiate into a variety of cell types, inducing tissue repair and regeneration. Therefore, the need to accurately and precisely mediate stem cell fate decisions holds a tremendous medical potential.

The study of native stem cell niches in the human body has revealed that the cellular microenvironment is linked to providing the internal cues responsible for stimulating and directing stem cell behaviour. The spatial organisation and mechanical properties of the niche influence the adhesion dynamics provided by the niche are directly linked with stem cell survival, proliferation and differentiation[422]. Stem cells therapeutic potential has instigated research into the identification and recapitulation of the most widely recognised niche cues associated with clinically relevant stem cell-based medical outcomes.

For most adherent cells, like MSCs, the principal link between the cell and the extracellular environment is provided by membrane-spanning integrins. Upon cell adhesion, integrins start forming clusters and initiate the recruitment of other proteins including talin, paxillin and vinculin, resulting in the formation of focal adhesion complexes (FAs)[423]. Except for the structural proteins, FAs are coupled to a variety of intracellular signalling molecules that directly activate further signalling pathways. These include activation of the Rac, RhoA and

Cdc42 GTPases, that translate changes (biochemical, mechanical) in the ECM into signalling processes that directly influence the morphotype and phenotype of the cell by mediating cell migration and adhesion to its surroundings[424,425]. More precisely, at the initial stages of cell adhesion to the ECM, integrin-mediated activation of Rho initiates the downstream ROCK effector that regulates the myosin light chain[426]. This signalling cascade is crucial in the maintenance of the balance between internal stiffness and extracellular force exerted at the FAs[427]. Furthermore, Rho directly regulates cell contractility and migration by microtubule-associated guanine nucleotide exchange factor (GEF)-H1-dependent activation[428]. Cell adhesion is also mediated through the Rac/Cdc42 pathway through p21-activated kinase-signalling and via activation of the Arp2/3 complex. More precisely, p21-activated kinase has been shown to induce cytoskeletal reorganisation and its activity has been linked with cell spreading and migration[429]. Additionally, Arp2/3 forms modular 'hybrid complexes' consisting of the actin-nucleating subunits of Arp2/3 and either vinculin or vinculin and α-actinin, resulting in actin polymerisation, that regulates lamellipodia formation[430], and in turn mediates cell adhesion and migration[431]. These main molecular interactions between the cells and ECM are summarised in figure 4.1.

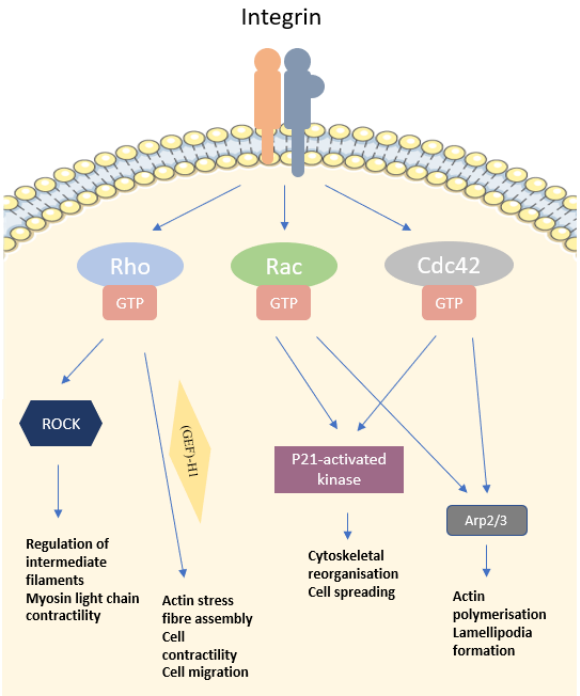

Figure 4.1. Major regulatory pathways in cell adhesion and migration. Rho family members are key regulators of actin reorganization and intermediate filaments. Activation of different members of the family of GTPases results in direct reorganisation of the cellular cytoskeleton, mediating cell morphology and localisation.

In contrast, cell survival, proliferation and differentiation are closely interconnected and rely mostly on stimulation by tissue-specific soluble signalling[432]. Cell proliferation and renewal is particularly important in stem cell studies and is regulated by the cell cycle, that can in turn be influenced by external stimuli to drive tissue and organ homeostasis and in some cases the development of malignant cell phenotypes and tumorigenesis[433]. Furthermore, stemness and differentiation is a bidirectional, dynamic state that is largely governed by the stem cell niche, allowing for plasticity and adaptability to changing conditions[434,435]. Given its central role in mediating stem cell behaviour, the biophysical and biochemical composition of the niche (figure 4.2) has been a major focus of scientific research. The closer study of the niche factors and signalling pathways that can promote stem cell function, enrich for cells with stem cell properties, or direct their differentiation towards specific lineages could have significant implications in regenerative medicine and tissue engineering.

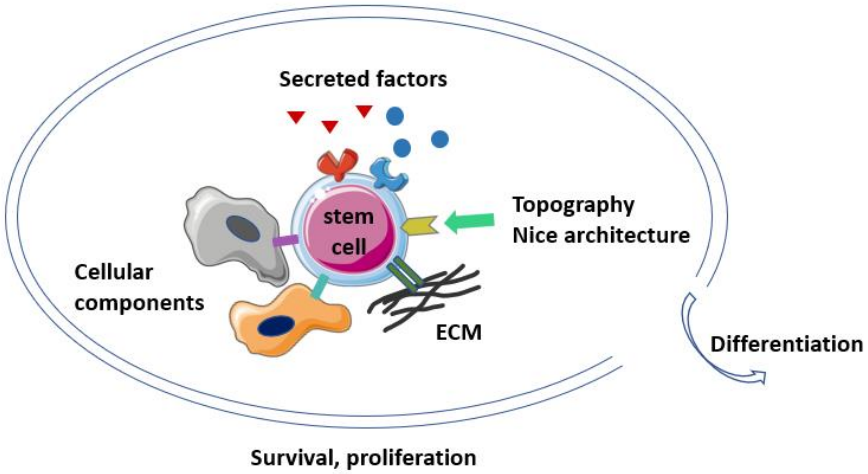

Figure 4.2. Schematic diagram of the stem cell niche. Shown here is a stem cell interacting with the various mechanical, topographical and soluble stimuli provided by its niche. In this image, the stem cell interacts with other cells residing in its microenvironment and the soluble signals provided by them. Furthermore, the stem cell adheres to the ECM, sensing the topography, mechanical characteristics and 3D architecture of the niche. The interplay between the niche-derived signals and stem cell responses mediate tissue homeostasis through regulating stem cell survival, proliferation and differentiation.

Even though MSCs are one of the most studied stem cell types, given their central role in regulation of the bone marrow niche[436,437] and their potential for differentiation for biomedical applications[438,439], their interplay and regulation by their niche is not completely

understood. In contrast, most scientific efforts have been focused on the understanding of the mechanisms through which MSCs contribute to niche homeostasis and drive the maintenance and expansion of other cell types, such as HSCs[440,441]. Recent studies have also examined the role of MSCs in healing processes, with wound[442,443] and bone[444] repair being the most prominent. Furthermore, MSC behaviour has been investigated in response to different substrate characteristics, such as nanotopography[445,446], stiffness[447,448] as well as mechanical stimulation[449].

Efforts to better understand the intrinsic mechanisms of MSC function have mainly focused on the impact of specific gene regulation[450,451] and methylation patterns[452] on MSC activity, while few articles have been published on possible effects of microenvironmental cues, such as the availability of adhesion motifs[453] on MSC regulation. Outside of mechanical stimuli, the only interactions between MSCs and ECM proteins have focused on the effects of laminins[454,455] and fibronectin[456,457]. However, the complexity of the BM microenvironment and the variety of the biochemical and mechanical signals it provides to its cellular components have made efforts to understand the mechanisms of stem cell regulation highly challenging.

Outside of cell phenotype and differentiation, major research focus has been placed on cell migration as a driver of a variety of clinically significant physiological processes. Cell migration is integral in organ development, tissue morphogenesis[458] and repair[459], wound healing[460], immune responses[461,462], as well as the development, progression and invasiveness of malignant conditions such as cancer[463]. Therefore, the study and better understanding of cell motility and the effects of environmental cues on cell movements can better direct the design of more efficient and physiologically relevant biotechnologies for tissue engineering applications[464,465].

Different models have been developed to study cellular migration dynamics. In particular, research has been focused on multiple aspects of cell movement, tracking both individual cells or aggregates and focusing on the presence or absence of external cues, such as chemical stimuli, extracellular matrices, as well as substrate topography and polarity[466]. This variation on the specific characteristics of each cellular microenvironment can have a large impact on the directionality of cellular migration and is important to quantify, regardless of whether the migration is directed by chemical and mechanical signals or not.

The most commonly used method for individual cell tracking is the persistent random walk (PRW) model, that was developed to mathematically track cell migration occurring in isotropic media. The main assumption of PRW is that a cell follows a Brownian motion, where it is assumed to migrate directionally at short time intervals, but lose its persistence at longer time intervals[467]. The relationship between this persistent directional movement to the random one is characterised by the directional persistence time (P), an estimate of which can be obtained by fitting the mean square displacement (MSD) of the tracked cells to Fürth's formula (equation 4.1).

$$MSD(t) = 4D[t - P\left(1 - e^{-\frac{t}{P}}\right)] \qquad (1)$$

Equation 4.1. Fürth's formula. Calculation of MSC, where D is the diffusion coefficient, and t is time during which the migration takes place.

Initially, this fitting was performed with ordinary nonlinear least-squares regression analysis[467]. The equation involves fitting the experimental mean-squared displacement of the cell or population with a known speed and persistence in time as the two parameters. However, later studies observed that deviations for large time interval data were big enough to question the underlying assumption that migrating cells actually undergo PRW[468]. More precisely, studies have suggested that in the absence of external cues, mammalian cells undergo a persistent, random walk, rather than Brownian motion[469,470]. Careful analysis of mammalian cell migration trajectories suggested that cellular movement can alternate between two different modes, a directional mode and a reorientation, or zig-zag-like mode, where, in particular, the cell-tracks of starved cells exhibit many turns with the cells repeatedly visiting the same position[471].

The aim of this chapter is to study the interaction between genetically engineered *L. lactis* biofilms and MSCs. The recombinant proteins expressed by the bacteria (CXCL12, TPO, VCAM1, FN) are expressed by a variety of BM-residing cell types and therefore are an important regulator of the BM niche[472]. This provides us with the opportunity to create a dynamic microenvironment that mimics some of the biochemical characteristics of the BM and assess the impact of these stimuli on MSC behaviour. By closely monitoring the impact of the different adhesion and soluble proteins on MSCs, our goal is to further our understanding on the way BM signals affect MSC survival, maintenance, differentiation, and

migration as well as determine the conditions that best maintain a stem-like MSC phenotype in order to create an *ex-vivo* BM analogue.

4.2. Materials and Methods

4.2.1. MSC viability on *L. lactis*

Human BM-derived MSCs were cultured on genetically engineered *L. lactis* biofilms at an initial density of 10,000 cells/cm^2 for 3 and 5 days, with the aim of assessing the impact of the biofilm on cell viability. To distinguish live from dead cells, we used the LIVE/DEAD® Viability/Cytotoxicity Kit (ThermoFisher), that involves staining the sample with the green fluorescent calcein-acetoxymethyl ester (AM) staining and the red-fluorescent ethidium homodimer-1 (EthD-1) that indicate intracellular esterase activity and loss of plasma membrane integrity respectively. Dead cells are associated with a damaged plasma membrane. This feature allows EthD-1 to enter the cytoplasm, where it bins nucleic acids, resulting in a conformational change that enhances its fluorescence and results in the emission of a bright red signal (excitation ~495 nm, emission ~635 nm)[473]. In contrast, live cells display a uniform cell membrane that prevents the entry of EthD-1 into the intracellular space. However, the cell-permeant calcein AM can be transported into the cytoplasm, where it can be enzymatically converted to the intensely fluorescent calcein, producing an intense green fluorescent signal (excitation ~495 nm, emission ~515 nm)[474].

At the desired timepoint, MSCs were washed once with sterile phosphate buffered saline (PBS, Invitrogen) to remove any excess cell culture media. The samples were then stained with a mix of 1:2000 calcein plus 1:500 EthD-1 and incubated in a covered tissue culture plate for 30 minutes at room temperature in absence of light. The samples were then transferred to microscope slides and imaged in a Zeiss AxioObserver Z1 fluorescence microscope. Results were obtained by image analysis by counting the number of green-stained cells (live) versus the red-stained cells (dead). Image processing was conducted using the open-source software Fiji/ImageJ.

4.2.2. Cell adhesion and spreading on biofilms

The adhesion and spreading of cells on *L. lactis* biofilms on glass coverslips were assessed through vinculin and actin immunostaining, respectively. Human MSCs were cultured at a density of 5,000 cells/cm^2 and were incubated for 3 hours in DMEM with no added fetal bovine serum (FBS) in a humidified incubator at 37°C, 5% CO_2. Similarly, murine FN$^{-/-}$ fibroblasts were seeded at the same conditions to serve as a negative control. After the incubation period, the cells were washed in PBS and fixed in 4 % formaldehyde in PBS at 37 °C for 15 minutes. The samples were washed three times with PBS and the cells were then permeabilized after a 5-minute incubation in 0.5% Triton-X100 in PBS, in room temperature. Afterwards, the samples were incubated in 1 % bovine serum albumin (BSA) in PBS at room temperature for 1 hour to block reactive sites and subsequently decrease background fluorescence. Following the incubation period, the samples were incubated in a mouse monoclonal anti-vinculin antibody (Sigma, V9131, UK) diluted to 1:400 in 1 % BSA / PBS for 1 hour at room temperature. The samples were washed three times with 0.5% v/v Tween 20 in PBS and were then incubated in an antibody mix containing Cy-3-conjugated rabbit anti-mouse secondary antibody, and Alexa Fluor 488 phalloidin, diluted 1:200 and 1:100 in 1 % BSA / PBS, respectively. The reaction was run for 1 hour at room temperature, with the samples protected from light. Finally, the samples were washed three times with 0.5% v/v Tween20 in PBS. Each coverslip was stained with a drop of mounting media containing DAPI and transferred on to a clean microscope slide for visualisation and analysis, that was conducted under a fluorescence microscope (Zeiss AxioObserver- Z1).

4.2.3. In-Cell Western (ICW)

In order to evaluate any phenotypical changes on the MSCs in response to direct co-culture on genetically engineered *L. lactis* biofilms, we conducted an ICW analysis. Human BM-derived MSCs were seeded on biofilms cultured on clean glass coverslips at a density of 5,000 cells/cm^2. The cells were cultured in DMEM supplemented with 10% FBS and 10ug/ml antibiotic mix containing chloramphenicol, tetracycline, erythromycin, sulfamethoxazole and hemin. The samples were incubated for 14 days in a humidified atmosphere incubator at 37°C, 5% CO_2, with media changes every 3 days. The control conditions for this experiment were naïve MSCs, cultured on a glass coverslip in DMEM + 10% FBS + 10ug/ml

penicillin/streptomycin (P/S) for 24h to avoid loss of phenotype, and MSCs cultured in osteogenic differentiation media containing 25 ng/ml of BMP-2, cultured for 14 days. After the desired timepoint, the cells were fixed with 4% formaldehyde in PBS for 30 minutes at room temperature and were permeabilized during a following 5-minute incubation in 0.05% Triton X-100 in PBS. The samples were then incubated for 1.5 hours in 1% BSA in PBS on a rotary shaking platform at room temperature. The importance of this step lies in the blocking of reactive sites, reducing the nonspecific protein adsorption and thus background fluorescence at the end of the experiment. In order to determine if the MSCs had retained a stem-like phenotype or if they had differentiated towards the osteogenic lineage, we stained for the stemness markers Nestin, Stro1 and ALCAM, and the osteogenic markers osterix (OSX) and osteopontin (OPN). We also performed a normalization step to correct for well-to-well variation in cell number, by staining for the internal control protein beta-actin.

Mouse primary antibodies against the markers mentioned above were diluted in 1% BSA in PBS as described in table 4.1. The cell staining took place at room temperature for 1 hour. The primary antibody solution was then removed, and the samples were washed five times for 5 minutes on a shaking platform with washing buffer, consisting of 0.1% Tween-20 in PBS. A rabbit anti-mouse IRDye 800CW secondary antibody, diluted 1:800 in 1% BSA in PBS, along with an anti beta-actin antibody (1:500) were added to the samples, and incubated at room temperature for 1 hour, protected from light. After the incubation period, the samples were subjected to 5 washes, each lasting 5 minutes, in washing buffer. Finally, the buffer was removed, and the samples were dried overnight under laminar flow.

The plate containing the stained and dried samples was imaged using an Odyssey® CLx Imaging System (LI-COR Biosciences). The relative protein levels were normalised against b-actin and were quantified and analysed using the GraphPad Prism 8 graphing program.

Antibody	Dilution in 1% BSA / PBS
Anti-OPN primary antibody	1:200 w/w
Anti-OSX conjugated antibody	1:200 w/w
Anti-Stro1 primary antibody	1:200 w/w
Anti-ALCAM primary antibody	1:200 w/w
Anti-Nestin conjugated antibody	1:200 w/w
Anti-beta-actin primary antibody	1:100 w/w
IRDye 800CW secondary antibody	1:800 w/w
Anti-beta-actin secondary antibody	1:500 w/w

Table 4.1. The antibodies used for the ICW analysis of MSC phenotype on biofilms. All antibodies were purchased by abcam and were reconstituted and used according to the manufacturers' specifications.

4.2.4. Cell tracking

To determine cellular movement and migration patterns, we set up different timelapse experiments, with an aim to track human MSCs cultured on *L. lactis* biofilms. Biofilms were formed overnight on glass coverslips and were washed three times before MSC seeding. Human BM-derived MSCs were seeded on the prepared biofilms at a density of 8,000 cells/cm^2 and were incubated in DMEM + 10% FBS + AB mix in a humidified incubator at 37°C, 5% CO_2. For the conditions containing a hydrogel, the cells were allowed to adhere to the biofilm for 3h before the addition of a 5% w/v PEG hydrogel. Degradable hydrogels were formed by substituting 50% of the SH-PEG-SH with VPM.

For cellular tracking, we used an EVOS FL Auto 2 microscope (ThermoFisher). Results analysis was performed in Fiji/ImageJ and Microsoft Excel, using the macros in the protocol developed by Gorelik and Gautreau (2014)[475].

4.3. Results

4.3.1. MSC viability on biofilms

MSC viability was assessed on *L. lactis* NZ9020 biofilms expressing all recombinant proteins of interest (CXCL12, TPO, VCAM1 and FN) as well as the EMPTY population that expresses no protein. The single population biofilms were chosen rather than combinations of different populations in order to understand the direct impact of each population and perhaps of the recombinant cytokine on the viability of the co-cultured stem cells. Since our ultimate goal is

to use MSCs as a support layer for HSC expansion, we measured MSC viability after 3 and 5 days, according to the duration of our HSC cultures.

As shown in figure 4.3, MSC viability appears completely unaffected by the co-culture with the *L. lactis* biofilms. More precisely, no dead cells were recorded after imaging the Live/Dead assay, performed after either timepoint. This result is a clear improvement compared to previous studies conducted in our group, that noted a gradual decrease in MSC viability over a 14-day culture on *L. lactis* biofilms[293]. This difference can be attributed to a variety of factors. First, the strain used in the previous studies was NZ9000, a much more metabolically active strain, that produces lactic acid as its metabolic end product. This would result in a rapid decrease of the pH of the culture medium, that could explain a drop in MSC viability. The increased metabolic activity of the biofilm would also deplete the MSCs from the glucose and growth factors provided by the culture media, resulting in higher cell death. In contrast, the biofilms used in this work were made out of *L. lactis* strain NZ9020, where both known lactate dehydrogenase genes are knocked out and have been replaced with erythromycin and tetracycline resistance genes, to allow for positive screening[2]. The resulting strain has been associated with a metabolic shift, producing mainly ethanol and acetoin during fermentation instead of lactate[476]. A more detailed description of the metabolic end products of NZ9020 can be found in table 4.2.

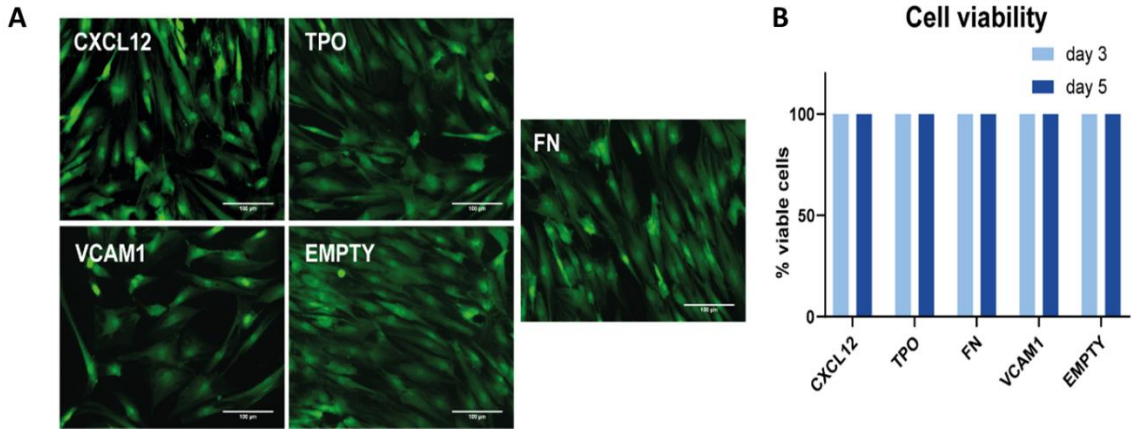

Figure 4.3. MSC viability on biofilms after 3 and 5 days of culture. (A) MSC viability on *L. lactis* biofilms. Representative images of the Live/Dead assay are shown for each condition. Live MSCs are displayed in green, while no dead MSCs were recorded (red channel). (B) MSC viability of cells cultured on CXCL12, TPO, FN, VCAM1 for 3 and 5 days was determined with a mammalian viability kit (Thermofisher). No non-viable (red-stained) cells were found in any of the conditions, assuming a 100% viability in all the tested conditions.

Species	Aerobe	Lactate	Formate	Acetate	Acetoin	Butanediol	Ethanol	Pyruvate
NZ9020	+	0.6 (1.0)	ND	12.0 (20.3)	17.9 (60.5)	0.1 (0.4)	1.4 (2.4)	2.6 (4.5)
NZ9020	-	1.5 (2.5)	ND	10.0 (16.9)	5.6 (18.9)	ND	25.2 (42.7)	0.5 (0.8)

Table 4.2. Growth and fermentation characteristics of ldh-deficient *L. lactis* strain NZ9020 cultured in aerobic and anaerobic conditions. Each value is displayed as concentration (mmol/L) of metabolic end product formed. ND: Not detected[477].

In aerobic cultures, the *ldh*-deficient bacteria maintain their intracellular redox balance through the activity of the endogenous NADH oxidase, that allows for continued sugar fermentation. In contrast, in the absence of oxygen, the metabolic rate of the bacteria is reduced, resulting in the production of acetate and ethanol. The metabolic shift that results in the conversion of pyruvate to ethanol and acetate instead of acetoin, suggests that these pathways are used as an alternative electron sink, since the reducing steps involved require NADH as a co-factor. Furthermore, the increased production of mannitol observed in the *ldh*-deficient strain NZ9020, suggests that the bacteria suffer from redox stress in anaerobic cultures and that the use of acetate is important for the maintenance of the redox balance during pyruvate metabolism[478]. The strain is therefore unable to produce as much lactate as a fermentation end product, preventing a large pH drop.

Nevertheless, anaerobic NZ9020 metabolism still yields significant amounts of ethanol, which is also detrimental for stem cell culture. To address this issue, studies have identified that heme can both prevent huge drops in pH and improve bacterial viability in aerobic conditions. Exogenous presence of heme in aerobic LAB cultures has been associated with the establishment of an aerobic respiratory chain, which reduces O_2 to H_2O in the presence of H^+ (Figure 4.4)[479]. More precisely, in the presence of oxygen and heme lactococcal growth occurs through glucose fermentation, and when the external pH drops to approximately 5.3 the bacteria switch to respiration[480]. The consequent shift in the NAD^+/NADH ratio, results in a metabolic change mediated by enzymatic use of either NAD or pyruvate as a substrate. This results in a more energetically favourable metabolism, that also protects the bacteria from oxidative and acid stress in the presence of oxygen[481], and for the purpose of our experiments provides a way of achieving a neutral pH, during the co-culture experiments

conducted in the presence of oxygen. Therefore, we performed all of our co-culture experiments in the presence of hemin at a concentration of 5 µg/mL.

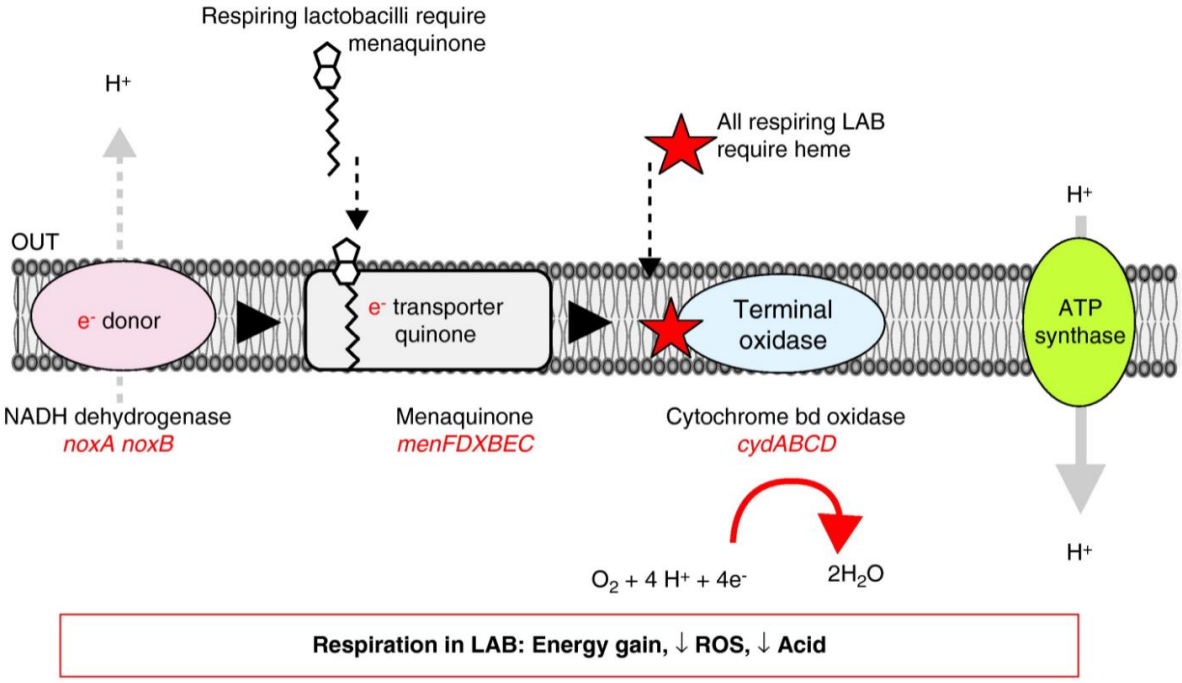

Figure 4.4. Schematic representation of the major electron transport chain components in respiration-competent LAB, in the presence of exogenous heme. The major components of the respiration chain include the electron donor (NADH dehydrogenase), electron transporter, and a heme-requiring terminal electron acceptor (cytochrome quinol oxidase, called CydAB, in LAB). *L. lactis* genes associated with each stage are indicated below each component. Several LAB, including lactobacilli require the presence of menaquinones that can be obtained by their environment. In aerobic conditions, LAB can establish a respiratory chain, based on the reduction of O_2 to H_2O in the presence of H^+, a reaction mediated by an ATP synthase. ROS, reactive oxygen species. Image adapted from Hatti-Kaul et al (2018)[479].

Furthermore, we have developed and optimised a mix of different antibiotics that reduce the metabolic rate of our bacteria. As discussed in previous chapter, except for chloramphenicol, to which NZ9020 is resistant, we used sulfamethoxazole[397], erythromycin and tetracycline[396] at 5 µg/mL in an effort to maintain the bacteria in a metabolically active, latent state. In this way, we could deter the over-proliferation of the bacteria and ensure that their minimal metabolic requirements do not deplete the culture medium of nutrients essential for MSC survival. The high MSC viability suggests that the stem cells can be used in combination with the biofilms in any future experimental setup that aims to create a BM analogue in order to either study or direct stem cell behaviour, expansion and proliferation.

4.3.2. Cell adhesion

The ECM is a major component of every natural stem cell niche and plays a key role in regulating stem cell morphology and behaviour. Except for structural support, the ECM binds and displays ligands and signalling molecules that can directly affect stem cell fate decisions, proliferation, and survival[482]. Given the importance of the interaction between stem cells and their surrounding microenvironment, we studied the mechanical interaction between human MSCs and *L. lactis* biofilms with emphasis on the cell morphology and adhesion dynamics.

The adhesion of MSCs to the bacteria was assessed on biofilms expressing CXCL12, TPO, VCAM1 and FN, as well as empty bacteria, producing no recombinant cytokine. After seeding, the MSCs were allowed to interact and adhere to the biofilms for 3 hours, before they were fixed and immunostained for actin and vinculin. MSCs cultured on the FN-expressing biofilm display a statistically significant more spread and elongated morphotype compared to the cells seeded on the other biofilms (figure 4.5 A). This resembles the behaviour of MSCs cultured on FN-treated substrates, showing that the biofilm has an observable effect on MSC adhesion and spreading behaviours, similar to the one directed by traditional methods[483]. Furthermore, the effect of the FN-expressing bacteria on the MSCs is obvious compared to the cells grown on a glass coverslip that do not display significant cell elongation and retain a more rounded shape. In terms of the other recombinant protein-producing bacterial populations, our data shows that MSCs do attach to the biofilms but remain in a rounded conformation, showing no observable cell spreading (figure 4.5 B). The cell shape observed on the CXCL12, TPO and VCAM1 biofilms has proven to be comparable to the one on the wild type bacteria (EMPTY) as well as the glass coverslip, therefore suggesting that the aforementioned cytokines have no measurable effect on cell adhesion and spreading. Since FN is a protein well known as an adhesion molecule associated with strong cell adhesion and a spread morphotype, this observation is expected and in agreement with previous research conducted on biointerface interaction dynamics between *L. lactis* and MSCs[187].

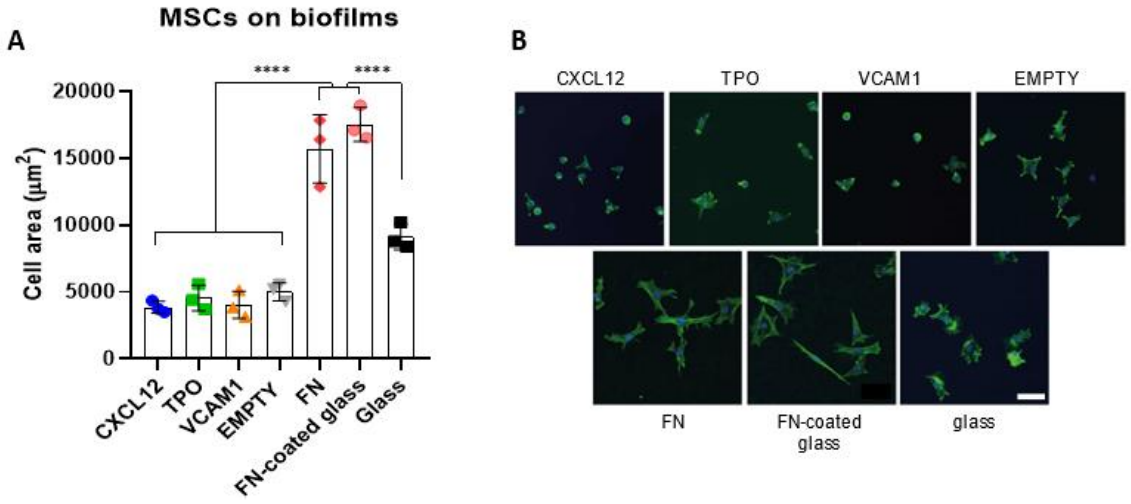

Figure 4.5. MSC spreading on biofilms 3 hours post-seeding. (A) The cell area of MSCs cultured on biofilms expressing CXCL12, TPO, VCAM1 and FN was measured by image analysis and was compared to an EMPTY biofilm as well as MSCs grown on FN-coated and uncoated glass coverslips. The cells grown on CXCL12, TPO, VCAM1 and EMPTY biofilms were found significantly smaller in size compared to cells grown on the FN-expressing biofilm and the two glass coverslip conditions ($n \geq 15$ cells analysed per condition, 3 biological triplicates) after a one-way non-parametric ANOVA with Kruskal-Wallis post-hoc test ($a = 0.05$). Data are presented as mean ± SD, (***p-value<0.001). (B) Actin immunostained Human MSCs cultured on the different biofilms. Scale bar: 100 µm. ANOVA; analysis of variance, SD; standard deviation.

Despite the differences in cell spreading, analysis of the focal adhesions (FAs) formed by the MSCs cultured on the biofilms suggests that the cells adhere to the bacteria in all conditions. Vinculin analysis after a 3-hour MSC-biofilm co-culture suggests that MSCs cultured on the FN-expressing biofilm display a larger area of FAs compared to cells cultured on biofilms made up of a combination of CXCL12/TPO and CXCL12/TPO/FN. However, no other significant difference was observed between the rest of the conditions (figure 4.6 A). Furthermore, we report no statistical difference between the circularity of the FAs between our conditions (figure 4.6 B). In this work, circularity was calculated as $c = 4\pi(area/perimeter^2)$, where $0 \leq c \leq 1$, with $c = 0$ for a straight line and $c = 1$ for a perfect circle. The circularity of the FAs is correlated to the stress that the cell is supporting, with higher circularities suggesting higher tension[484]. According to our data, the FAs examined show a range of conformations between the two values, a distribution that is uniform among all conditions. This observation suggests that the MSCs interact with the biofilm and experience a comparable degree of stress in all cases and regardless of the recombinant protein produced by the bacteria.

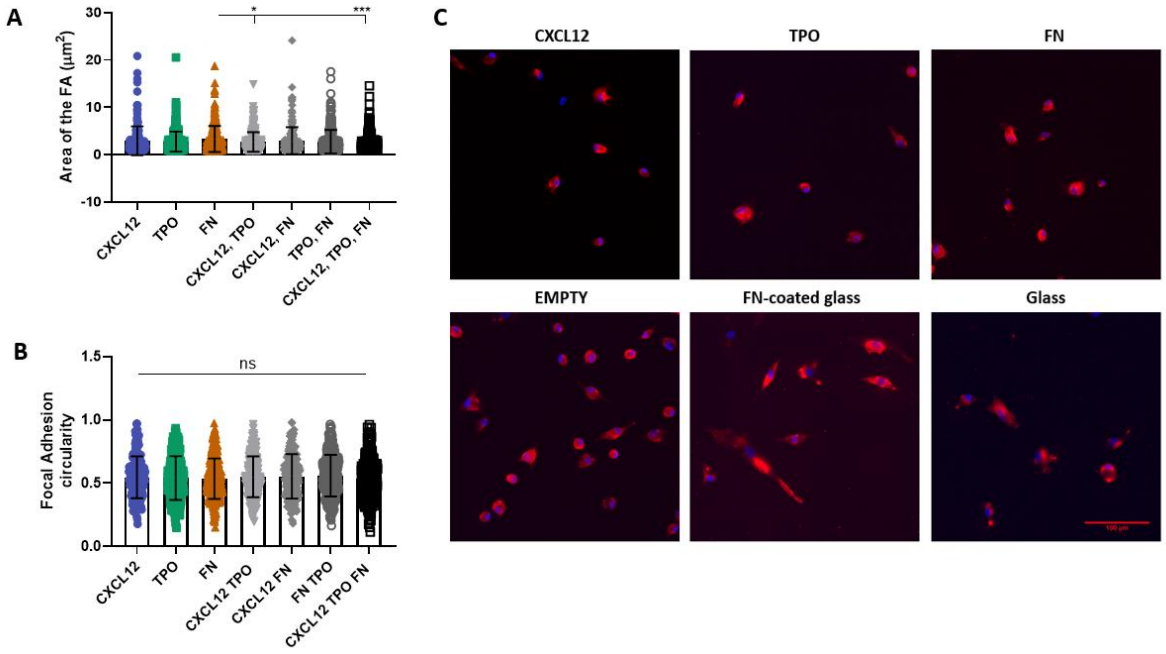

Figure 4.6. Area and circularity of focal adhesions on biofilms. (A) The area the FAs of MSCs cultured on biofilms expressing different cytokines was measured by image analysis. The area of the FAs of cells grown on biofilms expressing a combination of CXCL12/TPO and CXCL12/TPO/FN were found significantly smaller in size compared to FAs of cells grown on the FN-expressing biofilm (n ≥ 15 cells analysed per condition) after a one-way non-parametric ANOVA with Kruskal-Wallis post-hoc test (a = 0.05). (B) The circularity of the FAs was also determined by image analysis of vinculin immunostaining, where no significant difference was observed between the conditions. (C) Representative images of DAPI (blue) and vinculin (red) immunostaining of MSCs cultured on biofilms. Scale bar: 100 µm.

This claim is further supported by analysis of the area distribution of the FAs in the different conditions. As shown in figure 4.7 A, the area distribution of the FAs formed on CXCL12, TPO and FN-expressing biofilms appear statistically comparable after 3 hours, with and without the use of FBS. In particular, we divided the FAs by area, in order to classify them according to their maturation stage[485]. Therefore, we classified FAs into two categories; those smaller than 0.2 µm^2 were considered immature focal attachments and up to 2 µm^2, were classed as mature FAs. Comparison of the two classes of FAs demonstrated that their frequency is consistent among the different biofilms examined, supporting our claim that the mechanical stress exerted to the MSCs by the bacteria is independent of the recombinant protein produced by the biofilm. This trend could also be visually confirmed, as shown by the representative images in figure 4.7 B. Imaging of the vinculin immunostaining performed,

show clear FA development on the MSCs cultured on all biofilms (CXCL12, TPO and FN-expressing *L. lactis*), with and without the use of FBS, after 3 hours of culture.

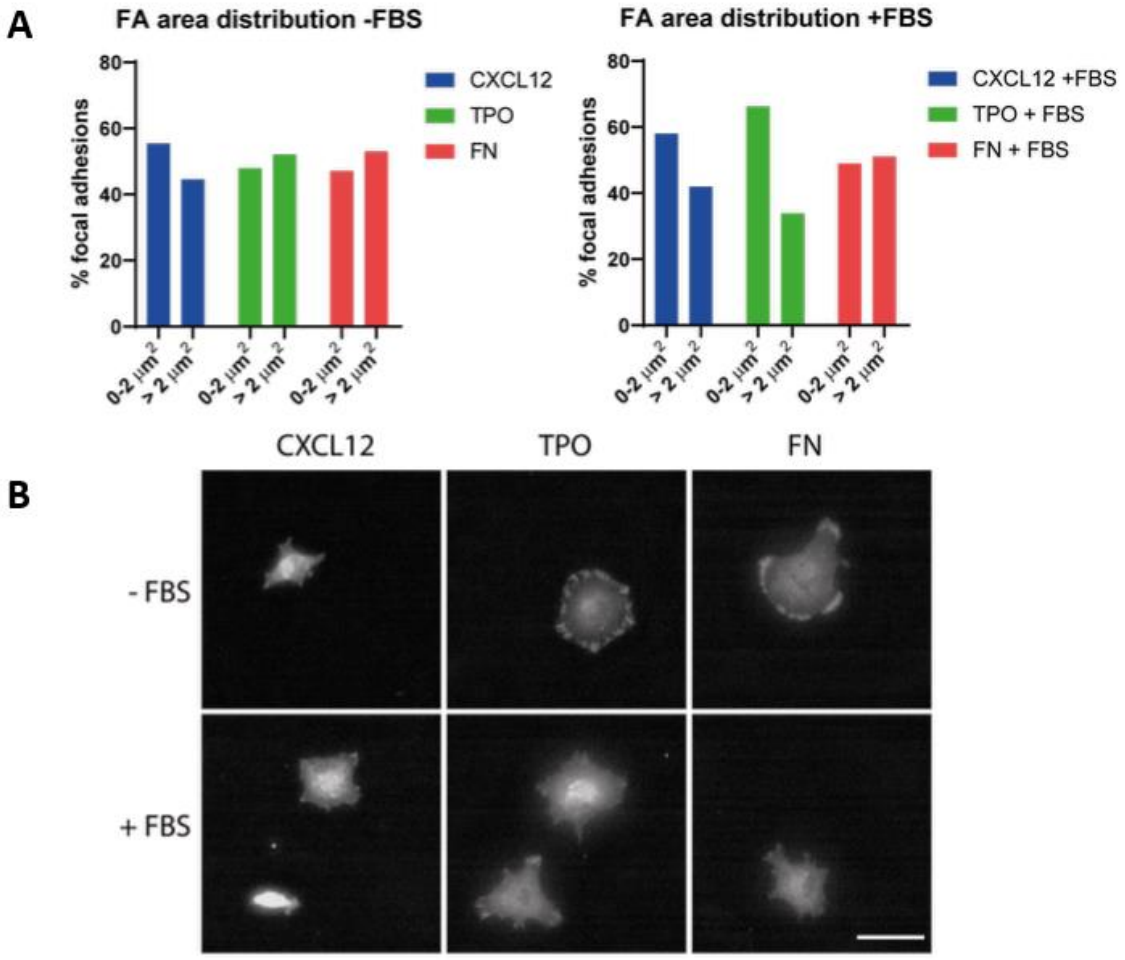

Figure 4.7. Area distribution of the focal adhesions of MSCs on biofilms. (A) The area distribution of FAs of MSCs cultured on biofilms expressing different cytokines, with and without the addition of FBS was measured by image analysis. No statistical difference was observed between the distribution of the FAs between the conditions in 3-hour cultures, with and without the addition of FBS ($n \geq 15$ cells analysed per condition) after a one-way non-parametric ANOVA with Kruskal-Wallis post-hoc test ($a = 0.05$). (B) Vinculin immunostained images of MSCs representative of each condition. Scale bar = 100 µm.

Finally, the number of focal adhesions of each cell were measured on bone marrow-derived MSCs cultured on biofilms expressing CXCL12, TPO or FN for 3 hours. Our observations suggest that the distribution of the FAs measured in MSCs cultured on all biofilms followed the same distribution (figure 4.8). The same trend was observed with and without the use of FBS. Collectively, our data supports the maintenance of a similar area and number of FAs

per cell, in all conditions. Therefore, FA turnover appears to be comparable and consistent among the conditions tested, further supporting our claim that the stem cells interact with the different bacterial populations in a fashion that is independent on the recombinant protein produced by each biofilm.

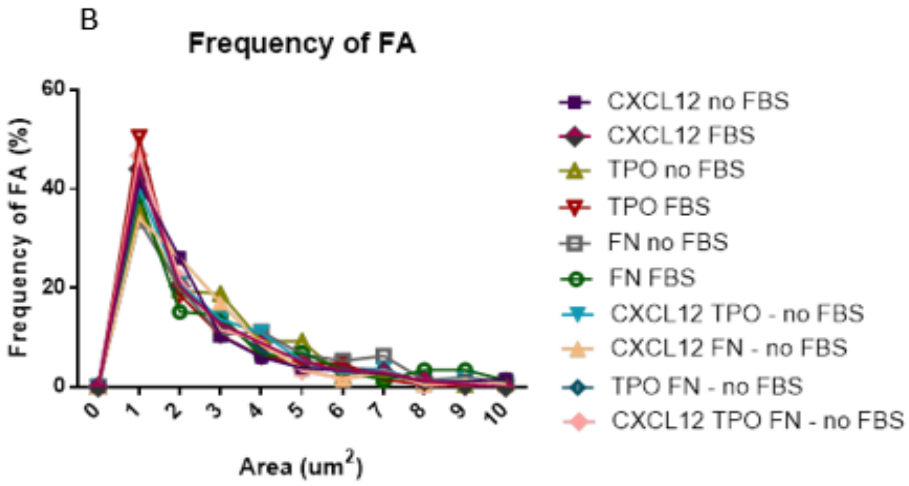

Figure 4.8. Frequency of the number of focal adhesions per cell. Human bone marrow isolated MSCs were cultured on *L. lactis* biofilms expressing CXCL12, TPO or FN, with and without the use of FBS. The number of focal adhesions was measured in a minimum of 30 cells per condition. No significant differences were observed in the frequency distribution of the FAs among the conditions. Furthermore, the number of FAs per cell appeared to be independent of the use of FBS in the culture media.

4.3.3. MSC phenotype on biofilms

MSCs have long been studied for their ability to differentiate into mature cell types for biomedical applications. Earlier studies focused on the capacity of MSCs to respond and regulate cell fate decisions in the presence of soluble cytokines. More precisely, a variety of growth factors and cytokines have been explored for their osteogenic, chondrogenic and adipogenic potential, as shown in table 4.3.

Cytokine / Growth factor / Hormone	Impact on MSC differentiation
TGF-β1	Osteogenesis[486], Chondrogenesis[487]
TGF-β3	Chondrogenesis[488]
TNF-a	Osteogenesis[489]
IGF1	Osteogenesis[490], Chondrogenesis[488]
VEGF	Osteogenesis[491]
FGF 1 and 2	Stemness Maintenance[492,493]
Insulin	Osteogenesis[494]
Estradiol	Osteogenesis[494]
Estrogen	Osteogenesis[495,496]
Growth Hormone	Adipogenesis[497]
BMP2	Osteogenesis , Chondrogenesis[498,499]
BMP4, BMP6	Chondrogenesis[500,499]
IL-1β, IL-6, IL-7 and IL-23	Osteogenesis[501,7]
IGFBP2	Adipogenesis[502]

Table 4.3. Key factors associated with MSC differentiation towards the osteogenic or adipogenic lineages. A variety of cytokines, hormones and growth factors have been examined for their effect on maintaining or changing the naïve MSC phenotype.

To evaluate the effect of the different bacteria-based interfaces, expressing different recombinant proteins on hMSC fate, we performed 14-day co-culture experiments and followed by in-cell Western (ICW) analysis of phenotype. We selected the osteogenic markers osteopontin (OPN)[503,504] and osterix (OSX)[504] and the stemness markers Nestin[505], Stro1[506,507] and Activated Leukocyte Cell Adhesion Molecule (ALCAM)[508] that have been widely used in the literature to assess MSC phenotype. The results were normalised against the housekeeping protein β-actin, commonly used in studies to obtain reliable and reproducible quantitative results in Real-Time PCR, Western Blot and ICW analysis[509]. In particular, Stro1, Nestin and ALCAM, have been described as markers commonly used to select for naïve BM MSCs[510,511,512]. In contrast, OPN and OSX have been identified as drivers of osteogenesis[513,514] and have been highly linked to MSC differentiation into osteoblasts[515]. The results were compared to osteogenic and a stem-like controls, consisting of MSCs cultured in osteogenic media (with the addition of 2.5 ng/ml BMP-2) for 14 days and MSCs cultured in base medium for 1 day, to prevent differentiation in longer timepoints, respectively (figure 4.9). The same phenotyping analysis was conducted on MSCs cultured on biofilms containing a combination of bacterial populations, expressing more than one recombinant protein at the same time, with the results shown in supplementary figure 1.

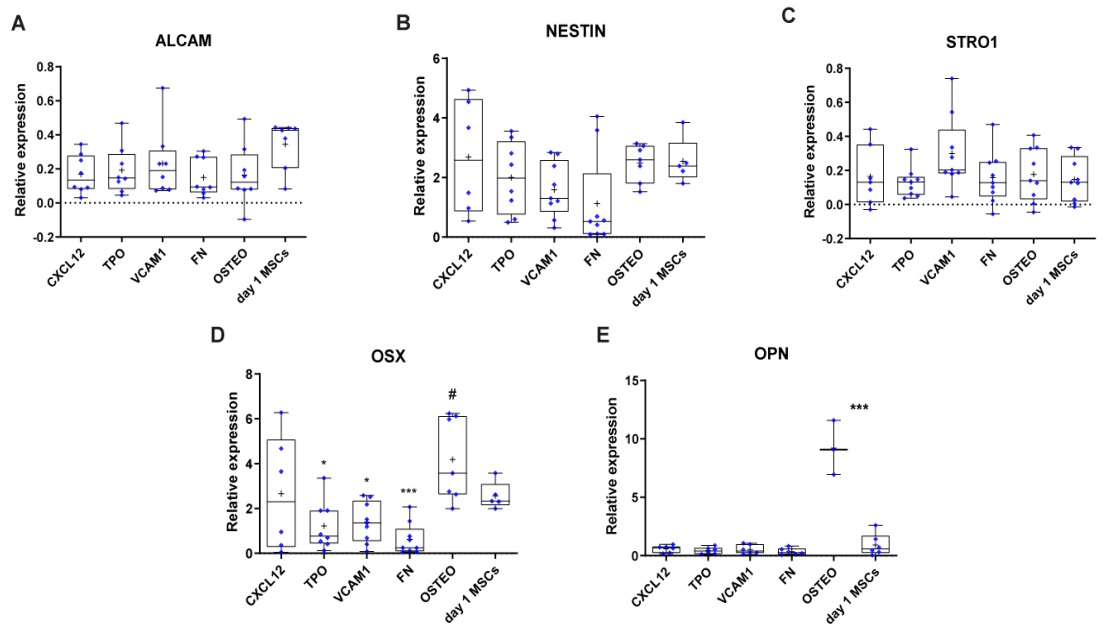

Figure 4.9. In-cell Western analysis of MSC phenotype on biofilms. MSC were phenotyped using in-cell Western to analyse relative expression of ALCAM, Nestin, Stro1, osterix (OSX) and osteopontin (OPN). Analysis was performed after a 14-day co-culture with the biofilms depicted in the graphs, namely CXCL12, TPO, VCAM1, FN, osteogenic medium (OSTEO) and glass-only control MSCs grown for one day to ensure phenotype preservation (day 1 MSCs). No statistical difference was observed between the stemness markers expressed by the control MSCs and the stem cells cultured on *L. lactis* (A-C). Interestingly, increased expression of osteogenic differentiation markers osteopontin and osterix (D, E) was not observed in any of the conditions except for the osteogenic medium, (*** $p < 0.001$) compared to the rest of the conditions (two-way ANOVA with Tukey post-hoc test) and in the OSX graph (* $p < 0.05$, ** $p < 0.01$, *** $p < 0.001$ compared to the reference condition, OSTEO, labelled as #).

ICW analysis of Stro1, Nestin and ALCAM expression revealed that all three markers of stemness are expressed by the MSCs after 14 days of culture on all biofilm conditions. Despite the notable overexpression of ALCAM and Stro1 by the MSCs cultured on biofilms consisting of mixed *L. lactis* populations expressing TPO/FN/VCAM-1 (figure 4.9 A, C), the difference is not significant compared to the MSC control. Furthermore, Nestin expression was comparable between the MSCs cultured on all biofilms and the control (figure 4.9 B). Together, these results suggest that MSCs cultured on recombinant *L. lactis* biofilms have the potential to maintain their stem-like phenotype in a similar level to naïve MSCs cultured for one day (MSC control).

Staining for osteogenic markers (figure 4.9 D, E), also suggested that all biofilms can maintain an undifferentiated state of MSCs compared to our osteogenic control. We selected OPN, a highly abundant non-collagenous protein found in bone tissue, that has been extensively used as a marker for the early osteogenic differentiation of MSCs[516,517] and OSX, a commonly used marker that may indicate the onset of the osteogenic differentiation of MSCs[518]. Our data suggests an observable difference between cells cultured on all biofilms and the osteogenic control (figure 4.9 D), and a comparable production of OPN between the biofilm conditions and the undifferentiated MSC control. MSCs cultured on all biofilm conditions, except for CXCL12, showed significantly less OSX expression than the osteogenic control (figure 4.9 E). Combined, our results suggest that the tested recombinant *L. lactis* biofilms can maintain a stem-like MSC phenotype for up to 14 days in culture, while reducing their potential for osteogenic differentiation.

To further verify our claim that the MSC phenotype is maintained in long term co-cultures with the biofilms, we repeated the 14-day cultures and stained for the early adipogenic differentiation marker Pref-1. Consistent with our hypothesis, the expression of Pref-1 by the MSCs was significantly downregulated compared to the adipogenic control (figure 4.10). This trend was consistent among all biofilm conditions, with the exemption of CXCL12, where Pref-1 was expressed at comparable levels to the differentiated cells. Combined with the results reported in figure 4.10, our data suggests a possible influence of the *L. lactis* biofilms in maintaining the MSCs in a stem-like phenotype for up to 14 days in co-culture without inducing their differentiation towards the osteogenic or the adipogenic lineage.

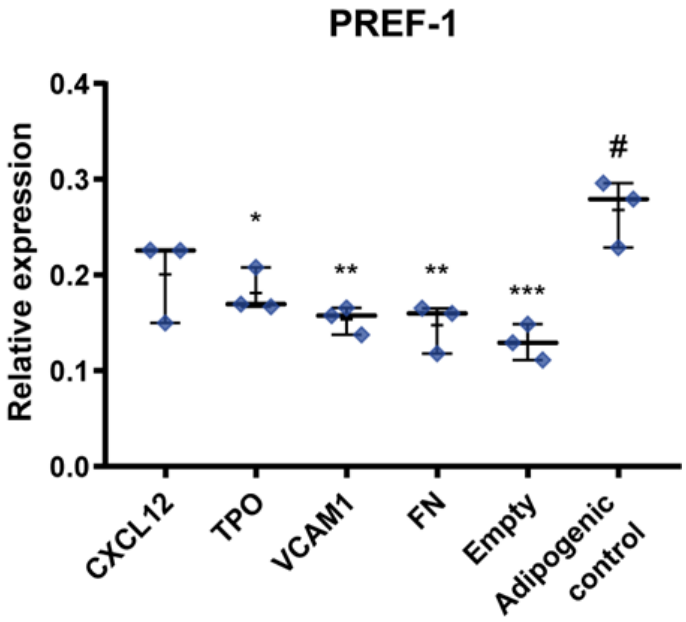

Figure 4.10. In-cell Western analysis of adipogenic potential of human BM-derived MSCs cultured on different biofilms. Stem cells grown on *L. lactis* were stained for Pref-1 and were compared to the adipogenic control. With the exception of CXCL12, cells grown on all other biofilms showed significantly downregulated expression of Pref-1, and no commitment to the adipogenic lineage. Data was analysed using a two-way ANOVA followed by a Tukey post-hoc test (* $p < 0.05$, ** $p < 0.01$, *** $p < 0.001$, compared to the adipogenic control).

The same analysis was conducted in the presence of a hydrogel in order to determine whether a 3D component would have any effect on the MSC phenotype after co-cultures with the biofilms. Like the experiment described above, human BM MSCs were seeded on CXCL12, TPO, FN, VCAM1 and EMPTY *L. lactis* biofilms, as well as a FN-coated coverslip and MSCs grown in osteogenic media, that served as the control conditions. To resemble the BM architecture more closely, we added a 5% w/v PEG hydrogel on top of the biofilm-MSC co-cultures, in all of the conditions and controls. The cells were co-cultured for 14 days and the MSC phenotype was assessed using ICW analysis and the same markers and normalisation procedure as described above.

Our data suggests that the stemness markers Nestin and Stro1 are not statistically different to the MSC control. At the same time, the EMPTY biofilms, as well as the osteogenic control displayed significantly lower Nestin expression compared to the MSC control, while the same trend was observed in the case of the osteogenic media and Stro1 expression when

compared to the MSCs (figure 4.11 A, B). ALCAM expression appeared statistically lower in all conditions compared to the MSC control (figure 4.11 C). At the same time, both osteogenic markers OPN and OSX were significantly upregulated in the osteogenic control compared to the biofilm conditions (figure 4.11 D, E). Together, this data suggests that even in the presence of a hydrogel, the biofilms have the potential to maintain a BM-resembling, stem-like MSC phenotype in long term cultures, while at the same time preventing the commitment of cultured MSCs towards osteogenic lineages. This observation solidifies our hypothesis that MSCs can be maintained in a stem-like state on the biofilms both in a 2D and 2.5D environment, and as an extension, this platform could more closely resemble the BM conditions, and could be used to more closely mimic the BM HSC niche.

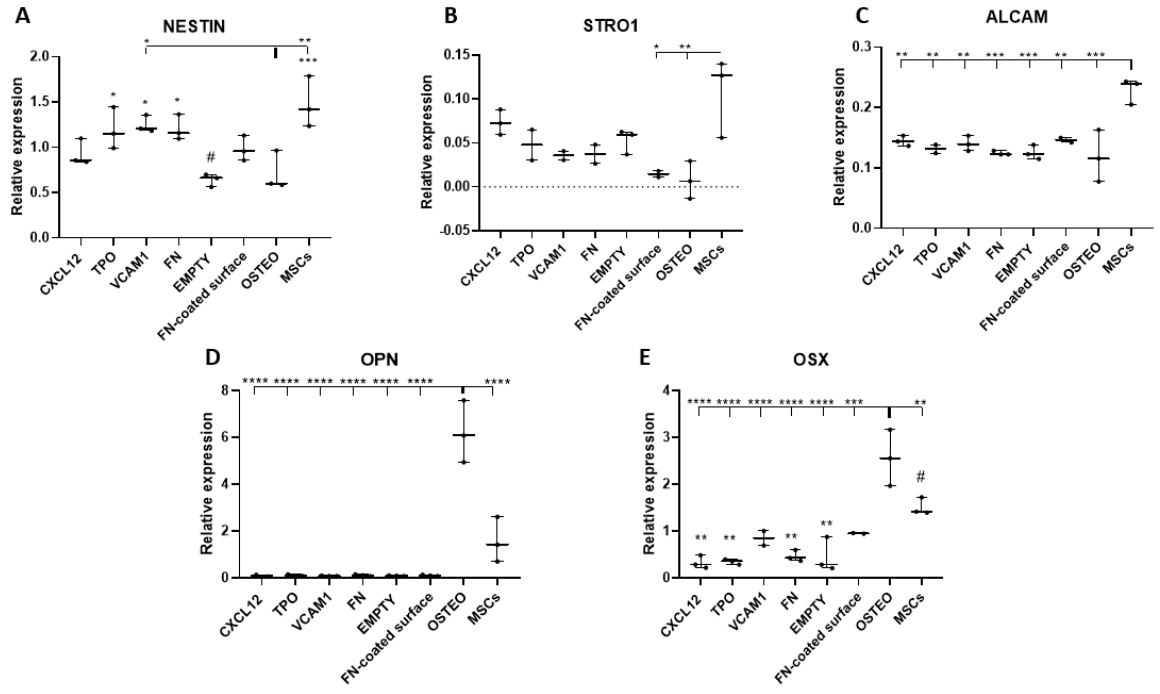

Figure 4.11. In-cell Western analysis of the phenotype of human BM-derived MSCs cultured on top of *L. lactis* biofilms in the presence of a 5% w/v hydrogel for 14 days. The phenotype of the cells was assessed by staining for Nestin, Stro1, ALCAM, OPN and OSX and the data was normalised against the housekeeping protein β-actin. Combined, this data suggests a maintenance of the stemness markers Nestin and Stro1 by the biofilm conditions, and no commitment of the stem cells towards osteogenic differentiation, as supported by the absence of statistically significant expression of OPN and OSX compared to the osteogenic control. Data was analysed using a two-way ANOVA followed by a Tukey post-hoc test (* $p < 0.05$, ** $p< 0.01$, *** $p < 0.001$, **** $p < 0.0001$ compared to the reference condition).

To sum up our findings, we compared the phenotype displayed by the MSCs when cultured with and without the PEG hydrogel. To easier visualise the data, we took the average of the readings obtained for each MSC-biofilm condition and normalised against the average MSC reading. The results are presented in figure 4.12. In the comparison between the stemness markers expressed by the MSCs in the gel and no gel conditions we observed a similar expression of Nestin and ALCAM (figure 4.12 A, B). At the same time, Stro1 appeared downregulated in the presence of a hydrogel, especially on MSCs cultured on TPO, VCAM1 and FN-expressing biofilms (figure 4.12 C). A similar trend was recorded in the expression of OPN, that was shown to be expressed at significantly higher levels in the absence of the hydrogel (figure 4.12 D). Finally, OSX was also expressed at a higher rate in 2D compared to stem cells cultured in the presence of a hydrogel, and especially on MSCs cultured on CXCL12-expressing bacteria (figure 4.12 E). Our results suggest that while most stemness markers show similar expression levels with and without the hydrogels present, the osteogenic markers appear over-expressed in the absence of the 3D element. Therefore, we can suggest that the presence of a hydrogel in the biofilm-MSC co-cultures may have a higher potential to maintain the MSCs in a more naïve state, resembling their BM phenotype, while also preventing their osteogenic differentiation compared to 2D cultures.

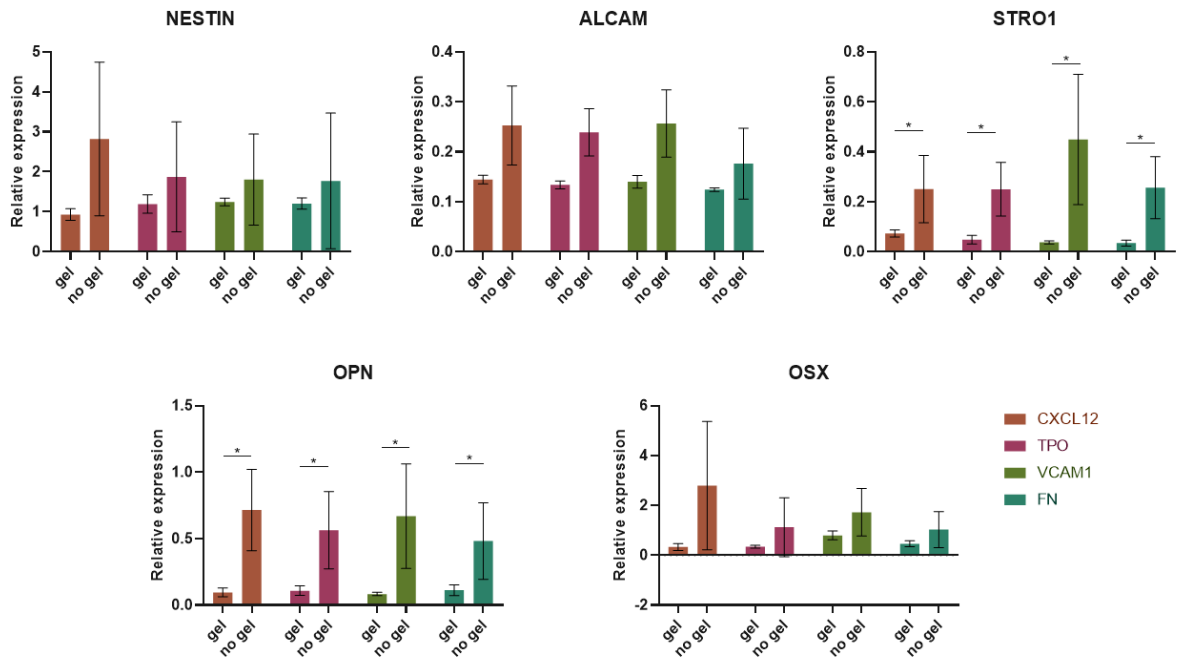

Figure 4.12. Comparison between the expression of stemness and osteogenic markers by human BM-derived MSCs. Stemness (A-C) and Osteogenic marker (D, E) expression was assessed on stem cells cultured on biofilms for 14 days with and without the addition of a non-degradable, 5% w/v PEG hydrogel. The data presented constitute the average of each condition (n ≥ 3), normalised against the MSC reading for each marker. In total, the data suggests that while there is no significant difference between the expression of nestin, alcam and Osterix, Osteopontin and Stro1 appear downregulated in the presence of a hydrogel. Data are presented as mean ± SD (*p-value<0.05), after a Student's t-test between the conditions.

Following our observation that the biofilms have the potential to maintain the cultured MSCs in a naïve state, we aimed to investigate whether the stem cells maintain their differentiation capacity following their co-culture with the engineered *L. lactis*. As previously, we cultured human BM-derived MSCs on *L. lactis* biofilms producing CXCL12, TPO, FN and VCAM1, as well as EMPTY bacteria. The co-cultures were maintained in base MSC culture media for 14 days, following another 14 days of culture in osteogenic media. After the total of 28 days, the MSCs were stained for OPN and OSX to assess their differentiation towards the osteogenic lineage. The results were compared to MSCs cultured on a glass coverslip in osteogenic media (labelled as MSC on the graphs) and are displayed in figure 4.13. ICW analysis revealed no significant difference in the expression of neither OPN nor OSX compared to the osteogenic control (figure 4.13 B, C), suggesting that the differentiation capacity of MSCs after long term co-cultures with the biofilms is maintained.

This interesting observation is consistent among all biofilms, suggesting that the expression of the different markers, combined by the active presence of the biointerface may provide a degree of resemblance to the BM, where MSCs reside in a naïve, stem-like state, while also retaining their characteristic ability to differentiate into other cell types.

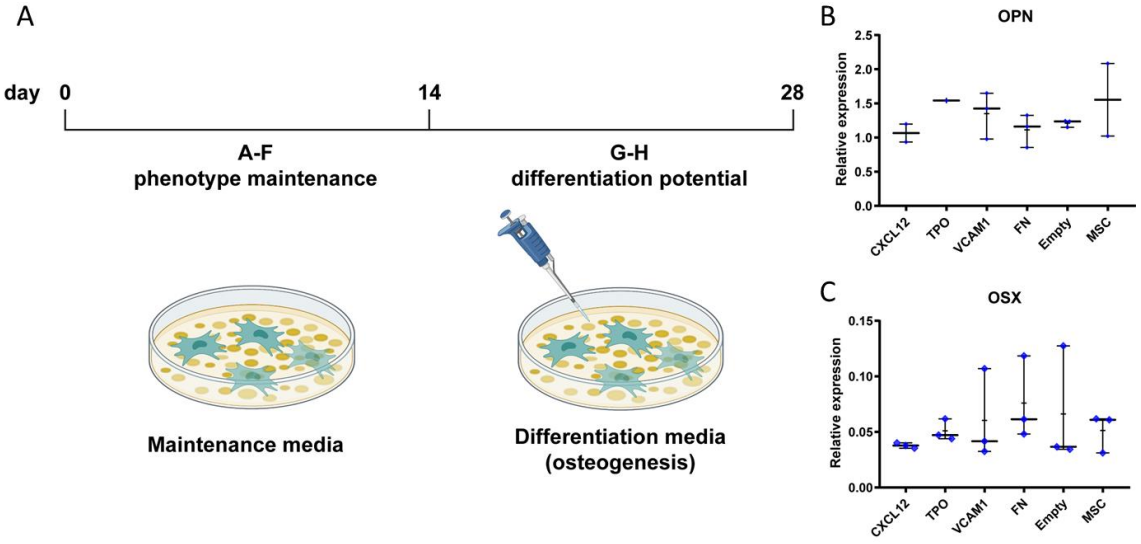

Figure 4.13. In-cell Western analysis of the phenotype of human BM-derived MSCs to assess the maintenance of their differentiation capacity. The cells were cultured on top of *L. lactis* biofilms in base medium for 14 days, following another 14-day culture in osteogenic media. The results were normalised against the housekeeping gene b-actin and were compared to MSCs grown in osteogenic media for 14 days (MSCs). No statistical difference was observed between the differentiated MSCs, and the stem cells cultured on the biofilms (two-way ANOVA, followed by a Tukey post-hoc test).

4.3.4. MSC tracking on biofilms

Following the study of the phenotype decisions of the MSCs in response to their interaction with the biofilms, we aimed to examine the movement and migration of the stem cells in our co-cultures. The mechanism by which cells control directional persistence during migration has been a major topic of research for a variety of applications, ranging from studies aiming to characterise the cell-material interactions[519], attempts to control and direct stem cell migration in tissue engineering and injury repair[459,520], and efforts to better understand pressing clinical issues such as immune cell migration[521] or cancer invasiveness and metastasis[522].

Inspired by the constant state of flux and remodelling that characterises native stem cell niches[523,524], we aimed to evaluate the way MSCs move and explore their surroundings in our dynamic system. To mimic the 3D structure of the niche, we tracked MSC trajectories on

different *L. lactis* biofilms, with and without the presence of a hydrogel, bearing stiffness within the range found in human BM[525]. Specifically, the hydrogels used in this work had been previously characterised and have been shown to have a stiffness of 5 kPa. Initially, we examined whether there is a difference between MSC movement in 2D and 3D, by tracking cells seeded directly on the biofilms and comparing them to cells seeded in a monolayer between the biofilms and a hydrogel. At the same time, we also investigated whether the biofilms, producing different recombinant proteins could be linked with any potential changes in the movement patterns of MSCs, in both 2D and 3d. Figure 4.3.13 depicts the movement trajectories followed by the cells, at different timepoints and in different culture conditions. Analysis of a 24h tracking of the cells displayed a significant difference between the range and speed of motion exhibited by the MSCs in the presence of a hydrogel compared to its absence (Figure 4.14 A). Cells seeded in 2D were highly mobile and appeared to actively explore their environment, following large trajectories. In contrast, the presence of the hydrogel appeared to significantly restrict cell movement, resulting in less active cells that largely remained attached to their initial seeding point. The same trend was observed after analysis of cell speed, with higher speeds measured in 2D compared to 3D.

Following this observation, we aimed to examine the effect of hydrogel degradability on cell movement. In a similar experiment, we seeded MSCs on the *L. lactis* biofilms and tracked cell movement in the presence of a non-degradable and a degradable hydrogel. To provide a close BM analogue, we fabricated protease-degradable hydrogels, using the crosslinking peptide GCRDVPMSMRGGDRCG (VPM)[526], which is rapidly cleaved by the matrix metalloproteinases MMP-1 and MMP-2[527]. The degradable hydrogels were manufactured at a 1:1 PEG:VPM ratio, while the non-degradable hydrogels consisted of 100% PEG.To allow enough time for the cells to degrade and remodel their 3D environment, we tracked cell movements at days 3, 5 and 7, after seeding. Analysis of the cell trajectories and average cell speed suggested a significant difference between the cells cultured in contact with the degradable and non-degradable hydrogels (Figure 4.14 B-D). The difference was more pronounced on days 3 and 7, with the MSCs cultured in the presence of the PEG-VPM hydrogel moving at an observably higher speed compared to the non-degradable condition. While most differences in cell movement appear to have settled by day 5, we again observed a significant change at day 7, with similar cell movement trends as in day 3.

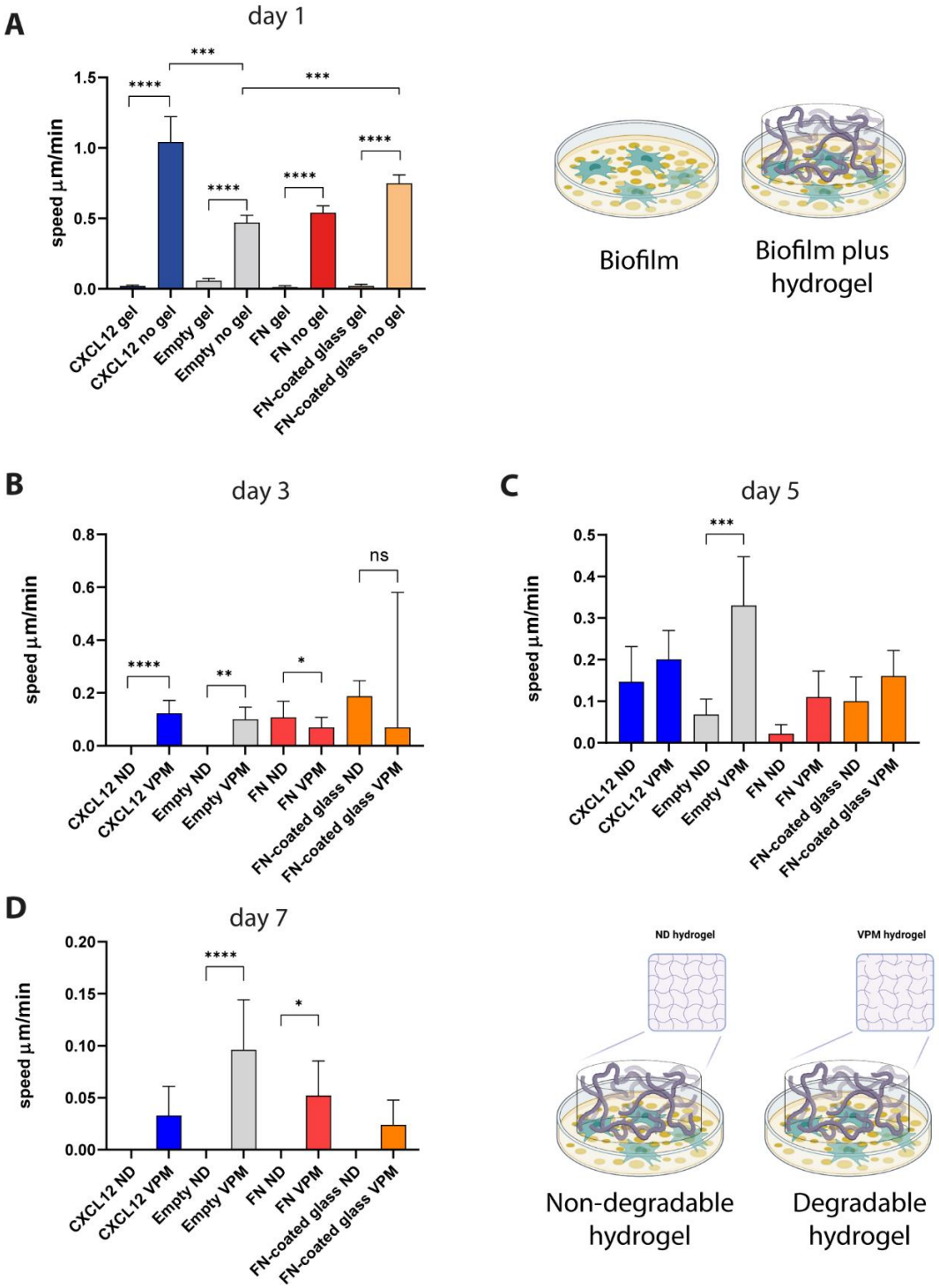

Figure 4.14. Average speed by cell. Human MSCs were seeded on *L. lactis* biofilms in either 2D or 3D conditions and were tracked at different timepoints. (A) The cells were initially tracked for 24h hours, with 5-minute intervals after overnight incubation, the average speed by cell was recorded and comparisons were drawn between the cells incubated with and without the presence of a hydrogel and between the different biofilm conditions. (B-D) Cells were incubated on top of *L. lactis* biofilms in the presence of either a non-degradable (PEG) or a degradable (VPM) hydrogel. Cell speed was measured after tracking for 1 hour with 2-minute intervals on days 3, 5 and 7 of the MSC-biofilm co-cultures. Data was analysed using a two-way ANOVA followed by a Tukey post-hoc test (* $p < 0.05$, ** $p < 0.01$, *** $p < 0.001$, **** < 0.0001).

The collective observation that MSCs cultured in the presence of degradable hydrogels are more active in exploring their surroundings and move at a higher speed compared to cells cultured in non-degradable 3D conditions is further supported by mean displacement (MSD) analysis data (Figure 4.15), that suggests a larger area explored by MSCs cultured in the degradable hydrogel conditions. For this analysis, we used the Excel plugin provided by Gorelik and Gautreau[475]. The program plots the average square displacements over increasing time intervals between positions of a migration trajectory, that in our experiment describes the displacement of MSCs as they move on the *L. lactis* biofilms. MSD is a commonly used in the context of cell migration, as it indicates the surface area explored by cells over time (Figure 4.15 A-C), which can be related to the overall efficiency of migration and carries information about both speed and directional persistence of the particles measured. MSD can also be expressed as a log-log plot, with log(MSD) on the y axis and log(time interval) on the x axis (Figure 4.15 D-F). The slope of these log-log plots, often called the α-value, is a handy index for directional persistence: it equals 1 for randomly moving cells and 2 for cells that move in a perfectly straight manner.

Our data suggests that, in general, MSCs move in a random manner. They appear to be relatively immobile in the presence of non-degradable hydrogels, exploring smaller areas and showing minimal cell movements around their area of initial attachment. In contrast, MSCs cultured in the presence of the degradable PEG-VPM hydrogels appear to follow larger trajectories and being significantly more mobile. There is a slight change of cell migration on day 5, as MSCs in almost all conditions appear to slow down their movement, a trend that disappears by day 7.

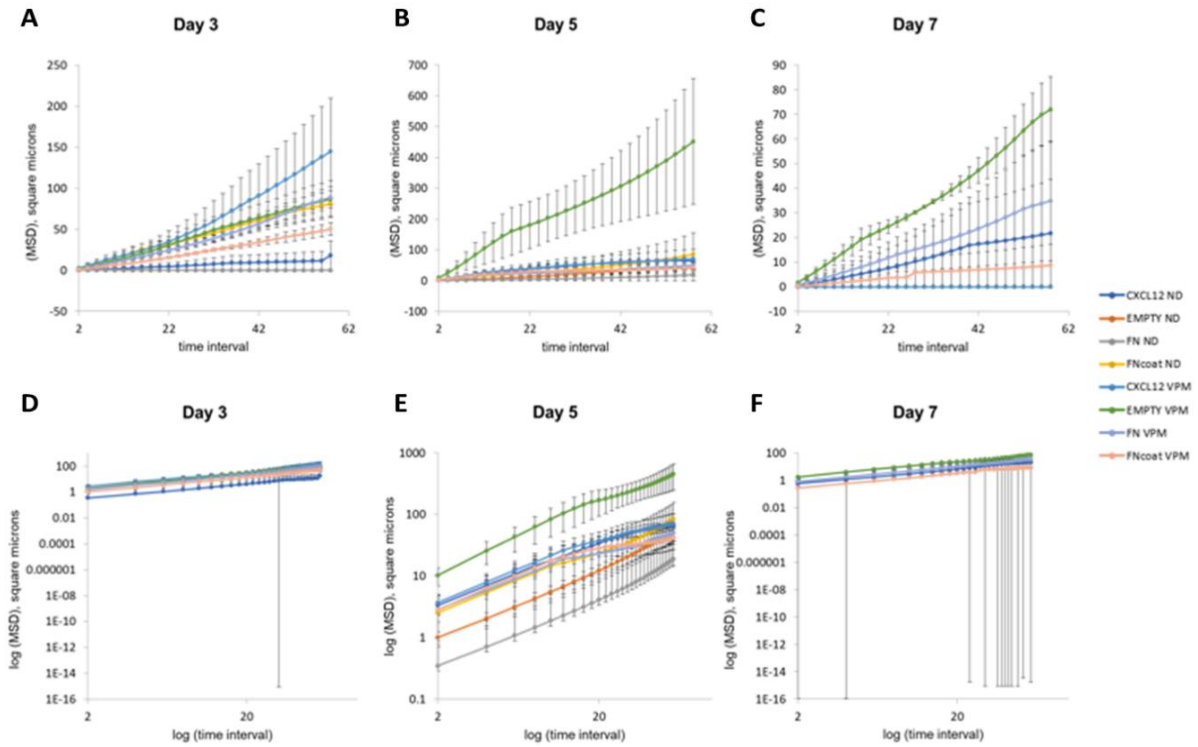

Figure 4.15. Mean square displacement analysis for MSC migration on different *L. lactis* biofilms in the presence of a degradable (VPM) or a non-degradable (ND) hydrogel. MSCs were cultured on *L. lactis* for 7 days and the cells were tracked on days 3, 5 and 7, for 1 hour with 2-minute intervals. MSD plotted on a linear scale top and a log-log scale, bottom for each timepoint. All cells appear to follow random cell movement and explore a larger area in the degradable gel conditions compared to the non-degradable. The large error bars shown in graphs D, E and F, represent outliers. N ≥ 3, error bars are standard error of the mean.

Overall, MSCs appear to actively explore their surrounding environment, especially in the presence of the degradable hydrogels, on all biofilms. Representative images of representative cell trajectories for all conditions are displayed in supplementary figure 2. Furthermore, the migration trends of MSCs in terms of MSD are consistent with the average speed by cell recorded in our experiment, showing that the stem cells how more efficient migration in the presence of degradable compared to non-degradable hydrogels. This result may suggest that except for displaying increased mobility, MSCs may also be actively remodelling their ECM, resulting in degradation of the PEG-VPM hydrogels that would allow them to move more freely and explore larger areas of the niche.

4.4. Discussion

The innate ability of multipotent MSCs to differentiate into a variety of mature tissue cells (Figure 4.16) has placed the cells in the spotlight of experimental bioengineering. The importance of MSCs in cellular therapeutics and regenerative medicine has directed scientific interest towards the development of innovative culture methods in order to provide more effective, cost efficient and safer strategies for stem cell transplantation. To address this medical need, a variety of studies have explored the use of different biomaterials, each bearing unique biochemical and mechanical properties for the *ex-vivo* MSC maintenance, differentiation, and expansion.

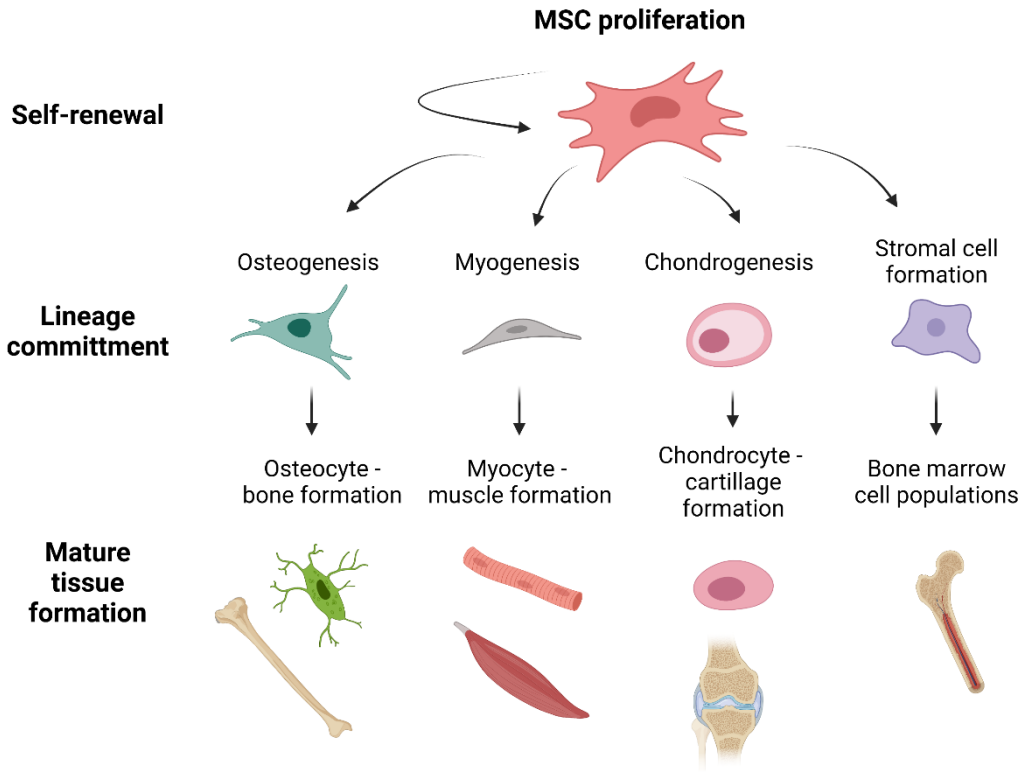

Figure 4.16. The differentiation capacity of MSCs. Multipotent MSCs have the capacity to commit to different lineages and differentiate to a variety of mature tissue cells.

The first and foremost attribute of any material designed for clinical applications is its biocompatibility. All clinically significant materials must therefore be engineered to interact with biological systems without affecting cell viability, in order to be successfully used for therapeutic or diagnostic purposes. The requirement for the lack of any adverse effects on

the human body has been recognized from the onsets of the field of biomaterials, with early studies suggesting that any clinically relevant material should not cause blood clotting, inflammation or any other immune response, and should generally be non-cytotoxic[528]. Advances in the field, combined with the need to address more complex clinical issues, drove the development of more sophisticated biomaterials with added characteristics, such as biofunctionality and the featuring of active components. More precisely, the ability of the biomaterial to encourage cell adhesion and spreading has been identified as a key feature of developed implants and transplants. In particular, cell adhesion has been highly associated with cell communication and regulation, through a variety of signals that regulate cell survival, migration, differentiation, and quiescence and is therefore fundamental for the development and maintenance of tissues[529]. The importance of cell adhesion has been further consolidated by evidence suggesting that changes or disruption in cell adhesion can lead to a variety of diseases, including osteoporosis[530], arthritis[531], and various forms of cancer[532].

Our findings, outlined in section 4.3, suggest that *L. lactis* NZ9020 can be used as a living biomaterial in co-cultures with human MSCs, without negatively affecting cell viability. Furthermore, the strain can be genetically engineered to encourage cell attachment and spreading by expressing human recombinant adhesion proteins, such as the FN $III_{7\text{-}10}$ fragment and the extracellular part of VCAM1. In particular, the FN-expressing *L. lactis* has been shown to induce a similar degree of cell spreading as observed in cells seeded on a FN-coated substrate. This finding is of particular interest, as it demonstrates that our living biointerface can induce the same effect on human stem cells, in terms of cell adhesion, as traditional culture methods. Moreover, our data support that the bacterial biointerface allows for the interaction between the MSCs and the biofilm, with MSCs forming focal adhesions when cultured biofilms expressing all recombinant proteins used in this work. Therefore, the characterisation of the interaction between the biofilms and MSCs has shown that the biointerface can be used successfully as a substrate for cell culture, as it displays the most relevant basic characteristics of biomaterials; biocompatibility and the potential for cell adhesion and spreading.

Another equally important feature of successful biomaterials is their ability to direct cell fate according to the clinical application they are designed to address[533]. In their natural niche,

stem cells are tightly regulated by a combination of physiochemical factors, thus, conventional cell culture approaches based on the addition of soluble factors to direct stem cell fate have resulted in limited success. This limitation has led to the development of bioactive materials, featuring surface modifications[534], as well as mechanical[535], electrical[536], morphological and chemical properties[537]. In this way, the designed materials aim to deliver stem-cell-regulatory signals in a precise and near-physiological fashion with the aim to mimic the native tissue microenvironment and elicit the target cultured stem cell response[538]. Hence, a variety of different natural and artificial biomaterials has been developed, each bearing different levels of biocompatibility, biodegradability, bioresorbability, low immunogenicity and low toxicity, providing a variety of tools that can be tuned to meet each clinical application[539]. Some of the most important aspects of successful biomaterials are their ability to induce cell adhesion, present and deliver soluble signals, and provide a form of architecture either in terms of a 3D environment or micro- or nanotopography in 2D settings[540].

In our work, we have created a system that aims to actively provide stem cells with adhesion molecules and soluble signals, directly produced by the bacteria, while also simulating a form of nanotopography with the presence of the biointerface. In this way, our engineered microenvironment provides the cultured stem cells with the required signals to induce cell fate decisions in a precise, tunable manner, to allow for an easy, adaptable and inexpensive way of controlling stem cell fate. Except for providing a substrate that encourages cell adhesion and spreading, we have shown that the adhesion molecules and soluble cytokines produced by NZ9020 can maintain human MSCs in a naïve state that resembles their phenotype in the bone marrow. After 14 days of cultures on the biofilms, the MSCs maintain high Nestin, ALCAM and Stro1 production, at similar levels as naïve BM MSCs, while they show no sign of commitment towards osteogenic differentiation, as suggested by the lack of OPN and OSX expression (section 4.3.3). Furthermore, the co-culture with the biointerface was not shown to induce the adipogenic differentiation of cultured MSCs either, as demonstrated by the absence of Pref-1 expression by the MSCs in the majority of the conditions. The same trend was observed in the presence of a hydrogel, as MSCs showed high maintenance and expression of the selected stemness markers, while also displaying no significant overexpression of OPN and OSX. This observation may suggest

that the combination of the biointerface, the chemical and adhesion signals it provides, and the 3D environment provided by the hydrogel may present the MSCs with a collection of conditions that closely resemble their natural niche in the bone marrow and as a result contribute to the maintenance of the cells in a naïve, stem-like state.

Another essential characteristic of stem cells and one of their most clinically significant attributes is their ability to differentiate to a variety of mature tissue cells. In our effort to engineer a platform to maintain MSCs in a naïve, stem-like phenotype for clinical applications, it is important to assess whether our system affects the differentiation potential of the cultured stem cells. To test this, we performed a 14-day culture of MSCs on different *L. lactis* biofilms, followed by another 14 days of incubation in osteogenic media. After the total of 28 days, phenotype analysis showed an overexpression of OPN and OSX in all conditions at statistically similar levels to the osteogenic control.

MSCs have been identified as a prominent candidate for cell-based therapies for a variety of immune-mediated, inflammatory, and degenerative diseases, due to their immunosuppressive, immunomodulatory, and regenerative potentials. However, limiting factors including the limited availability of clinically significant cell numbers due to the low *ex vivo* MSC survival, the difficulty of *ex vivo* cell overexpansion prior to infusions as well as the intrinsic differences between MSC and different sources and donors, variability of culturing protocols, have created an urgent need for the development of novel methods of long-term maintenance and expansion of MSCs. A variety of approaches to improving the immunosuppressive and immunomodulatory properties of MSCs aimed for transplantation have been explored, including cell priming with soluble cytokines[541], MSC priming using hypoxic environments[541], or pharmacological drugs such as isoflurane[542] and all-trans retinoic acid[543]. Additionally, a range of different biomaterials have been developed with a view to improving the therapeutic potential of MSCs has been reported. Such methods include the use of a variety of polymers as 3D culture systems[544], nanotopographical design[545], as well as the incorporation of functional properties on different polymer scaffolds[546], to provide MSCs with the appropriate signals in order to direct stem cell fate for each desired application. Nevertheless, the chemical and architectural complexity of the bone marrow and the constant state of flux directed by the ECM remodeling by other BM-

residing cells have significantly limited the progress and outcomes of efforts to mimic and recreate a BM niche *ex vivo*.

In the field of cellular therapeutics, current efforts to improve the clinical efficacy of MSCs include priming with interferon- γ (IFN-γ)[547], interleukin-17 (IL-17)[548], or other pro-inflammatory cytokine cocktails[549]. Combined with some of the aforementioned culture methods involving bioactive materials, these approaches have demonstrated an enhancement of the immunosuppressive properties of MSC and some regulation of their differentiation potential, however, the open question of generating high numbers of naïve MSCs that maintain their functional properties after long term cultures still remains unanswered. Our work has provided evidence that MSCs cultured on genetically engineered *L. lactis* biofilms remain phenotypically similar to their BM-residing state in long term cultures. Furthermore, we have shown that those MSCs retain their differentiation potential and can be easily directed towards the osteogenic lineage in a way comparable to traditional methods. This observation bears significant clinical potential, as we have demonstrated that our system can maintain MSCs without affecting their stemness, an attribute that would be of great medical significance for therapeutic applications.

Finally, we have shown that MSCs cultured in our system remain active and retain their ability to migrate and remodel their microenvironment, resembling their BM-residing state. In section 4.3.4, we demonstrate that the MSCs move freely on the *L. lactis* biofilms, constantly exploring their surroundings. We also suggest that the addition of a 3D component, in the form of a degradable or non-degradable hydrogel has a direct impact on MSC movement on the biointerface, with cells moving at a higher average speed and following longer trajectories in the presence of the degradable ECM compared to the non-degradable one. This result suggests that the MSCs maintain their active phenotype and their functional capacity to secrete matrix metalloproteinases, that allow them to degrade and remodel their surrounding microenvironment, resulting in increased cell movement in the degradable matrix. MSC migration has been identified as a key mechanism for successful cellular therapies based on the ability of the stem cells to “home” to areas of injury in response to signals of cellular damage and initiate tissue regeneration[550]. Consequently, by demonstrating that our system has the capacity to allow cell migration in 2D and 3D, provides evidence of a close representation of the native BM conditions *ex vivo*.

To our knowledge, there is a lack of studies of the characteristics of migration potential of MSCs on artificial BM-mimicking microenvironments. Nevertheless, recent research has identified a small number of chemokine receptors and adhesion molecules that mediate the homing of MSCs in the BM. In more detail, the chemokine receptor CXCR4 and its binding partner CXCL12[551], as well as VCAM1[552] have been recognized as significant regulators of MSC homing. CXCL12 in particular, has been used as a pretreatment to enhance the migration and increased the secretion of pro-survival and angiogenic cytokines in order to enhance the therapeutic potential of MSCs, while the CXCL12/CXCR4 signaling pathway has been described as critical for MSC survival, migration and cytokine secretion[553]. Our data, based on the use of recombinant CXCL12, is in line with previous research, both in terms of contributing to MSC phenotype maintenance and in inducing normal cell migration in our co-cultures. Furthermore, upregulation of the CXCR4 chemokine receptor has been identified as a key player in enhancing the migration ability[554] and inducing mobilization of MSCs to sites of tissue damage[555]. Consequently, we can suggest that the expression of CXCL12 by the biofilms may result in the overexpression of CXCR4 on the MSCs, that in turn upregulates the expression of stemness markers and prevents the differentiation of the stem cells, while also maintaining their migration capacity. FN has also been studied as a substrate for stem cell culture because of its wide presence in natural ECMs and its consequent potential to mediate cell adhesion and influence cell behaviour[556]. Our observations that MSCs attached and spread more on the FN-expressing bacteria and the FN-coated substrate is in agreement with previous research suggesting that MSC culture on FN-coated surfaces results in faster cell spreading, an enhanced formation of the actin cytoskeleton and its co-localization with proteins found in focal adhesions[557]. Similarly, the ability of our system to allow for normal MSC migration is consistent with the previously reported enhanced migration patterns of MSCs on FN-coated materials[558]. Despite the limited number of studies on the effect of cytokines and adhesion molecules on MSC phenotype, fate and migration capacity, our data supports the hypothesis that our engineered biointerface has the potential to closely mimic the BM conditions and contribute to the maintenance of cultured MSCs in an active, stem-like state, close to the one observed in the BM.

4.5. Conclusion

Having gathered increased scientific and medical interest, and having been used in more than 1000 clinical trials[559], MSCs have solidified their position as a major therapeutic strategy in the field of regenerative medicine. However, clinical outcomes can be negatively influenced by a variety of factors, such as the different tissue origins of used MSCs, donors of different gender, age, and medical history, variability in the tissue processing and culture conditions, freezing and thawing of the cells, and different administration routes[560]. Furthermore, to meet the high clinical demands, MSCs are cultured for long periods of time to obtain the required cell numbers, which results in important changes in gene expression and clonal selection, that affects their phenotype, biological and immunomodulatory properties[561]. Therefore, there is an urgent need to create novel culture systems that would provide increased, clinically relevant stem cell numbers, while also ensuring the maintenance of the phenotype, differentiation potential and functional properties of cultured MSCs for cellular therapeutics.

To address this issue, we have created a platform based on genetically engineered *L. lactis* biofilms that produce the key BM cytokines CXCL12 and TPO, and the adhesion molecules VCAM1 and FN. Our aim is to create an *ex vivo* BM-analogue with a view to providing the MSCs with the necessary signals to induce their proliferation and expansion, while at the same time maintaining their naïve phenotype and differentiation potential. Our initial results indicated that the biofilms have no negative effect on MSC viability during co-culture experiments. Furthermore, we have shown that the MSCs interact, attach, and spread on the biofilms, and especially on the FN-expressing bacteria, displaying strong focal adhesions and an elongated phenotype comparable to currently used traditional methods. Moreover, our data suggest that the MSCs are able to maintain both a naïve phenotype, similar to the one found in the BM, and retain their differentiation capacity when cultured on top of the biofilms. At the same time, we show that the biointerface does not induce stem cell differentiation towards the osteogenic or adipogenic lineages. Finally, tracking experiments have demonstrated that the MSCs cultured on the biofilms retain their innate active behaviour and showed increased cell movement and migration. At the same time, we have shown that the stem cells are able to remodel their microenvironment, after recording higher average speeds and longer migration trajectories of the MSCs cultured in the

presence of degradable compared to non-degradable hydrogels. Combined, our results suggest that our engineered biointerface can be successfully used as a substrate for stem cell culture and can be tuned to direct MSC fate to fit the desired medical applications. We aspire that our system be used in the future, in 2D, 3D or in a bioreactor setting, to provide the answer to current limitations associated with traditional stem cell culture methods for cellular therapeutics.

Chapter 5. Bacteria-HSC interactions

Summary

This chapter is focused on the interaction between *L. lactis* biofilms and human BM-derived HSCs. To study this interaction, we set up co-culture experiments, where the HSCs were seeded on biofilms of genetically engineered *L. lactis*, producing CXCL12, TPO, VCAM1 and FN, alone or in combinations. At an initial stage, we evaluated the interaction between the biointerface and the seeded CD34+ cell population (general cell population containing a number of HSCs) in 2D culture experiments, where the biofilm remained attached to a hydrophobic coverslip, while the stem cells were seeded directly on top of the bacteria at a density of 50,000 cells/ml. The populations that emerged from the CD34+ cell sample were assessed by flow cytometry after 5 days of culture. We also evaluated the force of adhesion and work of detachment between the stem cells and different biofilms, in order to assess their interaction dynamics in more detail. Furthermore, with the aim to move the system into 3D, we integrated a hydrogel into the system. In our 3D experiments, we encapsulated a sample of CD34+ cells in degradable or non-degradable PEG hydrogels of controlled stiffness and functional properties and cultured them on the same bacterial biofilms and in the same experimental settings as previously. We report no negative impact of the biointeface on CD34+ cell viability in both 2D and 3D environments. Our data also suggest that the biofilms can prevent lineage commitment of the CD34+ cells, maintaining them in a naïve state, and achieving a similar level of HSC expansion as traditional methods featuring 2D cultures in HSC expansion media and cytokine cocktails.

5.1. Introduction

Hematopoietic stem cells (HSCs) constitute a rare cellular population residing in the bone marrow (BM) and have recently gained traction in research due to their significant clinical potential. These multipotent, self-renewing cells have the unique capacity to regenerate the whole hematopoietic system in the event of hematological disorders[562,563]. Currently, there are two ways to obtain HSC grafts for regenerative medicine, including allogeneic HSC transplantation, in which hematopoietic stem and progenitor cells (HSPC) are procured from a healthy donor and used to reconstitute a patient's hematopoietic and immune systems;

and autologous HSC transplantation, in which the patient's own HSPC are isolated and cultured to make up the end transplant[564]. In clinical settings, human allogeneic stem cell therapy relies on HSC grafts that can be isolated from peripheral blood, bone marrow or cord blood. However, the scarcity of donors, combined with the additional requirement that immunological barriers need to be overcome to allow sustained engraftment while minimising risk of graft-versus-host disease developing in the recipient of transplanted stem cells pose a significant problem to widespread, successful, and easy to access transplants[565]. Combined with the need to identify and match donors for human leukocyte antigens (HLA) and the time required to identify and procure an HLA-matched unrelated donor, allogenic HSC transplantation may take too long for patients with rapidly progressive malignancies[566]. Furthermore, the long and painful HSC isolation procedure needed for autologous HSC transplantation, combined with the increased possibility of infection and often low isolated or surviving HSC numbers have posed significant limitations in the medical use of autologous grafts[567]. Given the importance of the presence of high numbers of definitive hematopoietic stem cells (HSCs) in the donor material for the long-term durability of this treatment, current research is focusing on the identification and study of the key HSC regulators of HSC fate decisions, including survival, proliferation and expansion[568,569]. Such efforts would pave the way to creating *ex vivo* culture methods aiming to achieve clinically relevant expansion of HSCs for transplantation and medical applications.

5.1.1. HSCs in the BM microenvironment

The complexity of the BM and the variety of signals that support HSC stemness and self-renewal have proven a limiting factor in current approaches to HSC expansion methods. Several studies in both mice and humans have reported a variety of distinct HSC niches (figure 5.1) including the endosteal niche, where HSCs are mainly supported by osteoblastic cells[570,571], the perivascular niche, in which HSCs are maintained by vascular and perivascular cells[572], as well as a third niche, formed and regulated mainly by Nestin^{+} mesenchymal stem cells[573].

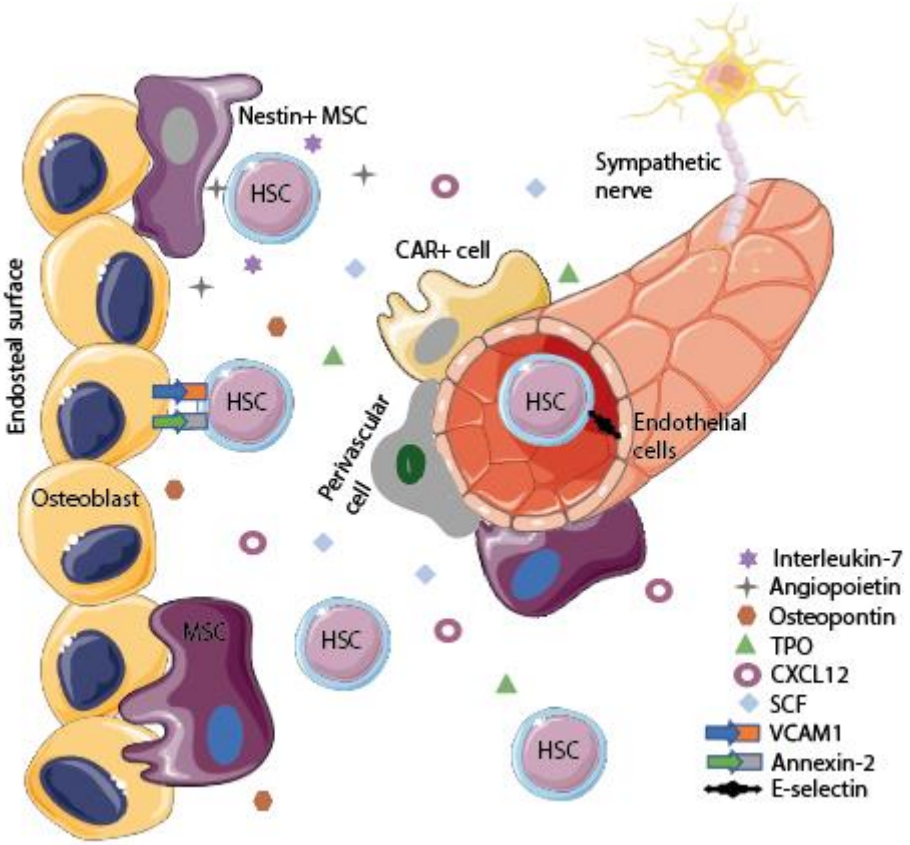

Figure 5.1. The HSC niches. The endosteal, perivascular, and Nestin+ MSC regulated HSC microenvironments.

Each HSC niche consists of a variety of cells, such as osteoblasts, mesenchymal stem cells (MSCs), adipocytes, endothelial, perivascular and stromal cells, that secrete a variety of chemical signals that influence HSC fate[55]. Furthermore, HSCs are regulated through hormonal and sympathetic nervous system signals as well as chemokines and adhesion proteins secreted by the other cells present in the BM. Except for the biological cues, the physical characteristics of the BM have played a critical role in HSC regulation. The stiffness of the niche, combined with the ligands present, have proven key determinants of the lineage specification of HSCs[56].

5.1.2. Cellular components of the HSC niches

The HSC niches are regulated by an intricate interplay between a variety of different cell types and the chemical stimuli they produce. A schematic representation of some of the key cellular components of the niche and the effect they induce on HSC fate through cytokine

production is depicted in figure 5.2. In all cases, HSCs appear to be in close proximity to mesenchymal stem cells, while HSCs with the highest hematopoietic potential have been reported to reside in the endosteal niche and adhere to the endosteal matrix[57]. MSCs that can differentiate into both osteogenic lineage cells, as well as adipocytes and chondrocytes, are another major component of the BM niche. Perivascular CXCL12-expressing mesenchymal progenitors are especially important in HSC maintenance as they induce cell maintenance and are associated with increased repopulation activity[61]. Additionally, MSCs have been reported to produce angiopoietin-1 (ANG1) and stem cell factor (SCF), key cytokines for HSC expansion and self-renewal. Nestin+ MSCs have also been reported to play a role in HSC maintenance and homing in the BM. Studies have shown that Angiopoietin-1 and Interleukin-7 secretion by Nestin+ MSCs has a direct effect on HSC phenotype quiescence and mobilisation in the BM[574].

Osteoblasts are the key regulators of the endosteal HSC niche. They produce a variety of chemical and adhesion stimuli that directly impact HSC fate. Specifically, osteoblasts produce SCF, TPO[60] and OPN, as well as angiopoietin 1 and 2, the levels of which regulate HSC maintenance, homing and quiescence[575]. Apart from providing attachment and homing for HSCs through N-cadherin[576] and annexin-2 expression[58], osteoblastic cells tightly regulate haematopoiesis through Wnt and Notch signalling[59].

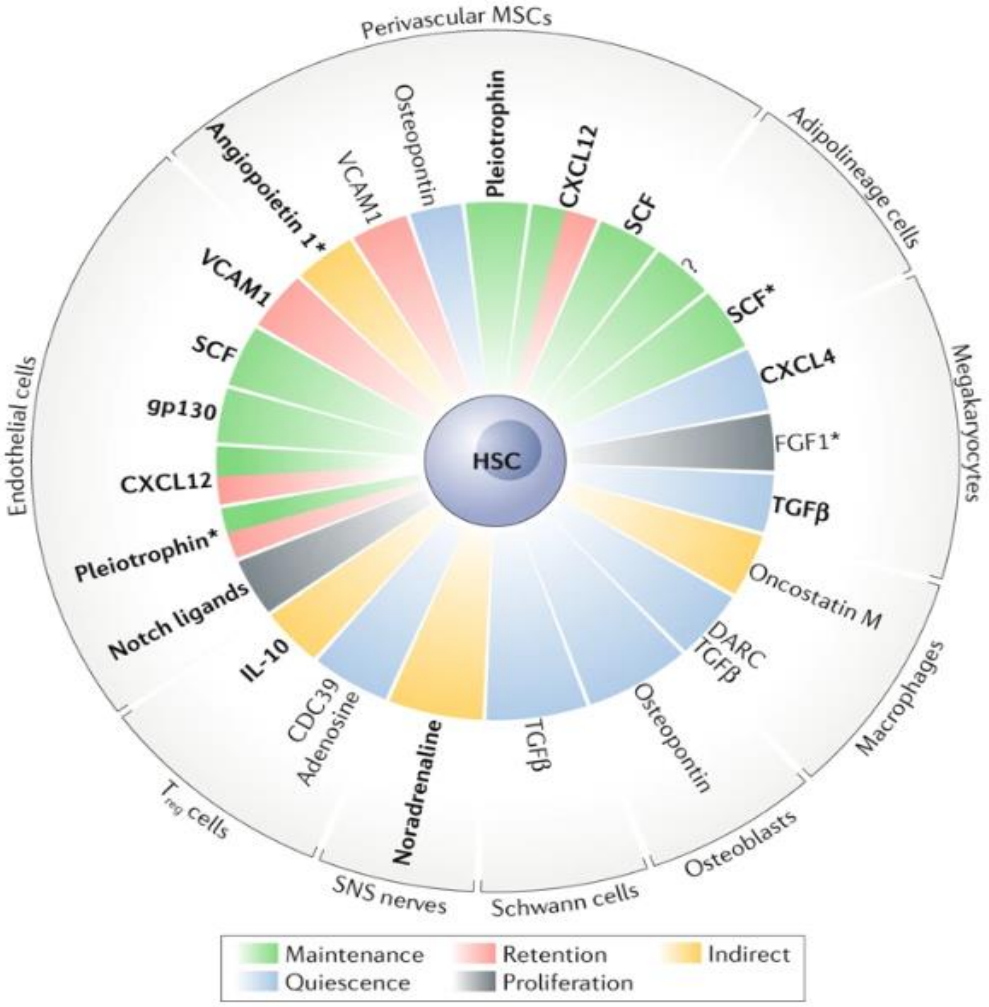

Figure 5.2. Cellular and molecular components of the HSC niche. The target plot depicts the different kinds of cells present in the HSC niches, the chemical stimuli they produce and the effect they induce on HSCs. Adapted from Pinho and Frenette (2019)[577].

Endothelial cells present in the BM, also serve as a source of secreted ANG1, CXCL12 and SCF[62]. Furthermore, the expression of E-selectin (CD62E)[578] and VCAM1 (CD106)[579] on endothelial cells has been associated with HSC adhesion to the BM through P-selectin glycoprotein ligand-1 (CD162) or integrins α4β1, α4β7 and α9β1[580]. Stromal cell populations including osteolineage cells, perivascular CXCL12-expressing cells, endothelial cells, adipocytes, neuronal, and glial cells are another component present in the perivascular HSC niche that also secrete maintenance factors and contribute in HSC expansion and proliferation[64]. Stromal N-cadherin and SCF expression has been shown as a key regulator of HSC homeostasis[65]. Stromal cell lines have also been used in *ex vivo* cultures to support HSC maintenance and self-renewal[66]. Neuronal and glial cells have also been implicated in HSC

fate decisions, inducing their mobilisation through CXCL12 production and quiescence through transforming growth factor β (TGF-β) signaling[67]. More specifically, the sympathetic nervous system has been shown to contribute to HSC trafficking from the bone marrow by coordinating the circadian egress of HSCs into the circulation through regulating local production of CXCL12[581].

5.1.3. HSC adhesion in the BM

The hematopoietic stem cell niche is a complex microenvironment, containing a variety of different cell types, including osteoblasts, vascular cells, and mesenchymal stem cells, all of which are directly implicated in the regulation of HSC fate. In addition to the cellular components, many aspects of HSC behaviour are directly regulated by the ECM, via the interaction of the cells with the soluble and adhesion factors presented by their surroundings, as well as the mechanical properties of their extracellular space[582]. These BM components control the HSC fate decision through direct cell–cell interactions, mediated mostly via cadherins, cell-ECM interactions, mediated mostly via integrins, or through soluble mediators like cytokines and extra-cellular vesicles (EVs).

Integrins are one of the most important classes of adhesion molecules mediating cell-ECM interactions. HSCs in particular, are known to express β1, β2, β3, and β7 integrins, the expression and activation of which has been associated with key fate decisions during the HSC lifecycle. More precisely, β1 integrin has been suggested to regulate HSC migration and homing[583]. Furthermore, integrins α4β1, α5β1, and αLβ2 are both important in the interplay between HSCs and endothelial and in the trans-endothelial migration of HSCs toward the stromal cell-derived factor (SDF)-1α (CXCL12)-expressing stromal cells. Additionally, integrins α4β1 and α5β1 have been identified as key mediators of FN-associated adhesion of the HSCs in the BM[584], while integrin αvβ3 has been linked to both FN and thrombopoietin mediated HSC maintenance in the niche[585].

Selectins are another set of molecules, highly associated with the homing of healthy as well as transplanted HSCs to the bone marrow niche. In particular, E-selectin has been identified to regulate a variety of HSC functions, including dormancy, self-renewal as well as chemoresistance and resistance to radiation in transplanted HSCs[586]. Furthermore, E- and P-selectins have been linked to HSC homing, through adhesion to endothelial cells in the

BM[587]. Finally, despite the controversy on the role of N-cadherin in the regulation of HSC fate, the protein has been determined to be expressed on a subset of the HSC population, and may play some role in hematopoiesis and HSC homing in the BM[588,589].

5.1.4. Current methods for HSC expansion

The increased demand for high HSC numbers to be used in cellular therapeutics, combined with the need to improve the efficacy of bone marrow transplantation and interest into new insights in the regulation and maintenance of HSCs in the field of regenerative biology has fuelled the development of a variety of culture methods that aim to provide different stimuli for HSC expansion. Inspired by the soluble factors associated with HSC survival and expansion in the BM, initial studies had focused on the addition of cytokine cocktails to HSC cultures. Stem cell factor (SCF), Flt-3 Ligand FLT3L, Thrombopoietin (TPO), and Interleukins 3 and 6 (IL3, IL6) have been among the most promising candidate cytokines associated with the highest *ex vivo* HSC expansion[590,591]. High throughput screening methods of different molecules with the potential to increase HSC proliferation has identified Prostaglandin E2 [592], Stemregenin 1 (SR1)[593] and UM171[594] as promising candidates for HSC expansion *in vitro*. Additionally, a variety of natural and synthetic polymers have been assessed for their potential in HSC expansion efforts. Materials made of proteins, polysaccharides, amino acids, and apatite, as well as decellularised ECM have been developed for tissue regeneration, based on the assumption that their natural origins may support stem cell survival and proliferation[595,596]. Other approaches have attempted to mimic the BM microenvironment by using MSCs[597], osteoblasts[598], or stromal cells[599] as feeder cells to improve the long-term survivability, migration, proliferation, differentiation, and maintenance of HSCs *in vitro*.

More recently, research groups have tried to incorporate dynamic elements in their developed BM-mimicking microenvironments and provide more multi-faceted approaches to the development of *ex vivo* HSC niches. Static and dynamic culture conditions in a perfused 3D PEG-hydrogel based bone marrow analogue[600], as well as a bone marrow on-a-chip 3D co-culture approach, based on a hydroxyapatite- coated zirconium oxide scaffold[601] have shown promising potential for HSC maintenance and expansion. Other alternative approaches include 3D hanging drop models of MSCs and HSPCs co-cultures[602], biomimetic

macroporous PEG hydrogel-based 3D scaffolds[603], computationally controlled “fed-batch” HSC cultures[604], and functionalised electrospun polymer nanofiber scaffolds[605]. Finally, decellularized ECM derived from both mouse[606] and human[607] cells has been investigated as a potential substrate to regulate the expansion potential of HSCs.

In the effort to design and engineer microenvironments for the *ex vivo* HSC expansion, the most commonly used method has been the use of 3D hydrogel platforms made of synthetic or natural polymers. Poly(ethylene glycol) (PEG) hydrogels have been previously identified as a suitable platform for the multiplication of human hematopoietic stem and progenitor cells[608]. Except for its mechanical properties, PEG hydrogels have also been used to covalently bind and present key HSC maintenance cytokines, such as stem cell factor (SCF) and interferon-γ (IFNγ), as well as the cell adhesion sequence Arg-Gly-Asp (RGD) and connecting segment 1 to more closely represent the BM conditions in culture[609]. Covalently immobilisation of stem cell factor has also been reported to induce the maintenance and expansion of HSCs cultured in gelatin methacrylamide (GelMA) hydrogels, while also preventing their rapid differentiation[610]. Glycosaminoglycan-based hydrogel systems have also been reported to balance the proliferation of human HSCs and maintain their quiescence through simultaneous regulation of exogenous biochemical and biophysical cues[611]. Zwitterionic materials bearing star-shaped poly(carboxybetaine acrylamide) and polypeptide crosslinkers containing alternating lysine and glutamic acid sequences and a metalloproteinase-degradable motifs have successfully supported the maintenance of stemness and self-renewal of HSCs during long-term cultures through inhibition of excessive reactive oxygen species (ROS) production[612].

Despite the plethora of resourceful biomaterial platforms available to examine the effect of the biophysical and biochemical properties of HSC niches, the current multifunctional biomaterial-based approaches have made small progress towards guiding HSC fate. The sensitive and highly active nature of HSCs has created the need for the study and engineering of highly complex microenvironments with the aim to closely mimic the BM. However, despite the scientific community’s increased progress and better understanding of the various signals associated with HSC maintenance and expansion *in vivo*, such complex environments have not yet been possible to recapitulate *in vitro*.

5.2. Materials and Methods

5.2.1. HSC culture

All cultures containing CD34+ cells were performed in Iscove's Modified Dulbecco's Medium (IMDM) supplemented with 20% BIT and 10% L-glutamine. IMDM is a serum-free media, developed by Guilbert and Iscove[613] as a modification of Dulbecco's Modified Eagle's Medium (DME). It contains selenium, additional amino acids and vitamins, sodium pyruvate, HEPES buffer, and potassium nitrate instead of ferric nitrate. A more comprehensive list of the components of IMDM is shown in table 5. 1.

In the 2D experiments, CD34+ cells were seeded directly on top of *L. lactis* biofilms producing the proteins of interest at a concentration of $2.5*10^5$ cells/ml. In our 3D cultures, the CD34+ cells were encapsulated in plain or functionalized PEG hydrogels at a concentration of 10^6 cells/ml, according to the current standard for HSC expansion 3D cultures. In both 2D and 3D, the cells were incubated in IMDM + 20% BIT and 10% L-glutamine. No soluble cytokines were added in the cultures where the bacteria produced recombinant proteins. In contrast, the media in the positive control conditions was supplemented with 10 μg/ml of SCF and FLT3L, and 5 μg/ml of TPO. All cultures were performed for 5 days, without media changes and were maintained in a humidified incubator at 37°C, 5% CO_2.

5.2.2. Flow cytometry

Prior to staining with antibodies for the flow cytometry analysis of the CD34+ cell populations, the cells were isolated from their culturing microenvironment depending on each experimental setup; either by direct aspiration, in the 2D experiments where the CD34+ cells were seeded directly on top of *L. lactis* biofilms, or after removal and subsequent degradation of the hydrogel containing the cells in the 3D experiments. More precisely, in our 3D setups, the hydrogel containing the encapsulated CD34+ cells was removed from the cultured well and biofilm, and was placed in a new sterile well. The hydrogel and cells were incubated in 1:1 IMDM:PBS media containing 2.5mg/ml collagenase D (Sigma) and the gels were allowed to degrade for 90 minutes in a humidified incubator at

37°C. The above media was selected for the incubation during the degradation of the hydrogels in order to allow for the optimal activity of collagenase D, by minimizing any inhibitory effects the IMDM could incur, while also keeping the CD34+ cells in close to physiological conditions for the duration of the hydrogel degradation.

To prepare the cells for flow cytometry, the cells were spun down and resuspended in flow buffer. Then they were stained with an antibody mix containing: 84% flow buffer, 10% Lineage antibody, 2% CD34, 2% CD90 and 1% CD38 antibodies (Thermo Fisher Scientific). The excitation and emission spectra of each antibody are displayed in table 5. 2. The cells were incubated with the antibody mix on ice for 30 minutes and were then washed twice with flow buffer. After resuspension in flow buffer, the cells were run in the flow cytometer. Compensation beads (Thermo Fisher Scientific) were used to ensure that the portion of the emission spectrum of each fluorochrome will not fall in the detection spectrum of another. More precisely, the beads work by capturing species-specific antibodies conjugated to fluorophores with the purpose of setting voltages and gating parameters for obtaining accurate fluorescence signals. The beads used in this work consisted of a mixture of antibody-coated positive compensation beads and uncoated negative compensation beads, combined in the same vial. The beads were prepared by incubating 4 populations of beads (1 for each fluorochrome) with the respective antibody, as above, at 4°C for 30 minutes. During the incubation period, the antibody-coated positive compensation beads bound the antibody, while the negative beads did not. This allowed us to set the correct compensation thresholds, in order to accurately detect and differentiate between the stained cells of interest to unstained cells[614].

Flow cytometry was performed on an Attune NxT Accoustic Focusing Cytometer and data analysis was performed using FlowJo, software Version vX.0.7 (Flowjo LLC, Ashland, OR).

Fluorophore	**Excitation**	**Emission**
Lineage antibody mix	490 nm	525 nm
CD34	488-561 nm	578 nm
CD38	488-561 nm	775 nm
CD90	488 nm	695 nm

Table 5.1. Excitation and emission spectra for the antibodies used in the flow cytometric analysis of the CD34+ cells used in this work.

5.2.3. Spinning Disk Microscopy

To image our engineered microenvironment in 3D, we used the K-562 HSCs reporter cell line (ATCC). The cells were GFP-tagged to allow for easier imaging and were encapsulated in plain or functionalized PEG hydrogels of different stiffnesses, placed on top of *L. lactis* biofilms. For visual purposes, we also used a GFP-tagged strain of *L. lactis*. The system was incubated in IMDM supplemented with 20% BIT, 10% L-glutamine and 10 µg/ml Chloramphenicol and was maintained overnight in a humidified incubator at 37°C, 5% CO_2. The following day, the culture was visualised using a Cell Observer Spinning Disk Confocal microscope (Zeiss), at 10x magnification. Image and z-stack analysis was performed using the Zeiss ZEN Blue image acquisition software.

5.2.4. Atomic Force Microscopy

In AFM measurements of cell-substrate interactions, a sensitive and small probe, the cantilever, is used to detect the nanoscopic deviations of the deflection of a laser beam relative to its positional change. An individual living cell can be attached to the tip of the cantilever and act as a probe for the adhesion strength measurement between cell-cell or cell-matrix adhesions.

To measure the adhesion forces between the biofilm and CD34+ cells in 2D, we used a Zeiss Axio Observer Aa1 atomic force microscope (AFM) (Zeiss). *L. lactis* biofilms producing different recombinant proteins were formed overnight on sterile hydrophobic, Sigmacote-treated glass coverslips. The following day, the biofilms were washed three times with sterile PBS. A population of CD34+ cells were seeded at the side of each well, but not on the biofilms, to allow for single cells to be “fished”. In this work, we used NanoWorld Arrow™ TL1 cantilevers (Micro Shop) with a known spring constant ranging from 0.03 to 0.09 N/m. Prior to the measurements, we performed the calibration of the cantilever. Initially, we calibrated the thermal noise of the cantilever, followed by its deflection. For that, we used the known spring constant to convert the measured distance that the cantilever deflects in a given change of photodetector voltage into a force, using Hooke’s law (equation 5.1). The force applied was small enough to ensure that only a limited amount of transient deformation was involved in our measurements, without causing large or permanent changes to the cell. The calibration was performed in water, using a set point of 2V, z-length

of 50 µm and speed of 5 µm/s.

$$F = -k * x$$

Equation 5.1. Hooke's law. The force (*F*) needed to extend or compress a spring (here the cantilever) by some distance (*x*) scales in a linear way with respect to that distance.

The sensitivity of the experimental setup was calculated by the force curve between a bare cantilever and a hard substrate (here the bottom of the petri dish). A sample force curve displaying the deflection of the cantilever in response to changes in the position of the piezo is shown in figure 5.3. The sensitivity is measured as the conversion factor of the true deflection in nm per Volt of measured deflection and can be used to convert the deflection into units of length. When the cantilever is far from the reference surface, the force of interaction is considered to be equal to zero, which is depicted as a flat part on the right side of the force curve.

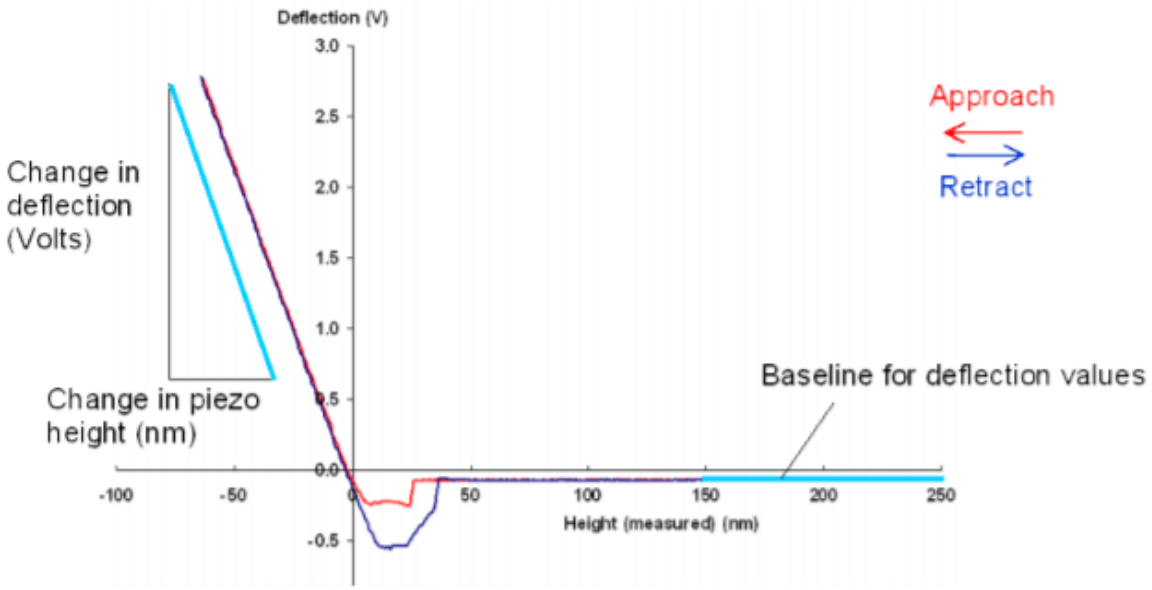

Figure 5.3. Sample force curve between a bare cantilever tip and a hard surface, used to calibrate the sensitivity of the experimental setup[615].

For the purpose of this experiment, *L. lactis* biofilms expressing CXCL12, TPO, VCAM1, and FN, as well as EMPTY biofilms, were cultured overnight on sterile glass coverslips and washed with sterile PBS in preparation for the experiment. The coverslips containing the biofilms were then transferred into a sterile petri dish filled with PBS, and a small number of

CD34+ cells was seeded in one side of the well, away from the biofilm. To measure the attachment of the cells on the biofilm, a single CD34+ cell was allowed to attach to the cantilever, as shown in figure 5.4A. More precisely, a single cell was first identified, the cantilever was then programmed to approach the cell and allow the tip to interact with the cell surface for 30 seconds, in order for the cell to attach to the tip. The cantilever and cell were then retracted from the surface of the well. To ensure a strong adhesion of the cell to the cantilever, we had previously coated the cantilever tip with Poly-D-lysine (Sigma), by incubating it in a 0.1 mg/mL Poly-D-lysine solution for 30 minutes. Poly-D-lysine is a positively charged amino acid polymer with approximately one HBr per lysine residue and provides a nonspecific attachment factor for cells[616]. This results in increased cell adhesion to solid substrates by enhancing the electrostatic interaction between negatively charged ions present on the cell membrane and the culture surface[617].

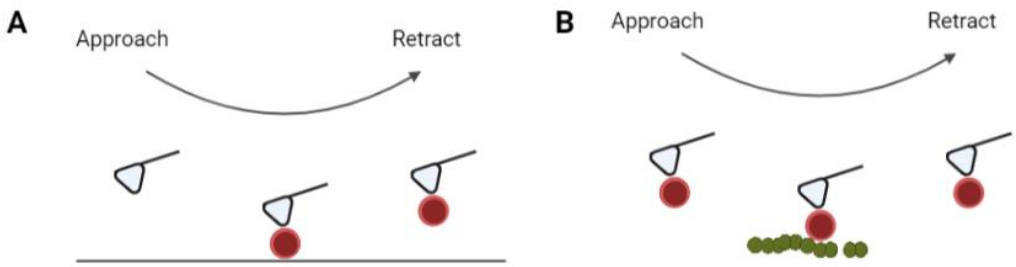

Figure 5.4. Schematic diagram of the vertical tip movement during the approach, cell attachment and retract parts of our experiment.

Once the cell had successfully attached to the cantilever tip, the cantilever was lowered again, and the cell was allowed to interact with the biofilm (figure 5.4. B) for various amounts of time. The same cell was allowed to interact with the different biofilms, that had been formed in different parts of the same well. The cantilever and cell were then retracted from the biofilm and the force of adhesion was recorded. The adhesion curves and force measurement data were analysed using the JPK BioAFM software.

The measurement of the interaction between the CD34+ cells and biofilm was measured by the changes in the position of the AFM cantilever as depicted in figure 5.5. More precisely, the position on a photodiode of a laser beam (red line, figure 5.5 A) that is reflected off the back of the cantilever measures the deflection of the cantilever and therefore the force that acts on the cantilever. During the approach of the cantilever towards the substrate (green

arrows), the cell (probe) is pressed onto the substrate until a pre-set force (here 2 nN) is reached. In this work, we allowed the cell to interact with the biofilm for 30 seconds, before retracting it from the substrate (blue arrows), and recording a force-distance curve like the one shown in figure 5.5 B. The generated curve corresponds to a cell-adhesion signature as the strain on the cell increases. The bonds that were formed between the substrate and the cell break gradually until the cell has completely separated from the surface. The maximum downward force exerted on the cantilever of the atomic force microscope is referred to as the detachment force (Fdetach). During the separation of the cell from the surface, two types of molecular unbinding events can occur. In the first event, the receptor remains anchored in the cell cortex and unbinds as the force increases (Jumps), while the second type of unbinding event occurs when receptor anchoring is lost and membrane tethers are pulled out of the cell, resulting in long plateaus of constant force (Tethers). The blue shaded area in figure 5.5 B denotes the work of detachment of the cell from the substrate.

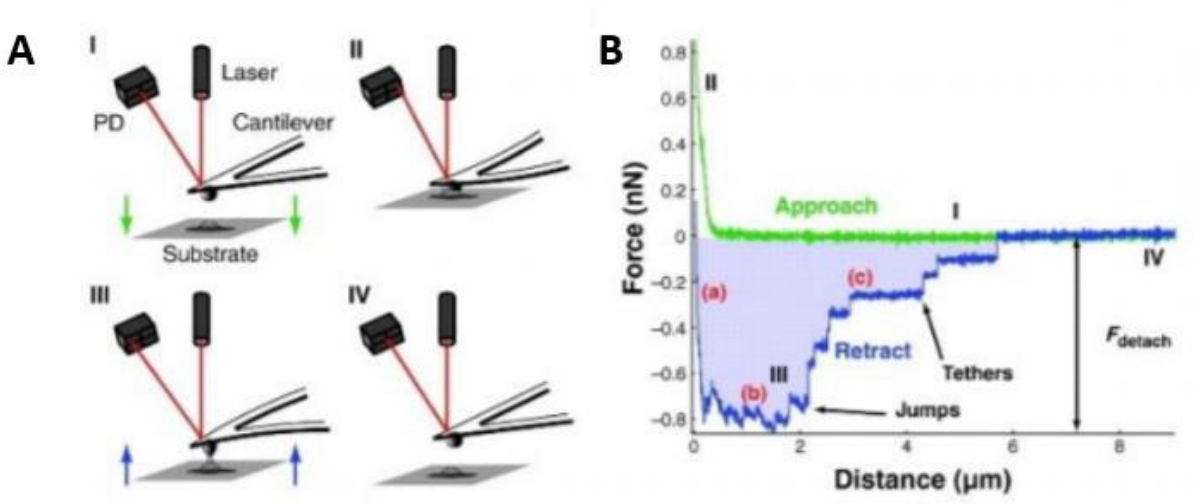

Figure 5.5. Atomic force microscopy. (A) Depiction of a cell-adhesion measurement, and characteristic force curve, depicting the approach (green) and retraction (blue) of the cantilever (B). Force curves are commonly used to set the imaging force in contact mode and to study attractive, repulsive, and adhesive interactions between the tip and the sample and plot the deflection of the cantilever as it contacts and separates from the sample during the extension and retraction of the scanner. On the force curve graph, the distance of the scanner movement is represented by the horizontal axis, and the cantilever deflection is represented by the vertical axis.

In contrast to the widely studied adhesion of MSCs to a variety of substrates, the adhesion dynamics between HSCs and their different culture environments has not been reported so far. While this may be due to the non-adherent nature of HSCs, that tend to mostly remain

in solution in traditional culture methods, we cannot disregard the fact that HSCs express integrins and adhesion molecules, through which they attach to their BM niche. The only previous literature report of the study of HSC adhesion dynamics has been conducted using non-invasive microscopy. In this work, we aimed to perform a more mechanically relevant assessment of the force of adhesion and work of detachment mediated by the HSCs in response to the different biofilms that act as culture substrates. This system can provide a quicker, more accurate and more direct evaluation of the interplay between the cells and substrate compared to microscopy. Nevertheless, the non-adherent characteristics of HSCs, their sensitivity to external manipulation and the conformation of the biofilm needs to be taken into account when using this system. Extra care needs to be taken when handling the HSCs both before and during the experiment, and an appropriate coating (such as poly-D-lysine used in this work) needs to be applied to the cantilever to ensure that the selected cell has properly attached to it.

5.3. Results

5.3.1. HSC adhesion on the *L. lactis* biofilms

The adhesion dynamics between the CD34+ cells and the biofilms were measured in 2D, using an atomic force microscope (AFM) and the results were compared to the adhesion dynamics between CD34+ cells and glass coverslips. Analysis of the AFM data suggested that the CD34+ cells form stronger attachments to the FN-expressing biofilms compared to both the other biofilm conditions and the glass coverslips (figure 5.6 A). The higher adhesion on the recombinantly produced FN appears to also have resulted in a higher work of detachment by the stem cells, as shown in figure 5.6 B.

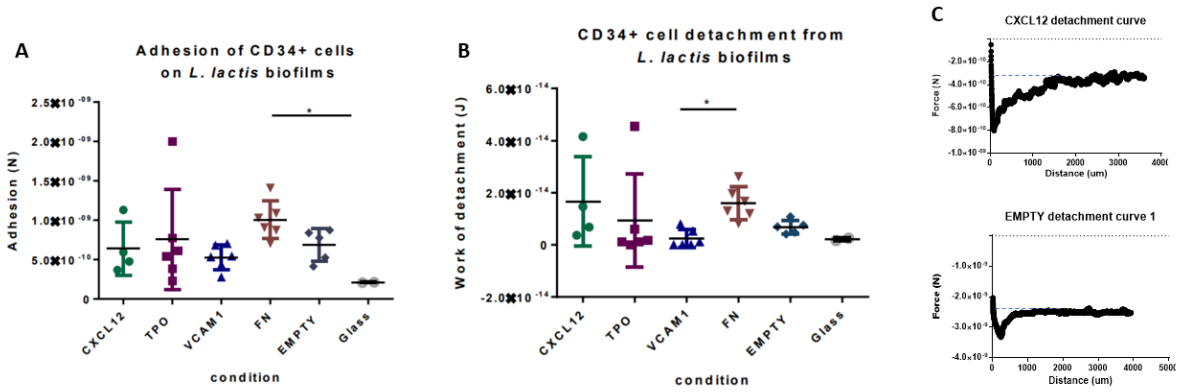

Figure 5.6. Interaction dynamics between CD34+ cells and *L. lactis* biofilms. The force of adhesion (A) and work of detachment (B) of the stem cells from *L. lactis* biofilms expressing CXCL12, TPO, VCAM1, and FN, as well as EMPTY biofilms and glass coverslips (controls) was measured using atomic force microscopy. The work of detachment was calculated as the area under the curve from Z = 0 to the detachment point, shown as the area between the curve and the dotted line in (C). Result analysis was performed using a one-way non-parametric ANOVA with Kruskal-Wallis post-hoc test (* $p < 0.05$). (C) Sample AFM curves showing the force of adhesion of CD34+ cells to CXCL12 and EMPTY biofilms.

Despite the small differences between the conditions, the higher adhesion dynamics between the CD34+ cells and the FN-expressing biofilms is consistent with current literature supporting the natural interactions between niche-resident HSCs and the FN present in the BM ECM[618,619]. Given the small time of interaction between the stem cells and biofilms, more research into the effect of longer interactions on the adhesion dynamics of the system would provide better insight into potential differences between the individual biofilms and the glass coverslip.

5.3.2. 2D experiments

Initial CD34+ cell viability and population expansion experiments were performed in 2D. A population of CD34+ cells was seeded on top of overnight grown *L. lactis* biofilms expressing different recombinant proteins, at a concentration of 2.5 * 10^5 cells/ml (Figure 5.7). After 5 days of culture, the cells were isolated from the biofilm by direct aspiration and were stained for population assessment using flow cytometry as described in section 5.2.2. Post assessment, the percentage of live cells is calculated, and the rest of the populations are determined in turn, as shown in figure 5.8.

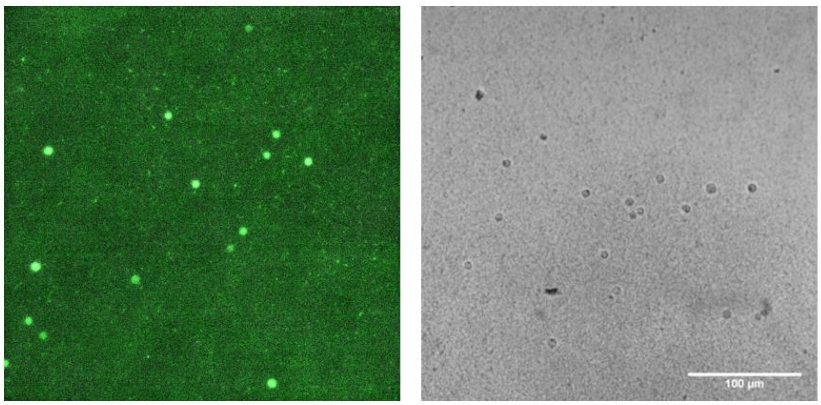

Figure 5.7. CD34+ cells on *L. lactis* biofilms. Fluorescence (left) and brightfield (right) images of CD34+ cells seeded on *L. lactis* biofilms expressing FN. In the fluorescence image, both CD34+ and bacterial cells express GFP and appear in green. The stem cells retain their round phenotype while interacting with the biofilms. Scale bar 100 µm

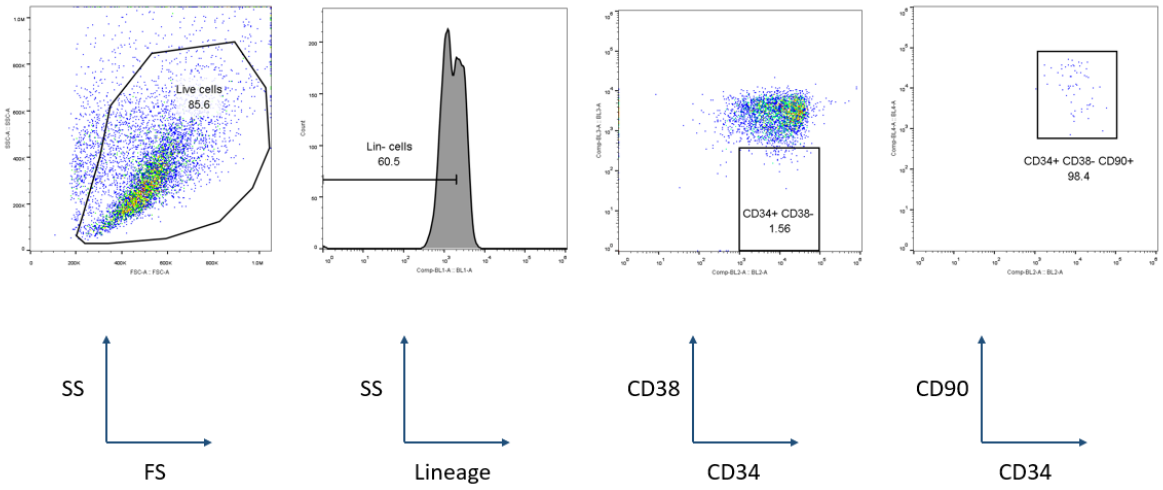

Figure 5.8. Representative flow cytometry plots depicting the populations of the CD34+ cells after 5 days of co-culture with the *L. lactis* biofilms. From left to right: cell viability is determined by size, after plotting the side scatter (SS) against the forward scatter (FS). The lineage negative cells are then determined by plotting the live cell population in a SS vs Lineage plot. Similarly, the CD34+/CD38- and CD34+/CD38-/CD90+ cell populations are determined by calculating the percentages of each population on the respective plots.

Analysis of the cell populations after the 5-day co-culture experiments displayed that the biofilms have no negative impact on the viability of the CD34+ cells. As displayed in figure 5.9 A, stem cell viability was recorded to be statistically comparable to the control conditions, where CD34+ cells were maintained in traditional expansion media, containing

soluble TPO, SCF and FLT3L, and without the presence of the bacteria. Similarly, the lineage negative phenotype of the CD34+ cells was maintained in all conditions, again showing no statistical difference compared to the controls (Figure 5.9 B). Further population analysis suggested that the commonly defined in the literature HSC population bearing the CD34+ CD38- phenotype[620], is also maintained in the stem cell-biofilm co-cultures at similar levels compared to the controls. Interestingly, this does not appear to be the case in when the biofilms do not produce recombinant cytokines (EMPTY bacteria), as the HSC phenotype appears to be lost in this condition (Figure 5.9 C). A similar trend is observed in the engrafting HSC population shown in figure 5.9 D. Despite some differences between the HSC numbers on samples retrieved from different biofilm conditions, the percentage of HSCs obtained after co-cultures with the biofilms does not statistically differ from the controls, suggesting that the bacteria and the recombinant proteins produced by the biofilms have a similar effect on the CD34+ cells as the added soluble cytokines used in traditional methods for HSC maintenance and expansion. Of particular interest has been the observation that the effect of the biofilms on the HSCs has been statistically comparable to the beneficial effect of the aryl hydrocarbon receptor antagonist StemRegenin 1 (SR1) that has been recently reported in the literature[621,622].

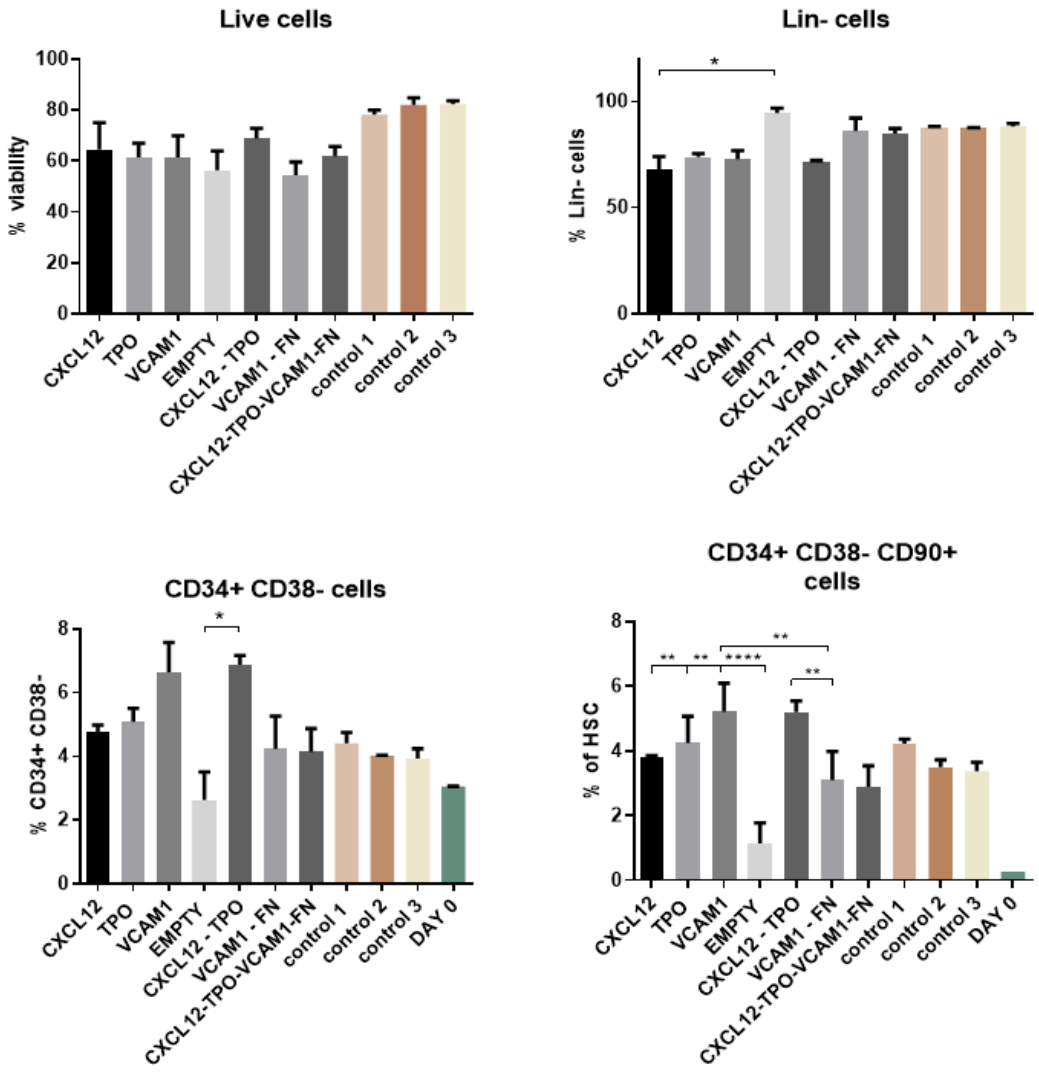

Figure 5.9. CD34+ cell populations as assessed by flow cytometry after 5 days of culture on top of *L. lactis* biofilms. (A) Stem cell viability remains unaffected by the presence of the biofilms and is comparable to the controls, that represent traditional HSC expansion methods. The co-cultures with the biofilms can also be associated with the maintenance of a lineage negative phenotype (B) and the traditionally recognised CD34+/38- cell phenotype (C). Finally, the engrafting population of HSCs, characterised by the CD34+/38-/90+ phenotype is also maintained in the conditions where a biofilm is present, at similar levels to the positive controls (D). Interestingly, this is not the case in the EMPTY condition, where the biofilm produces no recombinant proteins, and where both the CD34+/38- and CD90+ cell populations are significantly lower than all other conditions. In all cases, with the exception of the EMPTY condition, the stem cell populations of interest have shown increased expansion compared to the initially seeded population (shown as Day 0). The data was analysed using a two-way ANOVA with Tukey post-hoc test (* $p < 0.05$, ** $p < 0.01$, **** $p < 0.0001$, compared to the reference condition). Controls: Control 1: CD34+ cells cultured on Sigmacote-coated coverslips in the absence of bacteria in IMDM + 20% BIT + 10% L. glutamine + 10 ng/mL soluble SCF/FLT3L + 5 ng/mL TPO. Control 2: same as control 1, with added 1 µM of the SR1. Control 3: same as control 2, but no Sigmacote coverslip was used, the cells were cultured in an empty well, in 2D.

Again, the EMPTY biofilms did not show any effect on HSC expansion, as the percentage of engrafting HSCs measured in this condition was significantly lower compared to the other biofilm conditions. This result demonstrates that *L. lactis* can be successfully used as an active substrate for the maintenance and expansion of HSCs *ex vivo* and yield similar cell numbers compared to traditionally used methods.

5.3.3. 3D experiments

To more closely represent the architecture and mechanical properties of the BM in our system, we encapsulated the CD34+ cells in 3D hydrogels. We selected poly(ethylene glycol) (PEG), due to its versatility of applications and its ability to be functionalised with various biomolecules to study HSC proliferation and potentially induce their maintenance and expansion[623,624]. Initially, we identified Laminin-521 and Fibronectin, two key BM ECM molecules highly abundant in HSC niches[625,626], and used them to functionalise PEG hydrogels[627,628]. We then assessed the effect of these hydrogels on encapsulated CD34+ cell viability by Live/Dead assay. As shown in figure 5.10, neither hydrogel has any negative effect on stem cell viability, with viability values reordered above 85% for all conditions, after 5 days of culture.

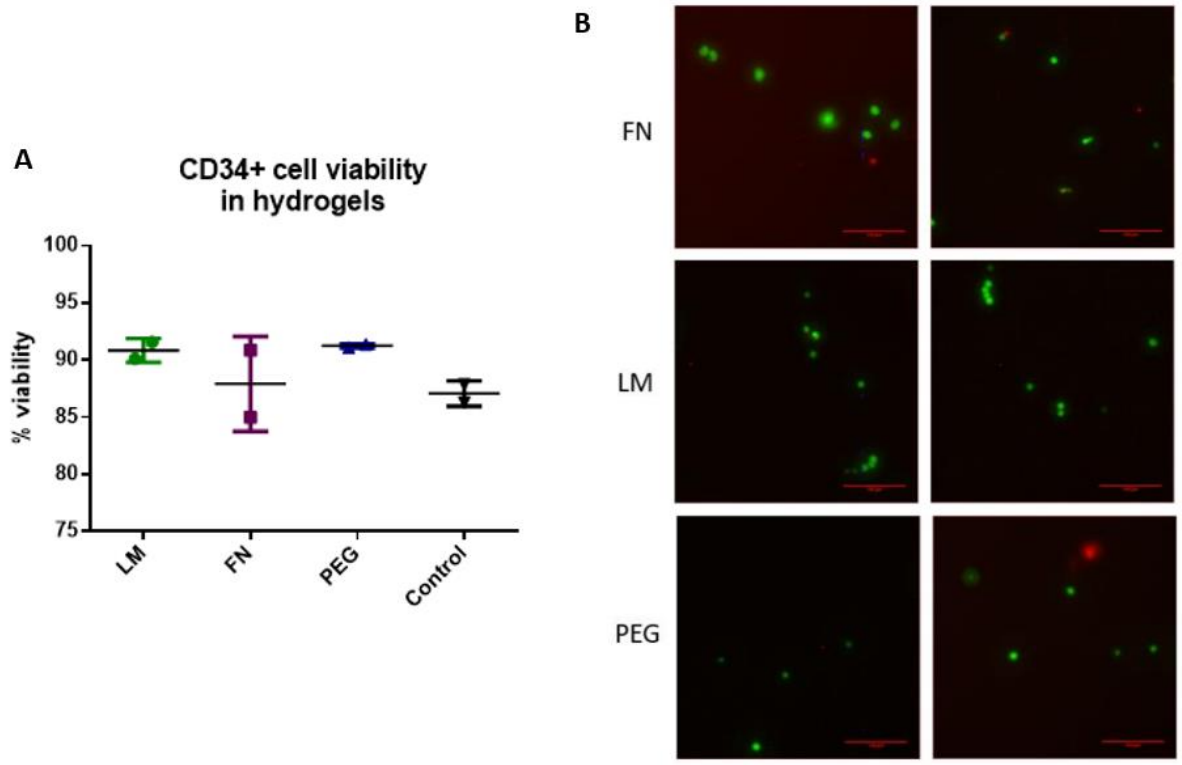

Figure 5.10. CD34+ cell viability in hydrogels. (A) CD34+ cell viability was recorded above 80% in all hydrogels, including plain PEG, PEG-LM (LM), and PEG-FN (FN) hydrogels. The results were compared to a 2D control, where the stem cells were cultured in the traditional HSC maintenance media, in the absence of a hydrogel. No statistical difference was observed between the cell viability in the hydrogels or the 2D control. (B) Representative images of the Live/Dead assay performed to assess CD34+ cell viability. The live cells are shown in green, and the dead cells are depicted in red. Control: CD34+ cells cultured in 2D, in HSC expansion media.

Following the viability assessment, we aimed to characterise the effect of the different proteins (LM or FN) compared to the plain PEG gels on the CD34+ cell populations. Except for providing functionality to the PEG hydrogels and therefore representing a more physiologically relevant HSC niche, the addition of LM and FN in the hydrogels may enable the capturing and presentation of either the recombinant secreted cytokines, expressed by the biofilms, or extra soluble factors expressed by the MSCs, when added as a support layer in the culture systems. In parallel, taking into account the varying stiffness of the BM microenvironment, we engineered hydrogels of different stiffnesses in order to determine the optimal microenvironmental cues for CD34+ cell culture. We conducted 5-day culture experiments with the CD34+ cells encapsulated in PEG hydrogels of different stiffnesses, ranging from 2 kPa (3% w/v polymer) to 5 kPa (5% w/v polymer), functionalised with either

FN or LM. The cultures were maintained in HSC expansion media with added SCF, TPO and FLT3L as described in section 5.2.1, and the population assessment at the end of the incubation period was conducted using flow cytometry. Except for the live population (Figure 5.11 A), we also assessed the lineage negative cell content, including the non-committed progenitor cells (Figure 5.11 B), as well as the HSC and engrafting HSC populations (Figure 5.11 C and D, respectively). In total, no statistical difference was observed between the different conditions. The viability of the CD34+ cell population remained high, above 80% in all hydrogels, while almost half of the seeded population retained the lineage negative phenotype. Furthermore, the HSC population bearing the CD34+/CD38- phenotype was maintained at similar levels among all conditions. Interestingly, the engrafting HSCs further classified by the expression of CD90, have been shown to be maintained at similar levels to the initially seeded population in all hydrogels after 5 days of culture. In total, our results are consistent with the previously reported literature, supporting the important role of LM and FN present in the ECM for the maintenance of HSCs[629]. Our observations are also in line with the hypothesis that HSCs could be maintained in 3D materials with a range of stiffness, since the cells can be found in different niches within the BM, ranging from the stiff endosteal niche (40-50 kPa) to the softer perivascular niche (1-3 kPa) and the even softer medullary region (0.3 kPa)[630].

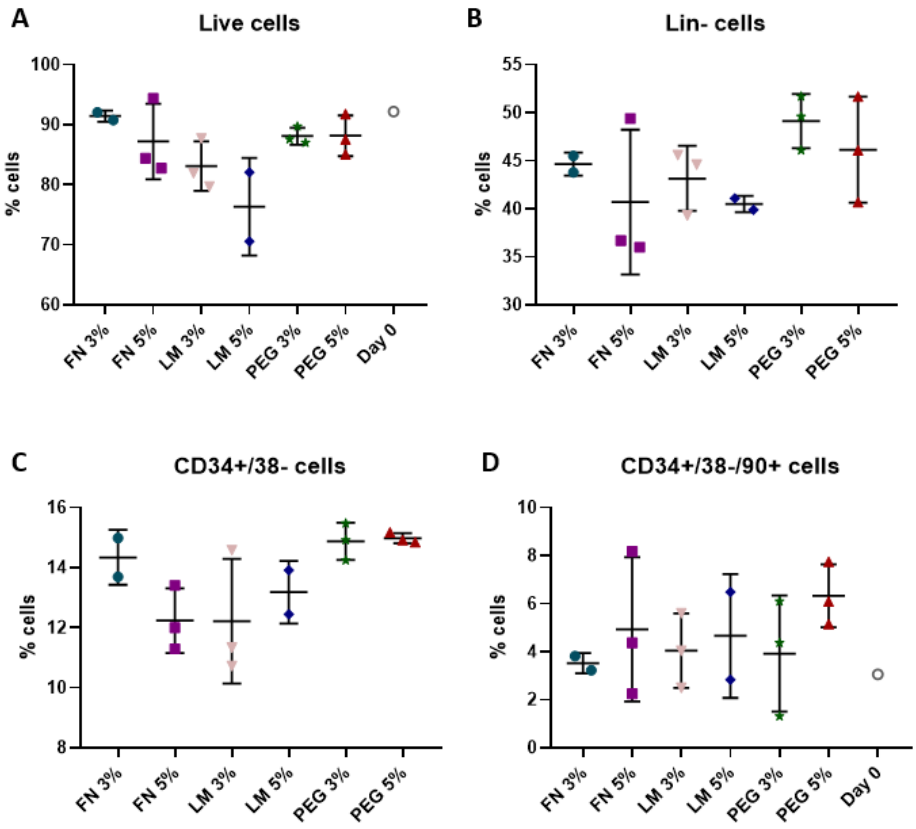

Figure 5.11. CD34+ populations in 3D hydrogels. (A) CD34+ cell viability, (B) the lineage negative CD34+ cell population, (C) the naïve HSC population and (D) the engrafting HSC population as measured by flow cytometry after a 5-day incubation in different PEG-based hydrogels. All hydrogels used in this experiment were based on PEG, with the addition of either the fibronectin fragment III_{7-10} (FN) or the laminin isoform 521 (LM). The hydrogels were engineered to display different stiffnesses, based on the percentage of the solids content (3% and 5% w/v of polymer), that ranged from 2 kPa (3% w/v polymer) to 5 kPa (5% w/v polymer). The results were compared to the initially seeded populations (day 0). No statistical differences were observed after data analysis using a two-way ANOVA with Tukey post-hoc test.

After assessing the suitability of all types of our selected hydrogels for HSC culture, we aimed to incorporate the biofilms expressing different recombinant proteins into the system. Our envisaged system is depicted in figure 5.12 and features a hydrogel containing encapsulated CD34+ cells, sitting on top of a *L. lactis* biofilm. In this work we tested hydrogels of different stiffness, as well as biofilms expressing different combinations of recombinant HSC maintenance cytokines and adhesion molecules in order to determine the optimal conditions for HSC expansion.

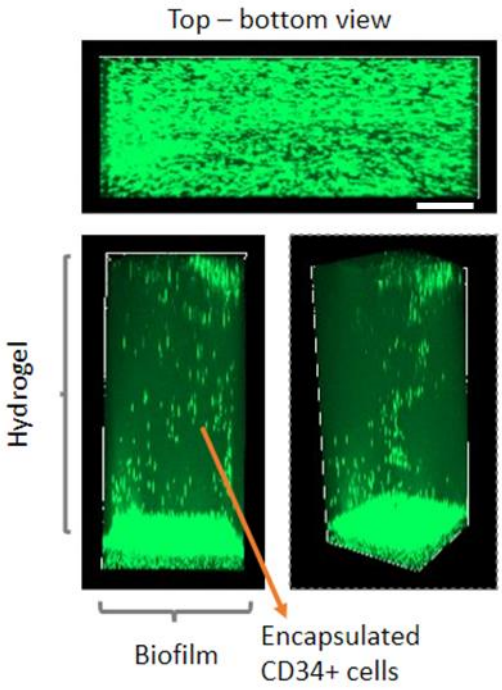

Figure 5.12. Our system in 3D. Z-stack image showing an EMPTY *L. lactis* biofilm and a hydrogel containing encapsulated CD34+ cells incubated on top of the bacteria. Both the biofilm and stem cells express GFP and are depicted in green for visual purposes. The image was obtained using a Zeiss Spinning Disk microscope. Scale bar: 100 µm.

Given the positive influence of the recombinant cytokines on HSC maintenance and expansion (section 5.3.1) and the high viability of the CD34+ cells cultured in both the plain PEG and functionalised hydrogels (section 5.3.2), we aimed to combine the two culture systems in order to produce a closer representation of the BM niche. More precisely, our goal was to encapsulate a population of CD34+ cells in hydrogels of different stiffness and functionality and culture them in the presence of *L. lactis* biofilms producing different recombinant cytokines. After 5 days of incubation, the CD34+ sub-populations that emerged from the 3D cultures in the presence of the biofilms were compared to 2D cultures between *L. lactis* and CD34+ cells, as well as traditional HSC expansion cultures, in 2D with the addition of soluble cytokines. The viability and cell populations were assessed using flow cytometry. For visual purposes, we show the best conditions in blue, compared to the initial population of CD34+ cells, seeded at the beginning of our experiment.

Initially, we measured and compared the cell viability between the different culture conditions (figure 5.13 A). After 5 days of culture, CD34+ cell viability had dropped

compared to the initially seeded population and the traditional culture methods (2D cytokine control), with statistical differences observed in most conditions. Interestingly, the viability of the CD34+ cells cultured on the *L. lactis* biofilm expressing all four recombinant cytokines (C/T/V/F), as well as the stem cells cultured in 3% PEG-FN and 3% PEG hydrogels in the presence of biofilms expressing CXCL12, TPO and VCAM1 (C/T/V) and all four cytokines respectively, remained high, and statistically comparable to the controls.

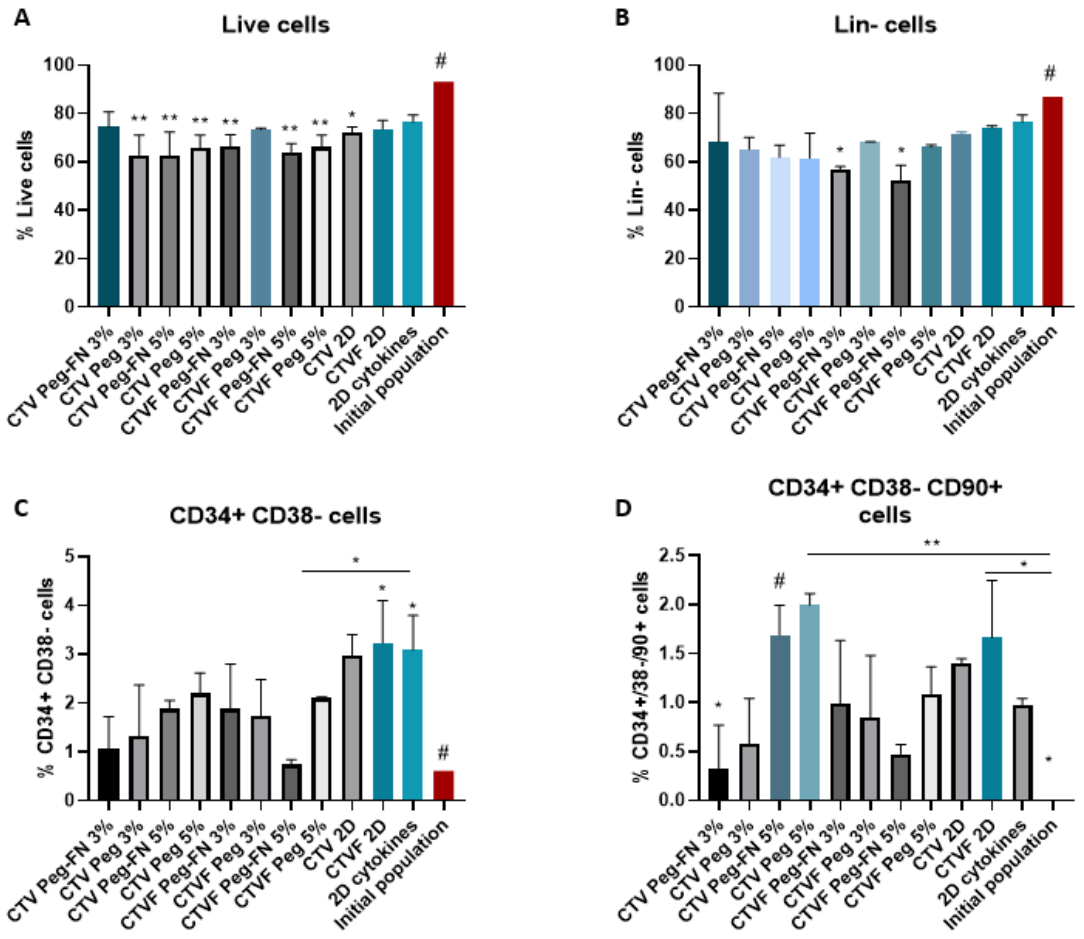

Figure 5.13. CD34+ viability and cell populations as assessed by flow cytometry after 5 days of culture inside different hydrogels, and in the presence of *L. lactis* biofilms expressing different recombinant cytokines. This experiment features PEG and PEG-FN hydrogels of different stiffnesses (3% and 5% w/v of polymer in each case), and *L. lactis* biofilms expressing different cytokines, including CXCL12 (C), TPO (T), VCAM1 (V), and FN (F). After 5 days of culture, we performed flow cytometric analysis of the populations, recording CD34+ cell viability (A), the Lineage negative cell population (B), as well as the HSC content (C), and engrafting HSC population (D). All conditions were compared to the initially seeded population, and a 2D control, where the stem cells were cultured in expansion media with added cytokines, without the presence of bacteria (2D cytokines). The data was analysed using a two-way ANOVA with Tukey post-hoc test (* $p < 0.05$, ** $p < 0.01$) and the statistical differences are shown compared to the reference condition (#).

Further population assessment revealed that the lineage negative phenotype of HSCs is maintained in the majority of our conditions, after 5 days of culture (figure 5.13 B). More precisely, more than 60% of the stem cells in all conditions showed no commitment to mature hematopoietic lineages. The only exception was observed in the case of CD34+ cells cultured in 3% and 5% PEG-FN hydrogels in the presence of *L. lactis* biofilms expressing all four cytokines, where the lineage negative phenotype of the sample was found to be statistically lower than both the controls and the other experimental conditions. Additionally, our data suggests that the HSC population (CD34+/38- cells) is also maintained after 5 days of culture, compared to the initially seeded CD34+ sample (figure 5.13 C). Interestingly, the percentage of HSCs cultured in 2D, in the presence of the biofilm expressing all 4 cytokines appears to have significantly expanded compared to the initial population, at similar levels compared to the 2D control containing the HSC expansion media and soluble cytokines. Finally, the engrafting population of HSCs expressing CD90, showed significant expansion when cultured in 5% PEG and PEG-FN hydrogels in the presence of biofilms expressing CXCL12, TPO and VCAM1 (figure 5.13 D). The same trend was also observed in the 2D co-culture of CD34+ cells and the biofilm expressing all four cytokines.

5.4. Discussion

Due to their increased clinical significance, HSCs are one of the best characterised adult cell lines, and the only one in routine clinical use. The importance of stem cell transplantation laid the foundations for the study of HSC behaviour with the view to developing novel cell therapies for healthcare applications. HSCs in particular, have received noteworthy attention due to their ability to give rise to all hemato/lymphoid lineages, leading to a life-long reconstitution of the entire hematopoietic system following transplantation, after acute injuries or the development of hematological disorders. However, the limited availability of health, transplantable, immune-compatible cells, combined with the difficulty of expansion methods that would give rise to clinically relevant cell numbers, pose a significant obstacle to the development of successful and affordable treatment regimes.

To address this issue, a variety of studies have focused on developing the appropriate conditions for large-scale HSC expansion, by either identifying exogenous soluble stimuli to

increase cell numbers[631,632], or by directly manipulating the cells[633] or their culture microenvironment[634]. Apart from the stimulation of cultured HSCs with growth factors or soluble molecules, that has been more extensively discussed in section 5.1, a variety of approaches have been focused on the genetic manipulation of HSCs in order to directly influence their behaviour. Efforts to increase the medical potential of HSCs have also suggested that genetically modified HSCs may even be more therapeutically potent than unmodified stem cells if they can be designed to overexpress a gene product of interest. This suggestion gave rise to two distinct methodologies for genetically modifying HSCs; lentiviral-mediated gene delivery and nuclease-based genome editing approaches[635]. Despite early inconsistencies with the clinical significance of lentiviral vectors as a therapeutic tool, more recent studies have suggested a strong medical potential of genetically modified HSC transplants as a cure for clinical disorders such as X-linked adrenoleukodystrophy[636] and adenosine deaminase-deficient immunodeficiency[637]. As an alternative to lentiviral-mediated gene integration, engineered nucleases have also been used to create site-specific DNA double-strand breaks in order to introduce precise changes to the locus of interest. Such methods have been successfully used in autologous HSC transplants to cure HIV infections[638].

Despite the recent progress on HSC expansion methods, the variety of medical and procedural risks associated with the transplantation of externally manipulated stem cell grafts has created the need for the better understanding of HSC biology and behaviour outside of their natural niche, as well as the creation of better, more efficient and reliable HSC expansion methods.

5.4.1. HSC adhesion

The extensive study of the BM microenvironment, and the HSC niches in particular, has indicated that fibronectin is one of the key molecules present in the BM, with a significant role in HSC adhesion and homing. This interaction has been suggested to be mediated by very late antigen 4 (VLA4) and VLA5[639,640], and has been suggested to support HSC function and growth *in vitro* and *in vivo*[641].

In this work, we aimed to characterise the response of CD34+ cells on different stimuli, including direct stimulation by recombinant cytokines produced by *L. lactis*, adhesion to

biofilms producing different recombinant proteins, as well as matrix functionality and stiffness. We therefore characterised the force of adhesion between CD34+ cells and different *L. lactis* biofilms expressing CXCL12, TPO, VCAM1 and FN, and compared the results with the adhesion dynamics between the cells and glass coverslips. Our data, displayed in section 5.3.1, suggests that the CD34+ cells formed stronger attachments with the FN-expressing biofilms compared to the glass coverslips. While the interaction of other stem cell types, such as MSCs with fibronectin has been well characterised, and the stronger adhesion of the cells on FN-coated substrates compared to uncoated surfaces has been demonstrated in a variety of studies, this interaction has not been investigated in HSCs. Despite the lack of literature on CD34+ cell attachment to biofilms, the higher adhesion forces recorded between the cells and the FN-expressing bacteria falls in line with studies of the HSC niche that have identified FN as an important mediator of stem cell homing. Interestingly, no statistical difference was observed between the adhesion of CD34+ cells on the biofilms used in this work. Despite some of the biofilms not expressing adhesion factors (CXCL12, TPO), this observation may suggest that the stem cells interact with the biofilm and may form weaker adhesions to the extracellular polymeric substances (EPS) including proteins, extracellular DNA, and a small amount of polysaccharides expressed by the bacteria during the formation of the biofilms. Furthermore, this observation can be attributed to a possible interaction of the stem cells with pili expressed by the bacteria, either by directly interacting with them, or by adhesion dynamics mediated by the 3D structure and local nanotopography of the biofilms[642]. However, the work of detachment of CD34+ cells was found to be statistically similar on the glass coverslip and the different biofilms. The only difference was observed between the FN and VCAM1-expressing biofilms, with a higher work of detachment being recorded on the FN-producing bacteria. While the expression of VCAM1 on HSCs has been reported previously, the interaction between VCAM1 on HSCs and the integrin a9 on niche cells has not been well characterised and the question of whether and how strongly the stem cells interact with either a9 integrins or VCAM1 present in their surroundings is not well understood[643,644]. Nevertheless, the stronger interaction dynamics of the CD34+ cells with the FN-expressing biofilms, may support our claim that the use of bacteria can provide an active, BM-mimicking microenvironment in our culture system, while also expressing recombinant proteins that directly influence CD34+ cell behaviour.

5.4.2. HSC expansion in 2D and 3D

Initial efforts to expand HSC populations *ex vivo* were conducted by using culture methods based on incubating the cells in chemokine cocktails. These expansion media were made up of a variety of soluble factors that have been previously identified to maintain and expand HSCs in the BM, and were traditionally used in 2D cultures, aiming to create a simplistic BM-mimicking niche in the lab. CXCL12 has been identified to be one of the most important HSC maintenance factors in the niche and has been described as the most potent naturally occurring chemoattractant for these stem cells[645]. The cytokine has been linked to HSC maintenance in the BM, due to its ability to induce HSC adhesion to both cellular (e.g., VCAM1) and matrix components (e.g., fibronectin) via integrin signalling[646]. A variety of studies have suggested that CXCL12 produced by a variety of cells, including CAR+ and Nestin+ cells[647], as well as stromal cells and osteoblasts[648,649], has the potential to induce HSC expansion *ex vivo*. Upregulation of the CXCL12/CXCR4 signalling cascade, has also been associated with radiation protection, and enhanced activity and mobilization of hematopoietic stem and progenitor cells, leading to an increase of the efficacy of HSC transplantation in clinical studies[650,651].

Thrombopoietin (TPO) has been initially identified as the major cytokine regulating megakaryocyte production, through signalling via its receptor, MPL. However, recent studies have shifted the attention of the scientific community towards the ability of TPO to directly regulate HSC fate decisions, including their maintenance and expansion[652,653]. More precisely, the direct influence of MPL signalling in HSC regulation has been underlined in a variety of studies on patients with congenital megakaryocytic thrombocytopenia (CAMT), where loss of TPO signalling was associated with gradual BM failure[654]. Furthermore, studies of TPO signalling in healthy HSCs have identified two roles for TPO in adult hematopoiesis; its ability to maintain naive HSCs in a quiescent state to preserve them with age, and to expand the stem cells in times of need such as in the case of hematological disorders or post-transplantation[655]. The direct impact of TPO on HSC behaviour has resulted in the cytokine been identified as a key additive in HSC expansion media for long-term cultures[656], and the effects of soluble TPO on HSC expansion have been reported by a variety of studies both in 2D and 3D culture systems[657,658]. TPO has also been identified as a key supplement for cell cultures aiming to expand HSCs. Significant *ex vivo* expansion of HSCs was reported

in 3D polycaprolactone nano-scaffolds coated with fibronectin (FN) in cultures containing recombinant human thrombopoietin and Flt3 ligand at 50 ng ml^{-1}[659]. The HSC-expanding potential of FN-coated substrates will be further examined in more detail below.

VCAM1 has been identified as an adhesion molecule, highly associated with the maintenance of a naïve, quiescent HSC phenotype. It is expressed by a variety of hematopoietic cells, including myeloid and lymphoid progenitors and has been associated with HSC activities including adhesion to the niche and mobilization upon activation[660]. VCAM1 has been found to be expressed by a variety of different cell types, including endothelial cells and macrophages, and has been suggested to contribute to HSC retention in different niches, including the BM and the spleen[661,662]. The activation of VCAM1 and the synergistic interaction between membrane bound VCAM1 and stem cell factor (SCF) has been reported to induce the maintenance of naïve HSCs through increased nuclear retention of FOXO3a[635]. In addition to the maintenance and quiescence signals it provides, VCAM1 has been identified as a "don't eat me" signal recognised by circulating macrophages on HSCs during their migration from the BM to different sites around the body, preventing their clearance by cells of the immune system[663].

Fibronectin has also been identified as a key BM adhesion molecule, with direct implications in HSC biology[664]. The protein is ubiquitously expressed in the BM, making it the main and most studied extracellular matrix protein, and resulting in its wide use as a necessary component in stem cell niche engineering[665]. In particular, fibronectin not only mediates HSC homing through adhesion to the BM, but it also modulates their behaviour by facilitating their binding to a variety of BM residing cells, such as adjacent HSCs and stromal cells. These effects are mainly mediated by a variety of integrins such as α4β1, α9β1, α4β7, α5β1, αvβ3, Toll-like receptor-4 (TLR-4), and CD44[666,667]. Early studies on the interactions between different BM extracellular matrix components suggested that the direct adhesion and interaction of HSCs to fibronectin may retain HSCs in a naïve state, inhibiting hematopoietic progenitor proliferation and differentiation[668]. Further research displayed a difference on the interactions between CD34+ cells with cellular BM components and FN expressed by the ECM. CD34+ adherence to mesenchymal stromal cells is mediated through Transforming Growth Factor-Beta-Induced Protein Ig-H3 (BIGH3) in an integrin-dependent manner, an interaction shown to inhibit their adhesion and CXCL12-induced migration

capacities. However, high BIGH3 expression has not been noted in FN-bound CD34+ cells, suggesting an enhanced maintenance of HSCs in the BM, which may be explained by reduced cell cycle progression and proliferation upon reduced BIGH3 levels[669]. Fibronectin has also been associated with HSC quiescence and maintenance in the endosteal BM niche. In particular, since the specific biomechanics of BM ECM can directly influence HSC quiescence, with stiffer microenvironments supporting more a more quiescent stem cell phenotype, FN has been associated with high HSC maintenance. These effects have been explored in studies aiming to maintain and expand HSCs in 3D, where a higher viability, spreading proliferation, and the retention of the cells in a more primitive, naïve state was observed on FN-coated, compared to collagen and laminin-coated scaffolds[670].

Furthermore, efforts towards long-term, *ex vivo* HSC expansion displayed that the addition of soluble thrombopoietin (TPO) synergize with low levels of stem-cell factor (SCF) and fibronectin to sustain HSC self-renewal. In particular, the addition of 100 ng ml^{-1} of TPO and 10 ng ml^{-1} of SCF have been shown to expand functional HSCs cultured on FN-coated substrates over 1 month[671]. A similar effect was observed in HSCs cultured on fibronectin coated substrates in media supplemented with 50 ng ml^{-1} SCF, 20 ng ml^{-1} IL-6, 10 ng ml^{-1} IL-3, and 25 ng ml^{-1} Flt-3 ligand, where researchers reported significant expansion of HSCs and improvement of their engrafting potential[625]. Additionally, HSCs cultured in media supplemented with IL-3, IL-6, SCF and Megakaryocyte growth and development factor (MGDF) showed significant proliferation in the presence of FN, compared to its absence, in 8-day cultures. This effect was more prominent where both FN and MGDF were added to the cell cultures, underlying the importance of their synergistic effect on HSC expansion[672]. Finally, studies of the effects of FN on HSC expansion where FN was either immobilized in 2D PET substrates or was supplemented in the medium of HSCs cultured in 3D scaffolds suggest that covalent conjugation of FN in 3D structures yields the highest expansion of CD34+ cells[673]. These cultures were performed in the presence of added cytokines including 100 ng ml^{-1} SCF, 100 ng ml^{-1} Flt-3 ligand, 50 ng ml^{-1} TPO, and 20 ng ml^{-1} IL-3.

5.4.3. HSCs and bacteria

Given the integral role of HSCs in regulating immune responses, the majority of research work conducted so far on the interaction between the stem cells and bacteria, has been focused on the biological events occurring during infections. Early studies have discussed the difference in susceptibility and response of HSCs and other hematopoietic cells to different infectious agents. More precisely, quiescent human HSCs have been reported to be show full resistance to infection by the intracellular bacteria *Listeria monocytogenes* and *Salmonella enterica serovariation typhimurium*, as well as the extracellular pathogen *Yersinia enterocolitica*[674]. The same authors report that incubation of HSCs in expansion media containing stem cell factor, thrombopoietin, and flt-3 ligand, induces the differentiation of HSCs towards the myeloid/monocytic lineages, resulting in the uptake of the above pathogenic bacterial species initially by micropinocytosis and at a later stage by receptor-mediated phagocytosis. Further research has also supported the myeloid differentiation of HSCs during infection with *Listeria monocytogenes* and *Yersinia enterocolitica*, in a process characterised by the secretion of granulocyte-macrophage colony-stimulating factor, interleukin (IL)-6, IL-8, IL-10, IL-12, and tumor necrosis factor-α by the HSCs[675]. Additionally, the metabolic events occurring during the rapid expansion of HSCs in response to stress stimuli have recently been investigated. Infection by Gram-negative bacteria has been reported to drive an increase in the mitochondrial mass in mammalian HSCs, resulting to a metabolic shift from glycolysis toward oxidative phosphorylation. This transition has been linked to the increased oxidative stress and reactive oxygen species formed during infections, and has been suggested to occur in a phosphoinositide 3-kinase (PI3K)-dependent manner, ultimately priming HSCs to differentiate into granulocytes[676].

In contrast to the abundance of studies on the response of HSCs to infections, few references can be found on the effects of bacteria on HSC expansion. Perhaps the only relevant study to our knowledge, has been focused on the effects of lipopolysaccharide (LPS) exposure of HSCs during bacterial infections by *Staphylococcus aureus*. The authors reported an induction of hematopoietic and progenitor cell activation and proliferation *in vitro* following *S. aureus* infections, in an interferon-β (IFN-β) dependent manner. Interestingly, despite their central role in regulating immune responses due to pathogens, Toll-like receptor and IFN-1 signaling has been found absent and hence independent of the

expansion of HSCs[677].

To this date, no scientific research has been conducted on the interactions between non-pathogenic, gram positive bacteria and HSCs in co-culture experiments. In contrast to previous studies, we did not aim to explore the effects of infections caused by bacteria on HSCs, but to use the bacteria as an active biointerface that could direct HSC fate. Our data suggests that our chosen bacterial species, *Lactococcus lactis*, does not have a significantly negative impact on CD34+ cell viability, both in 2D and in 3D cultures, where the stem cells are incubated directly on top of a biofilm or are encapsulated in a hydrogel that sits on top of the biofilm, respectively. A similar observation had been made in previous research on the interactions between MSCs and *L. lactis*, where, again, no decrease in stem cell viability was observed[187,292]. In 3D studies, a variety of research groups have used PEG hydrogels as a biomimetic substrate for HSC culture and expansion. Studies in mice have shown that PEG hydrogels functionalized with the cell adhesion peptide RGD (arginyl-glycyl-aspartic acid) and bearing gold nanoparticle block copolymer micelle nanolithography (BCML) arrays could be used to direct HSC fate towards T-cell differentiation[678]. The same cell adhesion peptide, in conjunction with connecting segment 1 (CS1) were also used to functionalized PEG hydrogels, displaying an ability of the system to retain covalently bound stem cell factor (SCF) and interferon-γ (IFNγ), and resulting in significant expansion of HSCs and progenitor cells[679]. In other studies, PEG hydrogels functionalized with covalently attached RGD and CS1, as well as tethered SCF, CXCL12, JAG1, and IFNγ showed evidence that the functionalized gels and different combinations of niche factors can directly impact cell behaviour. More precisely, while HSCs cultured on hydrogels functionalized with JAG1 and CXCL12 did not proliferate extensively and were able to maintain primitive HSC populations, cells cultured in the presence of SCF and IFNγ showed much more significant proliferation. Furthermore, the immobilization of SCF and CXCL12 onto the RGD and CS1-functionalised PEG hydrogels has been reported to result in increased HSC in adhesion and spreading[680].

Fibronectin (FN) has been widely recognised as a key glycoprotein that is found in abundance in the ECM, with important roles in cell adhesion due to its Arg-Gly-Asp (RGD) and Pro-His-Ser-Arg-Asp (PHSRN) motifs[681,682]. Laminins (LM) are a family of proteins also identified as primary component of the ECM and basement membrane protein mesh that supports and provides adhesion sites for a variety of stem cells, including HSCs in the BM[683].

Additionally, both FN and LMs play a significant role in sequestering growth factors in the extracellular space and presenting them to nearby cells, through their growth factor and heparin binding domains[684,685]. These attributes have classed FN and LMs as important ECM components that promote cell adhesion, survival, proliferation, and differentiation. Hence, a variety of attempts have been made to incorporate FN as either the whole protein[686] or the signaling parts of the molecule[687], and LM[688] into hydrogels, with a view to engineering niche-mimicking microenvironments for stem cell manipulation. Our data (section 5.3.3) suggest that PEG hydrogels containing both FN and LM (isoform 521 used in this work), support the maintenance of CD34+ cells as well as the naïve, engrafting HSC populations in 3D experiments. This data is consistent with previous reports in the literature that underline the importance of HSC adhesion to FN and LM in the BM for long-term hematopoiesis and their sustained proliferation *in vivo*[689]. Our observations are also in agreement with the reported effects of matrix-associated cues on HSC proliferation, where FN and LM-functionalised polyacrylamide substrates were shown to encourage HSC maintenance and proliferation[670]. The two ECM proteins have also been found critical in the maintenance of naïve HSC populations in studies of niche engineering based on bone marrow-mimetic decellularized extracellular matrix (ECM) scaffolds, as such FN and LM-rich scaffolds have been suggested to promote the development of focal contacts via Integrin β3 signaling, resulting in increased cell adhesion and maintenance of HSCs[690]. Our 3D co-culture experiments between *L. lactis* biofilms and CD34+ cells encapsulated in PEG or PEG-FN hydrogels of different stiffnesses, suggested that despite an initial drop in cell numbers compared to the originally seeded population, the stem cells retain their lineage negative phenotype in most conditions (figure 5.3.2.4). We also demonstrate that the HSC population (CD34+/38- cells) remains statistically similar to the initially seeded HSC population after 5 days of culture in all hydrogels and biofilm combinations. Interestingly, HSCs cultured in 2D, in direct contact with the *L. lactis* biofilm expressing all 4 recombinant cytokines (CXCL12, TPO, VCAM1 and FN) shows increased proliferation, at similar levels to the control, that features the addition of recombinant cytokines in the culture media, according to traditionally used protocols. Finally, a notable expansion of the engrafting HSC population (CD34+/38-/90+ cells) was observed, compared to the initially seeded population. Despite there being no significant increase of these naïve stem cells compared to traditional expansion methods (2D control), our results provide strong evidence and proof of concept

data that support the possibility of using genetically engineered, non-pathogenic bacteria for the *ex vivo* expansion of HSCs.

In total, we believe that the 2D biofilm and stem cell co-culture may have yielded better results in terms of HSC expansion due to the possibility of a direct interaction between the stem cells and biofilm. Since *L. lactis* has been engineered to produce two secreted (CXCL12, TPO) and two membrane-bound signaling molecules (VCAM1, FN), we suggest that the direct interaction between the CD34+ cells and the biointerface would allow the exposure of the stem cells to both soluble and adhesion molecules and provide a closer representation of the signaling occurring in their native BM microenvironments. Similarly, it has been shown that one of the conditions associated with the highest expansion of naïve HSCs has been the culture of the stem cells in 5% PEG-FN hydrogels on top of CXCL12, TPO and VCAM1-expressing biofilms (figure 5.3.2.4 D). As suggested previously, this culture system would present the cultured stem cells with all 4 signaling molecules, as CXCL12, TPO and VCAM1 would be expressed by the biofilm and FN would be presented as a functional group by the hydrogel. In addition, this particular culture condition, would provide the cells with structural support, as they remained encapsulated within the hydrogel. In total, we can suggest that all four cytokines we have chosen to include in our cultures have been shown important for HSC maintenance and expansion. Furthermore, our results demonstrate that the recombinant expression of the above cytokines by the bacteria has similar HSC maintenance and expansion potential as traditionally used methods, involving the addition of soluble cytokines to HSC expansion media. Finally, we can suggest that the combination of FN-functionalised PEG hydrogels, combined with the CXCL12/TPO/VCAM1 expressing biofilms can provide an *ex vivo* BM analogue, that has been shown to induce HSC maintenance and expansion.

5.5. Conclusion

This chapter describes the interactions between genetically engineered *L. lactis* biofilms that produce recombinant human CXCL12, TPO, VCAM1 and FN and human BM CD34+ cells. In this work, we have studied a variety of aspects of that interaction, including CD34+ cell adhesion to the different biofilms, as well as 2D and 3D co-cultures between the bacteria and the stem cells. We have shown that the biofilms do not negatively impact the viability of

the CD34+ cells, supporting our claim that our engineered biointerface can be used as an active biomaterial for stem cell culture. Furthermore, we have shown that the cells interact and attach to the biofilms, and in particular to the FN-expressing *L. lactis* populations, displaying that our biofilms can provide some of the native BM niche conditions that encourage HSC adhesion and have been found to be associated with stem cell homing. In 2D cultures, we have shown that the biofilms can induce HSC maintenance, preventing their commitment to differentiated lineages and encouraging self-renewal and proliferation at comparable levels to traditionally used methods featuring the use of HSC expansion media and cytokines (including TPO, SCF and FLT3L), as well as other promising HSC expansion molecules such as SR1. Furthermore, we have shown that the CD34+ cells can be successfully encapsulated and cultured in PEG hydrogels. The hydrogels used in this work have been functionalised with the BM niche proteins FN and laminin, in order to provide a closer representation of the HSC microenvironment. In our 3D, active culture systems featuring the CD34+ cells encapsulated in a hydrogel and incubated on top of *L. lactis* biofilms, we have observed the retention of an uncommitted CD34+ cell phenotype, as well as notable naïve HSC expansion, compared to both the initially seeded population and our positive controls. In total, we have shown that *L. lactis* can be successfully used as an active biomaterial for CD34+ cell culture, that has the potential to maintain the stem cells in a naïve state and encourage their self-renewal and proliferation.

Chapter 6. Discussion and Conclusion

6.1. General discussion

The recent advance of the synthetic biology field has enabled scientists to expand the clinical toolset in cellular therapeutics by enabling the use of genetically engineered cells, instead of small molecules or biologics, as the basis for the development of novel therapeutics[691]. This development has given rise to the establishment of the field of live biotherapeutic products (LBPs), defined by the FDA as live organisms developed to treat, cure, or prevent a disease or condition in humans[692]. In particular, a number of non-pathogenic bacterial species have been identified as suitable candidates for live therapeutics and have been used in a variety of applications including direct delivery to treat diseases, their use as carriers for therapeutic agents to increase the drug availability at the disease site and enhance the treatment efficacy[693]. In addition to their traditional use for recombinant protein production for medical applications[694], non-pathogenic bacteria have been used as probiotics[695], living diagnostics[696], vaccine carriers as well as treatment options in metabolic disorders[697] and cancer therapeutics[698]. *L. lactis* has gained increased scientific interest due to its versatility in clinical uses, including therapeutic protein production[699], metabolic disease management[700] and vaccine development and delivery[701].

Inspired by the versatility of *L. lactis* as a potential therapeutic tool, we designed an active stem cell culture system, where mammalian cells could be cultured in 2D or 3D and receive direct stimulation by the recombinant proteins produced by bacteria. Our engineered populations of *L. lactis* have been designed to produce recombinant soluble CXCL12 and TPO, and VCAM1 and FN in a membrane-bound form. We have used this platform for HSC and MSC culture, stimulating the cells with recombinant CXCL12, TPO, VCAM1 and FN, and showing that our biointerface can maintain both cell types in a naïve, undifferentiated state, and induce HSC expansion. This effect was not observed in EMPTY bacteria, that do not produce any recombinant protein, suggesting the bioactivity of our selected expressed factors, and supporting our claim that genetically modified bacteria can be the basis of a novel, efficient cell culture system for applications in cellular therapeutics.

Despite its widely recognised potential as a therapeutic tool in a variety of applications, *L. lactis* has not yet been fully explored for its potential in clinical application. We provide

evidence that the bacteria can be engineered to produce a variety of secreted proteins and adhesion molecules of interest, depending on the target use of the system described in this work. Furthermore, our data suggests that the biointerface reported in our study can be used successfully as a stem cell culture system, that has the potential to directly influence cell behaviour.

In general, this thesis provides proof-of-concept data that bacteria can be successfully used as a substrate for stem cell manipulation. The versatility and adaptability of the system to a variety of biomedical applications has significant clinical potential, both as an experimental tool to help better understand the natural niches of different cell types, and as a stem cell expansion or differentiation platform for uses in cellular therapeutics. Despite its promising potential, this work is largely based on the co-culture of human stem cells with bacteria, an idea that could be faced with apprehension by both clinicians and the general public. In addition to the scientific contribution to the field of biomedical engineering, and the experimental data that aims to establish *L. lactis* as a clinically significant biomaterial for stem cell manipulation, this work also aspires to provide evidence that non-pathogenic bacteria such as *L. lactis* could be used in biomedicine, without compromising the safety or reliability of the technique for future use in clinical settings.

6.2. Future work

The versatility of our proposed system provides a wide range of possibilities for further investigation of the potential of *L. lactis* as a therapeutic tool for biomedical applications. As an extension of our MSC work, it would be interesting to more closely explore the effect of the biointerface on stem cell proliferation. Having observed the ability of the biofilms to maintain the MSCs in an undifferentiated state, while also maintaining their differentiation potential, it would be interesting to investigate whether the same system can be used to induce MSC self-renewal. This could be explored by selecting the appropriate cytokines that are associated with MSC expansion in their natural niche, expressing them in our bacteria and culturing the MSCs with our biointerface as described in our co-culture experiments in chapter 4. Such an indication would carry huge clinical significance, due to the lack of reliable and efficient methods to provide clinically relevant stem cell numbers for transplants development and cellular therapeutic applications. Another exciting possibility

would include the further investigation of the HSC niche, as the bacteria could be engineered to produce further key HSC maintenance cytokines, such as SCF and FLT3L. These factors in particular have been identified as highly significant in HSC expansion, and have been traditionally used in most cytokine cocktails aimed at encouraging HSC proliferation[702,703]. Furthermore, having established that HSCs can be successfully cultured in 3D hydrogels, in the presence of the biointerface, it would be interesting to assess the effects of added MSCs in the co-culture. MSCs have been identified as one of the crucial modulators of the HSC niche and have been associated with the production of a variety of signals directly influencing HSC fate decisions, including homing, proliferation and differentiation[704,705]. We suggest that the combination of the protein-expressing biointerface, combined with the cultured MSCs and the hydrogel-encapsulated HSCs can provide a closer BM analogue that could enable both the study of the HSC niche, and the expansion of HSCs for biomedical applications. Except for the chemical and mechanical stimulation of the HSCs in our engineered niche analogue, it would be interesting to further investigate the adhesion dynamics between the cells and the biofilms. Such an experiment would provide valuable insight into the ability of the bacteria to mimic the parts of the BM niche where the stem cells would be maintained in a quiescent phenotype, attached to the ECM. Investigation of this interaction on a larger number of HSCs would also be necessary to reduce effects of the potential variance that could be observed between different cells of the same population.

Additionally, in addition to inducing stem cell maintenance and expansion, our system could be tailored to meet a variety of other applications, including cell differentiation. Previous studies have suggested that *L. lactis* can induce the myoblastic differentiation of myotubes[387] and the osteogenic differentiation of MSCs[280,292]. Given the range of available genetic tools and the indications provided in this work that *L. lactis* can produce a variety of different molecules of interest, our living interfaces can be designed to produce different growth or adhesion factors in order to drive the differentiation of stem cells into any desired lineage.

Finally, the system can be engineered to become more self-regulated. In particular, with the use of optogenetic tools, the system could be engineered to switch on and off the production of recombinant proteins according to the stimulation of the bacteria by a

specific optical wavelength. Additionally, positive and negative feedback loops could be engineered in order to regulate the levels of recombinant protein production in the system. For example, in a biofilm containing two *L. lactis* populations with the ability to produce two different recombinant proteins, one of the bacterial populations could be engineered to express a receptor that would get activated by the presence of the recombinant protein secreted by the other bacterial population, and this signal could then turn on or off its own recombinant protein expression.

Finally, further steps could be taken towards scaling up the platform discussed in this work. The creation of a larger biointerface would provide the possibility for a larger culture of stem cells, that would translate into the production of larger, clinically relevant cell numbers. The ability of *L. lactis* to colonise and form biofilms on a variety of substrates would enable the co-cultures to take place in larger wells, tissue culture plates or stacks. Furthermore, the system could be used in a bioreactor setting, where the bacteria could be isolated and kept separate from the stem cells, divided potentially by a porous membrane, which would enable the stimulation of the stem cells by the recombinant cytokines, without the direct contact of the human cells with the bacteria. While this approach would not be designed to involve recombinant adhesion molecules, since the stem cells would not be in direct contact with the bacteria, it could facilitate the isolation of the stem cells and would potentially be met with less scepticism by healthcare professionals and the public.

6.3. General conclusion

This thesis shows the biomedical potential and versatility of applications of genetically engineered bacteria in stem cell manipulation. *Lactococcus lactis* has been engineered to produce human recombinant CXCL12, TPO, and VCAM1. These populations, with the addition of the FN-expressing *L. lactis* NZ9020 that has been previously developed[293], have been investigated for their potential to maintain MSCs and HSCs in a naïve, undifferentiated state, while also inducing HSC expansion *ex vivo*. The biointerface has been shown to directly influence MSC behaviour, by encouraging cell adhesion and spreading. Furthermore, co-cultures between the protein-expressing biofilms and the MSCs have shown that *L. lactis* can maintain MSC stemness in long term cultures, while also retaining their differentiation potential. The same naïve phenotype maintenance was recorded in co-cultures between

CD34+ cells and *L. lactis*, where we show maintenance of a naïve HSC phenotype, as well as HSC self-renewal and proliferation. The versatile nature of this system enables further modifications that would tailor our proposed platform to produce a variety of different molecules for other biomedical applications. Overall, this thesis supports the ability of genetically engineered bacteria to directly control stem cell fate.

Supplementary figures and Tables

Element	DNA sequence
CXCL12 ORF	CATCACCACCATCATCACATGAATGCAAAAGTTGTTGTCGTTCTTGTTTTAGTTCTTACTGCGTTGTGC TTGAGTGATGGAAAGCCAGTCAGTTTATCATATCGTTGTCCTTGCCGTTTCTTTGAGTCTCATGTCGC TCGTGCCAATGTAAAGCACTTAAAGATATTAAACACGCCAAATTGCGCTTTACAAATCGTTGCTCGTT TGAAAAACAATAACAGACAGGTCTGTATAGACCCTAAGTTGAAATGGATTCAAGAGTACCTTGAAAA AGCATTGAATAAATAA
TPO ORF	ATGGAGTTAACCGAACTTCTTTTGGTAGTTATGCTTTTATTAACTGCAAGATTGACCTTATCTTCTCCA GCTCCGCCAGCATGTGACCTTCGTGTATTGAGCAAATTACTTAGAGACAGCCACGTGCTTCACAGCC GTTTGTCTCAATGTCCTGAAGTACATCCTTTGCCGACGCCGGTCTTGTTGCCTGCCGTCGATTTCTCAT TAGGAGAGTGGAAAACCCAGATGGAAGAGACTAAAGCCCAGGACATCTTGGGAGCGGTTACTCTTT TGCTTGAGGGAGTAATGGCTGCACGAGGCCAGTTAGGTCCTACTTGTTTAAGCAGCCTTTTAGGACA GTTATCTGGCCAGGTCAGACTTTTATTGGGCGCATTGCAGTCTTTGTTAGGGACTCAGCTTCCTCCTC AAGGGCGTACTACGGCTCACAAAGACCCTAATGCTATTTTCTTGTCATTTCAACATTTGTTGCGTGGA AAGGTGAGATTCTTGATGTTGGTAGGGGGCAGCACATTATGTGTGCGTCGAGCACCTCCAACCACA GCGGTTCCGAGCAGAACAAGTCTTGTTCTTACCTTGAACGAGCTTCCTAATAGAACATCTGGCTTATT AGAAACTAACTTCACGGCTTCAGCTCGTACTACCGGGAGCGGCCTTCTTAAATGGCAGCAGGGCTTC CGAGCGAAGATACCTGGCTTATTAAATCAAACCAGCAGATCTTTGGATCAGATACCGGGCTATTTAA ACAGAATCCATGAGTTACTTAACGGCACTCGTGGCTTGTTCCCAGGTCCGTCACGAAGAACGTTAGG AGCGCCTGATATAAGCAGCGGTACGTCAGATACCGGCAGTCTTCCACCTAATTTACAGCCTGGATAC TCTCCGAGTCCTACTCACCCGCCAACAGGACAGTACACGCTTTTTCCGTTACCTCCTACCTTACCGACG CCGGTAGTGCAGCTTCACCCGTTACTTCCGGATCCAAGTGCGCCTACCCCTACACCGACATCTCCACT TCTTAATACAAGTTATACTCACAGTCAAAACCTTAGTCAGGAGGGACATCACCACCATCATCACTAA
VCAM1 ORF	TTCAAGATAGAGACTACGCCAGAGAGCCGATATCTTGCACAAATAGGAGATAGCGTGTCTTTGACTT GCTCAACGACAGGGTGCGAATCTCCGTTCTTTTCTTGGAGAACACAGATAGATAGCCCGTTGAACGG GAAGGTAACCAATGAAGGAACAACAAGCACTTTAACAATGAACCCAGTTAGTTTTGGGAACGAACA TTCATATTTGTGTACCGCTACATGCGAGAGCCGAAAGTTAGAGAAAGGAATTCAAGTCGAGATATAC AGTTTTCCTAAGGATCCAGAAATTCACTTATCTGGTCCATTAGAGGCTGGTAAGCCAATAACCGTGA AATGCTCTGTGGCTGATGTTTATCCATTTGATAGATTGGAAATAGACCTTCTTAAAGGTGACCACTTA ATGAAAAGCCAAGAATTCCTTGAGGACGCAGATCGAAAGAGTCTTGAAACGAAATCTTTAGAGGTT ACGTTCACCCCTGTGATTGAAGATATTGGGAAGGTGTTGGTTTGTAGAGCGAAATTACACATTGACG AGATGGACTCAGTTCCTACTGTACGTCAGGCAGTGAAAGAATTGCAGGTATACATAAGCCCAAAGA ATACAGTTATATCAGTCAATCCATCAACAAAATTACAAGAAGGAGGTTCAGTGACGATGACATGCTC AAGTGAGGGCTTGCCAGCTCCAGAAATTTTTTGGTCTAAAAAGTTGGACAATGGCAATTTGCAACAC TTATCTGGGAACGCTACGCTTACGTTGATAGCAATGCGTATGGAAGATTCAGGCATCTACGTCTGCG AAGGGGTGAATTTGATTGGTAAGAACAGAAAGGAAGTAGAACTTATCGTCCAAGAGAAACCATTCA CGGTAGAAATCTCTCCAGGCCCTCGAATAGCCGCACAAATCGGCGACTCAGTGATGTTGACCTGTTC TGTGATGGGGTGTGAATCACCTTCATTCAGCTGGCGAACTCAAATCGACTCTCCATTAAGTGGAAAA GTTAGAAGCGAGGGAACAAACAGCACTCTTACGCTTAGTCCTGTGAGTTTCGAAAATGAGCACAGTT ACTTATGCACCGTAACATGTGGTCATAAAAAATTAGAAAAAGGGATACAGGTTGAACTTTATAGTTT CCCTCGTGACCCGGAGATAGAGATGTCTGGTGGTTTGGTCAATGGGAGCAGCGTGACAGTGTCTTG CAAGGTTCCATCAGTTTACCCGTTGGATCGTTTAGAAATTGAACTTTTAAAAGGCGAGACGATCCTTG AGAATATCGAATTTTTAGAAGATACAGATATGAAGAGCTTGGAGAACAAATCATTGGAAATGACGTT

	TATACCGACTATTGAGGATACAGGCAAAGCCCTTGTTTGTCAAGCCAAACTTCATATCGATGATATG GAATTTGAACCAAAGCAGCGTCAGAGCACTCAAACGTTATATGTCAATGTAGCCCCAAGAGACACAA CAGTATTGGTAAGTCCGAGTAGCATACTTGAAGAGGGGAGCAGCGTGAACATGACTTGCCTTTCTCA AGGTTTTCCTGCCCCTAAGATTCTTTGGAGCAGACAATTACCGAATGGCGAGCTTCAGCCGTTAAGC GAAAACGCTACACTTACCCTTATCTCAACTAAGATGGAAGATTCTGGAGTTTATTTGTGCGAGGGAA TAAATCAGGCGGGCCGTAGTAGAAAGGAGGTCGAGTTAATAATACAAGTCACTCCAAAAGACATCA AGCTTACCGCGTTCCCGAGTGAGTCTGTGAAGGAAGGAGACACTGTTATCATTTCATGCACTTGTGG TAACGTTCCTGAGACCTGGATCATACTTAAAAAGAAGGCTGAAACGGGCGACACTGTCTTAAAAAGC ATCGATGGCGCTTACACCATCAGAAAGGCACAGTTGAAAGACGCGGGAGTTTACGAGTGCGAAAGC AAGAACAAAGTCGGATCTCAATTGCGTTCATTAACCTTAGATGTGCAGGGAAGAGAGAACAATAAA GATTACTTTTCACCGGAGCATCACCACCATCATCAC
P1 promoter	GAATTCGATTAAGTCATCTTACCTCTTTTATTAGTTTTTTCTTATAATCTAATGATAACATTTTTATAAT TAATCTATAAACCATATCCCTCTTTGGAATCAAAATTTATTATCTACTCCTTTGTAGATATGTTATAATA CAAGTATCA
T7 gene 10 5’ UTR plus RBS	GATCTGGGAGACCACAACGGTTTCCCACTAGAAATAATTTTGTTTAACTTTAGAAAGGAGATATACG C
Usp45 secretion peptide	ATGAAAAAAAAGATTATCTCAGCTATTTTAATGTCTACAGTGATACTTTCTGCTGCAGCCCCGTTGTC AGGTGTTTACGCC
S. aureus protein A membrane binding domain (SpA)	GATCCAAAAGAGGAAGACAACAACAAGCCTGGTAAAGAAGACGGCAACAAACCTGGTAAAGAAGA CGGCAACAAACCTGGTAAAGAAGACAACAAAAAACCTGGCAAAGAAGACGGCAACAAACCTGGTA AAGAAGACAACAAAAAACCTGGCAAAGAAGATGGCAACAAACCTGGTAAAGAAGACGGCAACAAG CCTGGTAAAGAAGATGGCAACAAGCCTGGTAAAGAAGATGGCAACAAGCCTGGTAAAGAAGACGG CAACGGAGTACATGTCGTTAAACCTGGTGATACAGTAAATGACATTGCAAAAGCAAACGGCACTACT GCTGACAAAATTGCTGCAGATAACAAATTAGCTGATAAAAACATGATCAAACCTGGTCAAGAACTTG TTGTTGATAAGAAGCAACCAGCAAACCATGCAGATGCTAACAAAGCTCAAGCATTACCAGAAACTG GTGAAGAAAATCCATTCATCGGTACAACTGTATTTGGTGGATTATCATTAGCGTTAGGTGCAGCGTT ATTAGCTGGACGTCGTCGCGAACTATAA

Supplementary table 1. Genetic elements used in this work. 6xHis tag is highlighted in yellow.

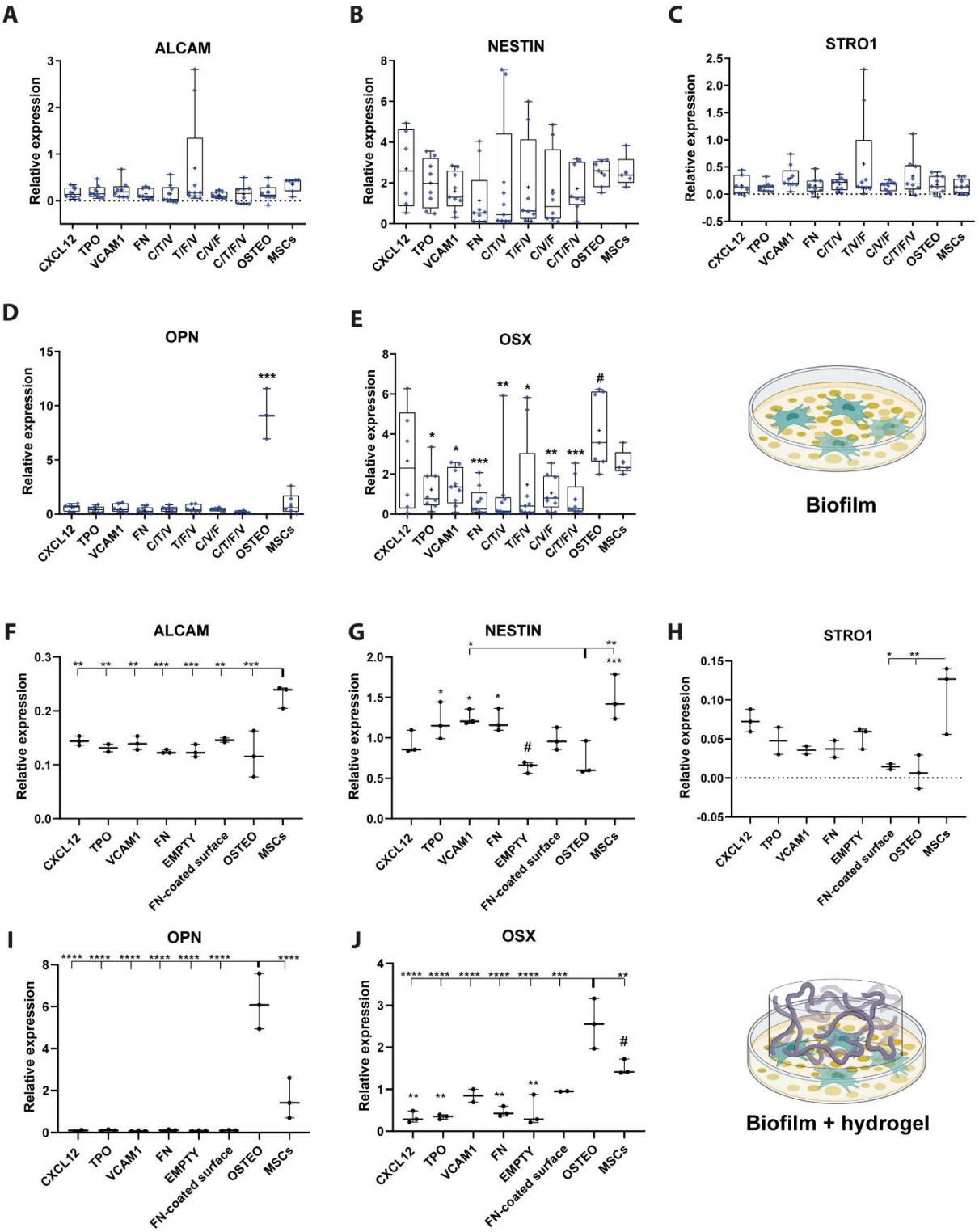

Supplementary figure 1. Collective phenotyping of MSCs using in-cell Western analysis. (A-E) Relative expression of ALCAM, Nestin, Stro1, osteopontin (OPN) and osterix OSX) compared to expression of beta-actin was measured after a 14-day co-culture with the biofilms. As depicted in the graphs, MSCs were cultured on CXCL12, TPO, VCAM1 and FN biofilms, as well as biofilms made up of combinations of the aforementioned recombinant protein-producing *L. lactis* populations. The results were compared to MSCs cultured in osteogenic medium (OSTEO) and a glass-only control containing cells after only one day of culture to avoid loss of stem-like phenotype. Preservation of

the stemness markers ALCAM, Nestin and Stro1 was suggested by the lack of statistical differences between the cells cultured on biofilms and the MSC control (A-C). Expression of osteogenic differentiation markers OPN and OSX (D, E) was not observed in any of the conditions except for the positive osteogenic medium, (*** $p < 0.001$) compared to the rest of the conditions (two-way ANOVA with Tukey post-hoc test) and in the OSX graph (* $p < 0.05$, ** $p< 0.01$, *** $p < 0.001$ compared to the reference condition, osteo, labelled as #). The same analysis was performed in the presence of a non-degradable PEG hydrogel (F-J). Similarly, we report the maintenance of a stem-like phenotype on the MSCs (F-H) and no commitment towards the osteogenic lineage (I, J). Data was analysed using a two-way ANOVA followed by a Tukey post-hoc test. C: CXCL12, T: TPO, V: VCAM1, F: FN.

A

1d
24h tracking

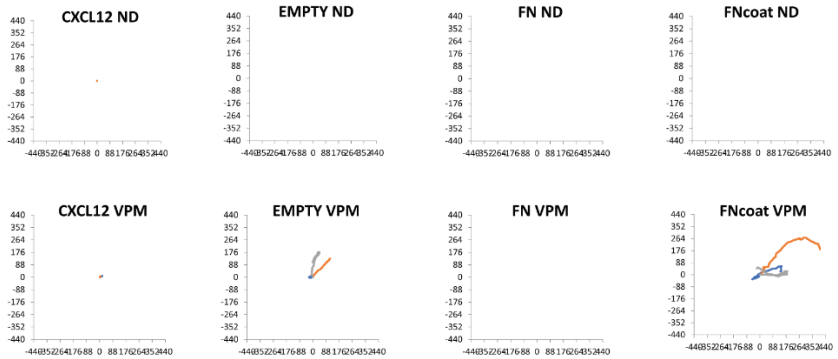

B

3d
1h tracking

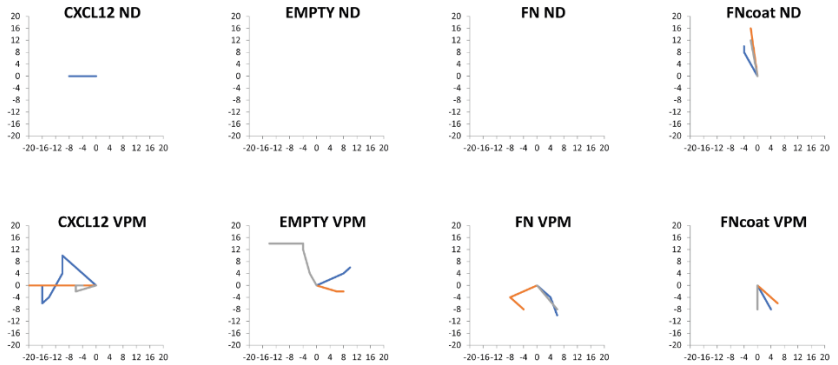

C

5d
1h tracking

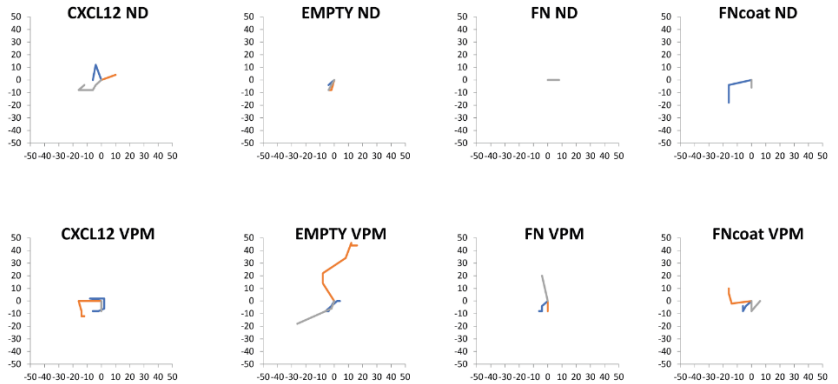

D

7d
1h tracking

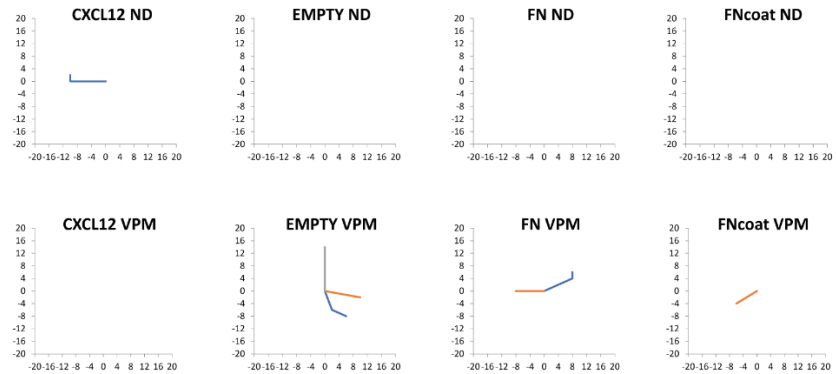

Supplementary figure 2. Movement trajectories of MSCs on *L. lactis* biofilms. MSCs were tracked for 24 h after an overnight culture (A) or for 1 hour after 3, 5 or 7 days of culture on the biofilms respectively (B-D). Cell movement was compared inn different culture conditions, in the presence or absence of a non-degradable PEG hydrogel (A), or between conditions containing a non-degradable (PEG) or degradable (VPM) hydrogels (B-D). Graphs were constructed using the Plot_At_Origin plugin for Microsoft Excel, provided by Gorelik and Gautreau (2014)[475].

References

1. Almouemen N, Kelly HM, O'Leary C. Tissue Engineering: Understanding the Role of Biomaterials and Biophysical Forces on Cell Functionality Through Computational and Structural Biotechnology Analytical Methods. *Comput Struct Biotechnol J*. 2019;17:591-598. doi:10.1016/j.csbj.2019.04.008
2. Han F, Wang J, Ding L, et al. Tissue Engineering and Regenerative Medicine: Achievements, Future, and Sustainability in Asia. *Front Bioeng Biotechnol*. 2020;8:83. doi:10.3389/fbioe.2020.00083
3. Mao AS, Mooney DJ. Regenerative medicine: Current therapies and future directions. *Proc Natl Acad Sci U S A*. 2015;112(47):14452-14459. doi:10.1073/pnas.1508520112
4. Mitragotri S, Lahann J. Physical approaches to biomaterial design. *Nat Mater*. 2009;8(1):15-23. doi:10.1038/nmat2344
5. Uludağ H. Grand challenges in biomaterials. *Front Bioeng Biotechnol*. 2014;2(OCT). doi:10.3389/fbioe.2014.00043
6. Matai I, Kaur G, Seyedsalehi A, McClinton A, Laurencin CT. Progress in 3D bioprinting technology for tissue/organ regenerative engineering. *Biomaterials*. 2020;226. doi:10.1016/j.biomaterials.2019.119536
7. Sharma K, Mujawar MA, Kaushik A. State-of-Art Functional Biomaterials for Tissue Engineering. *Front Mater*. 2019;6:172. doi:10.3389/fmats.2019.00172
8. Dehghanifard A, Shahjahani M, Soleimani M, Saki N. The Emerging Role of Mesenchymal Stem Cells in Tissue Engineering. *Int J Hematol Stem Cell Res*. 2013;7(1):46.
9. Bulati M, Miceli V, Gallo A, et al. The Immunomodulatory Properties of the Human Amnion-Derived Mesenchymal Stromal/Stem Cells Are Induced by INF-γ Produced by Activated Lymphomonocytes and Are Mediated by Cell-To-Cell Contact and Soluble Factors. *Front Immunol*. 2020;11:54. doi:10.3389/fimmu.2020.00054
10. Wang LT, Ting CH, Yen ML, et al. Human mesenchymal stem cells (MSCs) for treatment towards immune- and inflammation-mediated diseases: review of current clinical trials. *J Biomed Sci*. 2016;23(1):1-13. doi:10.1186/s12929-016-0289-5
11. Musiał-Wysocka A, Kot M, Majka M. The Pros and Cons of Mesenchymal Stem Cell-Based Therapies. *Cell Transplant*. 2019;28(7):801-812. doi:10.1177/0963689719837897
12. Čamernik K, Zupan J. Complete Assessment of Multilineage Differentiation Potential of Human Skeletal Muscle-Derived Mesenchymal Stem/Stromal Cells. In: *Methods in Molecular Biology*. Vol 2045. Humana Press Inc.; 2019:131-144. doi:10.1007/7651_2018_200
13. Haraszti RA, Didiot MC, Sapp E, et al. High-resolution proteomic and lipidomic analysis of exosomes and microvesicles from different cell sources. *J Extracell Vesicles*. 2016;5(1). doi:10.3402/jev.v5.32570
14. Zhou T, Yuan Z, Weng J, et al. Challenges and advances in clinical applications of mesenchymal stromal cells. *J Hematol Oncol*. 2021;14(1):24. doi:10.1186/s13045-021-01037-x
15. Younger EM, Chapman MW. Morbidity at bone graft donor sites. *J Orthop Trauma*. 1989;3(3):192-195. doi:10.1097/00005131-198909000-00002
16. Lozano-Calderón SA, Swaim SO, Federico A, Anderson ME, Gebhardt MC. Predictors of soft-tissue complications and deep infection in allograft reconstruction of the proximal tibia. *J Surg Oncol*. 2016;113(7):811-817. doi:10.1002/jso.24234
17. Yamasaki S, Hashimoto Y, Takigami J, et al. Effect of the direct injection of bone marrow mesenchymal stem cells in hyaluronic acid and bone marrow stimulation to treat chondral defects in the canine model. *Regen Ther*. 2015;2:42-48. doi:10.1016/j.reth.2015.10.003
18. Fischer UM, Harting MT, Jimenez F, et al. Pulmonary passage is a major obstacle for intravenous stem cell delivery: The pulmonary first-pass effect. *Stem Cells Dev*. 2009;18(5):683-691. doi:10.1089/scd.2008.0253
19. Aragón J, Salerno S, De Bartolo L, Irusta S, Mendoza G. Polymeric electrospun scaffolds for bone

morphogenetic protein 2 delivery in bone tissue engineering. *J Colloid Interface Sci*. 2018;531:126-137. doi:10.1016/j.jcis.2018.07.029

20. Ye K, Liu D, Kuang H, et al. Three-dimensional electrospun nanofibrous scaffolds displaying bone morphogenetic protein-2-derived peptides for the promotion of osteogenic differentiation of stem cells and bone regeneration. *J Colloid Interface Sci*. 2019;534:625-636. doi:10.1016/j.jcis.2018.09.071

21. Li N, Guo R, Zhang ZJ. Bioink Formulations for Bone Tissue Regeneration. *Front Bioeng Biotechnol*. 2021;9:630488. doi:10.3389/fbioe.2021.630488

22. Ghorbani F, Li D, Zhong Z, et al. Bioprinting a cell-laden matrix for bone regeneration: A focused review. *J Appl Polym Sci*. 2021;138(8):49888. doi:10.1002/app.49888

23. Cheng ZA, Alba-Perez A, Gonzalez-Garcia C, et al. High Efficiency BMP-2 Coatings: Nanoscale Coatings for Ultralow Dose BMP-2-Driven Regeneration of Critical-Sized Bone Defects (Adv. Sci. 2/2019). *Adv Sci*. 2019;6(2):1970009. doi:10.1002/advs.201970009

24. Emami A, Talaei-Khozani T, Tavanafar S, Zareifard N, Azarpira N, Vojdani Z. Synergic effects of decellularized bone matrix, hydroxyapatite, and extracellular vesicles on repairing of the rabbit mandibular bone defect model. *J Transl Med*. 2020;18(1):361. doi:10.1186/s12967-020-02525-3

25. Park B, Yoo KH, Kim C. Hematopoietic stem cell expansion and generation: The ways to make a breakthrough. *Blood Res*. 2015;50(4):194-203. doi:10.5045/br.2015.50.4.194

26. Herberts CA, Kwa MSG, Hermsen HPH. Risk factors in the development of stem cell therapy. *J Transl Med*. 2011;9:29. doi:10.1186/1479-5876-9-29

27. Chua KN, Chai C, Lee PC, et al. Surface-aminated electrospun nanofibers enhance adhesion and expansion of human umbilical cord blood hematopoietic stem/progenitor cells. *Biomaterials*. 2006;27(36):6043-6051. doi:10.1016/j.biomaterials.2006.06.017

28. Lee-Thedieck C, Rauch N, Fiammengo R, Klein G, Spatz JP. Impact of substrate elasticity on human hematopoietic stem and progenitor cell adhesion and motility. *J Cell Sci*. 2012;125(16):3765-3775. doi:10.1242/jcs.095596

29. Altrock E, Muth CA, Klein G, Spatz JP, Lee-Thedieck C. The significance of integrin ligand nanopatterning on lipid raft clustering in hematopoietic stem cells. *Biomaterials*. 2012;33(11):3107-3118. doi:10.1016/j.biomaterials.2012.01.002

30. Muth CA, Steinl C, Klein G, Lee-Thedieck C. Regulation of Hematopoietic Stem Cell Behavior by the Nanostructured Presentation of Extracellular Matrix Components. *PLoS One*. 2013;8(2). doi:10.1371/journal.pone.0054778

31. Xu Y, Chen C, Hellwarth PB, Bao X. Biomaterials for stem cell engineering and biomanufacturing. *Bioact Mater*. 2019;4:366-379. doi:10.1016/j.bioactmat.2019.11.002

32. Deng C, Chang J, Wu C. Bioactive scaffolds for osteochondral regeneration. *J Orthop Transl*. 2019;17:15-25. doi:10.1016/j.jot.2018.11.006

33. Jing D, Fonseca AV, Alakel N, et al. Hematopoietic stem cells in co-culture with mesenchymal stromal cells -modeling the niche compartments in vitro. *Haematologica*. 2010;95(4):542-550. doi:10.3324/haematol.2009.010736

34. Friel J, Heberlein C, Geldmacher M, Ostertag W. Diverse isoforms of colony-stimulating factor-1 have different effects on the development of stroma-dependent hematopoietic cells. *J Cell Physiol*. 2005;204(1):247-259. doi:10.1002/jcp.20291

35. Galán-Díez M, Kousteni S. The Osteoblastic Niche in Hematopoiesis and Hematological Myeloid Malignancies. *Curr Mol Biol Reports*. 2017;3(2):53-62. doi:10.1007/s40610-017-0055-9

36. Coskun S, Hirschi KK. Establishment and regulation of the HSC niche: Roles of osteoblastic and vascular compartments. *Birth Defects Res Part C - Embryo Today Rev*. 2010;90(4):229-242. doi:10.1002/bdrc.20194

37. Li H, Pei H, Wang S, et al. Arterial endothelium creates a permissive niche for expansion of human cord blood hematopoietic stem and progenitor cells. *Stem Cell Res Ther*. 2020;11(1):1-13.

doi:10.1186/s13287-020-01880-8

38. Fajardo-Orduña GR, Mayani H, Montesinos JJ. Hematopoietic Support Capacity of Mesenchymal Stem Cells: Biology and Clinical Potential. *Arch Med Res*. 2015;46(8):589-596. doi:10.1016/j.arcmed.2015.10.001

39. Budgude P, Kale V, Vaidya A. Mesenchymal stromal cell-derived extracellular vesicles as cell-free biologics for the ex vivo expansion of hematopoietic stem cells. *Cell Biol Int*. 2020;44(5):1078-1102. doi:10.1002/cbin.11313

40. Nichols JE, Cortiella J, Lee J, et al. In vitro analog of human bone marrow from 3D scaffolds with biomimetic inverted colloidal crystal geometry. *Biomaterials*. 2009;30(6):1071-1079. doi:10.1016/j.biomaterials.2008.10.041

41. Raic A, Rödling L, Kalbacher H, Lee-Thedieck C. Biomimetic macroporous PEG hydrogels as 3D scaffolds for the multiplication of human hematopoietic stem and progenitor cells. *Biomaterials*. 2014;35(3):929-940. doi:10.1016/j.biomaterials.2013.10.038

42. Leisten I, Kramann R, Ventura Ferreira MS, et al. 3D co-culture of hematopoietic stem and progenitor cells and mesenchymal stem cells in collagen scaffolds as a model of the hematopoietic niche. *Biomaterials*. 2012;33(6):1736-1747. doi:10.1016/j.biomaterials.2011.11.034

43. Zhou D, Chen L, Ding J, et al. A 3D engineered scaffold for hematopoietic progenitor/stem cell co-culture in vitro. *Sci Rep*. 2020;10(1):11485. doi:10.1038/s41598-020-68250-5

44. Housler GJ, Pekor C, Miki T, Schmelzer E, Zeilinger K, Gerlach JC. 3-D Perfusion Bioreactor Process Optimization for CD34+ Hematopoietic Stem Cell Culture and Differentiation towards Red Blood Cell Lineage. *J Bone Marrow Res*. 2014;2:3. doi:10.4172/2329-8820.1000150

45. Bourgine PE, Klein T, Paczulla AM, et al. In vitro biomimetic engineering of a human hematopoietic niche with functional properties. *Proc Natl Acad Sci U S A*. 2018;115(25):E5688-E5695. doi:10.1073/pnas.1805440115

46. Torisawa YS, Spina CS, Mammoto T, et al. Bone marrow-on-a-chip replicates hematopoietic niche physiology in vitro. *Nat Methods*. 2014;11(6):663-669. doi:10.1038/nmeth.2938

47. Ravichandran A, Liu Y, Teoh S-H. Review: bioreactor design towards generation of relevant engineered tissues: focus on clinical translation. *J Tissue Eng Regen Med*. 2018;12(1):e7-e22. doi:10.1002/term.2270

48. Grayson W, Stephenson M. Recent advances in bioreactors for cell-based therapies. *F1000Research*. 2018;7. doi:10.12688/f1000research.12533.1

49. Juric MK, Ghimire S, Ogonek J, et al. Milestones of hematopoietic stem cell transplantation - From first human studies to current developments. *Front Immunol*. 2016;7(NOV). doi:10.3389/fimmu.2016.00470

50. Ng AP, Alexander WS. Haematopoietic stem cells: Past, present and future. *Cell Death Discov*. 2017;3:17002. doi:10.1038/cddiscovery.2017.2

51. Tsao GJ, Allen JA, Logronio KA, Lazzeroni LC, Shizuru JA. Purified hematopoietic stem cell allografts reconstitute immunity superior to bone marrow. *Proc Natl Acad Sci U S A*. 2009;106(9):3288-3293. doi:10.1073/pnas.0813335106

52. Walasek MA, van Os R, de Haan G. Hematopoietic stem cell expansion: Challenges and opportunities. *Ann N Y Acad Sci*. 2012;1266(1):138-150. doi:10.1111/j.1749-6632.2012.06549.x

53. Hoffman CM, Calvi LM. Minireview: Complexity of hematopoietic stem cell regulation in the bone marrow microenvironment. *Mol Endocrinol*. 2014;28(10):1592-1601. doi:10.1210/me.2014-1079

54. Springuel L, Renauld JC, Knoops L. JAK kinase targeting in hematologic malignancies: A sinuous pathway from identification of genetic alterations towards clinical indications. *Haematologica*. 2015;100(10):1240-1253. doi:10.3324/haematol.2015.132142

55. Hoffman CM, Calvi LM. Minireview: Complexity of Hematopoietic Stem Cell Regulation in the Bone Marrow Microenvironment. *Mol Endocrinol*. 2014;28(10):1592. doi:10.1210/ME.2014-1079

56. Choi JS, Harley BAC. Marrow-inspired matrix cues rapidly affect early fate decisions of hematopoietic stem and progenitor cells. *Sci Adv*. 2017;3(1). doi:10.1126/sciadv.1600455

57. Haylock DN, Williams B, Johnston HM, et al. Hemopoietic Stem Cells with Higher Hemopoietic Potential Reside at the Bone Marrow Endosteum. *Stem Cells*. 2007;25(4):1062-1069. doi:10.1634/stemcells.2006-0528

58. Jung Y, Wang J, Song J, et al. Annexin II expressed by osteoblasts and endothelial cells regulates stem cell adhesion, homing, and engraftment following transplantation. *Blood*. 2007;110(1):82-90. doi:10.1182/blood-2006-05-021352

59. Calvi LM, Adams GB, Weibrecht KW, et al. Osteoblastic cells regulate the haematopoietic stem cell niche. *Nature*. 2003;425(6960):841-846. doi:10.1038/nature02040

60. Yoshihara H, Arai F, Hosokawa K, et al. Thrombopoietin/MPL Signaling Regulates Hematopoietic Stem Cell Quiescence and Interaction with the Osteoblastic Niche. *Cell Stem Cell*. 2007;1(6):685-697. doi:10.1016/j.stem.2007.10.020

61. Tzeng Y-S, Li H, Kang Y-L, Chen W-C, Cheng W-C, Lai D-M. Loss of Cxcl12/Sdf-1 in adult mice decreases the quiescent state of hematopoietic stem/progenitor cells and alters the pattern of hematopoietic regeneration after myelosuppression. *Blood*. 2011;117(2):429-439. doi:10.1182/blood-2010-01-266833

62. Chute JP, Muramoto GG, Dressman HK, Wolfe G, Chao NJ, Lin S. Molecular Profile and Partial Functional Analysis of Novel Endothelial Cell-Derived Growth Factors that Regulate Hematopoiesis. *Stem Cells*. 2006;24(5):1315-1327. doi:10.1634/stemcells.2005-0029

63. Winkler IG, Barbier V, Nowlan B, et al. Vascular niche E-selectin regulates hematopoietic stem cell dormancy, self renewal and chemoresistance. *Nat Med*. 2012;18(11):1651-1657. doi:10.1038/nm.2969

64. Sugiyama T, Kohara H, Noda M, Nagasawa T. Maintenance of the Hematopoietic Stem Cell Pool by CXCL12-CXCR4 Chemokine Signaling in Bone Marrow Stromal Cell Niches. *Immunity*. 2006;25(6):977-988. doi:10.1016/j.immuni.2006.10.016

65. Zhao M, Tao F, Venkatraman A, et al. N-Cadherin-Expressing Bone and Marrow Stromal Progenitor Cells Maintain Reserve Hematopoietic Stem Cells. *Cell Rep*. 2019;26(3):652-669.e6. doi:10.1016/J.CELREP.2018.12.093

66. Kokkaliaris KD, Drew E, Endele M, et al. Identification of factors promoting ex vivo maintenance of mouse hematopoietic stem cells by long-term single-cell quantification. *Blood*. 2016;128(9):1181-1192. doi:10.1182/blood-2016-03-705590

67. Yamazaki S, Iwama A, Takayanagi S -i., Eto K, Ema H, Nakauchi H. TGF- as a candidate bone marrow niche signal to induce hematopoietic stem cell hibernation. *Blood*. 2009;113(6):1250-1256. doi:10.1182/blood-2008-04-146480

68. Mansour A, Abou-Ezzi G, Sitnicka E, Jacobsen SEW, Wakkach A, Blin-Wakkach C. Osteoclasts promote the formation of hematopoietic stem cell niches in the bone marrow. *J Exp Med*. 2012;209(3):537-549. doi:10.1084/jem.20110994

69. Xie Y, Yin T, Wiegraebe W, et al. Detection of functional haematopoietic stem cell niche using real-time imaging. *Nature*. 2009;457(7225):97-101. doi:10.1038/nature07639

70. Adams GB, Chabner KT, Alley IR, et al. Stem cell engraftment at the endosteal niche is specified by the calcium-sensing receptor. *Nature*. 2006;439(7076):599-603. doi:10.1038/nature04247

71. Crisan M, Kartalaei PS, Vink C, et al. BMP signalling differentially regulates distinct haematopoietic stem cell types. *Nat Commun*. 2015;6(1):1-9. doi:10.1038/ncomms9040

72. Vaidya A, Kale VP. TGF-β signaling and its role in the regulation of hematopoietic stem cells. *Syst Synth Biol*. 2015;9(1-2):1. doi:10.1007/s11693-015-9161-2

73. Amnon Peled, Orit Kollet, Tanya Ponomaryov, Isabelle Petit, Suzanna Franitza, Valentin Grabovsky, Michal Magid Slav, Arnon Nagler, Ofer Lider, Ronen Alon DZ and TL. The chemokine SDF-1 activates the integrins LFA-1, VLA-4, and VLA-5 on immature human CD34+ cells: role in transendothelial/stromal

migration and engraftment of NOD/SCID mice. *Blood*. 2000;95(11):3289-3296. doi:https://doi.org/

74. Chabanon A, Desterke C, Rodenburger E, et al. A Cross-Talk Between Stromal Cell-Derived Factor-1 and Transforming Growth Factor-β Controls the Quiescence/Cycling Switch of CD34 + Progenitors Through FoxO3 and Mammalian Target of Rapamycin. *Stem Cells*. 2008;26(12):3150-3161. doi:10.1634/stemcells.2008-0219

75. Lennartsson J, Rönnstrand L. Stem Cell Factor Receptor/c-Kit: From Basic Science to Clinical Implications. *Physiol Rev*. 2012;92(4):1619-1649. doi:10.1152/physrev.00046.2011

76. Ding L, Saunders TL, Enikolopov G, Morrison SJ. Endothelial and perivascular cells maintain haematopoietic stem cells. *Nature*. 2012;481(7382):457-462. doi:10.1038/nature10783

77. Zhou BO, Yu H, Yue R, et al. Bone marrow adipocytes promote the regeneration of stem cells and haematopoiesis by secreting SCF. *Nat Cell Biol*. 2017;19(8):891-903. doi:10.1038/ncb3570

78. Xu C, Gao X, Wei Q, et al. Stem cell factor is selectively secreted by arterial endothelial cells in bone marrow. *Nat Commun*. 2018;9(1):2449. doi:10.1038/s41467-018-04726-3

79. Anastasia Guerriero, Lydia Worford, H. Kent Holland, Gui-Rong Guo KS and EKW. Thrombopoietin Is Synthesized by Bone Marrow Stromal Cells. *Blood*. 1992;90(9):3444-3455. http://www.ncbi.nlm.nih.gov/pubmed/1382698. Accessed April 10, 2019.

80. Decker M, Leslie J, Liu Q, Ding L. Hepatic thrombopoietin is required for bone marrow hematopoietic stem cell maintenance. *Science*. 2018;360(6384):106-110. doi:10.1126/science.aap8861

81. Kubota Y, Takubo K, Suda T. Bone marrow long label-retaining cells reside in the sinusoidal hypoxic niche. *Biochem Biophys Res Commun*. 2008;366(2):335-339. doi:10.1016/J.BBRC.2007.11.086

82. Simsek T, Kocabas F, Zheng J, et al. The Distinct Metabolic Profile of Hematopoietic Stem Cells Reflects Their Location in a Hypoxic Niche. *Cell Stem Cell*. 2010;7(3):380-390. doi:10.1016/j.stem.2010.07.011

83. Parmar K, Mauch P, Vergilio J-A, Sackstein R, Down JD. Distribution of hematopoietic stem cells in the bone marrow according to regional hypoxia. *Proc Natl Acad Sci U S A*. 2007;104(13):5431-5436. doi:10.1073/pnas.0701152104

84. Roy S, Tripathy M, Mathur N, Jain A, Mukhopadhyay A. Hypoxia improves expansion potential of human cord blood-derived hematopoietic stem cells and marrow repopulation efficiency. *Eur J Haematol*. 2012;88(5):396-405. doi:10.1111/j.1600-0609.2012.01759.x

85. Chow DC, Wenning LA, Miller WM, Papoutsakis ET. Modeling pO2 Distributions in the Bone Marrow Hematopoietic Compartment. II. Modified Kroghian Models. *Biophys J*. 2001;81(2):685-696. doi:10.1016/S0006-3495(01)75733-5

86. Roy S, Tripathy M, Mathur N, Jain A, Mukhopadhyay A. Hypoxia improves expansion potential of human cord blood-derived hematopoietic stem cells and marrow repopulation efficiency. *Eur J Haematol*. 2012;88(5):396-405. doi:10.1111/j.1600-0609.2012.01759.x

87. Lévesque J-P, Winkler IG, Hendy J, et al. Hematopoietic Progenitor Cell Mobilization Results in Hypoxia with Increased Hypoxia-Inducible Transcription Factor-1 ⌴ and Vascular Endothelial Growth Factor A in Bone Marrow. *Stem Cells*. 2007;25:1954-1965. doi:10.1634/stemcells.2006-0688

88. Simsek T, Kocabas F, Zheng J, et al. The distinct metabolic profile of hematopoietic stem cells reflects their location in a hypoxic niche. *Cell Stem Cell*. 2010;7(3):380-390. doi:10.1016/j.stem.2010.07.011

89. Discher DE, Mooney DJ, Zandstra PW. Growth Factors, Matrices, and Forces Combine and Control Stem Cells. *Science (80-)*. 2009;324(5935):1673-1677. doi:10.1126/science.1171643

90. Tse JR, Engler AJ. Stiffness Gradients Mimicking In Vivo Tissue Variation Regulate Mesenchymal Stem Cell Fate. Leipzig ND, ed. *PLoS One*. 2011;6(1):e15978. doi:10.1371/journal.pone.0015978

91. Adamo L, Naveiras O, Wenzel PL, et al. Biomechanical forces promote embryonic haematopoiesis. *Nature*. 2009;459(7250):1131-1135. doi:10.1038/nature08073

92. Choi JS, Harley BAC. The combined influence of substrate elasticity and ligand density on the viability and biophysical properties of hematopoietic stem and progenitor cells. *Biomaterials*.

2012;33(18):4460-4468. doi:10.1016/J.BIOMATERIALS.2012.03.010

93. Lee-Thedieck C, Rauch N, Fiammengo R, Klein G, Spatz JP. Impact of substrate elasticity on human hematopoietic stem and progenitor cell adhesion and motility. *J Cell Sci*. 125:3765-3775. doi:10.1242/jcs.095596

94. Holst J, Watson S, Lord MS, et al. Substrate elasticity provides mechanical signals for the expansion of hemopoietic stem and progenitor cells. *Nat Biotechnol*. 2010;28(10):1123-1128. doi:10.1038/nbt.1687

95. Vogel V, Sheetz M. Local force and geometry sensing regulate cell functions. *Nat Rev Mol Cell Biol*. 2006;7(4):265-275. doi:10.1038/nrm1890

96. Orr AW, Helmke BP, Blackman BR, Schwartz MA. Mechanisms of mechanotransduction. *Dev Cell*. 2006;10(1):11-20. doi:10.1016/j.devcel.2005.12.006

97. Arnaout MA, Goodman SL, Xiong JP. Structure and mechanics of integrin-based cell adhesion. *Curr Opin Cell Biol*. 2007;19(5):495-507. doi:10.1016/j.ceb.2007.08.002

98. Maître JL, Heisenberg CP. Three functions of cadherins in cell adhesion. *Curr Biol*. 2013;23(14):R626. doi:10.1016/j.cub.2013.06.019

99. McEver RP. Selectins: Initiators of leucocyte adhesion and signalling at the vascular wall. *Cardiovasc Res*. 2015;107(3):331-339. doi:10.1093/cvr/cvv154

100. Samanta D, Almo SC. Nectin family of cell-adhesion molecules: Structural and molecular aspects of function and specificity. *Cell Mol Life Sci*. 2015;72(4):645-658. doi:10.1007/s00018-014-1763-4

101. Sumarokova M, Iturri J, Weber A, et al. Influencing the adhesion properties and wettability of mucin protein films by variation of the environmental pH. *Sci Rep*. 2018;8(1):1-10. doi:10.1038/s41598-018-28047-z

102. Takada Y, Ye X, Simon S. The integrins. *Genome Biol*. 2007;8(5):215. doi:10.1186/gb-2007-8-5-215

103. García AJ. Get a grip: Integrins in cell-biomaterial interactions. *Biomaterials*. 2005;26(36):7525-7529. doi:10.1016/j.biomaterials.2005.05.029

104. Bershadsky AD, Ballestrem C, Carramusa L, et al. Assembly and mechanosensory function of focal adhesions: Experiments and models. *Eur J Cell Biol*. 2006;85(3-4):165-173. doi:10.1016/j.ejcb.2005.11.001

105. Biggs MJP, Richards RG, Dalby MJ. Nanotopographical modification: A regulator of cellular function through focal adhesions. *Nanomedicine Nanotechnology, Biol Med*. 2010;6(5):619-633. doi:10.1016/j.nano.2010.01.009

106. Kim DH, Wirtz D. Focal adhesion size uniquely predicts cell migration. *FASEB J*. 2013;27(4):1351-1361. doi:10.1096/fj.12-220160

107. Cao X, Ban E, Baker BM, et al. Multiscale model predicts increasing focal adhesion size with decreasing stiffness in fibrous matrices. *Proc Natl Acad Sci U S A*. 2017;114(23):E4549-E4555. doi:10.1073/pnas.1620486114

108. Katoh K. Activation of Rho-kinase and focal adhesion kinase regulates the organization of stress fibers and focal adhesions in the central part of fibroblasts. *PeerJ*. 2017;2017(11). doi:10.7717/peerj.4063

109. Geiger B, Yamada KM. Molecular architecture and function of matrix adhesions. *Cold Spring Harb Perspect Biol*. 2011;3(5):1-21. doi:10.1101/cshperspect.a005033

110. Lin YH, Park ZY, Lin D, et al. Regulation of cell migration and survival by focal adhesion targeting of Lasp-1. *J Cell Biol*. 2004;165(3):421-432. doi:10.1083/jcb.200311045

111. Yam JWP, Tse EYT, Ng IOL. Role and significance of focal adhesion proteins in hepatocellular carcinoma. *J Gastroenterol Hepatol*. 2009;24(4):520-530. doi:10.1111/j.1440-1746.2009.05813.x

112. Windisch R, Pirschtat N, Kellner C, et al. Oncogenic deregulation of cell adhesion molecules in Leukemia. *Cancers (Basel)*. 2019;11(3):311. doi:10.3390/cancers11030311

113. Swaminathan V, Kalappurakkal JM, Mehta SB, et al. Actin retrograde flow actively aligns and orients

ligand-engaged integrins in focal adhesions. *Proc Natl Acad Sci U S A*. 2017;114(40):10648-10653. doi:10.1073/pnas.1701136114

114. Elosegui-Artola A, Trepat X, Roca-Cusachs P. Control of Mechanotransduction by Molecular Clutch Dynamics. *Trends Cell Biol*. 2018;28(5):356-367. doi:10.1016/j.tcb.2018.01.008

115. Case LB, Waterman CM. Integration of actin dynamics and cell adhesion by a three-dimensional, mechanosensitive molecular clutch. *Nat Cell Biol*. 2015;17(8):955-963. doi:10.1038/ncb3191

116. Tusan CG, Man YH, Zarkoob H, et al. Collective Cell Behavior in Mechanosensing of Substrate Thickness. *Biophys J*. 2018;114(11):2743-2755. doi:10.1016/j.bpj.2018.03.037

117. Bennett M, Cantini M, Reboud J, Cooper JM, Roca-Cusachs P, Salmeron-Sanchez M. Molecular clutch drives cell response to surface viscosity. *Proc Natl Acad Sci U S A*. 2018;115(6):1192-1197. doi:10.1073/pnas.1710653115

118. Yeh YC, Corbin EA, Caliari SR, et al. Mechanically dynamic PDMS substrates to investigate changing cell environments. *Biomaterials*. 2017;145:23-32. doi:10.1016/j.biomaterials.2017.08.033

119. Daliri K, Pfannkuche K, Garipcan B. Effects of physicochemical properties of polyacrylamide (PAA) and (polydimethylsiloxane) PDMS on cardiac cell behavior. *Soft Matter*. 2021;17(5):1156-1172. doi:10.1039/d0sm01986k

120. Whitehead AK, Barnett HH, Caldorera-Moore ME, Newman JJ. Poly (ethylene glycol) hydrogel elasticity influences human mesenchymal stem cell behavior. *Regen Biomater*. 2018;5(3):167-175. doi:10.1093/RB/RBY008

121. Cady E, Orkwis JA, Weaver R, Conlin L, Madigan NN, Harris GM. Micropatterning decellularized ecm as a bioactive surface to guide cell alignment, proliferation, and migration. *Bioengineering*. 2020;7(3):1-14. doi:10.3390/bioengineering7030102

122. Chaudhuri O, Gu L, Darnell M, et al. Substrate stress relaxation regulates cell spreading. *Nat Commun*. 2015;6:6364. doi:10.1038/ncomms7365

123. Rens EG, Merks RMH. Cell Shape and Durotaxis Explained from Cell-Extracellular Matrix Forces and Focal Adhesion Dynamics. *iScience*. 2020;23(9). doi:10.1016/j.isci.2020.101488

124. Wei WC, Lin HH, Shen MR, Tang MJ. Mechanosensing machinery for cells under low substratum rigidity. *Am J Physiol - Cell Physiol*. 2008;295(6). doi:10.1152/ajpcell.00223.2008

125. Yeh YC, Ling JY, Chen WC, Lin HH, Tang MJ. Mechanotransduction of matrix stiffness in regulation of focal adhesion size and number: Reciprocal regulation of caveolin-1 and β1 integrin. *Sci Rep*. 2017;7(1):1-14. doi:10.1038/s41598-017-14932-6

126. Shih YR V., Tseng KF, Lai HY, Lin CH, Lee OK. Matrix stiffness regulation of integrin-mediated mechanotransduction during osteogenic differentiation of human mesenchymal stem cells. *J Bone Miner Res*. 2011;26(4):730-738. doi:10.1002/jbmr.278

127. Navarrete RO, Lee EM, Smith K, et al. Substrate stiffness controls osteoblastic and chondrocytic differentiation of mesenchymal stem cells without exogenous stimuli. *PLoS One*. 2017;12(1):170312. doi:10.1371/journal.pone.0170312

128. Russo J Di, Young JL, Wegner JWR, Steins T, Kessler H, Spatz JP. Integrin a5b1 nano-presentation regulates collective keratinocyte migration independent of substrate rigidity. *bioRxiv*. March 2021:2021.03.08.434437. doi:10.1101/2021.03.08.434437

129. Nagano M, Hoshino D, Koshikawa N, Akizawa T, Seiki M. Turnover of focal adhesions and cancer cell migration. *Int J Cell Biol*. 2012. doi:10.1155/2012/310616

130. Roca-Cusachs P, Conte V, Trepat X. Quantifying forces in cell biology. *Nat Cell Biol*. 2017;19(7):742-751. doi:10.1038/ncb3564

131. Selig M, Lauer JC, Hart ML, Rolauffs B. Mechanotransduction and stiffness-sensing: Mechanisms and opportunities to control multiple molecular aspects of cell phenotype as a design cornerstone of cell-instructive biomaterials for articular cartilage repair. *Int J Mol Sci*. 2020;21(15):1-42. doi:10.3390/ijms21155399

132. Sun M, Chi G, Xu J, et al. Extracellular matrix stiffness controls osteogenic differentiation of mesenchymal stem cells mediated by integrin α5. *Stem Cell Res Ther*. 2018;9(1):52. doi:10.1186/s13287-018-0798-0

133. Rowlands AS, George PA, Cooper-White JJ. Directing osteogenic and myogenic differentiation of MSCs: Interplay of stiffness and adhesive ligand presentation. *Am J Physiol - Cell Physiol*. 2008;295(4):1037-1044. doi:10.1152/ajpcell.67.2008

134. Engler AJ, Sen S, Sweeney HL, Discher DE. Matrix Elasticity Directs Stem Cell Lineage Specification. *Cell*. 2006;126(4):677-689. doi:10.1016/j.cell.2006.06.044

135. Jing D, Wobus M, Poitz DM, Bornhäuser M, Ehninger G, Ordemann R. Oxygen tension plays a critical role in the hematopoietic microenvironment in vitro. *Haematologica*. 2012;97(3):331-339. doi:10.3324/haematol.2011.050815

136. Kohn DH, Sarmadi M, Helman JI, Krebsbach PH. Effects of pH on human bone marrow stromal cells in vitro: Implications for tissue engineering of bone. *J Biomed Mater Res*. 2002;60(2):292-299. doi:10.1002/jbm.10050

137. Monfoulet LE, Becquart P, Marchat D, et al. The pH in the microenvironment of human mesenchymal stem cells is a critical factor for optimal osteogenesis in tissue-engineered constructs. *Tissue Eng - Part A*. 2014;20(13-14):1827-1840. doi:10.1089/ten.tea.2013.0500

138. Nelson CM, Bissell MJ. Of Extracellular Matrix, Scaffolds, and Signaling: Tissue Architecture Regulates Development, Homeostasis, and Cancer. *Annu Rev Cell Dev Biol*. 2006;22(1):287-309. doi:10.1146/annurev.cellbio.22.010305.104315

139. Tsimbouri P, Gadegaard N, Burgess K, et al. Nanotopographical effects on mesenchymal stem cell morphology and phenotype. *J Cell Biochem*. 2014;115(2):380-390. doi:10.1002/jcb.24673

140. Her GJ, Wu HC, Chen MH, Chen MY, Chang SC, Wang TW. Control of three-dimensional substrate stiffness to manipulate mesenchymal stem cell fate toward neuronal or glial lineages. *Acta Biomater*. 2013;9(2):5170-5180. doi:10.1016/j.actbio.2012.10.012

141. d'Angelo M, Benedetti E, Tupone MG, et al. The Role of Stiffness in Cell Reprogramming: A Potential Role for Biomaterials in Inducing Tissue Regeneration. *Cells*. 2019;8(9). doi:10.3390/cells8091036

142. Watt FM, Huck WTS. Role of the extracellular matrix in regulating stem cell fate. *Nat Rev Mol Cell Biol*. 2013;14(8):467-473. doi:10.1038/nrm3620

143. Lutolf MP, Blau HM. Artificial stem cell niches. *Adv Mater*. 2009;21(32-33):3255-3268. doi:10.1002/adma.200802582

144. Lutolf MP, Gilbert PM, Blau HM. Designing materials to direct stem-cell fate. *Nature*. 2009;462(7272):433-441. doi:10.1038/nature08602

145. Lovecchio J, Gargiulo P, Vargas Luna JL, Giordano E, Sigurjónsson ÓE. A standalone bioreactor system to deliver compressive load under perfusion flow to hBMSC-seeded 3D chitosan-graphene templates. *Sci Rep*. 2019;9(1):1-11. doi:10.1038/s41598-019-53319-7

146. Campsie P, Childs PG, Robertson SN, et al. Design, construction and characterisation of a novel nanovibrational bioreactor and cultureware for osteogenesis. *Sci Rep*. 2019;9(1):1-12. doi:10.1038/s41598-019-49422-4

147. Yamada KM, Sixt M. Mechanisms of 3D cell migration. *Nat Rev Mol Cell Biol*. 2019;20(12):738-752. doi:10.1038/s41580-019-0172-9

148. Schlie-Wolter S, Ngezahayo A, Chichkov BN. The selective role of ECM components on cell adhesion, morphology, proliferation and communication in vitro. *Exp Cell Res*. 2013;319(10):1553-1561. doi:10.1016/j.yexcr.2013.03.016

149. Kechagia JZ, Ivaska J, Roca-Cusachs P. Integrins as biomechanical sensors of the microenvironment. *Nat Rev Mol Cell Biol*. 2019;20(8):457-473. doi:10.1038/s41580-019-0134-2

150. Niklason LE. Understanding the Extracellular Matrix to Enhance Stem Cell-Based Tissue Regeneration. *Cell Stem Cell*. 2018;22(3):302-305. doi:10.1016/j.stem.2018.02.001

151. Kular JK, Basu S, Sharma RI. The extracellular matrix: Structure, composition, age-related differences, tools for analysis and applications for tissue engineering. *J Tissue Eng*. 2014;5:204173141455711. doi:10.1177/2041731414557112

152. Cawston TE, Young DA. Proteinases involved in matrix turnover during cartilage and bone breakdown. *Cell Tissue Res*. 2010;339(1):221-235. doi:10.1007/s00441-009-0887-6

153. Lu P, Takai K, Weaver VM, Werb Z. Extracellular Matrix degradation and remodeling in development and disease. *Cold Spring Harb Perspect Biol*. 2011;3(12). doi:10.1101/cshperspect.a005058

154. Bansode S, Bashtanova U, Li R, et al. Glycation changes molecular organization and charge distribution in type I collagen fibrils. *Sci Rep*. 2020;10(1):1-13. doi:10.1038/s41598-020-60250-9

155. Sant S, Wang D, Agarwal R, Dillender S, Ferrell N. Glycation alters the mechanical behavior of kidney extracellular matrix. *Matrix Biol Plus*. April 2020:100035. doi:10.1016/j.mbplus.2020.100035

156. Merl-Pham J, Basak T, Knüppel L, et al. Quantitative proteomic profiling of extracellular matrix and site-specific collagen post-translational modifications in an in vitro model of lung fibrosis. *Matrix Biol Plus*. 2019;1:100005. doi:10.1016/j.mbplus.2019.04.002

157. Kloxin AM, Kasko AM, Salinas CN, Anseth KS. Photodegradable hydrogels for dynamic tuning of physical and chemical properties. *Science (80-)*. 2009;324(5923):59-63. doi:10.1126/science.1169494

158. Maitz MF, Freudenberg U, Tsurkan M V., Fischer M, Beyrich T, Werner C. Bio-responsive polymer hydrogels homeostatically regulate blood coagulation. *Nat Commun*. 2013;4. doi:10.1038/ncomms3168

159. Bacharouche J, Badique F, Fahs A, et al. Biomimetic cryptic site surfaces for reversible chemo-and cyto-mechanoresponsive substrates. *ACS Nano*. 2013;7(4):3457-3465. doi:10.1021/nn400356p

160. Yeo WS, Mrksich M. Electroactive Substrates that Reveal Aldehyde Groups for Bio-Immobilization. *Adv Mater*. 2004;16(15):1352-1356. doi:10.1002/adma.200400591

161. Lee TT, García JR, Paez JI, et al. Light-triggered in vivo activation of adhesive peptides regulates cell adhesion, inflammation and vascularization of biomaterials. *Nat Mater*. 2015;14(3):352-360. doi:10.1038/nmat4157

162. Auernheimer J, Dahmen C, Hersel U, Bausch A, Kessler H. Photoswitched cell adhesion on surfaces with RGD peptides. *J Am Chem Soc*. 2005;127(46):16107-16110. doi:10.1021/ja053648q

163. Petersen S, Alonso JM, Specht A, Duodu P, Goeldner M, Del Campo A. Phototriggering of cell adhesion by caged cyclic RGD peptides. *Angew Chemie - Int Ed*. 2008;47(17):3192-3195. doi:10.1002/anie.200704857

164. Nagahama K, Kimura Y, Takemoto A. Living functional hydrogels generated by bioorthogonal cross-linking reactions of azide-modified cells with alkyne-modified polymers. *Nat Commun*. 2018;9(1):1-11. doi:10.1038/s41467-018-04699-3

165. Gopinathan J, Noh I. Click Chemistry-Based Injectable Hydrogels and Bioprinting Inks for Tissue Engineering Applications. *Tissue Eng Regen Med*. 2018;15(5):531-546. doi:10.1007/s13770-018-0152-8

166. Tekin H, Sanchez JG, Tsinman T, Langer R, Khademhosseini A. Thermoresponsive platforms for tissue engineering and regenerative medicine. *AIChE J*. 2011;57(12):3249-3258. doi:10.1002/aic.12801

167. Ravichandran R, Astrand C, Patra HK, Turner APF, Chotteau V, Phopase J. Intelligent ECM mimetic injectable scaffolds based on functional collagen building blocks for tissue engineering and biomedical applications. 2017. doi:10.1039/c7ra02927f

168. Bai T, Li J, Sinclair A, et al. Expansion of primitive human hematopoietic stem cells by culture in a zwitterionic hydrogel. *Nat Med*. 2019;25(10):1566-1575. doi:10.1038/s41591-019-0601-5

169. Barros D, Conde-Sousa E, Gonçalves AM, et al. Engineering hydrogels with affinity-bound laminin as 3D neural stem cell culture systems. *Biomater Sci*. 2019;7(12):5338-5349. doi:10.1039/c9bm00348g

170. Trujillo S, Gonzalez-Garcia C, Rico P, et al. Engineered full-length Fibronectin-based hydrogels sequester and present growth factors to promote regenerative responses in vitro and in vivo.

doi:10.1101/687244

171. Gilbert C, Ellis T. Biological Engineered Living Materials: Growing Functional Materials with Genetically Programmable Properties. *ACS Synth Biol*. 2019;8:1-15.

172. Bertani B, Ruiz N. Function and biogenesis of lipopolysaccharides. *EcoSal Plus*. 2018;8(1). doi:10.1128/ECOSALPLUS.ESP-0001-2018

173. Dickson K, Lehmann C. Inflammatory Response to Different Toxins in Experimental Sepsis Models. *Int J Mol Sci*. 2019;20(18). doi:10.3390/IJMS20184341

174. Sivanathan V, Hochschild A. Generating extracellular amyloid aggregates using E. coli cells. *Genes Dev*. 2012;26(23):2659-2667. doi:10.1101/gad.205310.112

175. Nguyen PQ, Botyanszki Z, Kun P, Tay R, Joshi NS. ARTICLE Programmable biofilm-based materials from engineered curli nanofibres. *Nat Commun*. 2014. doi:10.1038/ncomms5945

176. Drachuk I, Harbaugh S, Geryak R, Kaplan DL, Tsukruk V V., Kelley-Loughnane N. Immobilization of Recombinant E. coli Cells in a Bacterial Cellulose-Silk Composite Matrix to Preserve Biological Function. *ACS Biomater Sci Eng*. 2017;3(10):2278-2292. doi:10.1021/acsbiomaterials.7b00367

177. Chuang E, Hori AM, Hesketh CD, Shorter J. Amyloid assembly and disassembly. *J Cell Sci*. 2018;131(8). doi:10.1242/jcs.189928

178. Jacob RS, George E, Singh PK, et al. Cell adhesion on amyloid fibrils lacking integrin recognition motif. *J Biol Chem*. 2016;291(10):5278-5298. doi:10.1074/jbc.M115.678177

179. Li C, Qin R, Liu R, Miao S, Yang P. Functional amyloid materials at surfaces/interfaces. *Biomater Sci*. 2018;6(3):462-472. doi:10.1039/c7bm01124e

180. Lamour G, Nassar R, Chan PHW, et al. Mapping the Broad Structural and Mechanical Properties of Amyloid Fibrils. *Biophys J*. 2017;112(4):584-594. doi:10.1016/j.bpj.2016.12.036

181. Nguyen PQ, Botyanszki Z, Tay PKR, Joshi NS. Programmable biofilm-based materials from engineered curli nanofibres. *Nat Commun*. 2014;5(1):1-10. doi:10.1038/ncomms5945

182. Noemie-Manuelle DC, Pei Kun T, Peter N, Neel J. Engineering E. coli to enable electron transfer along curli protein nanofibers. *Front Bioeng Biotechnol*. 2016;4. doi:10.3389/conf.fbioe.2016.01.01972

183. Wang J, Tang Y, Huang Y. Bacterial-Cellulose-Based Biomaterials for Tissue Engineering Applications. In: *Materials Science and Technology*. Wiley; 2019:1-25. doi:10.1002/9783527603978.mst0478

184. Park S, Park J, Jo I, et al. In situ hybridization of carbon nanotubes with bacterial cellulose for three-dimensional hybrid bioscaffolds. *Biomaterials*. 2015;58:93-102. doi:10.1016/j.biomaterials.2015.04.027

185. Pigossi SC, De Oliveira GJPL, Finoti LS, et al. Bacterial cellulose-hydroxyapatite composites with osteogenic growth peptide (OGP) or pentapeptide OGP on bone regeneration in critical-size calvarial defect model. *J Biomed Mater Res - Part A*. 2015;103(10):3397-3406. doi:10.1002/jbm.a.35472

186. Yang J, Du M, Wang L, et al. Bacterial Cellulose as a Supersoft Neural Interfacing Substrate. *ACS Appl Mater Interfaces*. 2018;10(39):33049-33059. doi:10.1021/acsami.8b12083

187. Hay JJ, Rodrigo-Navarro A, Hassi K, Moulisova V, Dalby MJ, Salmeron-Sanchez M. Living biointerfaces based on non-pathogenic bacteria support stem cell differentiation. *Sci Rep*. 2016;6. doi:10.1038/srep21809

188. Hay JJ, Rodrigo-Navarro A, Petaroudi M, et al. Bacteria-Based Materials for Stem Cell Engineering. *Adv Mater*. 2018;30(43):1804310. doi:10.1002/adma.201804310

189. Sankaran S, Zhao S, Muth C, Paez J, del Campo A. Toward Light-Regulated Living Biomaterials. *Adv Sci*. 2018;5(8). doi:10.1002/advs.201800383

190. Kim J, Hegde M, Jayaraman A. Co-culture of epithelial cells and bacteria for investigating host-pathogen interactions. *Lab Chip*. 2010;10(1):43-50. doi:10.1039/b911367c

191. Rodrigo-Navarro A, Rico P, Saadeddin A, Garcia AJ, Salmeron-Sanchez M. Living biointerfaces based on

non-pathogenic bacteria to direct cell differentiation. *Sci Rep*. 2014;4(1):1-10. doi:10.1038/srep05849

192. Hay JJ, Rodrigo-Navarro A, Petaroudi M, et al. Bacteria-Based Materials for Stem Cell Engineering. *Adv Mater*. 2018;30(43):1804310. doi:10.1002/adma.201804310

193. Sankaran S, Zhao S, Muth C, Paez J, del Campo A. Toward Light-Regulated Living Biomaterials. *Adv Sci*. 2018;5(8):1800383. doi:10.1002/advs.201800383

194. Navarro AR. *Functional Living Biointerfaces to Direct Cell-Material Interaction Acknowledgements*.; 2015.

195. Beadle GW, Tatum EL. Genetic Control of Biochemical Reactions in Neurospora. *Proc Natl Acad Sci*. 1941;27(11):499-506. doi:10.1073/pnas.27.11.499

196. Liang P, Xu Y, Zhang X, et al. CRISPR/Cas9-mediated gene editing in human tripronuclear zygotes. *Protein Cell*. 2015;6(5):363-372. doi:10.1007/s13238-015-0153-5

197. Silva G, Poirot L, Galetto R, et al. Meganucleases and Other Tools for Targeted Genome Engineering: Perspectives and Challenges for Gene Therapy. *Curr Gene Ther*. 2011;11(1):11-27. doi:10.2174/156652311794520111

198. Urnov FD, Rebar EJ, Holmes MC, Zhang HS, Gregory PD. Genome editing with engineered zinc finger nucleases. *Nat Rev Genet*. 2010;11(9):636-646. doi:10.1038/nrg2842

199. Joung JK, Sander JD. TALENs: A widely applicable technology for targeted genome editing. *Nat Rev Mol Cell Biol*. 2013;14(1):49-55. doi:10.1038/nrm3486

200. Ran FA, Hsu PD, Wright J, Agarwala V, Scott DA, Zhang F. Genome engineering using the CRISPR-Cas9 system. *Nat Protoc*. 2013;8(11):2281-2308. doi:10.1038/nprot.2013.143

201. Fellmann C, Lowe SW. Stable RNA interference rules for silencing. *Nat Cell Biol*. 2014;16(1):10-18. doi:10.1038/ncb2895

202. Rinaldi C, Wood MJA. Antisense oligonucleotides: The next frontier for treatment of neurological disorders. *Nat Rev Neurol*. 2018;14(1):9-22. doi:10.1038/nrneurol.2017.148

203. Lewin AS, Hauswirth WW. Ribozyme gene therapy: Applications for molecular medicine. *Trends Mol Med*. 2001;7(5):221-228. doi:10.1016/S1471-4914(01)01965-7

204. Koppolu V, Vasigala VK. Role of Escherichia coli in Biofuel Production . *Microbiol Insights*. 2016;9:MBI.S10878. doi:10.4137/mbi.s10878

205. Yang D, Park SY, Park YS, Eun H, Lee SY. Metabolic Engineering of Escherichia coli for Natural Product Biosynthesis. 2020. doi:10.1016/j.tibtech.2019.11.007

206. Antonovsky N, Gleizer S, Noor E, et al. Sugar Synthesis from CO2 in Escherichia coli. *Cell*. 2016;166(1):115-125. doi:10.1016/j.cell.2016.05.064

207. Ferrer-Miralles N, Domingo-Espín J, Corchero J, Vázquez E, Villaverde A. Microbial factories for recombinant pharmaceuticals. *Microb Cell Fact*. 2009;8:17. doi:10.1186/1475-2859-8-17

208. Sharma A, Chaudhuri TK. Revisiting Escherichia coli as microbial factory for enhanced production of human serum albumin. *Microb Cell Fact*. 2017;16(1). doi:10.1186/s12934-017-0784-8

209. Zieliński M, Romanik-Chruścielewska A, Mikiewicz D, et al. Expression and purification of recombinant human insulin from E. coli 20 strain. *Protein Expr Purif*. 2019;157:63-69. doi:10.1016/j.pep.2019.02.002

210. Caraceni P, Tufoni M, Bonavita ME. Clinical use of albumin. *Blood Transfus*. 2013;11(SUPPL. 4):s18. doi:10.2450/2013.005s

211. Baeshen NA, Baeshen MN, Sheikh A, et al. Cell factories for insulin production. *Microb Cell Fact*. 2014;13(1). doi:10.1186/s12934-014-0141-0

212. Martín R, Chain F, Miquel S, et al. Effects in the use of a genetically engineered strain of Lactococcus lactis delivering in situ IL-10 as a therapy to treat low-grade colon inflammation. *Hum Vaccines Immunother*. 2014;10(6):1611-1621. doi:10.4161/hv.28549

213. Gu Q, Song D, Zhu M. Oral vaccination of mice against Helicobacter pylori with recombinant

Lactococcus lactis expressing urease subunit B. *FEMS Immunol Med Microbiol*. 2009;56(3):197-203. doi:10.1111/j.1574-695X.2009.00566.x

214. Bahey-El-Din M, Casey PG, Griffin BT, Gahan CGM. Lactococcus lactis-expressing listeriolysin O (LLO) provides protection and specific CD8+ T cells against Listeria monocytogenes in the murine infection model. *Vaccine*. 2008;26(41):5304-5314. doi:10.1016/j.vaccine.2008.07.047

215. Sybesma W, Burgess C, Starrenburg M, Van Sinderen D, Hugenholtz J. Multivitamin production in Lactococcus lactis using metabolic engineering. *Metab Eng*. 2004;6(2):109-115. doi:10.1016/j.ymben.2003.11.002

216. Mao R, Zhou K, Han Z, Wang Y. Subtilisin QK-2: Secretory expression in Lactococcus lactis and surface display onto gram-positive enhancer matrix (GEM) particles. *Microb Cell Fact*. 2016;15(1):80. doi:10.1186/s12934-016-0478-7

217. Zhang B, Li A, Zuo F, et al. Recombinant Lactococcus lactis NZ9000 secretes a bioactive kisspeptin that inhibits proliferation and migration of human colon carcinoma HT-29 cells. *Microb Cell Fact*. 2016;15(1):102. doi:10.1186/s12934-016-0506-7

218. Goldstein DA, Thomas JA. Biopharmaceuticals derived from genetically modified plants. *Q J Med*. 2004;97:705-716. doi:10.1093/qjmed/hch121

219. Doehmer J, Schneider A, Faßbender M, Soballa V, Schmalix WA, Greim H. Genetically engineered mammalian cells and applications. *Toxicol Lett*. 1995;82-83(C):823-827. doi:10.1016/0378-4274(95)03523-0

220. Tacon W, Carey N, Emtage S. The construction and characterisation of plasmid vectors suitable for the expression of all DNA phases under the control of the E. coli tryptophan promoter. *MGG Mol Gen Genet*. 1980;177(3):427-438. doi:10.1007/BF00271481

221. Kouprina N, Earnshaw WC, Masumoto H, Larionov V. A new generation of human artificial chromosomes for functional genomics and gene therapy. *Cell Mol Life Sci*. 2013;70(7):1135-1148. doi:10.1007/s00018-012-1113-3

222. Rosa P, Samuels DS, Hogan D, Stevenson B, Casjens S, Tilly K. Directed insertion of a selectable marker into a circular plasmid of Borrelia burgdorferi. *J Bacteriol*. 1996;178(20):5946-5953. doi:10.1128/jb.178.20.5946-5953.1996

223. Fornwald JA, Schmidt FJ, Adams CW, Rosenberg M, Brawner ME. Two promoters, one inducible and one constitutive, control transcription of the Streptomyces lividans galactose operon. *Proc Natl Acad Sci U S A*. 1987;84(8):2130-2134. doi:10.1073/pnas.84.8.2130

224. Albers SC, Peebles CAM. Evaluating Light-Induced Promoters for the Control of Heterologous Gene Expression in Synechocystis sp. PCC 6803. *Biotechnol Prog*. 2017;33(1):45-53. doi:10.1002/btpr.2396

225. Madsen SM, Arnau J, Vrang A, Givskov M, Israelsen H. Molecular characterization of the pH-inducible and growth phase-dependent promoter P170 of Lactococcus lactis. *Mol Microbiol*. 1999;32(1):75-87. doi:10.1046/j.1365-2958.1999.01326.x

226. Chandrapati S, O'Sullivan DJ. Nisin independent induction of the *nisA* promoter in *Lactococcus lactis* during growth in lactose or galactose. *FEMS Microbiol Lett*. 1999;170(1):191-198. doi:10.1111/j.1574-6968.1999.tb13374.x

227. Pathogens NL of E, Microbiology B of, Control LC for D. The polymerase chain reaction: An overview and development of diagnostic PCR protocols at the LCDC. *Can J Infect Dis*. 1991;2(2):89. doi:10.1155/1991/580478

228. Pathogens NL of E, Microbiology B of, Control LC for D. The polymerase chain reaction: An overview and development of diagnostic PCR protocols at the LCDC. *Can J Infect Dis*. 1991;2(2):89. doi:10.1155/1991/580478

229. Crut A, Nair PA, Koster DA, Shuman S, Dekker NH. Dynamics of phosphodiester synthesis by DNA ligase. *Proc Natl Acad Sci U S A*. 2008;105(19):6894-6899. doi:10.1073/pnas.0800113105

230. Mullis KB. The unusual origin of the polymerase chain reaction. *Sci Am*. 1990;262(4):56-65.

doi:10.1038/scientificamerican0490-56

231. Notomi T, Okayama H, Masubuchi H, et al. *Loop-Mediated Isothermal Amplification of DNA*. Vol 28.; 2000.

232. Lizardi PM, Huang X, Zhu Z, Bray-Ward P, Thomas DC, Ward DC. Mutation detection and single-molecule counting using isothermal rolling-circle amplification. *Nat Genet*. 1998;19(3):225-232. doi:10.1038/898

233. Gibriel AA, Adel O. Advances in ligase chain reaction and ligation-based amplifications for genotyping assays: Detection and applications. *Mutat Res - Rev Mutat Res*. 2017;773:66-90. doi:10.1016/j.mrrev.2017.05.001

234. Aich P, Patra M, Chatterjee AK, Roy SS, Basu T. Calcium chloride made e. coli competent for uptake of extraneous DNA through overproduction of ompC protein. *Protein J*. 2012;31(5):366-373. doi:10.1007/s10930-012-9411-z

235. Heravi RM, Nasiraii LR, Sankian M, Kermanshahi H, Varasteh AR. Optimization and comparison of two electrotransformation methods for lactobacilli. *Biotechnology*. 2012;11(1):50-54. doi:10.3923/biotech.2012.50.54

236. Tarazanova M, Huppertz T, Beerthuyzen M, et al. Cell surface properties of Lactococcus lactis reveal milk protein binding specifically evolved in dairy isolates. *Front Microbiol*. 2017;8(SEP):1691. doi:10.3389/fmicb.2017.01691

237. Kelly WJ, Ward LJH, Leahy SC. Chromosomal diversity in Lactococcus lactis and the origin of dairy starter cultures. *Genome Biol Evol*. 2010;2(1):729-744. doi:10.1093/gbe/evq056

238. Parapouli M, Delbès-Paus C, Kakouri A, Koukkou A-I, Montel M-C, Samelis J. Characterization of a Wild, Novel Nisin A-Producing Lactococcus Strain with an L. lactis subsp. *cremoris* Genotype and an L. lactis subsp. *lactis* Phenotype, Isolated from Greek Raw Milk. *Appl Environ Microbiol*. 2013;79(11):3476-3484. doi:10.1128/AEM.00436-13

239. Song AAL, In LLA, Lim SHE, Rahim RA. A review on Lactococcus lactis: From food to factory. *Microb Cell Fact*. 2017;16(1). doi:10.1186/s12934-017-0669-x

240. Bolotin A, Wincker P, Mauger S, et al. The complete genome sequence of the lactic acid bacterium lactococcus lactis ssp. lactis IL1403. *Genome Res*. 2001;11(5):731-753. doi:10.1101/gr.GR-1697R

241. Di Cagno R, Coda R, De Angelis M, Gobbetti M. Exploitation of vegetables and fruits through lactic acid fermentation. *Food Microbiol*. 2013;33(1):1-10. doi:10.1016/j.fm.2012.09.003

242. Ricci A, Allende A, Bolton D, et al. Update of the list of QPS-recommended biological agents intentionally added to food or feed as notified to EFSA 8: suitability of taxonomic units notified to EFSA until March 2018. *EFSA J*. 2018;16(7). doi:10.2903/j.efsa.2018.5315

243. Liu Y, van Bennekom EO, Zhang Y, Abee T, Smid EJ. Long-chain vitamin K2 production in Lactococcus lactis is influenced by temperature, carbon source, aeration and mode of energy metabolism. *Microb Cell Fact*. 2019;18(1):129. doi:10.1186/s12934-019-1179-9

244. Sybesma W, Burgess C, Starrenburg M, van Sinderen D, Hugenholtz J. Multivitamin production in Lactococcus lactis using metabolic engineering. *Metab Eng*. 2004;6(2):109-115. doi:10.1016/j.ymben.2003.11.002

245. Sybesma W, Starrenburg M, Kleerebezem M, Mierau I, de Vos WM, Hugenholtz J. Increased production of folate by metabolic engineering of Lactococcus lactis. *Appl Environ Microbiol*. 2003;69(6):3069-3076. doi:10.1128/aem.69.6.3069-3076.2003

246. Medina M, Vintiñi E, Villena J, Raya R, Alvarez S. Lactococcus lactis as an adjuvant and delivery vehicle of antigens against pneumococcal respiratory infections. *Bioeng Bugs*. 2010;1(5):313-325. doi:10.4161/bbug.1.5.12086

247. Azizpour M, Hosseini SD, Jafari P, Akbary N. Lactococcus lactis : A New Strategy for Vaccination. *Avicenna J Med Biotechnol*. 2017;9(4):163-168. http://www.ncbi.nlm.nih.gov/pubmed/29090064. Accessed September 16, 2019.

248. Todorov SD, Botes M, Danova ST, Dicks LMT. Probiotic properties of Lactococcus lactis ssp. lactis HV219, isolated from human vaginal secretions. *J Appl Microbiol*. 2007;103(3):629-639. doi:10.1111/j.1365-2672.2007.03290.x

249. Cook DP, Gysemans C, Mathieu C. Lactococcus lactis As a Versatile Vehicle for Tolerogenic Immunotherapy. *Front Immunol*. 2018;8:1961. doi:10.3389/fimmu.2017.01961

250. Liu M, Zhang X, Hao Y, et al. Protective effects of a novel probiotic strain, *Lactococcus lactis* ML2018, in colitis: *in vivo* and *in vitro* evidence. *Food Funct*. 2019;10(2):1132-1145. doi:10.1039/C8FO02301H

251. Gurien LA, Stallings-Archer K, Smith SD. Probiotic Lactococcus lactis decreases incidence and severity of necrotizing enterocolitis in a preterm animal model. *J Neonatal Perinatal Med*. 2018;11(1):65-69. doi:10.3233/NPM-181740

252. Lee N-K, Han KJ, Son S-H, Eom SJ, Lee S-K, Paik H-D. Multifunctional effect of probiotic Lactococcus lactis KC24 isolated from kimchi. *LWT - Food Sci Technol*. 2015;64(2):1036-1041. doi:10.1016/J.LWT.2015.07.019

253. Kimoto-Nira H. New lactic acid bacteria for skin health via oral intake of heat-killed or live cells. *Anim Sci J*. 2018;89(6):835-842. doi:10.1111/asj.13017

254. Boumaiza M, Colarusso A, Parrilli E, et al. Getting value from the waste: recombinant production of a sweet protein by Lactococcus lactis grown on cheese whey. *Microb Cell Fact*. 2018;17(1):126. doi:10.1186/s12934-018-0974-z

255. Gu W, Xia Q, Yao J, Fu S, Guo J, Hu X. Recombinant expressions of sweet plant protein mabinlin II in Escherichia coli and food-grade Lactococcus lactis. *World J Microbiol Biotechnol*. 2015;31(4):557-567. doi:10.1007/s11274-015-1809-2

256. Luerce TD, Gomes-Santos AC, Rocha CS, et al. Anti-inflammatory effects of Lactococcus lactis NCDO 2118 during the remission period of chemically induced colitis. *Gut Pathog*. 2014;6:33. doi:10.1186/1757-4749-6-33

257. Liu M, Zhang X, Hao Y, et al. Protective effects of a novel probiotic strain, *Lactococcus lactis* ML2018, in colitis: *in vivo* and *in vitro* evidence. *Food Funct*. 2019;10(2):1132-1145. doi:10.1039/C8FO02301H

258. Liu Q, Li J, Zhao J, Wu J, Shao T. Enhancement of lignocellulosic degradation in high-moisture alfalfa via anaerobic bioprocess of engineered Lactococcus lactis with the function of secreting cellulase. *Biotechnol Biofuels*. 2019;12(1):88. doi:10.1186/s13068-019-1429-4

259. Dunière L, Sindou J, Chaucheyras-Durand F, Chevallier I, Thévenot-Sergentet D. Silage processing and strategies to prevent persistence of undesirable microorganisms. *Anim Feed Sci Technol*. 2013;182(1-4):1-15. doi:10.1016/J.ANIFEEDSCI.2013.04.006

260. Liu J, Dantoft SH, Würtz A, Jensen PR, Solem C. A novel cell factory for efficient production of ethanol from dairy waste. *Biotechnol Biofuels*. 2016;9:33. doi:10.1186/s13068-016-0448-7

261. Abdel-Rahman MA, Tashiro Y, Sonomoto K. Recent advances in lactic acid production by microbial fermentation processes. *Biotechnol Adv*. 2013;31(6):877-902. doi:10.1016/J.BIOTECHADV.2013.04.002

262. Cano-Garrido O, Seras-Franzoso J, Garcia-Fruitós E. Lactic acid bacteria: reviewing the potential of a promising delivery live vector for biomedical purposes. *Microb Cell Fact*. 2015;14:137. doi:10.1186/s12934-015-0313-6

263. Remaut E, Braat H, Vandenbroucke K, Rotteiers P, Steidler L. Clinical Potential of Lactococcus lactis Mediated Delivery of Human Interleukin-10 and Trefoil Factors. *Biosci Microflora*. 2006;25(3):81-97. doi:10.12938/bifidus.25.81

264. Feizollahzadeh S, Khanahmad H, Rahimmanesh I, et al. Expression of biologically active murine interleukin-18 in *Lactococcus lactis*. Sauer M, ed. *FEMS Microbiol Lett*. 2016;363(21):fnw234. doi:10.1093/femsle/fnw234

265. Zhang B, Li A, Zuo F, et al. Recombinant Lactococcus lactis NZ9000 secretes a bioactive kisspeptin that inhibits proliferation and migration of human colon carcinoma HT-29 cells. *Microb Cell Fact*. 2016;15(1):102. doi:10.1186/s12934-016-0506-7

266. Ciaćma K, Więckiewicz J, Kędracka-Krok S, et al. Secretion of tumoricidal human tumor necrosis factor-related apoptosis-inducing ligand (TRAIL) by recombinant Lactococcus lactis: optimization of in vitro synthesis conditions. *Microb Cell Fact*. 2018;17(1):177. doi:10.1186/s12934-018-1028-2

267. Jacouton E, Torres Maravilla E, Boucard A-S, et al. Anti-tumoral Effects of Recombinant Lactococcus lactis Strain Secreting IL-17A Cytokine. *Front Microbiol*. 2019;9:3355. doi:10.3389/fmicb.2018.03355

268. Shenyang Gao, Dandan Li, Ying Liu, Tiezhing Zhou XY. Oral immunization with recombinant hepatitis E virus antigen displayed on the Lactococcus lactis surface enhances ORF2-specific mucosal and systemic immune responses in mice. *Int Immunopharmacol*. 2015;24(1):140-145. doi:10.1016/J.INTIMP.2014.10.032

269. Hansenanderwin PA, Lessel F. *Lactobacillus Casei (Orla-Jensen) Comb. Nov*. Vol 21.; 1971.

270. Heller P, Casaletto J, Ruiz G, Geller J, Characteristic Metazoa S. Data Descriptor: A database of metazoan cytochrome c oxidase subunit I gene sequences derived from GenBank with CO-ARBitrator Background & Summary. 2018. doi:10.1038/sdata.2018.156

271. Janda JM, Abbott SL. 16S rRNA gene sequencing for bacterial identification in the diagnostic laboratory: Pluses, perils, and pitfalls. *J Clin Microbiol*. 2007;45(9):2761-2764. doi:10.1128/JCM.01228-07

272. Schleifer KH, Ludwig W. Phylogenetic relationships of lactic acid bacteria. In: *The Genera of Lactic Acid Bacteria*. Springer US; 1995:7-18. doi:10.1007/978-1-4615-5817-0_2

273. Zhang Z-G, Ye Z-Q, Yu L, Shi P. *Phylogenomic Reconstruction of Lactic Acid Bacteria: An Update*.; 2011. doi:10.1186/1471-2148-11-1

274. Van De Bunt B, Bron PA, Sijtsma L, De Vos WM, Hugenholtz J. Use of non-growing Lactococcus lactis cell suspensions for production of volatile metabolites with direct relevance for flavour formation during dairy fermentations. *Microb Cell Fact*. 2014;13(1):176. doi:10.1186/s12934-014-0176-2

275. Samazan F, Rokbi B, Seguin D, et al. Production, secretion and purification of a correctly folded staphylococcal antigen in Lactococcus lactis. *Microb Cell Fact*. 2015;14(1):104. doi:10.1186/s12934-015-0271-z

276. Funayama H, Huang L, Sato T, et al. Pharmacological characterization of anaphylaxis-like shock responses induced in mice by mannan and lipopolysaccharide. *Int Immunopharmacol*. 2009;9(13-14):1518-1524. doi:10.1016/j.intimp.2009.09.006

277. Zielen S, Trischler J, Schubert R. Lipopolysaccharide challenge: immunological effects and safety in humans. *Expert Rev Clin Immunol*. 2015;11(3):409-418. doi:10.1586/1744666X.2015.1012158

278. Habimana O, Le Goff C, Juillard V, et al. Positive role of cell wall anchored proteinase PrtP in adhesion of lactococci. *BMC Microbiol*. 2007;7(1):36. doi:10.1186/1471-2180-7-36

279. Rodrigo-Navarro A, Rico P, Saadeddin A, Garcia AJ, Salmeron-Sanchez M. Living biointerfaces based on non-pathogenic bacteria to direct cell differentiation. *Sci Rep*. 2015;4(1):5849. doi:10.1038/srep05849

280. Hay JJ, Rodrigo-Navarro A, Hassi K, Moulisova V, Dalby MJ, Salmeron-Sanchez M. Living biointerfaces based on non-pathogenic bacteria support stem cell differentiation. *Sci Rep*. 2016;6(1):21809. doi:10.1038/srep21809

281. Bolotin A, Quinquis B, Ehrlich SD, Sorokin A. Complete Genome Sequence of Lactococcus lactis subsp. cremoris A76. *J Bacteriol*. 2012;194(5):1241-1242. doi:10.1128/JB.06629-11

282. Mierau I, Kleerebezem M. 10 years of the nisin-controlled gene expression system (NICE) in Lactococcus lactis. *Appl Microbiol Biotechnol*. 2005;68(6):705-717. doi:10.1007/s00253-005-0107-6

283. Jørgensen CM, Vrang A, Madsen SM. Recombinant protein expression in *Lactococcus lactis* using the P170 expression system. *FEMS Microbiol Lett*. 2014;351(2):170-178. doi:10.1111/1574-6968.12351

284. Gitton C, Meyrand M, Wang J, et al. Proteomic Signature of Lactococcus lactis NCDO763 Cultivated in Milk. *Appl Environ Microbiol*. 2005;71(11):7152-7163. doi:10.1128/AEM.71.11.7152-7163.2005

285. Silva WM, Sousa CS, Oliveira LC, et al. Comparative proteomic analysis of four biotechnological strains

Lactococcus lactis through label-free quantitative proteomics. *Microb Biotechnol*. 2019;12(2):265-274. doi:10.1111/1751-7915.13305

286. Frazier CL, San Filippo J, Lambowitz AM, Mills DA. Genetic manipulation of Lactococcus lactis by using targeted group II introns: Generation of stable insertions without selection. *Appl Environ Microbiol*. 2003;69(2):1121-1128. doi:10.1128/AEM.69.2.1121-1128.2003

287. Jørgensen CM, Vrang A, Madsen SM. Recombinant protein expression in *Lactococcus lactis* using the P170 expression system. *FEMS Microbiol Lett*. 2014;351(2):170-178. doi:10.1111/1574-6968.12351

288. van der Els S, James JK, Kleerebezem M, Bron PA. Versatile Cas9-driven subpopulation selection toolbox for Lactococcus lactis. *Appl Environ Microbiol*. 2018;84(8). doi:10.1128/AEM.02752-17

289. Mierau I, Olieman K, Mond J, Smid EJ. Optimization of the Lactococcus lactis nisin-controlled gene expression system NICE for industrial applications. *Microb Cell Fact*. 2005;4:16. doi:10.1186/1475-2859-4-16

290. Berlec A, Škrlec K, Kocjan J, Olenic M, Štrukelj B. Single plasmid systems for inducible dual protein expression and for CRISPR-Cas9/CRISPRi gene regulation in lactic acid bacterium Lactococcus lactis. *Sci Rep*. 2018;8(1):1-11. doi:10.1038/s41598-018-19402-1

291. Rodrigo-Navarro A, Rico P, Saadeddin A, Garcia AJ, Salmeron-Sanchez M. Living biointerfaces based on non-pathogenic bacteria to direct cell differentiation. *Sci Rep*. 2014;4(1):5849. doi:10.1038/srep05849

292. Hay JJ, Rodrigo-Navarro A, Petaroudi M, et al. Bacteria-Based Materials for Stem Cell Engineering. *Adv Mater*. 2018;30(43):1804310. doi:10.1002/adma.201804310

293. Hay JJ, Rodrigo-Navarro A, Hassi K, Moulisova V, Dalby MJ, Salmeron-Sanchez M. Living biointerfaces based on non-pathogenic bacteria support stem cell differentiation. *Sci Rep*. 2016;6(1):21809. doi:10.1038/srep21809

294. Steidler L, Wells JM, Raeymaekers A, Vandekerckhove J, Fiers W, Remaut E. Secretion of biologically active murine interleukin-2 by Lactococcus lactis subsp. lactis. *Appl Environ Microbiol*. 1995;61(4):1627-1629. doi:10.1128/aem.61.4.1627-1629.1995

295. Alimolaei M, Golchin M, Abshenas J, Ezatkhah M, Bafti MS. A Recombinant Probiotic, Lactobacillus casei, Expressing the Clostridium perfringens α-toxoid, as an Orally Vaccine Candidate Against Gas Gangrene and Necrotic Enteritis. *Probiotics Antimicrob Proteins*. 2018;10(2):251-257. doi:10.1007/s12602-017-9276-8

296. Saha P, Chassaing B, Yeoh BS, et al. Ectopic Expression of Innate Immune Protein, Lipocalin-2, in Lactococcus lactis Protects Against Gut and Environmental Stressors. *Inflamm Bowel Dis*. 2017;23(7):1120-1132. doi:10.1097/MIB.0000000000001134

297. Mertens N, Remaut E, Fiers W. Increased stability of phage T7g10 mRNA is mediated by either a 5'- or a 3'-terminal stem-loop structure. *Biol Chem*. 1996;377(12):811-817. http://www.ncbi.nlm.nih.gov/pubmed/8997491. Accessed October 22, 2019.

298. van Asseldonk M, Rutten G, Oteman M, Siezen RJ, de Vos WM, Simons G. Cloning of usp45, a gene encoding a secreted protein from Lactococcus lactis subsp. lactis MG1363. *Gene*. 1990;95(1):155-160. doi:10.1016/0378-1119(90)90428-T

299. Le Loir Y, Nouaille S, Commissaire J, Brétigny L, Gruss A, Langella P. Signal Peptide and Propeptide Optimization for Heterologous Protein Secretion in Lactococcus lactis. *Appl Environ Microbiol*. 2001;67(9):4119-4127. doi:10.1128/AEM.67.9.4119-4127.2001

300. Steidler L, Viaene J, Fiers W, Remaut E. Functional display of a heterologous protein on the surface of Lactococcus lactis by means of the cell wall anchor of Staphylococcus aureus protein A. *Appl Environ Microbiol*. 1998;64(1):342-345. doi:10.1128/aem.64.1.342-345.1998

301. Schneewind O, Model P, Fischetti VA. *Sorting of Protein A to the Staphylococcal Cell Wall*. Vol 70.; 1992.

302. Navarre WW, Schneewind O. Proteolytic cleavage and cell wall anchoring at the LPXTG motif of surface proteins in Gram-positive bacteria. *Mol Microbiol*. 1994;14(1):115-121. doi:10.1111/j.1365-

2958.1994.tb01271.x

303. Buza-Vidas N, Antonchuk J, Qian H, et al. Cytokines regulate postnatal hematopoietic stem cell expansion: Opposing roles of thrombopoietin and LNK. *Genes Dev*. 2006;20(15):2018-2023. doi:10.1101/gad.385606

304. Itkin T, Lapidot T. SDF-1 keeps HSC quiescent at home. *Blood*. 2011;117(2):373-374. doi:10.1182/blood-2010-09-307843

305. Kandler O. *Carbohydrate Metabolism in Lactic Acid Bacteria*. Vol 49.; 1983.

306. Deutscher J, Aké FMD, Derkaoui M, et al. The Bacterial Phosphoenolpyruvate:Carbohydrate Phosphotransferase System: Regulation by Protein Phosphorylation and Phosphorylation-Dependent Protein-Protein Interactions. *Microbiol Mol Biol Rev*. 2014;78(2):231-256. doi:10.1128/mmbr.00001-14

307. Neves AR, Pool WA, Kok J, Kuipers OP, Santos H. Overview on sugar metabolism and its control in Lactococcus lactis — The input from in vivo NMR . *FEMS Microbiol Rev*. 2005;29(3):531-554. doi:10.1016/j.fmrre.2005.04.005

308. Jing J, And YE, Saier MH. *Regulation of Sugar Uptake via the Phosphoenolpyruvate-Dependent Phosphotransferase Systems in Bacillus Subtilis and Lactococcus Lactis Is Mediated by ATP-Dependent Phosphorylation of Seryl Residue 46 in HPr*. Vol 178.; 1996.

309. Aleksandrzak-Piekarczyk T. Lactose and β-Glucosides Metabolism and Its Regulation in Lactococcus lactis: A Review. In: *Lactic Acid Bacteria - R & D for Food, Health and Livestock Purposes*. InTech; 2013. doi:10.5772/50889

310. Davidson AL, Dassa E, Orelle C, Chen J. Structure, Function, and Evolution of Bacterial ATP-Binding Cassette Systems. *Microbiol Mol Biol Rev*. 2008;72(2):317-364. doi:10.1128/mmbr.00031-07

311. Deutscher J, Saier MH. ATP-dependent protein kinase-catalyzed phosphorylation of a seryl residue in HPr, a phosphate carrier protein of the phosphotransferase system in Streptococcus pyogenes. *Proc Natl Acad Sci U S A*. 1983;80(22):6790-6794. doi:10.1073/pnas.80.22.6790

312. Ye JJ, Reizer J, Cui X, Saier MHS. Inhibition of the Phosphoeno1pyruvate:Lactose Phosphotransferase System and Activation of a Cytoplasmic Sugar-phosphate Phosphatase in Lactococcus Zactis by ATP-dependent Metabolite-activated Phosphorylation of Serine 46 in the Phosphocarrier Protein HPr*. *J BIOLCOICAL Chem* . 1994;269(16):11837-11844.

313. DeWaal D, Nogueira V, Terry AR, et al. Hexokinase-2 depletion inhibits glycolysis and induces oxidative phosphorylation in hepatocellular carcinoma and sensitizes to metformin. *Nat Commun*. 2018;9(1):1-14. doi:10.1038/s41467-017-02733-4

314. Boels IC, Kleerebezem M, De Vos WM. Engineering of carbon distribution between glycolysis and sugar nucleotide biosynthesis in Lactococcus lactis. *Appl Environ Microbiol*. 2003;69(2):1129-1135. doi:10.1128/AEM.69.2.1129-1135.2003

315. Kang TS, Korber DR, Tanaka T. Regulation of dual glycolytic pathways for fructose metabolism in heterofermentative Lactobacillus panis PM1. *Appl Environ Microbiol*. 2013;79(24):7818-7826. doi:10.1128/AEM.02377-13

316. Pokusaeva K, Fitzgerald GF, Van Sinderen D. Carbohydrate metabolism in Bifidobacteria. *Genes Nutr*. 2011;6(3):285-306. doi:10.1007/s12263-010-0206-6

317. SCHRAMM M, KLYBAS V, RACKER E. Phosphorolytic cleavage of fructose-6-phosphate by fructose-6-phosphate phosphoketolase from Acetobacter xylinum. *J Biol Chem*. 1958;233(6):1283-1288. http://www.jbc.org/. Accessed July 1, 2020.

318. K. T, A. K, K. S, A. I, S. H, P. S. Two different pathways for D -xylose metabolism and the effect of xylose concentration on the yield coefficient of L -lactate in mixed-acid fermentation by the lactic acid bacterium Lactococcus lactis IO-1. *Appl Microbiol Biotechnol*. 2002;60(1-2):160-167. doi:10.1007/s00253-002-1078-5

319. Novák L, Loubiere P. The metabolic network of Lactococcus lactis: Distribution of 14C- labeled substrates between catabolic and anabolic pathways. *J Bacteriol*. 2000;182(4):1136-1143.

doi:10.1128/JB.182.4.1136-1143.2000

320. Azizan KA, Baharum SN, Noor NM. Metabolic profiling of Lactococcus lactis under different culture conditions. *Molecules*. 2012;17(7):8022-8036. doi:10.3390/molecules17078022

321. Wagner N, Tran QH, Richter H, Selzer PM, Unden G. Pyruvate fermentation by Oenococcus oeni and Leuconostoc mesenteroides and role of pyruvate dehydrogenase in anaerobic fermentation. *Appl Environ Microbiol*. 2005;71(9):4966-4971. doi:10.1128/AEM.71.9.4966-4971.2005

322. Papagianni M. Metabolic engineering of lactic acid bacteria for the production of industrially important compounds. *Comput Struct Biotechnol J*. 2012;3(4):e201210003. doi:10.5936/csbj.201210003

323. Burgé G, Saulou-Bérion C, Moussa M, Allais F, Athes V, Spinnler HE. Relationships between the use of Embden Meyerhof pathway (EMP) or Phosphoketolase pathway (PKP) and lactate production capabilities of diverse Lactobacillus reuteri strains. *J Microbiol*. 2015;53(10):702-710. doi:10.1007/s12275-015-5056-x

324. Novák L, Loubiere P. The metabolic network of Lactococcus lactis: distribution of (14)C-labeled substrates between catabolic and anabolic pathways. *J Bacteriol*. 2000;182(4):1136-1143. doi:10.1128/jb.182.4.1136-1143.2000

325. Novák L, Loubiere P. The metabolic network of Lactococcus lactis: Distribution of 14C- labeled substrates between catabolic and anabolic pathways. *J Bacteriol*. 2000;182(4):1136-1143. doi:10.1128/JB.182.4.1136-1143.2000

326. Cantó C, Menzies K, Auwerx J. NAD+ metabolism and the control of energy homeostasis - a balancing act between mitochondria and the nucleus. *Cell Metab*. 2015;22(1):31. doi:10.1016/J.CMET.2015.05.023

327. Melchiorsen CR, Jensen NBS, Christensen B, Jokumsen KV, Villadsen J. Dynamics of pyruvate metabolism in Lactococcus lactis. *Biotechnol Bioeng*. 2001;74(4):271-279. doi:10.1002/bit.1117

328. Nordkvist M, Bang N, Jensen S, Villadsen J. Glucose Metabolism in Lactococcus lactis MG1363 under Different Aeration Conditions: Requirement of Acetate To Sustain Growth under Microaerobic Conditions. *Appl Environ Microbiol*. 2003;69(6):3462-3468. doi:10.1128/AEM.69.6.3462-3468.2003

329. Benthin S, Nielsen J, Villadsen J. *Two Uptake Systems for Fructose in Lactococcus Lactis Subsp. Cremoris FD1 Produce Glycolytic and Gluconeogenic Fructose Phosphates and Induce Oscillations in Growth and Lactic Acid Formation*. Vol 59. American Society for Microbiology (ASM); 1993. /pmc/articles/PMC182438/?report=abstract. Accessed July 3, 2020.

330. Aleksandrzak-Piekarczyk T, Kok J, Renault P, Bardowski J. Alternative lactose catabolic pathway in Lactococcus lactis IL1403. *Appl Environ Microbiol*. 2005;71(10):6060-6069. doi:10.1128/AEM.71.10.6060-6069.2005

331. Kaur M, Jayaraman G. Hyaluronan production and molecular weight is enhanced in pathway-engineered strains of lactate dehydrogenase-deficient Lactococcus lactis. *Metab Eng Commun*. 2016;3:15-23. doi:10.1016/J.METENO.2016.01.003

332. Bongers RS, Hoefnagel MHN, Starrenburg MJC, et al. IS981-mediated adaptive evolution recovers lactate production by ldhB transcription activation in a lactate dehydrogenase-deficient strain of Lactococcus lactis. *J Bacteriol*. 2003;185(15):4499-4507. doi:10.1128/JB.185.15.4499-4507.2003

333. Hoefnagel MHN, Starrenburg MJC, Martens DE, et al. Metabolic engineering of lactic acid bacteria, the combined approach: Kinetic modelling, metabolic control and experimental analysis. *Microbiology*. 2002;148(4):1003-1013. doi:10.1099/00221287-148-4-1003

334. Neves AR, Ramos A, Costa H, et al. Effect of different NADH oxidase levels on glucose metabolism by Lactococcus lactis: kinetics of intracellular metabolite pools determined by in vivo nuclear magnetic resonance. *Appl Environ Microbiol*. 2002;68(12):6332-6342. doi:10.1128/aem.68.12.6332-6342.2002

335. Hugenholtz J, Kleerebezem M, Starrenburg M, Delcour J, De Vos W, Hols P. Lactococcus lactis as a cell factory for high-level diacetyl production. *Appl Environ Microbiol*. 2000;66(9):4112-4114. doi:10.1128/AEM.66.9.4112-4114.2000

336. Neves AR, Ramos A, Shearman C, Gasson MJ, Almeida JS, Santos H. Metabolic characterization of Lactococcus lactis deficient in lactate dehydrogenase using in vivo13C-NMR. *Eur J Biochem*. 2000;267(12):3859-3868. doi:10.1046/j.1432-1327.2000.01424.x

337. Zomer AL, Buist G, Larsen R, Kok J, Kuipers OP. Time-resolved determination of the CcpA regulon of Lactococcus lactis subsp. cremons MG1363. In: *Journal of Bacteriology*. Vol 189. ; 2007:1366-1381. doi:10.1128/JB.01013-06

338. Barrière C, Veiga-da-Cunha M, Pons N, et al. Fructose utilization in Lactococcus lactis as a model for low-GC gram-positive bacteria: Its regulator, signal, and DNA-binding site. *J Bacteriol*. 2005;187(11):3752-3761. doi:10.1128/JB.187.11.3752-3761.2005

339. Larsen R, Van Hijum SAFT, Martinussen J, Kuipers OP, Kok J. Transcriptome analysis of the Lactococcus lactis ArgR and AhrC regulons. In: *Applied and Environmental Microbiology*. Vol 74. ; 2008:4768-4771. doi:10.1128/AEM.00117-08

340. Breüner A, Frees D, Varmanen P, et al. Ribosomal dimerization factor YfiA is the major protein synthesized after abrupt glucose depletion in Lactococcus lactis. *Microbiol (United Kingdom)*. 2016;162(10):1829-1839. doi:10.1099/mic.0.000362

341. Sepideh Dolatshahi LLF and EOV. New insights into the complex regulation of the glycolytic pathway in Lactococcus lactis. II. Inference of the precisely timed control system regulating glycolysis. *Mol BioSysyems*. 2016;12:37-47. https://pubs.rsc.org/en/content/articlepdf/2016/mb/c5mb00726g. Accessed October 15, 2019.

342. Nelson MR, Roy K. Bone-marrow mimicking biomaterial niches for studying hematopoietic stem and progenitor cells. *J Mater Chem B*. 2016;4(20):3490-3503. doi:10.1039/c5tb02644j

343. Rosalem GS, Torres LAG, de Las Casas EB, Mathias FAS, Ruiz JC, Carvalho MGR. Microfluidics and organ-on-a-chip technologies: A systematic review of the methods used to mimic bone marrow. *PLoS One*. 2020;15(12 December):e0243840. doi:10.1371/journal.pone.0243840

344. Burmølle M, Webb JS, Rao D, Hansen LH, Sørensen SJ, Kjelleberg S. Enhanced biofilm formation and increased resistance to antimicrobial agents and bacterial invasion are caused by synergistic interactions in multispecies biofilms. *Appl Environ Microbiol*. 2006;72(6):3916-3923. doi:10.1128/AEM.03022-05

345. Dominici M, Le Blanc K, Mueller I, et al. Minimal criteria for defining multipotent mesenchymal stromal cells. The International Society for Cellular Therapy position statement. *Cytotherapy*. 2006;8(4):315-317. doi:10.1080/14653240600855905

346. AbuSamra DB, Aleisa FA, Al-Amoodi AS, et al. Not just a marker: CD34 on human hematopoietic stem/progenitor cells dominates vascular selectin binding along with CD44. *Blood Adv*. 2017;1(27):2799-2816. doi:10.1182/bloodadvances.2017004317

347. Schindelin J, Arganda-Carreras I, Frise E, et al. Fiji: An open-source platform for biological-image analysis. *Nat Methods*. 2012;9(7):676-682. doi:10.1038/nmeth.2019

348. Sommer C, Straehle C, Köthe U, Hamprecht FA. ilastik: Interactive Learning and Segmentation Toolkit. 2011. www.ilastik.org. Accessed July 23, 2021.

349. Berg S, Kutra D, Kroeger T, et al. ilastik: interactive machine learning for (bio)image analysis. *Nat Methods*. 2019;16(12):1226-1232. doi:10.1038/s41592-019-0582-9

350. Gest H. The discovery of microorganisms by Robert Hooke and Antoni van Leeuwenhoek, fellows of the Royal Society. *Notes Rec R Soc*. 2004;58(2):187-201. doi:10.1098/rsnr.2004.0055

351. Daniels C, Ramos JL. Microbial Biotechnology from medicine to bacterial population dynamics. *Microb Biotechnol*. 2009;2(3):304-307. doi:10.1111/j.1751-7915.2009.00110.x

352. Cavicchioli R, Ripple WJ, Timmis KN, et al. Scientists' warning to humanity: microorganisms and climate change. *Nat Rev Microbiol*. 2019;17(9):569-586. doi:10.1038/s41579-019-0222-5

353. Videmšek U, Hagn A, Suhadolc M, et al. Abundance and diversity of CO2-fixing bacteria in grassland soils close to natural carbon dioxide springs. *Microb Ecol*. 2009;58(1):1-9. doi:10.1007/s00248-008-

9442-3

354. Ettwig KF, Speth DR, Reimann J, Wu ML, Jetten MSM, Keltjens JT. Bacterial oxygen production in the dark. *Front Microbiol*. 2012;3(AUG). doi:10.3389/fmicb.2012.00273

355. Hwangbo M, Chu KH. Recent advances in production and extraction of bacterial lipids for biofuel production. *Sci Total Environ*. 2020;734. doi:10.1016/j.scitotenv.2020.139420

356. Yurina V. Live Bacterial Vectors—A Promising DNA Vaccine Delivery System. *Med Sci*. 2018;6(2):27. doi:10.3390/medsci6020027

357. Avery OT, Macleod CM, McCarty M. Studies on the chemical nature of the substance inducing transformation of pneumococcal types: Induction of transformation by a desoxyribonucleic acid fraction isolated from pneumococcus type III. *J Exp Med*. 1979;149(2):297-326. doi:10.1084/jem.149.2.297

358. Lederberg J. Cell genetics and hereditary symbiosis. *Physiol Rev*. 1952;32(4):403-430. doi:10.1152/physrev.1952.32.4.403

359. Casjens SR, Hendrix RW. Bacteriophage lambda: Early pioneer and still relevant. *Virology*. 2015;479-480:310-330. doi:10.1016/j.virol.2015.02.010

360. Couturier M, Bex F, Bergquist PL, Maas WK. Identification and classification of bacterial plasmids. *Microbiol Rev*. 1988;52(3):375-395. doi:10.1128/mmbr.52.3.375-395.1988

361. Soler N, Marguet E, Cortez D, et al. Two novel families of plasmids from hyperthermophilic archaea encoding new families of replication proteins. *Nucleic Acids Res*. 2010;38(15):5088-5104. doi:10.1093/nar/gkq236

362. Volkert FC, Wilson DW, Broach JR. Deoxyribonucleic acid plasmids in yeasts. *Microbiol Rev*. 1989;53(3):299-317. doi:10.1128/mmbr.53.3.299-317.1989

363. Lacroix B, Citovsky V. Pathways of DNA Transfer to Plants from Agrobacterium tumefaciens and Related Bacterial Species . *Annu Rev Phytopathol*. 2019;57(1):231-251. doi:10.1146/annurev-phyto-082718-100101

364. del Solar G, Giraldo R, Ruiz-Echevarría MJ, Espinosa M, Díaz-Orejas R. Replication and Control of Circular Bacterial Plasmids. *Microbiol Mol Biol Rev*. 1998;62(2):434-464. doi:10.1128/mmbr.62.2.434-464.1998

365. Zhong C, Peng D, Ye W, et al. Determination of plasmid copy number reveals the total plasmid DNA amount is greater than the chromosomal DNA amount in Bacillus thuringiensis YBT-1520. *PLoS One*. 2011;6(1). doi:10.1371/journal.pone.0016025

366. Tarazanova M, Huppertz T, Kok J, Bachmann H. Altering textural properties of fermented milk by using surface-engineered Lactococcus lactis. *Microb Biotechnol*. 2018;11(4):770-780. doi:10.1111/1751-7915.13278

367. Mazhar SF, Afzal M, Almatroudi A, et al. The Prospects for the Therapeutic Implications of Genetically Engineered Probiotics. *J Food Qual*. July 2020:1-11. https://web.b.ebscohost.com/abstract?direct=true&profile=ehost&scope=site&authtype=crawler&jrnl=01469428&AN=142612877&h=w%2B5jppaEuDI6FzU8WUQwMv79JUQQFFlFJu5zKJ4nvXAI5NKOIZetMqfypFbvowgY43bCuJOUsJ1aIQtMmZhxMw%3D%3D&crl=c&resultNs=AdminWebAuth&resultLocal=ErrCrlNotAuth&crlhashurl=login.aspx%3Fdirect%3Dtrue%26profile%3Dehost%26scope%3Dsite%26authtype%3Dcrawler%26jrnl%3D01469428%26AN%3D142612877. Accessed July 14, 2020.

368. Sun N, Zhang R, Duan G, et al. An engineered food-grade Lactococcus lactis strain for production and delivery of heat-labile enterotoxin B subunit to mucosal sites. *BMC Biotechnol*. 2017;17(1):25. doi:10.1186/s12896-017-0345-6

369. Guimarâes VD, Innocentin S, Lefèvre F, et al. Use of native lactococci as vehicles for delivery of DNA into mammalian epithelial cells. *Appl Environ Microbiol*. 2006;72(11):7091-7097. doi:10.1128/AEM.01325-06

370. Ribeiro LA, Azevedo V, Le Loir Y, et al. Production and targeting of the Brucella abortus antigen L7/L12

in Lactococcus lactis: A first step towards food-grade live vaccines against brucellosis. *Appl Environ Microbiol*. 2002;68(2):910-916. doi:10.1128/AEM.68.2.910-916.2002

371. Mancha-Agresti P, de Castro CP, dos Santos JSC, et al. Recombinant Invasive Lactococcus lactis Carrying a DNA Vaccine Coding the Ag85A Antigen Increases INF-γ, IL-6, and TNF-α Cytokines after Intranasal Immunization. *Front Microbiol*. 2017;8(JUL):1263. doi:10.3389/fmicb.2017.01263

372. Mannam P, Jones KF, Geller BL. Mucosal vaccine made from live, recombinant Lactococcus lactis protects mice against pharyngeal infection with Streptococcus pyogenes. *Infect Immun*. 2004;72(6):3444-3450. doi:10.1128/IAI.72.6.3444-3450.2004

373. Braat H, Rottiers P, Hommes DW, et al. A Phase I Trial With Transgenic Bacteria Expressing Interleukin-10 in Crohn's Disease. *Clin Gastroenterol Hepatol*. 2006;4(6):754-759. doi:10.1016/j.cgh.2006.03.028

374. Zurita-Turk M, del Carmen S, Santos ACG, et al. Lactococcus lactis carrying the pValac DNA expression vector coding for IL-10 reduces inflammation in a murine model of experimental colitis. *BMC Biotechnol*. 2014;14(1):73. doi:10.1186/1472-6750-14-73

375. Steidler L, Hans W, Schotte L, et al. Treatment of murine colitis by Lactococcus lactis secreting interleukin-10. *Science (80-)*. 2000;289(5483):1352-1355. doi:10.1126/science.289.5483.1352

376. Borrero J, Jiménez JJ, Gútiez L, Herranz C, Cintas LM, Hernández PE. Use of the usp45 lactococcal secretion signal sequence to drive the secretion and functional expression of enterococcal bacteriocins in Lactococcus lactis. *Appl Microbiol Biotechnol*. 2011;89(1):131-143. doi:10.1007/s00253-010-2849-z

377. Integrated DNA Technologies. https://www.idtdna.com/500.aspx?aspxerrorpath=/CodonOpt. Accessed January 30, 2020.

378. Cloud-Based Informatics Platform for Life Sciences R&D | Benchling. https://www.benchling.com/. Accessed July 16, 2020.

379. Louis S. Gold Biotechnology Protocol Lactococcus lactis IL1403 Electrocompetent Cells Transformation Protocol.

380. Gibson DG, Young L, Chuang RY, Venter JC, Hutchison CA, Smith HO. Enzymatic assembly of DNA molecules up to several hundred kilobases. *Nat Methods*. 2009;6(5):343-345. doi:10.1038/nmeth.1318

381. Cole JN, Djordjevic SP, Walker MJ. Isolation and Solubilization of Gram-Positive Bacterial Cell Wall-Associated Proteins. In: *Methods in Molecular Biology (Clifton, N.J.)*. Vol 425. ; 2008:295-311. doi:10.1007/978-1-60327-210-0_24

382. Bongers RS, Hoefnagel MHN, Starrenburg MJC, et al. IS981-mediated adaptive evolution recovers lactate production by ldhB transcription activation in a lactate dehydrogenase-deficient strain of Lactococcus lactis. *J Bacteriol*. 2003;185(15):4499-4507. doi:10.1128/JB.185.15.4499-4507.2003

383. Ng DTW, Sarkar CA. Engineering signal peptides for enhanced protein secretion from Lactococcus lactis. *Appl Environ Microbiol*. 2013;79(1):347-356. doi:10.1128/AEM.02667-12

384. Gibson DG, Young L, Chuang RY, Venter JC, Hutchison CA, Smith HO. Enzymatic assembly of DNA molecules up to several hundred kilobases. *Nat Methods*. 2009;6(5):343-345. doi:10.1038/nmeth.1318

385. Khurana S, Melacarne A, Yadak R, et al. SMAD signaling regulates CXCL12 expression in the bone marrow niche, affecting homing and mobilization of hematopoietic progenitors. *Stem Cells*. 2014;32(11):3012-3022. doi:10.1002/stem.1794

386. Khurana S, Melacarne A, Yadak R, et al. SMAD signaling regulates CXCL12 expression in the bone marrow niche, affecting homing and mobilization of hematopoietic progenitors. *Stem Cells*. 2014;32(11):3012-3022. doi:10.1002/STEM.1794

387. Rodrigo-Navarro A, Rico P, Saadeddin A, Garcia AJ, Salmeron-Sanchez M. Living biointerfaces based on non-pathogenic bacteria to direct cell differentiation. *Sci Rep*. 2014;4(February):5849. doi:10.1038/srep05849

388. Marshall KC, Cruickshank RH. Cell surface hydrophobicity and the orientation of certain bacteria at interfaces. *Arch Mikrobiol*. 1973;91(1):29-40. doi:10.1007/BF00409536

389. Giaouris E, Chapot-Chartier MP, Briandet R. Surface physicochemical analysis of natural Lactococcus lactis strains reveals the existence of hydrophobic and low charged strains with altered adhesive properties. *Int J Food Microbiol*. 2009;131(1):2-9. doi:10.1016/j.ijfoodmicro.2008.09.006

390. van Oss CJ. Hydrophobicity of biosurfaces - Origin, quantitative determination and interaction energies. *Colloids Surfaces B Biointerfaces*. 1995;5(3-4):91-110. doi:10.1016/0927-7765(95)01217-7

391. Bayoudh S, Othmane A, Mora L, Ben Ouada H. Assessing bacterial adhesion using DLVO and XDLVO theories and the jet impingement technique. *Colloids Surfaces B Biointerfaces*. 2009;73(1):1-9. doi:10.1016/j.colsurfb.2009.04.030

392. Flemming HC, Wingender J. The biofilm matrix. *Nat Rev Microbiol*. 2010;8(9):623-633. doi:10.1038/nrmicro2415

393. Oxaran V, Ledue-Clier F, Dieye Y, et al. Pilus Biogenesis in Lactococcus lactis: Molecular Characterization and Role in Aggregation and Biofilm Formation. Biswas I, ed. *PLoS One*. 2012;7(12):e50989. doi:10.1371/journal.pone.0050989

394. Donlan RM. Biofilm Formation: A Clinically Relevant Microbiological Process. *Clin Infect Dis*. 2001;33(8):1387-1392. doi:10.1086/322972

395. Regina VR, Lokanathan AR, Modrzyński JJ, Sutherland DS, Meyer RL. Surface Physicochemistry and Ionic Strength Affects eDNA's Role in Bacterial Adhesion to Abiotic Surfaces. Desvaux M, ed. *PLoS One*. 2014;9(8):e105033. doi:10.1371/journal.pone.0105033

396. Chopra I, Roberts M. Tetracycline Antibiotics: Mode of Action, Applications, Molecular Biology, and Epidemiology of Bacterial Resistance. *Microbiol Mol Biol Rev*. 2001;65(2):232-260. doi:10.1128/mmbr.65.2.232-260.2001

397. Hitchings GH. Mechanism of action of trimethoprim-sulfamethoxazole. *J Infect Dis*. 1973;128(Supplement_3):S433-S436. doi:10.1093/infdis/128.Supplement_3.S433

398. Kanoh S, Rubin BK. Mechanisms of action and clinical application of macrolides as immunomodulatory medications. *Clin Microbiol Rev*. 2010;23(3):590-615. doi:10.1128/CMR.00078-09

399. Nagayasu M, Wardani AK, Nagahisa K, Shimizu H, Shioya S. Analysis of hemin effect on lactate reduction in Lactococcus lactis. *J Biosci Bioeng*. 2007;103(6):529-534. doi:10.1263/jbb.103.529

400. Wang T, Guo Z, Shen Y, Cui Z, Goodwin A. Accumulation mechanism of biofilm under different water shear forces along the networked pipelines in a drip irrigation system. *Sci Rep*. 2020;10(1):1-13. doi:10.1038/s41598-020-63898-5

401. Webb K, Hlady V, Tresco PA. Relationships among cell attachment, spreading, cytoskeletal organization, and migration rate for anchorage-dependent cells on model surfaces. *J Biomed Mater Res*. 2000;49(3):362-368. doi:10.1002/(SICI)1097-4636(20000305)49:3<362::AID-JBM9>3.0.CO;2-S

402. Seo JH, Chen LJ, Verkhoturov S V., Schweikert EA, Revzin A. The use of glass substrates with bi-functional silanes for designing micropatterned cell-secreted cytokine immunoassays. *Biomaterials*. 2011;32(23):5478-5488. doi:10.1016/j.biomaterials.2011.04.026

403. Hu B, Zhu Q, Xu Z, Wu X. *High Binding Yields of Viable Cancer Cells on Amino Silane Functionalized Surfaces*. Vol 26. Allied Academies; 2015. www.biomedres.info. Accessed July 18, 2020.

404. Syga Ł, Spakman D, Punter CM, Poolman B. Method for immobilization of living and synthetic cells for high-resolution imaging and single-particle tracking. *Sci Rep*. 2018;8(1):13789. doi:10.1038/s41598-018-32166-y

405. Lam ATL, Li J, Chen AKL, Birch WR, Reuveny S, Oh SKW. Improved human pluripotent stem cell attachment and spreading on xeno-free laminin-521-coated microcarriers results in efficient growth in agitated cultures. *Biores Open Access*. 2015;4(1):242-257. doi:10.1089/biores.2015.0010

406. Witte K, Rodrigo-Navarro A, Salmeron-Sanchez M. Bacteria-laden microgels as autonomous three-dimensional environments for stem cell engineering. *Mater Today Bio*. 2019;2:100011. doi:10.1016/j.mtbio.2019.100011

407. Susarrey-Arce A, Sorzabal-Bellido I, Oknianska A, et al. Bacterial viability on chemically modified silicon

nanowire arrays. *J Mater Chem B*. 2016;4(18):3104-3112. doi:10.1039/c6tb00460a

408. Ray B, Chopra N, Long JM, Lahiri DK. Human primary mixed brain cultures: Preparation, differentiation, characterization and application to neuroscience research. *Mol Brain*. 2014;7(1):1-15. doi:10.1186/s13041-014-0063-0

409. Garrett TR, Bhakoo M, Zhang Z. Bacterial adhesion and biofilms on surfaces. *Prog Nat Sci*. 2008;18(9):1049-1056. doi:10.1016/j.pnsc.2008.04.001

410. Fleming D, Rumbaugh K. Approaches to Dispersing Medical Biofilms. *Microorganisms*. 2017;5(2):15. doi:10.3390/microorganisms5020015

411. Jacouton E, Maravilla ET, Boucard AS, et al. Anti-tumoral effects of recombinant lactococcus lactisstrain secreting IL-17A cytokine. *Front Microbiol*. 2019;10(JAN). doi:10.3389/fmicb.2018.03355

412. Namai F, Murakami A, Ueda A, et al. Construction of Genetically Modified Lactococcus lactis Producing Anti-human-CTLA-4 Single-Chain Fragment Variable. *Mol Biotechnol*. September 2020:1-8. doi:10.1007/s12033-020-00274-8

413. Zhang B, Li A, Zuo F, et al. Recombinant Lactococcus lactis NZ9000 secretes a bioactive kisspeptin that inhibits proliferation and migration of human colon carcinoma HT-29 cells. *Microb Cell Fact*. 2016;15(1):102. doi:10.1186/s12934-016-0506-7

414. Mohseni AH, Sedigheh Taghinezhad S, Keyvani H. The First Clinical Use of a Recombinant Lactococcus lactis Expressing Human Papillomavirus Type 16 E7 Oncogene Oral Vaccine: A phase I safety and immunogenicity trial in healthy women volunteers. *Mol Cancer Ther*. 2020;19(2):717-727. doi:10.1158/1535-7163.MCT-19-0375

415. Rosano GL, Ceccarelli EA. Recombinant protein expression in Escherichia coli: Advances and challenges. *Front Microbiol*. 2014;5(APR). doi:10.3389/fmicb.2014.00172

416. Slouka C, Kopp J, Spadiut O, Herwig C. Perspectives of inclusion bodies for bio-based products: curse or blessing? *Appl Microbiol Biotechnol*. 2019;103(3):1143-1153. doi:10.1007/s00253-018-9569-1

417. Epstein J, Kelly CE, Lee MM, Donahoe PK. Effect of E. Coli endotoxin on mammalian cell growth and recombinant protein production. *Vitr Cell Dev Biol*. 1990;26(12):1121-1122. doi:10.1007/BF02623686

418. Hufnagel DA, Depas WH, Chapman MR. The Biology of the Escherichia coli Extracellular Matrix. *Microbiol Spectr*. 2015;3(3). doi:10.1128/microbiolspec.mb-0014-2014

419. Hochuli E, Bannwarth W, Dobeli H, Gentzi R, Stuber D. Genetic approach to facilitate purification of recombinant proteins with a novel metal chelate adsorbent. *Bio/Technology*. 1988;6(11):1321-1325. doi:10.1038/nbt1188-1321

420. Van Leewenhoeck A. Observations, Communicated to the Publisher by Mr. Antony van Leewenhoeck, in a Dutch Letter of the 9th of Octob. 1676. Here English'd: concerning Little Animals by Him Observed in Rain-Well-Sea. and Snow Water; as Also in Water Wherein Pepper Had Lain Infused on JSTOR. *Philos Trans Biol Sci*. 1677;12:821-831. https://www.jstor.org/stable/101758?seq=1#metadata_info_tab_contents. Accessed June 30, 2021.

421. Anbu P, Gopinath SCB, Chaulagain BP, Lakshmipriya T. Microbial Enzymes and Their Applications in Industries and Medicine 2016. *Biomed Res Int*. 2017;2017. doi:10.1155/2017/2195808

422. Frith JE, Mills RJ, Cooper-White JJ. Lateral spacing of adhesion peptides influences human mesenchymal stem cell behaviour. *J Cell Sci*. 2012;125(2):317-327. doi:10.1242/jcs.087916

423. Gilmore AP, Burridge K. Molecular mechanisms for focal adhesion assembly through regulation of protein-protein interactions. *Structure*. 1996;4(6):647-651. doi:10.1016/S0969-2126(96)00069-X

424. Allen, W, Jones G, Pollard J, Ridley A. Rho, Rac and Cdc42 regulate actin organization and cell adhesion in macrophages - PubMed. *J Cell Sci*. March 1997:707-720. https://pubmed.ncbi.nlm.nih.gov/9099945/. Accessed October 5, 2020.

425. Lawson CD, Burridge K. The on-off relationship of Rho and Rac during integrin-mediated adhesion and cell migration. *Small GTPases*. 2014;5(MAR). doi:10.4161/sgtp.27958

426. Matthews BD, Overby DR, Mannix R, Ingber DE. Cellular adaptation to mechanical stress: Role of integrins, Rho, cytoskeletal tension and mechanosensitive ion channels. *J Cell Sci*. 2006;119(3):508-518. doi:10.1242/jcs.02760

427. Amano M, Nakayama M, Kaibuchi K. Rho-kinase/ROCK: A key regulator of the cytoskeleton and cell polarity. *Cytoskeleton*. 2010;67(9):545-554. doi:10.1002/cm.20472

428. Nalbant P, Chang YC, Birkenfeld J, Chang ZF, Bokoch GM. Guanine nucleotide exchange factor-H1 regulates cell migration via localized activation of RhoA at the leading edge. *Mol Biol Cell*. 2009;20(18):4070-4082. doi:10.1091/mbc.E09-01-0041

429. Itakura A, Aslan JE, Kusanto BT, et al. p21-Activated Kinase (PAK) Regulates Cytoskeletal Reorganization and Directional Migration in Human Neutrophils. Hotchin NA, ed. *PLoS One*. 2013;8(9):e73063. doi:10.1371/journal.pone.0073063

430. Wu C, Asokan SB, Berginski ME, et al. Arp2/3 is critical for lamellipodia and response to extracellular matrix cues but is dispensable for chemotaxis. *Cell*. 2012;148(5):973-987. doi:10.1016/j.cell.2011.12.034

431. Chorev DS, Moscovitz O, Geiger B, Sharon M. Regulation of focal adhesion formation by a vinculin-Arp2/3 hybrid complex. *Nat Commun*. 2014;5(1):1-11. doi:10.1038/ncomms4758

432. Cho M, Titushkin I, Sun S, Shin J. Physicochemical control of adult stem cell differentiation: Shedding light on potential molecular mechanisms. *J Biomed Biotechnol*. 2010;2010. doi:10.1155/2010/743476

433. Chacón-Martínez CA, Koester J, Wickström SA. Signaling in the stem cell niche: regulating cell fate, function and plasticity. *Development*. 2018;145(15):dev165399. doi:10.1242/dev.165399

434. Ritsma L, Ellenbroek SIJ, Zomer A, et al. Intestinal crypt homeostasis revealed at single-stem-cell level by in vivo live imaging. *Nature*. 2014;507(7492):362-365. doi:10.1038/nature12972

435. Donnelly H, Salmeron-Sanchez M, Dalby MJ. Designing stem cell niches for differentiation and self-renewal. *J R Soc Interface*. 2018;15(145). doi:10.1098/rsif.2018.0388

436. Frenette PS, Pinho S, Lucas D, Scheiermann C. Mesenchymal Stem Cell: Keystone of the Hematopoietic Stem Cell Niche and a Stepping-Stone for Regenerative Medicine. *Annu Rev Immunol*. 2013;31(1):285-316. doi:10.1146/annurev-immunol-032712-095919

437. Azadniv M, Myers JR, McMurray HR, et al. Bone marrow mesenchymal stromal cells from acute myelogenous leukemia patients demonstrate adipogenic differentiation propensity with implications for leukemia cell support. *Leukemia*. 2020;34(2):391-403. doi:10.1038/s41375-019-0568-8

438. Pittenger MF, Discher DE, Péault BM, Phinney DG, Hare JM, Caplan AI. Mesenchymal stem cell perspective: cell biology to clinical progress. *npj Regen Med*. 2019;4(1):1-15. doi:10.1038/s41536-019-0083-6

439. Guo Y, Yu Y, Hu S, Chen Y, Shen Z. The therapeutic potential of mesenchymal stem cells for cardiovascular diseases. *Cell Death Dis*. 2020;11(5):1-10. doi:10.1038/s41419-020-2542-9

440. Crippa S, Bernardo ME. Mesenchymal Stromal Cells: Role in the BM Niche and in the Support of Hematopoietic Stem Cell Transplantation. *HemaSphere*. 2018;2(6). doi:10.1097/HS9.0000000000000151

441. Wei Q, Frenette PS. Niches for Hematopoietic Stem Cells and Their Progeny. *Immunity*. 2018;48(4):632-648. doi:10.1016/j.immuni.2018.03.024

442. Lee DE, Ayoub N, Agrawal DK. Mesenchymal stem cells and cutaneous wound healing: Novel methods to increase cell delivery and therapeutic efficacy. *Stem Cell Res Ther*. 2016;7(1):37. doi:10.1186/s13287-016-0303-6

443. Whelan DS, Caplice NM, Clover AJP. Mesenchymal stromal cell derived CCL2 is required for accelerated wound healing. *Sci Rep*. 2020;10(1):1-12. doi:10.1038/s41598-020-59174-1

444. Bielby R, Jones E, McGonagle D. The role of mesenchymal stem cells in maintenance and repair of bone. *Injury*. 2007;38(SUPPL. 1). doi:10.1016/j.injury.2007.02.007

445. Tsimbouri P, Gadegaard N, Burgess K, et al. Nanotopographical Effects on Mesenchymal Stem Cell Morphology and Phenotype. *J Cell Biochem*. 2014;115(2):380-390. doi:10.1002/jcb.24673

446. Lee LCY, Gadegaard N, de Andrés MC, et al. Nanotopography controls cell cycle changes involved with skeletal stem cell self-renewal and multipotency. *Biomaterials*. 2017;116:10-20. doi:10.1016/j.biomaterials.2016.11.032

447. Olivares-Navarrete R, Lee EM, Smith K, et al. Substrate Stiffness Controls Osteoblastic and Chondrocytic Differentiation of Mesenchymal Stem Cells without Exogenous Stimuli. van Wijnen A, ed. *PLoS One*. 2017;12(1):e0170312. doi:10.1371/journal.pone.0170312

448. Sun M, Chi G, Li P, et al. Effects of matrix stiffness on the morphology, adhesion, proliferation and osteogenic differentiation of mesenchymal stem cells. *Int J Med Sci*. 2018;15(3):257-268. doi:10.7150/ijms.21620

449. Robertson SN, Campsie P, Childs PG, et al. Control of cell behaviour through nanovibrational stimulation: Nanokicking. *Philos Trans R Soc A Math Phys Eng Sci*. 2018;376(2120). doi:10.1098/rsta.2017.0290

450. Mushtaq M, Kovalevska L, Darekar S, et al. Cell stemness is maintained upon concurrent expression of rb and the mitochondrial ribosomal protein s18-2. *Proc Natl Acad Sci U S A*. 2020;117(27):15673-15683. doi:10.1073/pnas.1922535117

451. Jeong SY, Lyu J, Kim JA, Oh IH. Ryk modulates the niche activity of mesenchymal stromal cells by fine-tuning canonical Wnt signaling. *Exp Mol Med*. 2020;52(7):1140-1151. doi:10.1038/s12276-020-0477-y

452. Bentivegna A, Roversi G, Riva G, et al. The effect of culture on human bone marrow mesenchymal stem cells: Focus on DNA methylation profiles. *Stem Cells Int*. 2016;2016. doi:10.1155/2016/5656701

453. Chosa N, Ishisaki A. Two novel mechanisms for maintenance of stemness in mesenchymal stem cells: SCRG1/BST1 axis and cell–cell adhesion through N-cadherin. *Jpn Dent Sci Rev*. 2018;54(1):37-44. doi:10.1016/j.jdsr.2017.10.001

454. Peng KY, Liu YH, Li YW, Yen BL, Yen ML. Extracellular matrix protein laminin enhances mesenchymal stem cell (MSC) paracrine function through αvβ3/CD61 integrin to reduce cardiomyocyte apoptosis. *J Cell Mol Med*. 2017;21(8):1572-1583. doi:10.1111/jcmm.13087

455. Saleh NT, Sohi AN, Esmaeili E, Karami S, Soleimanifar F, Nasoohi N. Immobilized Laminin-derived Peptide Can Enhance Expression of Stemness Markers in Mesenchymal Stem Cells. *Biotechnol Bioprocess Eng*. 2019;24(6):876-884. doi:10.1007/s12257-019-0118-2

456. Kasten A, Naser T, Brüllhoff K, et al. Guidance of Mesenchymal Stem Cells on Fibronectin Structured Hydrogel Films. Engler AJ, ed. *PLoS One*. 2014;9(10):e109411. doi:10.1371/journal.pone.0109411

457. Yeo GC, Weiss AS. Soluble matrix protein is a potent modulator of mesenchymal stem cell performance. *Proc Natl Acad Sci U S A*. 2019;116(6):2042-2051. doi:10.1073/pnas.1812951116

458. Friedl P, Gilmour D. Collective cell migration in morphogenesis, regeneration and cancer. *Nat Rev Mol Cell Biol*. 2009;10(7):445-457. doi:10.1038/nrm2720

459. Qu F, Guilak F, Mauck RL. Cell migration: implications for repair and regeneration in joint disease. *Nat Rev Rheumatol*. 2019;15(3):167-179. doi:10.1038/s41584-018-0151-0

460. Xiao Y, Riahi R, Torab P, Zhang DD, Wong PK. Collective Cell Migration in 3D Epithelial Wound Healing. *ACS Nano*. 2019;13(2). doi:10.1021/acsnano.8b06305

461. Kinashi T, Katagiri K. Regulation of immune cell adhesion and migration by regulator of adhesion and cell polarization enriched in lymphoid tissues. *Immunology*. 2005;116(2):164-171. doi:10.1111/j.1365-2567.2005.02214.x

462. Hampton HR, Chtanova T. Lymphatic migration of immune cells. *Front Immunol*. 2019;10(MAY):1168. doi:10.3389/fimmu.2019.01168

463. Novikov NM, Zolotaryova SY, Gautreau AM, Denisov E V. Mutational drivers of cancer cell migration and invasion. *Br J Cancer*. 2021;124(1):102-114. doi:10.1038/s41416-020-01149-0

464. Yang D, Zhao Z, Bai F, Wang S, Tomsia AP, Bai H. Promoting Cell Migration in Tissue Engineering Scaffolds with Graded Channels. *Adv Healthc Mater*. 2017;6(18). doi:10.1002/adhm.201700472

465. Wismayer K, Mehrban N, Bowen J, Birchall M. Improving cellular migration in tissue-engineered laryngeal scaffolds. *J Laryngol Otol*. 2019;133(2):135-148. doi:10.1017/S0022215119000082

466. Petrie RJ, Doyle AD, Yamada KM. Random versus directionally persistent cell migration. *Nat Rev Mol Cell Biol*. 2009;10(8):538-549. doi:10.1038/nrm2729

467. Dunn GA. Characterising a kinesis response: time averaged measures of cell speed and directional persistence. *Agents Actions Suppl*. 1983;12:14-33. doi:10.1007/978-3-0348-9352-7_1

468. Dickinson RB, Tranquillo RT. Optimal estimation of cell movement indices from the statistical analysis of cell tracking data. *AIChE J*. 1993;39(12):1995-2010. doi:10.1002/aic.690391210

469. Li L, Nørrelykke SF, Cox EC. Persistent Cell Motion in the Absence of External Signals: A Search Strategy for Eukaryotic Cells. Hatakeyama M, ed. *PLoS One*. 2008;3(5):e2093. doi:10.1371/journal.pone.0002093

470. Bosgraaf L, Van Haastert PJM. The Ordered Extension of Pseudopodia by Amoeboid Cells in the Absence of External Cues. Hotchin N, ed. *PLoS One*. 2009;4(4):e5253. doi:10.1371/journal.pone.0005253

471. Van Haastert PJM, Bosgraaf L. Food Searching Strategy of Amoeboid Cells by Starvation Induced Run Length Extension. Dornhaus A, ed. *PLoS One*. 2009;4(8):e6814. doi:10.1371/journal.pone.0006814

472. Choi JS, Harley BAC. Marrow-inspired matrix cues rapidly affect early fate decisions of hematopoietic stem and progenitor cells. *Sci Adv*. 2017;3(1):1600455. doi:10.1126/sciadv.1600455

473. Edwards JR, Diamantakos EA, Peuler JD, Lamar PC, Prozialeck WC. A novel method for the evaluation of proximal tubule epithelial cellular necrosis in the intact rat kidney using ethidium homodimer. *BMC Physiol*. 2007;7(1):1. doi:10.1186/1472-6793-7-1

474. Holló Z, Homolya L, Davis CW, Sarkadi B. Calcein accumulation as a fluorometric functional assay of the multidrug transporter. *BBA - Biomembr*. 1994;1191(2):384-388. doi:10.1016/0005-2736(94)90190-2

475. Gorelik R, Gautreau A. Quantitative and unbiased analysis of directional persistence in cell migration. *Nat Protoc*. 2014;9(8):1931-1943. doi:10.1038/nprot.2014.131

476. Kaur M, Jayaraman G. Hyaluronan production and molecular weight is enhanced in pathway-engineered strains of lactate dehydrogenase-deficient Lactococcus lactis. *Metab Eng Commun*. 2016;3:15-23. doi:10.1016/j.meteno.2016.01.003

477. Bongers RS, Hoefnagel MHN, Starrenburg MJC, et al. IS981-mediated adaptive evolution recovers lactate production by ldhB transcription activation in a lactate dehydrogenase-deficient strain of Lactococcus lactis. *J Bacteriol*. 2003;185(15):4499-4507. doi:10.1128/JB.185.15.4499-4507.2003

478. Hoefnagel MHN, Starrenburg MJC, Martens DE, et al. Metabolic engineering of lactic acid bacteria, the combined approach: Kinetic modelling, metabolic control and experimental analysis. *Microbiology*. 2002;148(4):1003-1013. doi:10.1099/00221287-148-4-1003

479. Hatti-Kaul R, Chen L, Dishisha T, Enshasy H El. Lactic acid bacteria: From starter cultures to producers of chemicals. *FEMS Microbiol Lett*. 2018;365(20):213. doi:10.1093/femsle/fny213

480. Duwat P, Sourice S, Cesselin B, et al. Respiration capacity of the fermenting bacterium Lactococcus lactis and its positive effects on growth and survival. *J Bacteriol*. 2001;183(15):4509-4516. doi:10.1128/JB.183.15.4509-4516.2001

481. Lechardeur D, Cesselin B, Fernandez A, et al. Using heme as an energy boost for lactic acid bacteria. *Curr Opin Biotechnol*. 2011;22(2):143-149. doi:10.1016/j.copbio.2010.12.001

482. Hynes RO. The extracellular matrix: Not just pretty fibrils. *Science (80-)*. 2009;326(5957):1216-1219. doi:10.1126/science.1176009

483. Salzig D, Leber J, Merkewitz K, Lange MC, Köster N, Czermak P. Attachment, Growth, and Detachment of Human Mesenchymal Stem Cells in a Chemically Defined Medium. *Stem Cells Int*. 2016;2016.

doi:10.1155/2016/5246584

484. Elosegui-Artola A, Jorge-Peñas A, Moreno-Arotzena O, et al. Image Analysis for the Quantitative Comparison of Stress Fibers and Focal Adhesions. Janody F, ed. *PLoS One*. 2014;9(9):e107393. doi:10.1371/journal.pone.0107393

485. Stricker J, Beckham Y, Davidson MW, Gardel ML. Myosin II-Mediated Focal Adhesion Maturation Is Tension Insensitive. Kumar S, ed. *PLoS One*. 2013;8(7):e70652. doi:10.1371/journal.pone.0070652

486. Van Zoelen EJ, Duarte I, Hendriks JM, Van Der Woning SP. TGFβ-induced switch from adipogenic to osteogenic differentiation of human mesenchymal stem cells: Identification of drug targets for prevention of fat cell differentiation. *Stem Cell Res Ther*. 2016;7(1). doi:10.1186/s13287-016-0375-3

487. Zayed MN, Schumacher J, Misk N, Dhar MS. Effects of pro-inflammatory cytokines on chondrogenesis of equine mesenchymal stromal cells derived from bone marrow or synovial fluid. *Vet J*. 2016;217:26-32. doi:10.1016/j.tvjl.2016.05.014

488. Indrawattana N, Chen G, Tadokoro M, et al. Growth factor combination for chondrogenic induction from human mesenchymal stem cell. *Biochem Biophys Res Commun*. 2004;320(3):914-919. doi:10.1016/j.bbrc.2004.06.029

489. Bastidas-Coral AP, Bakker AD, Zandieh-Doulabi B, et al. Cytokines TNF-α, IL-6, IL-17F, and IL-4 Differentially Affect Osteogenic Differentiation of Human Adipose Stem Cells. *Stem Cells Int*. 2016;2016. doi:10.1155/2016/1318256

490. Crane JL, Cao X. Function of matrix IGF-1 in coupling bone resorption and formation. *J Mol Med*. 2014;92(2):107-115. doi:10.1007/s00109-013-1084-3

491. Liu Y, Berendsen AD, Jia S, et al. Intracellular VEGF regulates the balance between osteoblast and adipocyte differentiation. *J Clin Invest*. 2012;122(9):3101-3113. doi:10.1172/JCI61209

492. Le Blanc S, Simann M, Jakob F, Schütze N, Schilling T. Fibroblast growth factors 1 and 2 inhibit adipogenesis of human bone marrow stromal cells in 3D collagen gels. *Exp Cell Res*. 2015;338(2):136-148. doi:10.1016/j.yexcr.2015.09.009

493. Simann M, Le Blanc S, Schneider V, et al. Canonical FGFs Prevent Osteogenic Lineage Commitment and Differentiation of Human Bone Marrow Stromal Cells Via ERK1/2 Signaling. *J Cell Biochem*. 2017;118(2):263-275. doi:10.1002/jcb.25631

494. Gopalakrishnan V, Vignesh RC, Arunakaran J, Aruldhas MM, Srinivasan N. Effects of glucose and its modulation by insulin and estradiol on BMSC differentiation into osteoblastic lineages. *Biochem Cell Biol*. 2006;84(1):93-101. doi:10.1139/o05-163

495. Okazaki RYO, Inoue D, Shibata M, et al. Estrogen promotes early osteoblast differentiation and inhibits adipocyte differentiation in mouse bone marrow stromal cell lines that express estrogen receptor (ER) α or β. *Endocrinology*. 2002;143(6):2349-2356. doi:10.1210/endo.143.6.8854

496. Li L, Yao XL, He XL, et al. Role of mechanical strain and estrogen in modulating osteogenic differentiation of mesenchymal stem cells (MSCs) from normal and ovariectomized rats. *Cell Mol Biol*. 2013;59(2):1889-1893. https://www.cellmolbiol.org/index.php/CMB/article/view/473. Accessed December 30, 2020.

497. Ma Q, Xia X, Tao Q, et al. Profound Actions of an Agonist of Growth Hormone-Releasing Hormone on Angiogenic Therapy by Mesenchymal Stem Cells. *Arterioscler Thromb Vasc Biol*. 2016;36(4):663-672. doi:10.1161/ATVBAHA.116.307126

498. Schmitt B, Ringe J, Häupl T, et al. BMP2 initiates chondrogenic lineage development of adult human mesenchymal stem cells in high-density culture. *Differentiation*. 2003;71(9-10):567-577. doi:10.1111/j.1432-0436.2003.07109003.x

499. Sekiya I, Larson BL, Vuoristo JT, Reger RL, Prockop DJ. Comparison of effect of BMP-2, -4, and -6 on in vitro cartilage formation of human adult stem cells from bone marrow stroma. *Cell Tissue Res*. 2005;320(2):269-276. doi:10.1007/s00441-004-1075-3

500. Estes BT, Wu AW, Guilak F. Potent induction of chondrocytic differentiation of human adipose-derived

adult stem cells by bone morphogenetic protein 6. *Arthritis Rheum*. 2006;54(4):1222-1232. doi:10.1002/art.21779

501. Pourgholaminejad A, Aghdami N, Baharvand H, Moazzeni SM. The effect of pro-inflammatory cytokines on immunophenotype, differentiation capacity and immunomodulatory functions of human mesenchymal stem cells. *Cytokine*. 2016;85:51-60. doi:10.1016/j.cyto.2016.06.003

502. Wang Y, Liu Y, Fan Z, Liu D, Wang F, Zhou Y. IGFBP2 enhances adipogenic differentiation potentials of mesenchymal stem cells from Wharton's jelly of the umbilical cord via JNK and Akt signaling pathways. Hare JM, ed. *PLoS One*. 2017;12(8):e0184182. doi:10.1371/journal.pone.0184182

503. Zohar R, Cheifetz S, McCulloch CAG, Sodek J. Analysis of intracellular osteopontin as a marker of osteoblastic cell differentiation and mesenchymal cell migration. *Eur J Oral Sci*. 1998;106(1 SUPPL.):401-407. doi:10.1111/j.1600-0722.1998.tb02206.x

504. Choi J-W, Shin S, Lee CY, et al. Rapid Induction of Osteogenic Markers in Mesenchymal Stem Cells by Adipose-Derived Stromal Vascular Fraction Cells. *Cell Physiol Biochem*. 2017;44(1):53-65. doi:10.1159/000484582

505. Xie L, Zeng X, Hu J, Chen Q. Characterization of Nestin, a Selective Marker for Bone Marrow Derived Mesenchymal Stem Cells. *Stem Cells Int*. 2015;2015. doi:10.1155/2015/762098

506. Gronthos S, Zannettino ACW, Hay SJ, et al. Molecular and cellular characterisation of highly purified stromal stem cells derived from human bone marrow. *J Cell Sci*. 2003;116(9):1827-1835. doi:10.1242/JCS.00369

507. Simmons P, Torok-Storb B. Identification of stromal cell precursors in human bone marrow by a novel monoclonal antibody, STRO-1. *Blood*. 1991;78(1). http://www.bloodjournal.org/content/78/1/55.long?sso-checked=true. Accessed March 26, 2019.

508. Arai F, Ohneda O, Miyamoto T, Zhang XQ, Suda T. Mesenchymal stem cells in perichondrium express activated leukocyte cell adhesion molecule and participate in bone marrow formation. *J Exp Med*. 2002;195(12):1549-1563. doi:10.1084/jem.20011700

509. Lin J, Redies C. Histological evidence: Housekeeping genes beta-actin and GAPDH are of limited value for normalization of gene expression. *Dev Genes Evol*. 2012;222(6):369-376. doi:10.1007/s00427-012-0420-x

510. Xie L, Zeng X, Hu J, Chen Q. Characterization of Nestin, a Selective Marker for Bone Marrow Derived Mesenchymal Stem Cells. *Stem Cells Int*. 2015;2015. doi:10.1155/2015/762098

511. Kolf CM, Cho E, Tuan RS. Mesenchymal stromal cells. Biology of adult mesenchymal stem cells: regulation of niche, self-renewal and differentiation. *Arthritis Res Ther*. 2007;9(1):204. doi:10.1186/ar2116

512. Morrison SJ, Scadden DT. The bone marrow niche for haematopoietic stem cells. *Nature*. 2014;505(7483):327-334. doi:10.1038/nature12984

513. Chen Q, Shou P, Zhang L, et al. An osteopontin-integrin interaction plays a critical role in directing adipogenesis and osteogenesis by mesenchymal stem cells. *Stem Cells*. 2014;32(2):327-337. doi:10.1002/stem.1567

514. Xiao W, Zhang D, Fan C, Yu B. Intermittent Stretching and Osteogenic Differentiation of Bone Marrow Derived Mesenchymal Stem Cells via the p38MAPK-Osterix Signaling Pathway. *Cell Physiol Biochem*. 2015;36(3):1015-1025. doi:10.1159/000430275

515. Shen C, Yang C, Xu S, Zhao H. Comparison of osteogenic differentiation capacity in mesenchymal stem cells derived from human amniotic membrane (AM), umbilical cord (UC), chorionic membrane (CM), and decidua (DC). *Cell Biosci*. 2019;9(1):17. doi:10.1186/s13578-019-0281-3

516. Aubin JE. Regulation of Osteoblast Formation and Function. *Rev Endocr Metab Disord*. 2001;2(1):81-94. doi:10.1023/A:1010011209064

517. Rickard DJ, Sullivan TA, Shenker BJ, Leboy PS, Kazhdan I. Induction of Rapid Osteoblast Differentiation in Rat Bone Marrow Stromal Cell Cultures by Dexamethasone and BMP-2. *Dev Biol*. 1994;161(1):218-

228. doi:10.1006/DBIO.1994.1022

518. Barry FP, Murphy JM. Mesenchymal stem cells: clinical applications and biological characterization. *Int J Biochem Cell Biol*. 2004;36(4):568-584. doi:10.1016/J.BIOCEL.2003.11.001

519. Wu S, Wells A, Griffith LG, Lauffenburger DA. Controlling multipotent stromal cell migration by integrating “course-graining” materials and “fine-tuning” small molecules via decision tree signal-response modeling. *Biomaterials*. 2011;32(30):7524-7531. doi:10.1016/j.biomaterials.2011.06.050

520. Fu, Liu, Halim, Ju, Luo, Song. Mesenchymal Stem Cell Migration and Tissue Repair. *Cells*. 2019;8(8):784. doi:10.3390/cells8080784

521. Shaebani MR, Jose R, Santen L, Stankevicins L, Lautenschläger F. Persistence-Speed Coupling Enhances the Search Efficiency of Migrating Immune Cells. *Phys Rev Lett*. 2020;125(26). doi:10.1103/PhysRevLett.125.268102

522. McAndrews KM, McGrail DJ, Ravikumar N, Dawson MR. Mesenchymal Stem Cells Induce Directional Migration of Invasive Breast Cancer Cells through TGF-β. *Sci Rep*. 2015;5(1):16941. doi:10.1038/srep16941

523. Ya-Hsuan Ho A, del Toro R, Rivera-Torres J, Louache F, André V, Mé ndez-Ferrer Correspondence S. Remodeling of Bone Marrow Hematopoietic Stem Cell Niches Promotes Myeloid Cell Expansion during Premature or Physiological Aging. *Cell Stem Cell*. 2019;25:407-418. doi:10.1016/j.stem.2019.06.007

524. Man Y, Yao X, Yang T, Wang Y. Hematopoietic Stem Cell Niche During Homeostasis, Malignancy, and Bone Marrow Transplantation. *Front Cell Dev Biol*. 2021;9:14. doi:10.3389/fcell.2021.621214

525. Zhang P, Zhang C, Li J, Han J, Liu X, Yang H. The physical microenvironment of hematopoietic stem cells and its emerging roles in engineering applications. *Stem Cell Res Ther*. 2019;10(1):1-13. doi:10.1186/s13287-019-1422-7

526. Foster GA, Headen DM, González-García C, Salmerón-Sánchez M, Shirwan H, García AJ. Protease-degradable microgels for protein delivery for vascularization. *Biomaterials*. 2017;113:170-175. doi:10.1016/j.biomaterials.2016.10.044

527. Patterson J, Hubbell JA. Enhanced proteolytic degradation of molecularly engineered PEG hydrogels in response to MMP-1 and MMP-2. *Biomaterials*. 2010;31(30):7836-7845. doi:10.1016/j.biomaterials.2010.06.061

528. Scales JT, Winter GD. Clinical considerations in the choice of materials for orthopedic internal prostheses. *J Biomed Mater Res*. 1975;9(4):167-176. doi:10.1002/jbm.820090420

529. Khalili AA, Ahmad MR. A Review of cell adhesion studies for biomedical and biological applications. *Int J Mol Sci*. 2015;16(8):18149-18184. doi:10.3390/ijms160818149

530. Perinpanayagam H, Zaharias R, Stanford C, Brand R, Keller J, Schneider G. Early cell adhesion events differ between osteoporotic and non-osteoporotic osteoblasts. *J Orthop Res*. 2001;19(6):993-1000. doi:10.1016/S0736-0266(01)00045-6

531. Szekanecz Z, Koch AE. Cell-cell interactions in synovitis. Endothelial cells and immune cell migration. *Arthritis Res*. 2000;2(5):368-373. doi:10.1186/ar114

532. Hirohashi S, Kanai Y. Cell adhesion system and human cancer morphogenesis. *Cancer Sci*. 2003;94(7):575-581. doi:10.1111/j.1349-7006.2003.tb01485.x

533. Lutolf MP, Gilbert PM, Blau HM. Designing materials to direct stem-cell fate. *Nature*. 2009;462(7272):433-441. doi:10.1038/nature08602

534. Amani H, Arzaghi H, Bayandori M, et al. Controlling Cell Behavior through the Design of Biomaterial Surfaces: A Focus on Surface Modification Techniques. *Adv Mater Interfaces*. 2019;6(13):1900572. doi:10.1002/admi.201900572

535. Uwais ZA, Hussein MA, Samad MA, Al-Aqeeli N. Surface Modification of Metallic Biomaterials for Better Tribological Properties: A Review. *Arab J Sci Eng*. 2017;42(11):4493-4512. doi:10.1007/s13369-017-2624-x

536. Tandon B, Magaz A, Balint R, Blaker JJ, Cartmell SH. Electroactive biomaterials: Vehicles for controlled delivery of therapeutic agents for drug delivery and tissue regeneration. *Adv Drug Deliv Rev*. 2018;129:148-168. doi:10.1016/j.addr.2017.12.012

537. Zhang K, Wang S, Zhou C, et al. Advanced smart biomaterials and constructs for hard tissue engineering and regeneration. *Bone Res*. 2018;6(1):1-15. doi:10.1038/s41413-018-0032-9

538. Martino S, D'Angelo F, Armentano I, Kenny JM, Orlacchio A. Stem cell-biomaterial interactions for regenerative medicine. *Biotechnol Adv*. 2012;30(1):338-351. doi:10.1016/j.biotechadv.2011.06.015

539. Xu Y, Chen C, Hellwarth PB, Bao X. Biomaterials for stem cell engineering and biomanufacturing. *Bioact Mater*. 2019;4:366-379. doi:10.1016/j.bioactmat.2019.11.002

540. Jang HK, Kim BS. Modulation of stem cell differentiation with biomaterials. *Int J Stem Cells*. 2010;3(2):80-84. doi:10.15283/ijsc.2010.3.2.80

541. Najar M, Krayem M, Merimi M, et al. Insights into inflammatory priming of mesenchymal stromal cells: functional biological impacts. *Inflamm Res*. 2018;67(6):467-477. doi:10.1007/s00011-018-1131-1

542. Sun Y, Li QF, Yan J, Hu R, Jiang H. Isoflurane Preconditioning Promotes the Survival and Migration of Bone Marrow Stromal Cells. *Cell Physiol Biochem*. 2015;36(4):1331-1345. doi:10.1159/000430300

543. Takeda K, Ning F, Domenico J, et al. Activation of p70S6 Kinase-1 in Mesenchymal Stem Cells Is Essential to Lung Tissue Repair. *Stem Cells Transl Med*. 2018;7(7):551-558. doi:10.1002/sctm.17-0200

544. Zippel N, Schulze M, Tobiasch E. Biomaterials and Mesenchymal Stem Cells for Regenerative Medicine. *Recent Pat Biotechnol*. 2009;4(1):1-22. doi:10.2174/187220810790069497

545. Wu YN, Law JBK, He AY, et al. Substrate topography determines the fate of chondrogenesis from human mesenchymal stem cells resulting in specific cartilage phenotype formation. *Nanomedicine Nanotechnology, Biol Med*. 2014;10(7):1507-1516. doi:10.1016/j.nano.2014.04.002

546. Yu J, Du KT, Fang Q, et al. The use of human mesenchymal stem cells encapsulated in RGD modified alginate microspheres in the repair of myocardial infarction in the rat. *Biomaterials*. 2010;31(27):7012-7020. doi:10.1016/j.biomaterials.2010.05.078

547. De Witte SFH, Franquesa M, Baan CC, Hoogduijn MJ. Toward development of imesenchymal stem cells for immunomodulatory therapy. *Front Immunol*. 2016;6(JAN). doi:10.3389/fimmu.2015.00648

548. Huang H, Kim HJ, Chang EJ, et al. IL-17 stimulates the proliferation and differentiation of human mesenchymal stem cells: Implications for bone remodeling. *Cell Death Differ*. 2009;16(10):1332-1343. doi:10.1038/cdd.2009.74

549. Najar M, Raicevic G, Kazan HF, et al. Immune-Related Antigens, Surface Molecules and Regulatory Factors in Human-Derived Mesenchymal Stromal Cells: The Expression and Impact of Inflammatory Priming. *Stem Cell Rev Reports*. 2012;8(4):1188-1198. doi:10.1007/s12015-012-9408-1

550. Kang SK, Shin IS, Ko MS, Jo JY, Ra JC. Journey of mesenchymal stem cells for homing: Strategies to enhance efficacy and safety of stem cell therapy. *Stem Cells Int*. 2012. doi:10.1155/2012/342968

551. Zhuang Y, Chen X, Xu M, Zhang LY, Xiang F. Chemokine stromal cell-derived factor 1/CXCL12 increases homing of mesenchymal stem cells to injured myocardium and neovascularization following myocardial infarction. *Chin Med J (Engl)*. 2009;122(2):183-187. doi:10.3760/cma.j.issn.0366-6999.2009.02.014

552. Krampera M, Pizzolo G, Aprili G, Franchini M. Mesenchymal stem cells for bone, cartilage, tendon and skeletal muscle repair. *Bone*. 2006;39(4):678-683. doi:10.1016/j.bone.2006.04.020

553. Liu X, Duan B, Cheng Z, et al. SDF-1/CXCR4 axis modulates bone marrow mesenchymal stem cell apoptosis, migration and cytokine secretion. *Protein Cell*. 2011;2(10):845-854. doi:10.1007/s13238-011-1097-z

554. Marquez-Curtis LA, Janowska-Wieczorek A. Enhancing the migration ability of mesenchymal stromal cells by targeting the SDF-1/CXCR4 axis. *Biomed Res Int*. 2013;2013. doi:10.1155/2013/561098

555. Ryu CH, Park SA, Kim SM, et al. Migration of human umbilical cord blood mesenchymal stem cells

mediated by stromal cell-derived factor-1/CXCR4 axis via Akt, ERK, and p38 signal transduction pathways. *Biochem Biophys Res Commun*. 2010;398(1):105-110. doi:10.1016/j.bbrc.2010.06.043

556. Parisi L, Toffoli A, Ghezzi B, Mozzoni B, Lumetti S, Macaluso GM. A glance on the role of fibronectin in controlling cell response at biomaterial interface. *Jpn Dent Sci Rev*. 2020;56(1):50-55. doi:10.1016/j.jdsr.2019.11.002

557. Kim JH, Jekarl DW, Kim M, et al. Effects of ECM protein mimetics on adhesion and proliferation of chorion derived mesenchymal stem cells. *Int J Med Sci*. 2014;11(3):298-308. doi:10.7150/ijms.6672

558. Kasten A, Naser T, Brüllhoff K, et al. Guidance of mesenchymal stem cells on fibronectin structured hydrogel films. *PLoS One*. 2014;9(10):109411. doi:10.1371/journal.pone.0109411

559. Home - ClinicalTrials.gov. https://clinicaltrials.gov/. Accessed June 27, 2021.

560. Galipeau J, Sensébé L. Mesenchymal Stromal Cells: Clinical Challenges and Therapeutic Opportunities. *Cell Stem Cell*. 2018;22(6):824-833. doi:10.1016/j.stem.2018.05.004

561. Gomez-Salazar M, Gonzalez-Galofre ZN, Casamitjana J, Crisan M, James AW, Péault B. Five Decades Later, Are Mesenchymal Stem Cells Still Relevant? *Front Bioeng Biotechnol*. 2020;8:148. doi:10.3389/fbioe.2020.00148

562. Henrich TJ, Lelièvre JD. Progress towards obtaining an HIV cure: slow but sure. *Curr Opin HIV AIDS*. 2018;13(5):381-382. doi:10.1097/COH.0000000000000492

563. Hogan LE, Hanhauser E, Hobbs KS, et al. Human Herpes Virus 8 in HIV-1 infected individuals receiving cancer chemotherapy and stem cell transplantation. *PLoS One*. 2018;13(5). doi:10.1371/journal.pone.0197298

564. Talib S, Shepard KA. Unleashing the cure: Overcoming persistent obstacles in the translation and expanded use of hematopoietic stem cell-based therapies. *Stem Cells Transl Med*. 2020;9(4):420-426. doi:10.1002/sctm.19-0375

565. Newman RG, Ross DB, Barreras H, et al. The allure and peril of hematopoietic stem cell transplantation: Overcoming immune challenges to improve success. *Immunol Res*. 2013;57(1-3):125-139. doi:10.1007/s12026-013-8450-7

566. Lou X, Zhao C, Chen H. Unrelated donor umbilical cord blood transplant versus unrelated hematopoietic stem cell transplant in patients with acute leukemia: A meta-analysis and systematic review. *Blood Rev*. 2018;32(3):192-202. doi:10.1016/j.blre.2017.11.003

567. Nucci M, Anaissie E. Infections after high-dose chemotherapy and autologous hematopoietic stem cell transplantation. In: *Infections in Hematology*. Springer Berlin Heidelberg; 2015:49-61. doi:10.1007/978-3-662-44000-1_4

568. Marx-Blümel L, Marx C, Weise F, et al. Biomimetic reconstruction of the hematopoietic stem cell niche for in vitro amplification of human hematopoietic stem cells. *PLoS One*. 2020;15(6):e0234638. doi:10.1371/JOURNAL.PONE.0234638

569. Wilkinson AC, Ishida R, Nakauchi H, Yamazaki S. Long-term ex vivo expansion of mouse hematopoietic stem cells. *Nat Protoc*. 2020;15(2):628-648. doi:10.1038/s41596-019-0263-2

570. Calvi LM, Adams GB, Weibrecht KW, et al. Osteoblastic cells regulate the haematopoietic stem cell niche. *Nature*. 2003;425(6960):841-846. doi:10.1038/nature02040

571. Lévesque JP, Helwani FM, Winkler IG. The endosteal osteoblastic niche and its role in hematopoietic stem cell homing and mobilization. *Leukemia*. 2010;24(12):1979-1992. doi:10.1038/leu.2010.214

572. Ding L, Saunders TL, Enikolopov G, Morrison SJ. Endothelial and perivascular cells maintain haematopoietic stem cells. *Nature*. 2012;481(7382):457-462. doi:10.1038/nature10783

573. Méndez-Ferrer S, Michurina T V., Ferraro F, et al. Mesenchymal and haematopoietic stem cells form a unique bone marrow niche. *Nature*. 2010;466(7308):829-834. doi:10.1038/nature09262

574. Pinho S, Frenette PS. Haematopoietic stem cell activity and interactions with the niche. *Nat Rev Mol Cell Biol*. 2019;20(5):303-320. doi:10.1038/s41580-019-0103-9

575. Coskun S, Hirschi KK. Establishment and regulation of the HSC niche: Roles of osteoblastic and vascular compartments. *Birth Defects Res Part C - Embryo Today Rev*. 2010;90(4):229-242. doi:10.1002/bdrc.20194

576. Haug JS, He XC, Grindley JC, et al. N-Cadherin Expression Level Distinguishes Reserved versus Primed States of Hematopoietic Stem Cells. *Cell Stem Cell*. 2008;2(4):367-379. doi:10.1016/j.stem.2008.01.017

577. Pinho S, Frenette PS. Haematopoietic stem cell activity and interactions with the niche. *Nat Rev Mol Cell Biol*. 2019;20(5):303-320. doi:10.1038/s41580-019-0103-9

578. Winkler IG, Nowlan B, Barbier V, Levesque J-P. Absence of E-Selectin at the Vascular Niche Delays Hematopoietic Stem Cell Turn-Over. *Blood*. 2007;110(11):609-609. doi:10.1182/blood.v110.11.609.609

579. Ulyanova T, Scott LM, Priestley G V., et al. VCAM-1 expression in adult hematopoietic and nonhematopoietic cells is controlled by tissue-inductive signals and reflects their developmental origin. *Blood*. 2005;106(1):86-94. doi:10.1182/blood-2004-09-3417

580. Grassinger J, Haylock DN, Storan MJ, et al. Thrombin-cleaved osteopontin regulates hemopoietic stem and progenitor cell functions through interactions with α9β1and α4β1 integrins. *Blood*. 2009;114(1):49-59. doi:10.1182/blood-2009-01-197988

581. Katayama Y, Battista M, Kao WM, et al. Signals from the sympathetic nervous system regulate hematopoietic stem cell egress from bone marrow. *Cell*. 2006;124(2):407-421. doi:10.1016/j.cell.2005.10.041

582. Chen S, Lewallen M, Xie T. Adhesion in the stem cell niche: biological roles and regulation. *Development*. 2013;140(2):255. doi:10.1242/DEV.083139

583. Wagers AJ, Allsopp RC, Weissman IL. Changes in integrin expression are associated with altered homing properties of Lin−/loThy1.1loSca-1+c-kit+ hematopoietic stem cells following mobilization by cyclophosphamide/granulocyte colony-stimulating factor. *Exp Hematol*. 2002;30(2):176-185. doi:10.1016/S0301-472X(01)00777-9

584. Muth CA, Steinl C, Klein G, Lee-Thedieck C. Regulation of Hematopoietic Stem Cell Behavior by the Nanostructured Presentation of Extracellular Matrix Components. *PLoS One*. 2013;8(2):e54778. doi:10.1371/JOURNAL.PONE.0054778

585. Choi JS, Harley BAC. Marrow-inspired matrix cues rapidly affect early fate decisions of hematopoietic stem and progenitor cells. *Sci Adv*. 2017;3(1). doi:10.1126/sciadv.1600455

586. IG W, V B, B N, et al. Vascular niche E-selectin regulates hematopoietic stem cell dormancy, self renewal and chemoresistance. *Nat Med*. 2012;18(11):1651-1657. doi:10.1038/NM.2969

587. Levesque J-P, Winkler IG. Cell Adhesion Molecules in Normal and Malignant Hematopoiesis: from Bench to Bedside. *Curr Stem Cell Reports 2016 24*. 2016;2(4):356-367. doi:10.1007/S40778-016-0066-0

588. P L, LI Z. Resolving the controversy about N-cadherin and hematopoietic stem cells. *Cell Stem Cell*. 2010;6(3):199-202. doi:10.1016/J.STEM.2010.02.007

589. Hosokawa K, Arai F, Yoshihara H, et al. Knockdown of N-cadherin suppresses the long-term engraftment of hematopoietic stem cells. *Blood*. 2010;116(4):554-563. doi:10.1182/BLOOD-2009-05-224857

590. Roβmanith T, Schröder B, Bug G, et al. Interleukin 3 Improves the Ex Vivo Expansion of Primitive Human Cord Blood Progenitor Cells and Maintains the Engraftment Potential of SCID Repopulating Cells. *Stem Cells*. 2001;19(4):313-320. doi:10.1634/stemcells.19-4-313

591. Branco A, Bucar S, Moura-Sampaio J, et al. Tailored Cytokine Optimization for ex vivo Culture Platforms Targeting the Expansion of Human Hematopoietic Stem/Progenitor Cells. *Front Bioeng Biotechnol*. 2020;8:1154. doi:10.3389/fbioe.2020.573282

592. Porter RL, Georger MA, Bromberg O, et al. Prostaglandin E2 increases hematopoietic stem cell survival and accelerates hematopoietic recovery after radiation injury. *Stem Cells*. 2013;31(2):372-383. doi:10.1002/stem.1286

593. Tao L, Togarrati PP, Choi KD, Suknuntha K. Stemregenin 1 selectively promotes expansion of

multipotent hematopoietic progenitors derived from human embryonic stem cells. *J Stem Cells Regen Med*. 2017;13(2):P75-P79. doi:10.46582/jsrm.1302011

594. Cohen S, Roy J, Lachance S, et al. Hematopoietic stem cell transplantation using single UM171-expanded cord blood: a single-arm, phase 1–2 safety and feasibility study. *Lancet Haematol*. 2020;7(2):e134-e145. doi:10.1016/S2352-3026(19)30202-9

595. Tiwari A, Tursky ML, Mushahary D, et al. Ex vivo expansion of haematopoietic stem/progenitor cells from human umbilical cord blood on acellular scaffolds prepared from MS-5 stromal cell line. *J Tissue Eng Regen Med*. 2013;7(11):871-883. doi:10.1002/term.1479

596. Congrains A, Bianco J, Rosa RG, Mancuso RI, Saad STO. 3d scaffolds to model the hematopoietic stem cell niche: Applications and perspectives. *Materials (Basel)*. 2021;14(3):1-18. doi:10.3390/ma14030569

597. Yin X, Hu L, Zhang Y, et al. PDGFB-expressing mesenchymal stem cells improve human hematopoietic stem cell engraftment in immunodeficient mice. *Bone Marrow Transplant*. 2020;55(6):1029-1040. doi:10.1038/s41409-019-0766-z

598. Stier S, Ko Y, Forkert R, et al. Osteopontin is a hematopoietic stem cell niche component that negatively regulates stem cell pool size. *J Exp Med*. 2005;201(11):1781-1791. doi:10.1084/jem.20041992

599. Magnusson M, Sierra MI, Sasidharan R, et al. Expansion on Stromal Cells Preserves the Undifferentiated State of Human Hematopoietic Stem Cells Despite Compromised Reconstitution Ability. *PLoS One*. 2013;8(1):53912. doi:10.1371/journal.pone.0053912

600. Rödling L, Schwedhelm I, Kraus S, Bieback K, Hansmann J, Lee-Thedieck C. 3D models of the hematopoietic stem cell niche under steady-state and active conditions. *Sci Reports 2017 71*. 2017;7(1):1-15. doi:10.1038/s41598-017-04808-0

601. S S, L W, N C, et al. Bone marrow-on-a-chip: Long-term culture of human haematopoietic stem cells in a three-dimensional microfluidic environment. *J Tissue Eng Regen Med*. 2018;12(2):479-489. doi:10.1002/TERM.2507

602. O S, J S, TE S, CB W, WK A, G K. Hematopoietic Stem and Progenitor Cell Expansion in Contact with Mesenchymal Stromal Cells in a Hanging Drop Model Uncovers Disadvantages of 3D Culture. *Stem Cells Int*. 2016;2016. doi:10.1155/2016/4148093

603. A R, L R, H K, C L-T. Biomimetic macroporous PEG hydrogels as 3D scaffolds for the multiplication of human hematopoietic stem and progenitor cells. *Biomaterials*. 2014;35(3):929-940. doi:10.1016/J.BIOMATERIALS.2013.10.038

604. E C, DC K, M Y, et al. Rapid expansion of human hematopoietic stem cells by automated control of inhibitory feedback signaling. *Cell Stem Cell*. 2012;10(2):218-229. doi:10.1016/J.STEM.2012.01.003

605. KN C, C C, PC L, S R, KW L, HQ M. Functional nanofiber scaffolds with different spacers modulate adhesion and expansion of cryopreserved umbilical cord blood hematopoietic stem/progenitor cells. *Exp Hematol*. 2007;35(5):771-781. doi:10.1016/J.EXPHEM.2007.02.002

606. A T, ML T, D M, et al. Ex vivo expansion of haematopoietic stem/progenitor cells from human umbilical cord blood on acellular scaffolds prepared from MS-5 stromal cell line. *J Tissue Eng Regen Med*. 2013;7(11):871-883. doi:10.1002/TERM.1479

607. W L, Y L, S M, et al. Reconstitution of bone-like matrix in osteogenically differentiated mesenchymal stem cell-collagen constructs: A three-dimensional in vitro model to study hematopoietic stem cell niche. *J Tissue Eng*. 2013;4(1):1-14. doi:10.1177/2041731413508668

608. Raic A, Rödling L, Kalbacher H, Lee-Thedieck C. Biomimetic macroporous PEG hydrogels as 3D scaffolds for the multiplication of human hematopoietic stem and progenitor cells. *Biomaterials*. 2014;35(3):929-940. doi:10.1016/J.BIOMATERIALS.2013.10.038

609. ML C, S C, OA B, KL H, KK H, JL W. Bioactive poly(ethylene glycol) hydrogels to recapitulate the HSC niche and facilitate HSC expansion in culture. *Biotechnol Bioeng*. 2016;113(4):870-881. doi:10.1002/BIT.25848

610. Mahadik BP, Pedron Haba S, Skertich LJ, Harley BAC. The use of covalently immobilized stem cell factor to selectively affect hematopoietic stem cell activity within a gelatin hydrogel. *Biomaterials*. 2015;67:297-307. doi:10.1016/J.BIOMATERIALS.2015.07.042

611. Gvaramia D, Müller E, Müller K, et al. Combined influence of biophysical and biochemical cues on maintenance and proliferation of hematopoietic stem cells. *Biomaterials*. 2017;138:108-117. doi:10.1016/J.BIOMATERIALS.2017.05.023

612. Bai T, Li J, Sinclair A, et al. Expansion of primitive human hematopoietic stem cells by culture in a zwitterionic hydrogel. *Nat Med 2019 2510*. 2019;25(10):1566-1575. doi:10.1038/s41591-019-0601-5

613. LJ G, NN I. Partial replacement of serum by selenite, transferrin, albumin and lecithin in haemopoietic cell cultures. *Nature*. 1976;263(5578):594-595. doi:10.1038/263594A0

614. Cossarizza A, Chang HD, Radbruch A, et al. Guidelines for the use of flow cytometry and cell sorting in immunological studies. *Eur J Immunol*. 2017;47(10):1584-1797. doi:10.1002/eji.201646632

615. NanoWizard ® AFM Handbook JPK Instruments NanoWizard ® Handbook Version 2.2a 1. 2012.

616. A M, J G. The structure of poly-L-lysine in different solvents. *Biophys Chem*. 2013;175-176:47-53. doi:10.1016/J.BPC.2013.02.004

617. YH K, NS B, YH H, MA C, SD J. Enhancement of neuronal cell adhesion by covalent binding of poly-D-lysine. *J Neurosci Methods*. 2011;202(1):38-44. doi:10.1016/J.JNEUMETH.2011.08.036

618. Franke K, Pompe T, Bornhäuser M, Werner C. Engineered matrix coatings to modulate the adhesion of CD133+ human hematopoietic progenitor cells. *Biomaterials*. 2007;28(5):836-843. doi:10.1016/j.biomaterials.2006.09.031

619. Muth CA, Steinl C, Klein G, Lee-Thedieck C. Regulation of Hematopoietic Stem Cell Behavior by the Nanostructured Presentation of Extracellular Matrix Components. *PLoS One*. 2013;8(2). doi:10.1371/journal.pone.0054778

620. Dorrell C, Gan OI, Pereira DS, Hawley RG, Dick JE. Expansion of human cord blood CD34+CD38−cells in ex vivo culture during retroviral transduction without a corresponding increase in SCID repopulating cell (SRC) frequency: dissociation of SRC phenotype and function. *Blood*. 2000;95(1):102-110. doi:10.1182/BLOOD.V95.1.102

621. Boitano AE, Wang J, Romeo R, et al. Aryl hydrocarbon receptor antagonists promote the expansion of human hematopoietic stem cells. *Science (80-)*. 2010;329(5997):1345-1348. doi:10.1126/science.1191536

622. L T, PP T, KD C, K S. StemRegenin 1 selectively promotes expansion of Multipotent Hematopoietic Progenitors derived from Human Embryonic Stem Cells. *J Stem Cells Regen Med*. 2017;13(2):P75-P79. doi:10.46582/JSRM.1302011

623. Lutolf MP, Blau HM. Artificial Stem Cell Niches. *Adv Mater*. 2009;21(32-33):3255. doi:10.1002/ADMA.200802582

624. Cuchiara ML, Coşkun S, Banda OA, Horter KL, Hirschi KK, West JL. Bioactive poly(ethylene glycol) hydrogels to recapitulate the HSC niche and facilitate HSC expansion in culture. *Biotechnol Bioeng*. 2016;113(4):870-881. doi:10.1002/BIT.25848

625. Sagar BMM, Rentala S, Gopal PNV, Sharma S, Mukhopadhyay A. Fibronectin and laminin enhance engraftibility of cultured hematopoietic stem cells. *Biochem Biophys Res Commun*. 2006;350(4):1000-1005. doi:10.1016/J.BBRC.2006.09.140

626. Choi JS, Harley BAC. Marrow-inspired matrix cues rapidly affect early fate decisions of hematopoietic stem and progenitor cells. *Sci Adv*. 2017;3(1):1600455. doi:10.1126/SCIADV.1600455

627. Trujillo S, Gonzalez-Garcia C, Rico P, et al. Engineered 3D hydrogels with full-length fibronectin that sequester and present growth factors. *Biomaterials*. 2020;252:120104. doi:10.1016/j.biomaterials.2020.120104

628. Dobre O, Oliva MAG, Ciccone G, et al. Hydrogel Platforms: A Hydrogel Platform that Incorporates Laminin Isoforms for Efficient Presentation of Growth Factors – Neural Growth and Osteogenesis. *Adv*

Funct Mater. 2021;31(21):2170150. doi:10.1002/adfm.202170150

629. Aasebø E, Birkeland E, Selheim F, Berven F, Brenner AK, Bruserud Ø. The extracellular bone marrow microenvironment—a proteomic comparison of constitutive protein release by in vitro cultured osteoblasts and mesenchymal stem cells. *Cancers (Basel)*. 2021;13(1):1-24. doi:10.3390/cancers13010062

630. Zhang P, Zhang C, Li J, Han J, Liu X, Yang H. The physical microenvironment of hematopoietic stem cells and its emerging roles in engineering applications. *Stem Cell Res Ther*. 2019;10(1). doi:10.1186/s13287-019-1422-7

631. I F, J C, Y G, et al. Cord blood expansion. Pyrimidoindole derivatives are agonists of human hematopoietic stem cell self-renewal. *Science*. 2014;345(6203):1509-1512. doi:10.1126/SCIENCE.1256337

632. HA H, CM T, L S, et al. Distinct Bone Marrow Sources of Pleiotrophin Control Hematopoietic Stem Cell Maintenance and Regeneration. *Cell Stem Cell*. 2018;23(3):370-381.e5. doi:10.1016/J.STEM.2018.07.003

633. Wang X, Rivière I. Genetic Engineering and Manufacturing of Hematopoietic Stem Cells. *Mol Ther Methods Clin Dev*. 2017;5:96. doi:10.1016/J.OMTM.2017.03.003

634. Ingavle G, Vaidya A, Kale V. Constructing Three-Dimensional Microenvironments Using Engineered Biomaterials for Hematopoietic Stem Cell Expansion. *Tissue Eng - Part B Rev*. 2019;25(4):312-329. doi:10.1089/TEN.TEB.2018.0286

635. Talib S, Shepard KA. Unleashing the cure: Overcoming persistent obstacles in the translation and expanded use of hematopoietic stem cell-based therapies. *Stem Cells Transl Med*. 2020;9(4):420-426. doi:10.1002/sctm.19-0375

636. N C, S H-B-A, CC B, et al. Hematopoietic stem cell gene therapy with a lentiviral vector in X-linked adrenoleukodystrophy. *Science*. 2009;326(5954):818-823. doi:10.1126/SCIENCE.1171242

637. KL S, E G, S M, et al. Clinical efficacy of gene-modified stem cells in adenosine deaminase-deficient immunodeficiency. *J Clin Invest*. 2017;127(5):1689-1699. doi:10.1172/JCI90367

638. Tebas P, Stein D, Tang WW, et al. Gene Editing of CCR5 in Autologous CD4 T Cells of Persons Infected with HIV. *N Engl J Med*. 2014;370(10):901-910. doi:10.1056/nejmoa1300662

639. Robledo MM, Sanz-Rodriguez F, Hidalgo A, Teixidó J. Differential use of very late antigen-4 and -5 integrins by hematopoietic precursors and myeloma cells to adhere to transforming growth factor-β1-treated bone marrow stroma. *J Biol Chem*. 1998;273(20):12056-12060. doi:10.1074/JBC.273.20.12056

640. Wierenga PK, Weersing E, Dontje B, de Haan G, van Os R. Differential role for very late antigen-5 in mobilization and homing of hematopoietic stem cells. *Bone Marrow Transplant*. 2006;38(12):789-797. doi:10.1038/SJ.BMT.1705534

641. Yokota T, Oritani K, Mitsui H, et al. Growth-Supporting Activities of Fibronectin on Hematopoietic Stem/Progenitor Cells In Vitro and In Vivo: Structural Requirement for Fibronectin Activities of CS1 and Cell-Binding Domains. *Blood*. 1998;91(9):3263-3272. doi:10.1182/BLOOD.V91.9.3263

642. Drame I, Lafforgue C, Formosa-Dague C, et al. Pili and other surface proteins influence the structure and the nanomechanical properties of Lactococcus lactis biofilms. *Sci Reports 2021 111*. 2021;11(1):1-13. doi:10.1038/s41598-021-84030-1

643. Forsberg EC, Smith-Berdan S. Parsing the niche code: the molecular mechanisms governing hematopoietic stem cell adhesion and differentiation. *Haematologica*. 2009;94(11):1477. doi:10.3324/HAEMATOL.2009.013730

644. Ulyanova T, Scott LM, Priestley G V., et al. VCAM-1 expression in adult hematopoietic and nonhematopoietic cells is controlled by tissue-inductive signals and reflects their developmental origin. *Blood*. 2005;106(1):86. doi:10.1182/BLOOD-2004-09-3417

645. DE W, EP B, AJ W, EC B, IL W. Hematopoietic stem cells are uniquely selective in their migratory response to chemokines. *J Exp Med*. 2002;195(9):1145-1154. doi:10.1084/JEM.20011284

646. Peled A, Kollet O, Ponomaryov T, et al. The chemokine SDF-1 activates the integrins LFA-1, VLA-4, and VLA-5 on immature human CD34+ cells: role in transendothelial/stromal migration and engraftment of NOD/SCID mice. *Blood*. 2000;95(11):3289-3296. doi:10.1182/BLOOD.V95.11.3289

647. S M-F, TV M, F F, et al. Mesenchymal and haematopoietic stem cells form a unique bone marrow niche. *Nature*. 2010;466(7308):829-834. doi:10.1038/NATURE09262

648. Sugiyama T, Kohara H, Noda M, Nagasawa T. Maintenance of the Hematopoietic Stem Cell Pool by CXCL12-CXCR4 Chemokine Signaling in Bone Marrow Stromal Cell Niches. *Immunity*. 2006;25(6):977-988. doi:10.1016/J.IMMUNI.2006.10.016

649. Mishima S, Nagai A, Abdullah S, et al. Effective ex vivo expansion of hematopoietic stem cells using osteoblast-differentiated mesenchymal stem cells is CXCL12 dependent. *Eur J Haematol*. 2010;84(6):538-546. doi:10.1111/J.1600-0609.2010.01419.X

650. Reid JC, Tanasijevic B, Golubeva D, et al. CXCL12/CXCR4 Signaling Enhances Human PSC-Derived Hematopoietic Progenitor Function and Overcomes Early In Vivo Transplantation Failure. *Stem Cell Reports*. 2018;10(5):1625-1641. doi:10.1016/j.stemcr.2018.04.003

651. Rajendiran S, Smith-Berdan S, Kunz L, et al. Ubiquitous overexpression of CXCL12 confers radiation protection and enhances mobilization of hematopoietic stem and progenitor cells. *bioRxiv*. January 2020:2020.01.08.899427. doi:10.1101/2020.01.08.899427

652. H Q, N B-V, CD H, et al. Critical role of thrombopoietin in maintaining adult quiescent hematopoietic stem cells. *Cell Stem Cell*. 2007;1(6):671-684. doi:10.1016/J.STEM.2007.10.008

653. O'Neill A, Chin D, Tan D, Majeed AQBBA, Nakamura-Ishizu A, Suda T. Thrombopoietin maintains cell numbers of hematopoietic stem and progenitor cells with megakaryopoietic potential. *Haematologica*. 2021;106(7):1883-1891. doi:10.3324/HAEMATOL.2019.241406

654. M B, M G, S K, K W. Thrombopoietin is essential for the maintenance of normal hematopoiesis in humans: development of aplastic anemia in patients with congenital amegakaryocytic thrombocytopenia. *Ann N Y Acad Sci*. 2003;996:17-25. doi:10.1111/J.1749-6632.2003.TB03228.X

655. Graaf CA de, Metcalf D. Thrombopoietin and hematopoietic stem cells. *Cell Cycle*. 2011;10(10):1582. doi:10.4161/CC.10.10.15619

656. Buza-Vidas N, Antonchuk J, Qian H, et al. Cytokines regulate postnatal hematopoietic stem cell expansion: opposing roles of thrombopoietin and LNK. *Genes Dev*. 2006;20(15):2018-2023. doi:10.1101/GAD.385606

657. Cui L, Moraga I, Lerbs T, et al. Tuning MPL signaling to influence hematopoietic stem cell differentiation and inhibit essential thrombocythemia. *Proc Natl Acad Sci U S A*. 2021;118(2). doi:10.1073/pnas.2017849118

658. Yagi M, Ritchie KA, Sitnicka E, Storey C, Roth GJ, Bartelmez S. Sustained ex vivo expansion of hematopoietic stem cells mediated by thrombopoietin. *Proc Natl Acad Sci*. 1999;96(14):8126-8131. doi:10.1073/PNAS.96.14.8126

659. Mousavi SH, Abroun S, Soleimani M, Mowla SJ. 3-Dimensional nano-fibre scaffold for ex vivo expansion of cord blood haematopoietic stem cells. *Artif Cells, Nanomedicine Biotechnol*. 2018;46(4):740-748. doi:10.1080/21691401.2017.1337026

660. Ulyanova T, Scott LM, Priestley G V., et al. VCAM-1 expression in adult hematopoietic and nonhematopoietic cells is controlled by tissue-inductive signals and reflects their developmental origin. *Blood*. 2005;106(1):86. doi:10.1182/BLOOD-2004-09-3417

661. Xu C, Gao X, Wei Q, et al. Stem cell factor is selectively secreted by arterial endothelial cells in bone marrow. *Nat Commun*. 2018;9(1). doi:10.1038/s41467-018-04726-3

662. P D, FF H, LS G, et al. Macrophages retain hematopoietic stem cells in the spleen via VCAM-1. *J Exp Med*. 2015;212(4):497-512. doi:10.1084/JEM.20141642

663. Pinho S, Qiaozhi W, Maryanovich M, Pierce H, Nakahara F, Frenette PS. Vcam1 Is a Don't-Eat-Me Signal on Healthy Hematopoietic and Leukemic Stem Cells. *Blood*. 2016;128(22):565-565.

doi:10.1182/BLOOD.V128.22.565.565

664. Hidalgo A. Hematopoietic stem cell homing: The long, winding and adhesive road to the bone marow. *Inmunología*. 2008;27(1):22-35. doi:10.1016/S0213-9626(08)70046-5

665. D V der V-Z, MA V, LH R, RA DW, JG V den T, P J. Fibronectin distribution in human bone marrow stroma: matrix assembly and tumor cell adhesion via alpha5 beta1 integrin. *Exp Cell Res*. 1997;230(1):111-120. doi:10.1006/EXCR.1996.3405

666. Wirth F, Lubosch A, Hamelmann S, Nakchbandi IA. Fibronectin and Its Receptors in Hematopoiesis. *Cells*. 2020;9(12). doi:10.3390/cells9122717

667. Umemoto T, Yamato M, Ishihara J, et al. Integrin-αvβ3 regulates thrombopoietin-mediated maintenance of hematopoietic stem cells. *Blood*. 2012;119(1):83-94. doi:10.1182/BLOOD-2011-02-335430

668. Hurley RW, McCarthy JB, Verfaillie CM. Direct adhesion to bone marrow stroma via fibronectin receptors inhibits hematopoietic progenitor proliferation. *J Clin Invest*. 1995;96(1):511-519. doi:10.1172/JCI118063

669. SE K, CG K, PL H, et al. BIGH3 modulates adhesion and migration of hematopoietic stem and progenitor cells. *Cell Adh Migr*. 2013;7(5):434-449. doi:10.4161/CAM.26596

670. Choi JS, Harley BAC. Marrow-inspired matrix cues rapidly affect early fate decisions of hematopoietic stem and progenitor cells. *Sci Adv*. 2017;3(1). doi:10.1126/SCIADV.1600455

671. Wilkinson AC, Ishida R, Kikuchi M, et al. Long-term ex vivo haematopoietic-stem-cell expansion allows nonconditioned transplantation. *Nat 2019 5717763*. 2019;571(7763):117-121. doi:10.1038/s41586-019-1244-x

672. Han P, Guo XH, Story CJ. Enhanced expansion and maturation of megakaryocytic progenitors by fibronectin. *Cytotherapy*. 2002;4(3):277-283. doi:10.1080/146532402320219790

673. Feng Q, Chai C, Jiang X-S, Leong KW, Mao H-Q. Expansion of engrafting human hematopoietic stem/progenitor cells in three-dimensional scaffolds with surface-immobilized fibronectin. *J Biomed Mater Res Part A*. 2006;78A(4):781-791. doi:10.1002/JBM.A.30829

674. Kolb-Mäurer A, Wilhelm M, Weissinger F, Bröcker EB, Goebel W. Interaction of human hematopoietic stem cells with bacterial pathogens. *Blood*. 2002;100(10):3703-3709. doi:10.1182/blood-2002-03-0898

675. Kolb-Mäurer A, Weissinger F, Kurzai O, Mäurer M, Wilhelm M, Goebel W. Bacterial infection of human hematopoietic stem cells induces monocytic differentiation. *FEMS Immunol Med Microbiol*. 2004;40(2):147-153. doi:10.1016/S0928-8244(03)00305-5

676. Mistry JJ, Marlein CR, Moore JA, et al. ROS-mediated PI3K activation drives mitochondrial transfer from stromal cells to hematopoietic stem cells in response to infection. *Proc Natl Acad Sci U S A*. 2019;116(49):24610-24619. doi:10.1073/pnas.1913278116

677. Scumpia PO, Kelly-Scumpia KM, Delano MJ, et al. Cutting Edge: Bacterial Infection Induces Hematopoietic Stem and Progenitor Cell Expansion in the Absence of TLR Signaling. *J Immunol*. 2010;184(5):2247-2251. doi:10.4049/jimmunol.0903652

678. Kratzer D, Ludwig-Husemann A, Junges K, Geckle U, Lee-Thedieck C. Nanostructured bifunctional hydrogels as potential instructing platform for hematopoietic stem cell differentiation. *Front Mater*. 2019;5:81. doi:10.3389/fmats.2018.00081

679. Cuchiara ML, Coşkun S, Banda OA, Horter KL, Hirschi KK, West JL. Bioactive poly(ethylene glycol) hydrogels to recapitulate the HSC niche and facilitate HSC expansion in culture. *Biotechnol Bioeng*. 2016;113(4):870-881. doi:10.1002/bit.25848

680. Cuchiara ML. Biomimetic PEG Hydrogels for ex vivo Hemapoietic Stem Cell Expansion. 2011. https://scholarship.rice.edu/handle/1911/70418. Accessed September 9, 2021.

681. Petrie TA, Capadona JR, Reyes CD, García AJ. Integrin specificity and enhanced cellular activities associated with surfaces presenting a recombinant fibronectin fragment compared to RGD supports. *Biomaterials*. 2006;27(31):5459-5470. doi:10.1016/j.biomaterials.2006.06.027

682. Salinas CN, Anseth KS. The influence of the RGD peptide motif and its contextual presentation in PEG gels on human mesenchymal stem cell viability. *J Tissue Eng Regen Med*. 2008;2(5):296-304. doi:10.1002/term.95

683. Kruegel J, Miosge N. Basement membrane components are key players in specialized extracellular matrices. *Cell Mol Life Sci 2010 6717*. 2010;67(17):2879-2895. doi:10.1007/S00018-010-0367-X

684. Ishihara J, Ishihara A, Fukunaga K, et al. Laminin heparin-binding peptides bind to several growth factors and enhance diabetic wound healing. *Nat Commun 2018 91*. 2018;9(1):1-14. doi:10.1038/s41467-018-04525-w

685. Zhu J, Clark RAF. Fibronectin at select sites binds multiple growth factors (GF) and enhances their activity: expansion of the collaborative ECM-GF paradigm. *J Invest Dermatol*. 2014;134(4):895. doi:10.1038/JID.2013.484

686. Trujillo S, Vega SL, Song KH, et al. Engineered Full-Length Fibronectin–Hyaluronic Acid Hydrogels for Stem Cell Engineering. *Adv Healthc Mater*. 2020;9(21):2000989. doi:10.1002/adhm.202000989

687. Petrie TA, Capadona JR, Reyes CD, García AJ. Integrin specificity and enhanced cellular activities associated with surfaces presenting a recombinant fibronectin fragment compared to RGD supports. *Biomaterials*. 2006;27(31):5459-5470. doi:10.1016/j.biomaterials.2006.06.027

688. Klotz BJ, Oosterhoff LA, Utomo L, et al. A Versatile Biosynthetic Hydrogel Platform for Engineering of Tissue Analogues. *Adv Healthc Mater*. 2019;8(19):1900979. doi:10.1002/ADHM.201900979

689. Susek KH, Korpos E, Huppert J, et al. Bone marrow laminins influence hematopoietic stem and progenitor cell cycling and homing to the bone marrow. *Matrix Biol*. 2018;67:47-62. doi:10.1016/j.matbio.2018.01.007

690. Kräter M, Jacobi A, Otto O, et al. Bone marrow niche-mimetics modulate HSPC function via integrin signaling. *Sci Rep*. 2017;7(1). doi:10.1038/s41598-017-02352-5

691. Kelly VW, Liang BK, Sirk SJ. Living Therapeutics: The Next Frontier of Precision Medicine. *ACS Synth Biol*. 2020;9(12):3184-3201. doi:10.1021/acssynbio.0c00444

692. FDA. Early Clinical Trials with Live Biotherapeutic Products: CMC Information - Guidance for Industry. *Guideline*. 2012;(February). http://www.fda.gov/BiologicsBloodVaccines/GuidanceComplianceRegulatoryInformation/Guida. Accessed November 4, 2021.

693. Charbonneau MR, Isabella VM, Li N, Kurtz CB. Developing a new class of engineered live bacterial therapeutics to treat human diseases. *Nat Commun*. 2020;11(1). doi:10.1038/s41467-020-15508-1

694. Rosano GL, Ceccarelli EA. Recombinant protein expression in Escherichia coli: Advances and challenges. *Front Microbiol*. 2014;5(APR):172. doi:10.3389/fmicb.2014.00172

695. Bober JR, Beisei CL, Nair NU. Synthetic Biology Approaches to Engineer Probiotics and Members of the Human Microbiota for Biomedical Applications. *Annu Rev Biomed Eng*. 2018;20:277. doi:10.1146/ANNUREV-BIOENG-062117-121019

696. Zhou Z, Chen X, Sheng H, et al. Engineering probiotics as living diagnostics and therapeutics for improving human health. *Microb Cell Fact*. 2020;19(1):1-12. doi:10.1186/s12934-020-01318-z

697. Isabella VM, Ha BN, Castillo MJ, et al. Development of a synthetic live bacterial therapeutic for the human metabolic disease phenylketonuria. *Nat Biotechnol*. 2018;36(9):857-867. doi:10.1038/nbt.4222

698. Rong L, Lei Q, Zhang XZ. Engineering Living Bacteria for Cancer Therapy. *ACS Appl Bio Mater*. 2020;3(12):8136-8145. doi:10.1021/acsabm.0c01286

699. van Tilburg AY, Cao H, van der Meulen SB, Solopova A, Kuipers OP. Metabolic engineering and synthetic biology employing Lactococcus lactis and Bacillus subtilis cell factories. *Curr Opin Biotechnol*. 2019;59:1-7. doi:10.1016/j.copbio.2019.01.007

700. Foligne B, Dessein R, Marceau M, et al. Prevention and Treatment of Colitis With Lactococcus lactis Secreting the Immunomodulatory Yersinia LcrV Protein. *Gastroenterology*. 2007;133(3):862-874. doi:10.1053/j.gastro.2007.06.018

701. Azizpour M, Hosseini SD, Jafari P, Akbary N. Lactococcus lactis: A new strategy for vaccination. *Avicenna J Med Biotechnol*. 2017;9(4):163-168. /pmc/articles/PMC5650732/. Accessed November 4, 2021.

702. Ueda T, Yasukawa K, Nakahata T. Expansion of human NOD/SCID-repopulating cells by stem cell factor, Flk2/Flt3 ligand, thrombopoietin, IL-6, and soluble IL-6 receptor. *J Clin Invest*. 2000;105(7):1013-1021. doi:10.1172/JCI8583

703. Oubari F, Amirizade N, Mohammadpour H, Nakhlestani M, Zarif MN. The important role of FLT3-L in ex vivo expansion of hematopoietic stem cells following co-culture with mesenchymal stem cells. *Cell J*. 2015;17(2):201-210. doi:10.22074/cellj.2016.3715

704. Méndez-Ferrer S, Michurina T V., Ferraro F, et al. Mesenchymal and haematopoietic stem cells form a unique bone marrow niche. *Nature*. 2010;466(7308):829-834. doi:10.1038/nature09262

705. Wei Q, Frenette PS. Niches for Hematopoietic Stem Cells and Their Progeny. *Immunity*. 2018;48(4):632-648. doi:10.1016/j.immuni.2018.03.024